Regulation of the diversification of the nodal and chamber myocardium

Horsthuis, T.

Publication date
2009
Document Version
Final published version

Regulation of the diversification of the nodal and chamber myocardium

Regulation of the diversification of the nodal and chamber myocardium
by Thomas Horsthuis / University of Amsterdam, 2009 / Thesis

Printed by Gildeprint Drukkerijen, Enschede

ISBN .....

On the front cover: Whole mount fluorescence microscopy image of transgenic mouse hearts. A modified bacterial artificial chromosome (*Bac337-Egfp*) with the enhanced green fluorescent protein (GFP) gene inserted into the ANF gene drives atrial expression in a healthy control heart (left side) and is activated in the ventricles during heart failure (right side). On the back: Whole mount fluorescence microscopy image of an E13.5 transgenic mouse embryo carrying *Bac336-Egfp*. *Egfp* expression is restricted to the heart. See related Chapter 2.

Regulation of the diversification of the nodal and chamber myocardium

ACADEMISCH PROEFSCHRIFT

ter verkrijging van de graad van doctor
aan de Universiteit van Amsterdam
op gezag van de Rector Magnificus
prof. dr. D.C. van den Boom
ten overstaan van een door de college voor promoties ingestelde
commissie, in het openbaar te verdedigen in de Agnietenkapel
op donderdag 11 juni 2009, te 12.00 uur

door

Thomas Horsthuis

geboren te Weerselo

Promotiecommissie:

Promotor:	Prof. dr. A.F.M. Moorman
Co-promotor:	Dr. V.M. Christoffels
Overige leden:	Dr. C.R. Bezzina Dr. P.A.C. ’t Hoen Prof. dr. A. Kispert Prof. dr. Y.M. Pinto Prof. dr. A.C. van Rossum

Faculteit der Geneeskunde

The study described in this thesis was carried out at the Heart Failure Research Center, Academic Medical Center, University of Amsterdam, the Netherlands. It was supported by grants from the Netherlands Heart Foundation (NHS) (1996T203) and European Community's Sixth Framework Programme contract ('HeartRepair') LSHM-CT-2005-018630.

Financial support by the Netherlands Heart Foundation for the publication of this thesis is gratefully acknowledged.

Additional financial support for the publication of this thesis was generously provided by the Department of Anatomy & Embryology, the University of Amsterdam, Boehringer Ingelheim B.V., Merck B.V., Novartis Pharma B.V., Pfizer B.V.

'Because it's there'

British mountaineer George H.L. Mallory (1886-1924) replied to the question
'Why do you want to climb Mt. Everest?'

Table of Contents

Scope

The heart is the first organ that is formed during development. In human it beats after 3 weeks of development, comparable with embryonic day E8.5 in mouse. At this early stage the heart is a contracting linear tube, of which the myocardial cells share important features, among which high automaticity, low conduction velocity and low contractility. By an interplay of proliferation, differentiation, cell growth and addition of extracardiac cells, the primitive tube eventually gives rise to the adult 4-chambered heart, containing many phenotypically different cells. When the atrial and ventricular chambers differentiate from the embryonic myocardium, they obtain the so-called 'working' myocardial phenotype, characterized by high contractility and conduction velocity, but low automaticity. The nodal components of the conduction system of the adult heart, the sinus node and the atrioventricular node, which arise from the embryonic myocardium of the primitive tube as well, maintain, in contrast to the chambers, the above-mentioned embryonic characteristics. Knowledge of the transcriptional gene programs regulating the diversification of the nodal and working myocardial phenotype during development is still incomplete. Research aiming to solve this puzzle not only is driven by pure scientific curiosity regarding the molecular processes underlying the development of the 4-chambered heart of higher vertebrates. Equally important is the insight this fundamental knowledge will give us in the underlying causes of congenital heart defects, which eventually will provide cues for new diagnostic and therapeutic interventions. The most challenging prospect would be to use this knowledge to experimentally differentiate (stem) cells into a specific - nodal or working myocardial - direction *in vitro* or *in vivo*. This would give us the tools to generate or renew any cardiac tissue. The work presented in this thesis focuses on the deciphering of the transcriptional pathways regulating the chamber- versus the atrioventricular node- specific gene program.

Chapter 1 starts with a brief introduction for those not familiar with the idiom of the molecular biologist. We discuss several transgenic mouse models, and explain how transcription factors regulate the activity of target genes. Then we review novel insights into the morphogenetic processes and transcriptional gene networks underlying cardiac development, and elaborate on the implications of this new knowledge for our understanding of congenital heart defects. In **Chapter 2** we describe a study on the regulatory DNA sequences driving expression of *Nppa*, the gene encoding atrial natriuretic factor (ANF), during development and disease. Before birth *Nppa* is expressed specifically in the evolving atrial and ventricular chambers, marking their development. After birth the gene is silenced in the ventricles, where it is reactivated in case of cardiac hypertrophy and heart failure, a feature which makes it an important cardiac biomarker. As a consequence, insight into the regulatory DNA sequences driving *Nppa* expression, and the transcriptional pathways converging on them, will reveal both the molecular pathways driving chamber development, and those

driving gene expression in the ventricles during cardiac stress. In **Chapter 3** we report on our findings on the interplay of three members of the T-box family of transcription factors, Tbx2, Tbx3 and Tbx20, and Bmp/Smad-signaling. In recent years these factors have been shown to play pivotal roles in correct development of the chambers and the atrioventricular canal (the embryonic connection between the atria and the ventricles from which both the atrioventricular node and the mesenchymal cushions, primordia of valves and septa, develop). However, the position in the transcriptional hierarchy of the separate regulators, and the way they interact, were still largely unknown. Combining diverse transgenic approaches, we reveal a novel protein-protein interaction playing a key role in this complex transcriptional gene network. Finally, in **Chapter 4**, we use regulatory DNA sequences of transcription factor Tbx3 to explore the transcriptional pathways underlying the development of the atrioventricular node, and to get insight into which genes are involved in its formation and function.

Can recent insights into cardiac development improve our understanding of congenitally malformed hearts?

Thomas Horsthuis[1], Vincent M. Christoffels[1], Robert H. Anderson[2], and Antoon F.M. Moorman[1]

[1]Heart Failure Research Center, Academic Medical Center, University of Amsterdam, the Netherlands, [2]Department of Anatomy, St George's Medical University, London, United Kingdom

Clinical Anatomy 2008. Nov 20;22:4-20.

Abstract

Congenital cardiac malformations account for one-quarter of all human congenital abnormalities. They are caused by environmental and genetic factors. Despite increasing efforts in fundamental research, as yet, the morphogenesis of only a limited number of malformations has been elucidated. Over the last decades, new genetic modifications have made it possible to manipulate the mammalian embryo. Evidence provided using these transgenic techniques has, over the past decade, necessitated re-evaluation of several developmental processes, important in the understanding of normal as opposed to abnormal cardiac development. In this review, we discuss current understanding of the patterning of the initial heart tube, new insights into formation of the atrial and ventricular chambers, and novel information on the origin of the cells that are added to the heart after formation of the initial tube. All of these advances modify our appreciation of malformations involving the venous and arterial poles. As we demonstrate, this new information sheds light not only on normal cardiac development, but also explains the structure of several previously controversial lesions seen in malformed human hearts.

Introduction

Congenitally malformed hearts are the commonest lesions seen in humans at birth, occur in nearly 1% of live births, and are found in up to one-tenth of spontaneously aborted fetuses (Hoffman, 1995). Although many investigators during the previous century speculated on the pathogenesis of these malformations, the precise developmental processes underlying the lesions remained poorly understood. It has been established, nonetheless, that both the

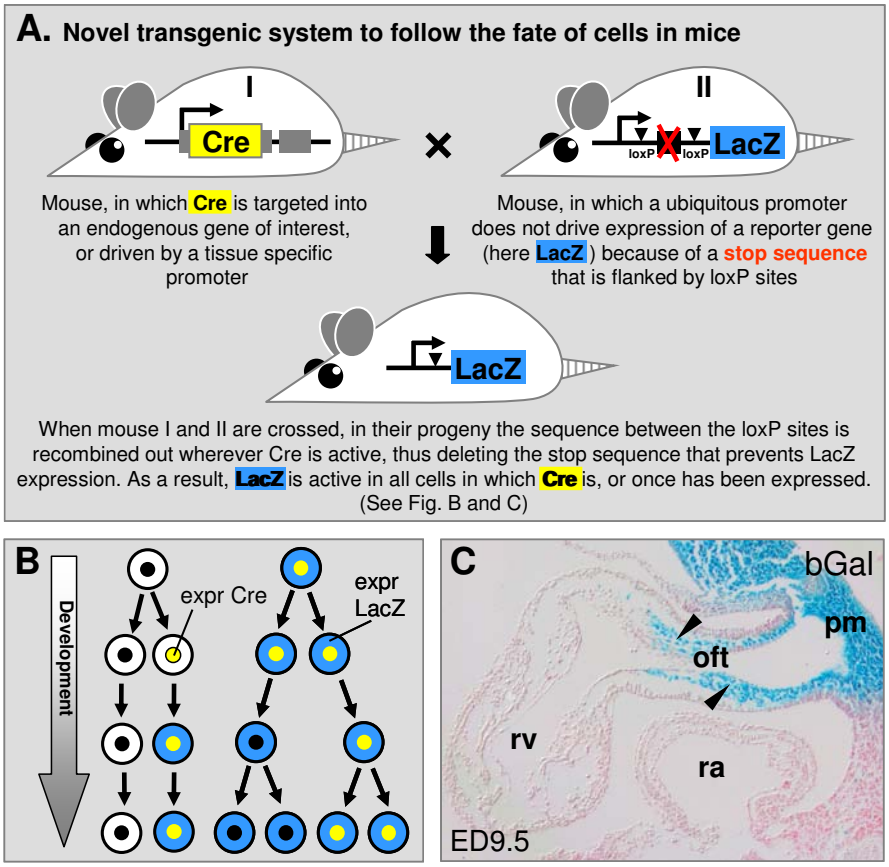

Figure 1. Transgenic Cre-loxP system to follow the fate of cells *in vivo*. (A) Irreversibly to label cells that do or once did express a gene of interest, two transgenic mouse lines are required. In one of the transgenes (mouse I) the coding sequence of Cre (Causes recombination enzyme) is cloned into the locus of the gene of interest. Another transgenic mouse (mouse II) holds a construct in which a ubiquitous promoter (that is, is active in all body cells) potentially drives expression of a reporter gene (here LacZ), however expression does not take place because of the insertion of a Stop sequence upstream of the reporter gene. This Stop sequence is flanked by loxP sites. When both mice are crossed, in all cells where Cre is expressed, the enzyme recombines the two loxP sites, thus removing the Stop sequence and facilitating expression of the reporter gene. (B) In all cells in which Cre (yellow) is expressed, LacZ (blue) is activated. Cells, and all their daughter cells, that ever expressed Cre, will appear blue, independently of whether Cre is inactivated afterwards. (C) Fate map of neural crest cells in ED9.5 mouse embryo (de Lange et al., 2004), by using a transgenic mouse line which holds a construct in which Cre is driven by the promoter of Wnt1. Wnt1 is expressed in neural crest cells and is inactivated before entering the heart. oft, outflow tract; ra, right atrium; rv, right ventricle; pm, pharyngeal mesoderm; arrow heads point at outflow tract cushions. pm, pharyngeal mesenchyme; oft, outflow tract; ra, right atrium; rv, right ventricle.

environment (extensively reviewed in Mone et al., 2004) and genetic factors play important causative roles.

With the huge expansion of knowledge and techniques in molecular biology accrued over the last decades of the 20th century, many genetic tools became available which provided important new knowledge. These advances in technology made it possible to generate transgenic mice, revealing the genetic networks underlying both normal and abnormal cardiac development. Using these techniques, it became possible to label irreversibly cells that once expressed a specific gene in the mouse embryo, thus permitting construction of "fate maps" to show the lineage of the marked cells and their progeny (for the interested reader, details of this novel technique are summarized in Figure 1). For the first time, therefore, it became possible to study the origin of the cells of the different components of the mature mammalian four-chambered heart, crucial information when we seek the cause of cardiovascular malformations. The information provided by these studies of cellular lineage often proved discordant with accepted views of cardiac development. Furthermore, the investigations validated in the mouse heart hypotheses made previously on the basis of labelling studies in chick embryos. Thus, it is now accepted that the initial linear heart tube does not contain all precursor cells of the mature heart, but rather gives rise only to part of the mature left ventricle (reviewed in Buckingham et al., 2005). The cells forming the remainder of the mature heart are added subsequently, by additional temporal migrations from the heart-forming areas. Additionally, the studies of lineage showed that the borders between the initial building blocks were not fixed. Rather, the cells initially present in the primitive heart tube differentiate continuously into the more mature myocardium of the cardiac chambers. This means that a structure seen at one particular stage of development will not necessarily retain its cellular composition at subsequent developmental stages. As a result, a malformation found in a specific part of the mature heart might well result from perturbed development of a different early component, or could even be due to abnormal development of components formed outside the embryonic heart.

Many decisions are needed before embryonic cardiac cells develop appropriately from their primitive to their mature phenotype. Many of these decisions are taken, or enforced, by transcription factors. These factors are proteins that are able to bind to specific sequences of DNA (Figure 2). When they bind, together with other transcription factors and co-factors, they turn on, or turn off, the transcription of downstream target genes. These genes, in turn, induce the changes in cellular differentiation. When transcription factors fail to act correctly, cellular differentiation, and hence morphogenesis, are at risk. We now know that many congenital cardiac malformations are caused by mutations that change the protein level or the function of a transcription factor. Since most transcription factors have a role in different processes, act in different parts in the embryo, and at different times of development, such mutations often lead to defects in multiple tissues. In other words, the mutations are pleiotropic.

Taking advantage of this new evidence, we begin this review with a discussion of recent knowledge relative to patterning of the early straight embryonic heart tube. We then

discuss the formation of the chambers by ballooning from this embryonic tube, and the significance of the addition of cells after initial formation of the linear heart tube. We conclude by discussing how these new insights improved our understanding of congenital cardiac malformations, in particular those involving the venous and arterial poles.

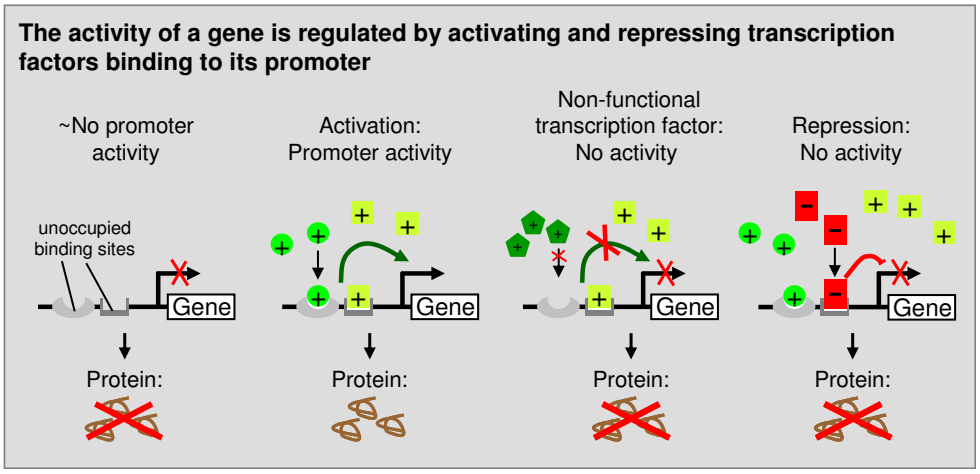

Figure 2. Schematic presentation of the regulation of the activity of genes by transcription factors. The promoter of a gene is defined as all non-coding DNA sequences which are important for the regulation of its activity, that is, which regulate its transcription into RNA. Transcription factors are DNA-binding proteins that regulate the activity of a gene by binding to specific binding sites in its promoter. The activity of a gene depends on a balance between activating and repressing transcription factors. Transcription factors never act alone, but always with other factors in transcription complexes. Black arrows depict DNA polymerase activity transcribing a gene; green shapes activating transcription factors, red shapes repressing transcription factors.

Patterning of the heart tube

Myocardial cells of the primary heart tube share important physiological characteristics

The heart is the first functional organ that is formed during development. Within 3 weeks of conception in humans, at a stage compatible with the mouse heart on embryonic day 8.5, it is already possible to see the beating heart. The heart needs to be functional from the onset of its formation because the subsequent development of the embryo depends on the circulatory system for the distribution and exchange of nutrients, oxygen, and waste products. At this early stage, the heart is a tube-like structure (Figure 3), which wall consists of an inner endocardial layer, a middle layer of extracellular matrix called the cardiac jelly, and an outer myocardial layer. The myocardium contracts in a peristaltoid fashion (Patten and Kramer, 1933), pumping the blood from the venous to the arterial pole . Already in the 1940s it was recognized that it is the cell-free cardiac jelly which plays an essential role in the pumping function of the tubular embryonic heart (Barry, 1948). All three layers have a mesodermal origin.

All myocytes, being embryonic or adult, share a number of important physiological characteristics (Figure 4 - reviewed in Moorman and Christoffels, 2003). In contrast to adult working myocardial myocytes, the cardiomyocytes of the embryonic heart tube have few contractile elements and a poorly developed sarcoplasmatic reticulum, they display high automaticity and have a low density of gap-junctions; consequently they are poorly coupled,

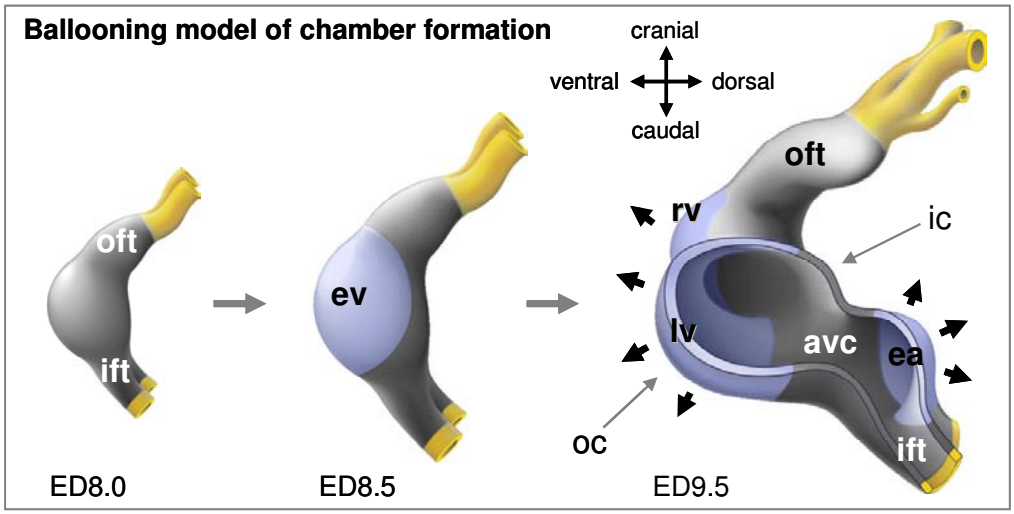

Figure 3. Ballooning model of chamber formation. At embryonic day ED8.0 in mouse, the heart tube consists of primary myocardium sharing important physiological characteristics (see Figure 4). At ED8.5 working myocardium of the ventricular, and only slightly later the atrial chambers, differentiates and balloons out only at the outer curvature of the looping heart. The inflow tract, atrioventricular canal and outflow tract maintain their embryonic phenotype and throughout development are connected at the inner curvature, which also maintains its primary phenotype. The boundary between grey and yellow reflects the pericardial deflection. a, atrium; ea, embryonic atrium; rv, right ventricle; lv, left ventricle; oft, outflow tract; avc, atrioventricular canal; ift, inflow tract; ev, embryonic ventricle.

Table: Phenotype of myocardial cells

phenotype	"primary" myocardium	"nodal" myocardium SAN/AVN	"chamber" myocardium
automaticity	**high** Hcn4	**high** Hcn4	low
conduction velocity	low	low	**high** Cx40/43
contractility	low	low	**high**
SR activity	low	low	**high**
proliferation	low	low	**high**

Figure 4. Table with the characteristic properties of the embryonic primary myocardium, the myocardium of the mature nodes, and chamber myocardium. The primary myocardium shares important characteristics with the mature sinus node (SAN) and atrioventricular node (AVN). Both display high automaticity because of high expression levels of the pacemaker channel gene HCN4. Chamber myocardium has a high conduction velocity due to the expression of high levels of fast c`onducting gap junctions Connexin40 and Connexin43. SR, sarcoplasmic reticulum.

resulting in a slow conduction of the activation wave throughout the heart. Therefore, we describe the myocardium of the embryonic tube as being primitive, or primary (Figure 4). Significantly, a number of transcription factors are expressed along the different axes of the tube, permitting recognition of the patterning of the tube along its cranio-caudal, dorso-ventral, and left-right axes (Figure 5). The patterning permits phenotypic differentiation of the different regions of the tube, ensuring its proper function.

Cranio-caudal patterning

Patterning along the cranio-caudal axis of the tube (Figure 5) can be recognized from the distribution of retinoic acid. This patterning is essential for the correct placement of the ventricles and the atrial chambers formed later in development (Yutzey et al., 1994). The importance of retinoic acid was shown by experiments in chicken. An excess of retinoic acid resulted in expansion of developing atrial structures, normally located caudally, while

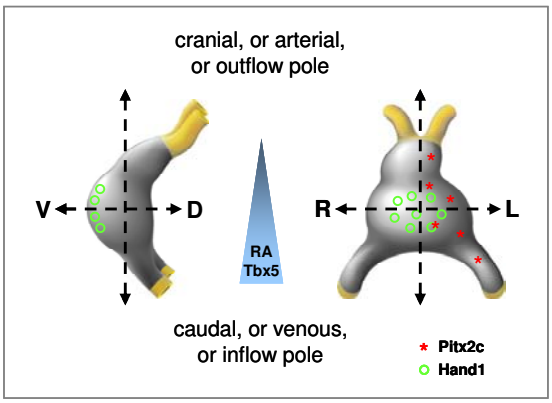

Figure 5. The heart tube is patterned along its cranio-caudal, dorso-ventral and left-right axes by transcription factors that are differentially expressed along these bodily axes. v, ventral; d, dorsal; r, right; l, left; RA, retinoic acid.

deficiency led to expansion of the ventricular compartment, which in the normal situation is positioned cranially (Yutzey et al., 1994; Hochgreb et al., 2003). Equally importantly, there is electric polarity along the cranio-caudal axis, with the cells showing the highest automaticity always found at the inflow to the developing heart. This feature insures that the dominant pacemaker is at the venous pole long before there is formation of a histological discrete conduction system. The overall effect is to produce slow peristaltoid contraction, which serves to propel the blood from the inflow to the outflow tract of the heart.

Equally important in determining cardiac design are the different members of the T-box family of transcription factors (Yutzey et al., 1994; Stennard and Harvey, 2005). One of the members of the family, *Tbx5*, acts downstream of retinoic acid and shows a similar caudo-cranial patterning, with the highest expression found caudally (Bruneau et al., 1999). Targeted

knockout of the factor in genetically modified mice reveals its function (for the interested reader, various transgenic possibilities in knock out mice are detailed in our Figure 6). The homozygous mutants show severe malformations, with particularly hypoplasia of the caudal structures of the heart (Bruneau et al., 2001). In humans, the majority of reported TBX5 mutations leads to loss-of-function, and consequently haploinsuffiency of the gene, producing Holt-Oram syndrome, a rare autosomal dominant disorder that is characterized by malformations of the limbs and the heart (Basson et al., 1997). More recently, patients have been observed with a mutation leading to gain-of-function. These subjects show a mild, atypical, phenotype of the Holt-Oram syndrome, but with associated paroxysmal atrial

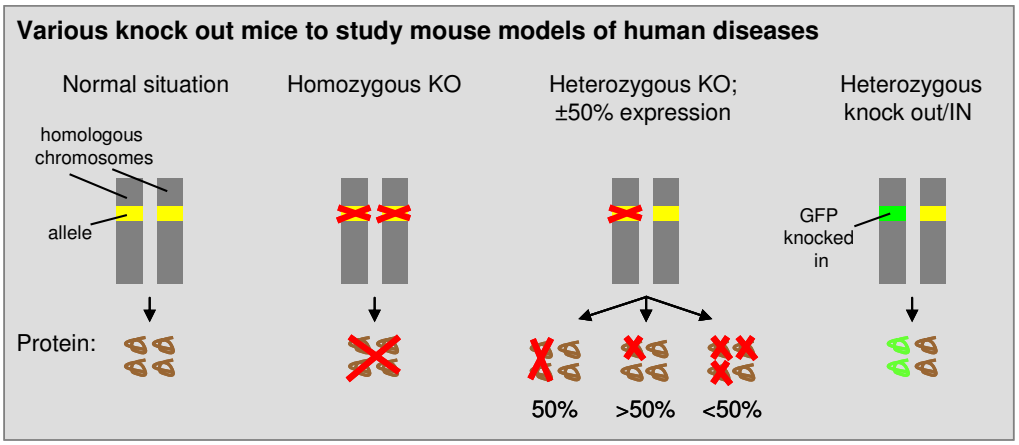

Figure 6. Schematic presentation of transgenic mouse models. In the normal situation one gene consists of two active alleles (one from both parents). In a homozygous knockout mouse both alleles have been disrupted and no protein is generated. In a heterozygous knockout mouse one of the alleles has been inactivated. Most often, this causes haploinsufficiency of the gene, i.e. the protein levels of the gene are half of the level in the normal situation. However, in the heterozygous knock out situation, the intact allele might become expressed more actively, resulting in higher than 50% of normal protein levels. Furthermore, if because of polymorphisms the allele that has been knocked out was the most active allele, this might lead to less than 50% of protein levels. Since many genetic disorders in human are caused by mutations resulting in dysfunction of only one of the alleles, heterozygous knockout mice mimic the genetic background of human diseases most closely. In a knock IN mouse, DNA encoding a transgenic gene is cloned into one of the alleles of the targeted gene. Therefore, the transgenic gene (for instance the reporter gene green fluorescent protein (GFP)) is expressed in the same spatiotemporal pattern as the endogenous gene. For clarity, in the model only two homologous chromosomes (represented by grey bars) with one gene (alleles represented by yellow boxes) are shown.

fibrillation (Postma et al., 2008). The cardiac malformations most commonly include defects of atrial and ventricular septation, but many other cardiac malformations have been reported.Among these, abnormalities of the morphologically left ventricle predominate, varying from aberrant trabecular patterning and mitral valvar prolapse to hypoplastic left heart syndrome (Basson et al., 1999). This is in keeping with the caudo-cranial patterning noted in the knockout mice, since as we will discuss, the apical part of the left ventricle balloons from the caudal part of the primary heart tube when considered relative to the right ventricle.

Furthermore, the diversity of the malformations caused by mutation in this single gene is a clear example of a pleiotropic effect.

Left/right patterning

The left/right axis of the developing embryo (Figure 5) is established well before formation of the heart tube. Left-right patterning specifies the laterality of most organs within the body, including eventually the heart. Abnormalities in patterning along this axis produce various malformations, including mirror-imagery and the right and left isomeric variants, the latter 2 usually grouped together in the clinical situation as visceral heterotaxy (Capdevila et al., 2000). When there is mirror-imagery, all organs of the body are formed in reverse, in other words with those organs usually formed on the right side retaining their normal anatomy, but being positioned on the left side of the body. In the setting of isomerism, in contrast, the organs on both sides of the body develop with the same morphological characteristics, so that, for example, in right isomerism both lungs have 3 lobes, with each lung supplied by a short bronchus (Figure 7). In the heart, it is only the atrial appendages which can be truly isomeric, since they are the only parts of the atrial chambers dependent on left-right patterning. This is because, as we will explain, both appendages balloon from the same segment of the heart tube, and hence both respond to the same signals. In contrast, the apical parts of the ventricles, these being the components that confer morphological specificity, balloon in series from the original ventral side of the primary tube, with the apical part of the morphologically left ventricle ballooning caudally relative to the apical component of the morphologically right ventricle. Since the ventricles develop in comparable fashion from consecutive parts of the

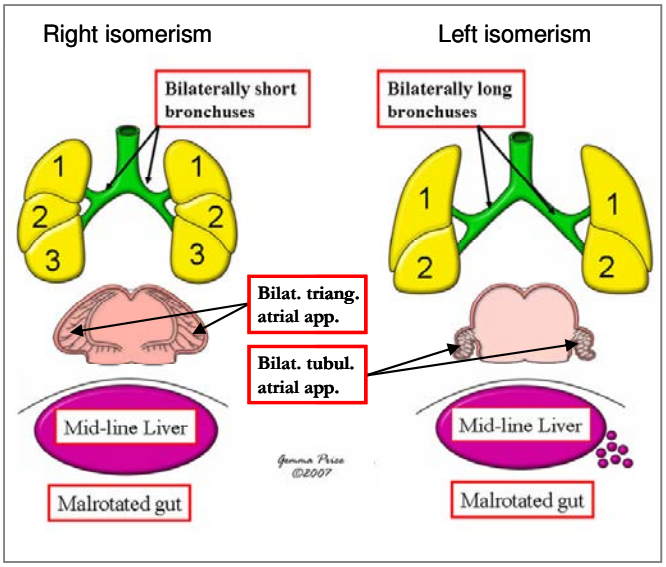

Figure 7. The arrangement of most lateralized organs: the lungs and bronchuses, the atrial appendages, liver, spleen, and gut, shown in right and left isomerism. bilat. triang. atrial app., bilaterally triangular atrial appendages; bilat. tubul. atrial app., bilaterally tubular atrial appendages. 1-3, lobes of the lungs.

tube, in molecular terms both have a right and a left side. Hence, both sides of each ventricle respond in comparable fashion to the genes determining laterality.

In molecular terms, evidence of left-right patterning can already be detected during gastrulation, when *nodal*, a member of the TGFβ family, is expressed only in the lateral plate mesoderm on the left side of the embryo. Its fundamental role in establishment of the bodily axis was shown in transgenic mice expressing *nodal* on the right side, instead of left-sided mesoderm. These mice developed with complete mirror-imagery, or so-called situs inversus (reviewed in Ramsdell, 2005). The essential regulator of cardiac left-right patterning is *Pitx2c* (Kitamura et al., 1999; Capdevila et al., 2000), a member of the homeobox gene transcription factor family that acts downstream of *nodal*. This gene is first detected prior to formation of the heart tube, when it is expressed exclusively in the left heart-forming field. When the heart tube is formed, it is found exclusively in the left part of the looping heart. Mice deficient for *Pitx2* have right isomerism of the atrial appendages, common atrioventricular junctions, anomalous pulmonary venous connections, and bilateral systemic venous tributaries (Liu et al., 2002). The mice also show isomerism of the sinus node (Mommersteeg et al., 2007), as do humans with right isomerism (Smith et al., 2006). In humans, mutations in the *PITX2* gene are also linked to the Rieger syndrome (reviewed in Amendt et al., 2000), an autosomal dominant disorder that is characterized by abnormalities of the eyes, teeth and umbilicus, but surprisingly not with deficient laterality. This can be explained by the effect of differential gene dosage, with one normal copy of the gene being sufficient to provide appropriate left-right patterning, but insufficient for adequate formation of the teeth and eyes (Liu et al., 2001). Other research with mice has shown that *Pitx2* is also expressed in the mesenchymal cells that are added to the heart after formation of the initial heart tube, where it again imposes laterality (Ai et al., 2006; Galli et al., 2008). This finding helps explain the abnormalities of the outflow tract and right ventricle seen in *Pitx2*-deficient mice, notably double outlet right ventricle or discordant ventriculo-arterial connections, since these structures are almost completely derived from cells added to the heart later in development.

Dorso-ventral patterning

When the heart starts to loop, it develops an outer and inner curvature (Figure 3). While cells are continuously added at both sides of the tube, first the ventricles develop at the cranio-ventral side, and only slightly later the atria form more caudally at both dorso-lateral sides. It is the apical parts of the ventricles, and the atrial appendages, which confer morphologic specificity on the ventricular and atrial chambers, respectively. Thus, formation of morphologically specific chambers is regulated not only by cranio-caudal, but also by dorso-ventral patterning (Figure 3 and 5). The principal signal inducing the dorso-ventral axis, however, remains unknown. Based on its pattern of expression, the helix-loop-helix transcription factor *Hand1* is a potential candidate (Christoffels et al., 2000). This gene is expressed at the ventral side of the heart tube, and subsequent to looping, along the outer curvature. It is from this side of the loop that the apical parts of the definitive ventricles

balloon, as demonstrated by the expression of genes that are specific for working-myocardium, such as atrial natriuretic factor (*anf*) and the gap junction protein Connexin40 *(Cx40)* (Christoffels et al., 2000; Moorman and Christoffels, 2003). When *Hand1* is knocked out in mice, the embryos die early in development because of defects of the placental trophoblast (Riley et al., 1998). If the gene is knocked out only in the embryo, and not in the developing placenta, the embryos live until mid-gestation. Cardiac looping does not occur, with the ventricles staying thin-walled, and failing to expand. The chamber-specific gene *anf,* however, continues to be expressed locally (Riley et al., 1998), indicating that *Hand1* is essential for development of the ventricles, but that it is not the primary signal inducing differentiation. Mutations of *HAND1* have yet to be detected in humans, most likely because heterozygous deficiency of the gene does not provoke a phenotype, just as has been shown in mice (Riley et al., 1998). An alternative explanation, of course, might be that such mutations are lethal because of extraembryonic defects.

Localized differentiation of working myocardium

Formation of the ventricular and atrial chambers

After its initial formation, the heart tube elongates by the continuous addition of cells at both poles of the heart. These cells are recruited from a highly proliferative pool of mesodermal cells located in the dorsal wall of the pericardial cavity and the pharyngeal arches (Kelly et al., 2001; Cai et al., 2003). Before they differentiate into myocytes, they cease to proliferate (Soufan et al., 2006). The myocytes forming the primary heart tube are in a low proliferative state (Figure 4). Then, only at very localized spots in the tube, the myocytes increase in size and re-initiate cell division (Soufan et al., 2006). Under the control of a chamber-specific genetic programme, these cells develop the properties of chamber myocardium, whilst the remainder of the tube maintains its embryonic, or primary, phenotype (Figure 3 and 4 - Moorman et al., 2000; Moorman and Christoffels, 2003). At the cranial part of the tube, at the original ventral side, primary myocardium begins to differentiate into the working myocardium of the embryonic left ventricle (Figure 3). More caudally, there is differentiation of primary myocardium into the chamber myocardium of the left and right atrial appendages on both dorso-lateral sides (Figure 3). Concomitant with chamber formation, typical apical trabeculated aspects of the chambers develop, much more pronounced in the ventricles than in the atria. The left and right ventricle develop a specific pattern of trabeculations, a feature used by the cardiac pathologist to identify their morphologic identity. The molecular background of this difference between both ventricles is unknown. As the myocytes become converted to a working phenotype, their velocity of conduction increases as they also develop gap-junctions containing Connexin40 and Connexin43 proteins. They also increase their contractile function by building up well-developed sarcomeric and sarcoplasmic reticular structures. These different morphogenetic processes - cell growth, proliferation and differentiation - cause the apical parts of the ventricles, and the atrial appendages, to expand locally. This process of differentiation of the myocardium of the primary heart tube along its outer curvature into the working myocardium of the chambers was initially illustrated by Davis following his studies of the human embryos held in the archive of the Carnegie Institution (Davis, 1927). In the 70ies the expansion from the outer curvature of the looping heart was also illustrated in the textbook of Goor and Lillehei (1975), and furthermore in the textbook of cardiac anatomy produced by Anderson and Becker (1978), albeit using an inappropriate segmental model for the initial heart tube. The concept was then brought to prominence as the ballooning model for formation of the cardiac chambers (Figure 3 - Moorman et al., 2000; Christoffels et al., 2000; Moorman and Christoffels, 2003).

The ballooning model has helped solve one of the major problems confronting generations of cardiac embryologists. This has been to explain how an initially solitary tube, with laminar flow through a single lumen, can transform into a 4-chambered heart in which the pulmonary and systemic circulations work in parallel (Kirby, 2001). The solution to this problem was difficult to understand when it was presumed that the primordiums for all

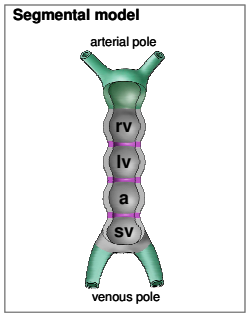

Figure 8. The segmental model of heart development, in which it was inaccurately assumed that already in the early heart tube all progenitors of the mature building blocks of the heart were present as a linear array of transverse precursor components. sv, sinus venosus. See legend to Figure 3 for other abbreviations.

cardiac chambers were already present in a linear array of transverse segments within the initial heart tube, as in the concept advanced by Anderson and Becker in their atlas of 1978. In this segmental model the atrioventricular canal and the outflow tract were separated by cells fated to become the left and right ventricle, respectively (Figure 8). The major difficulty to overcome was to understand how the mature atrioventricular canal could become connected to the right ventricle, and the mature left ventricle to the subaortic component of the outflow tract. Ingenious but complex solutions had been proposed previously, such as that put forward by Odgers (1938), but the accounts were remarkably difficult to understand. The essence of the ballooning model is the insight that the inflow tract, the atrioventricular canal, and the outflow tract maintain their primary myocardial phenotype, and are interconnected one to another at the inner curvature throughout development. Thus, from the outset the flows through the developing chambers are connected within the primary tube, the parietal wall of the right atrium already being in continuity via the right side of the atrioventricular canal with

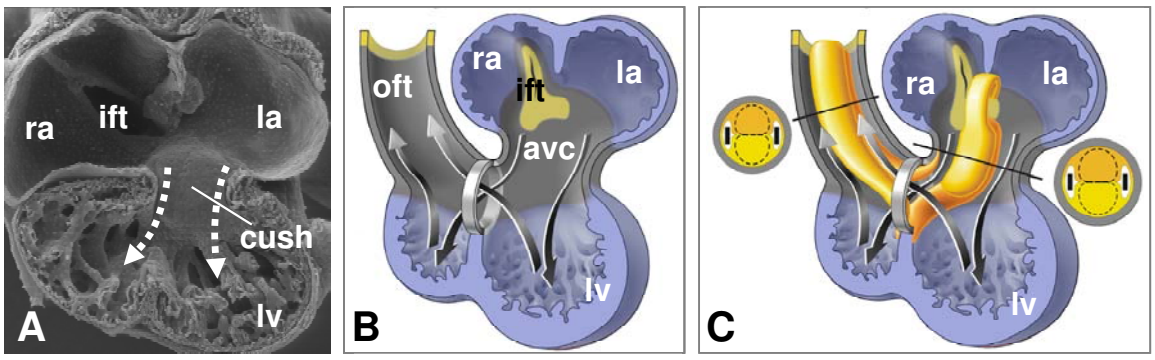

Figure 9. Already prior to and during septation, in the looping heart a left and right circulation act in parallel. Electron microscopic picture (A), model without cushions (B) and with atrioventricular and outflow tract cushions (C) of a frontal view of a ED10 septating mouse heart. In the models the outflow tract has been shifted sideward for clarity. The dotted arrows indicate the left (systemic) and right (pulmonal) circulation acting in parallel. In the models the cardiac cushions are indicated in yellow. cush, cardiac cushion. See legend to Figure 3 for other abbreviations.

the wall of the developing right ventricle, and the wall of the presumptive subaortic outlet already being in continuity, via the inner heart curvature, with the roof of the developing left ventricle. Long before overt cardiac septation, therefore, the systemic and pulmonary circulations are properly arranged in parallel (Figure 9 shows this parallel arrangement in the septating heart).

Chamber formation requires a network of activating and repressing transcription factors

We are just beginning to understand the molecular mechanisms underlying the strictly localized activation of the chamber-specific genetic programme. By an interplay of transcription factors, including Nkx2-5, Gata4, and the T-box transcription factors Tbx5 and Tbx20, the chamber-specific programme is potentially activated throughout the entire heart tube (Figure 10), inducing differentiation of primary into working myocardium (Bruneau et al., 2001; Hiroi et al., 2001). Formation of chamber myocardium, nonetheless, is prevented in the inflow tract, atrioventricular canal, inner curvature and outflow tract by the transcription factors Tbx2 and Tbx3, which repress the chamber-specific genetic programme (Figure 10 and 11 - Habets et al., 2002). Tbx2 is expressed from early stages onwards when formation of the chambers commences, and decreases prior to birth. Tbx3, however, is expressed until adulthood, and delineates the developing central conduction system (Hoogaars et al., 2004).

This mechanism of localized complementary repression has important consequences on our thinking about congenital malformations that might occur during formation of the chambers. If repression is incomplete, chamber-specific genes will be expressed ectopically,

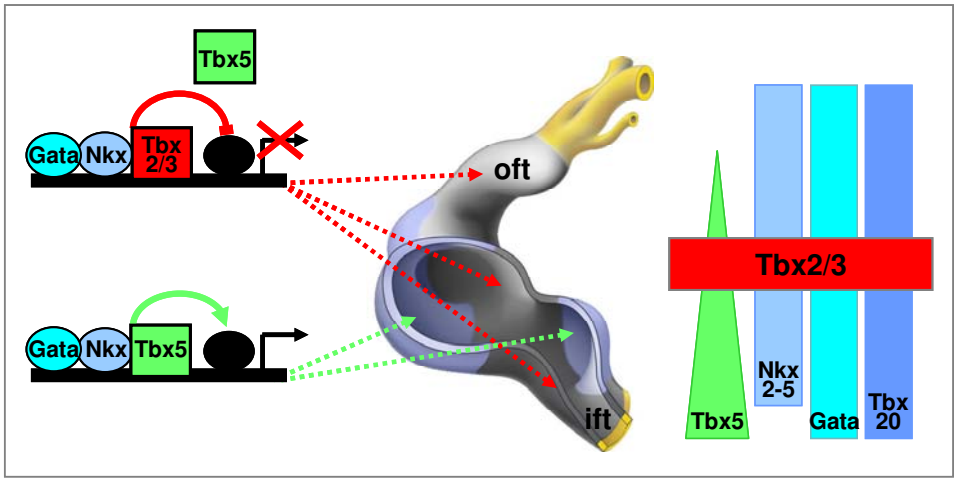

Figure 10. Model for the mechanism of transcriptional activation and repression of chamber genes. Broadly expressed transcription factors like GATA, Nkx2-5, Tbx5 and Tbx20 potentially activate chamber-specific genes throughout the looping heart. Tbx2 and Tbx3 are specifically expressed only in the forming inflow tract, atrioventricular canal, inner curvature and outflow tract. These transcriptional repressors compete with Tbx5 for DNA binding and for Nkx2-5 and as a result prevent the activation of the chamber-specific gene program in these regions. Black oval depicts DNA polymerase. See legend to Figure 3 for abbreviations.

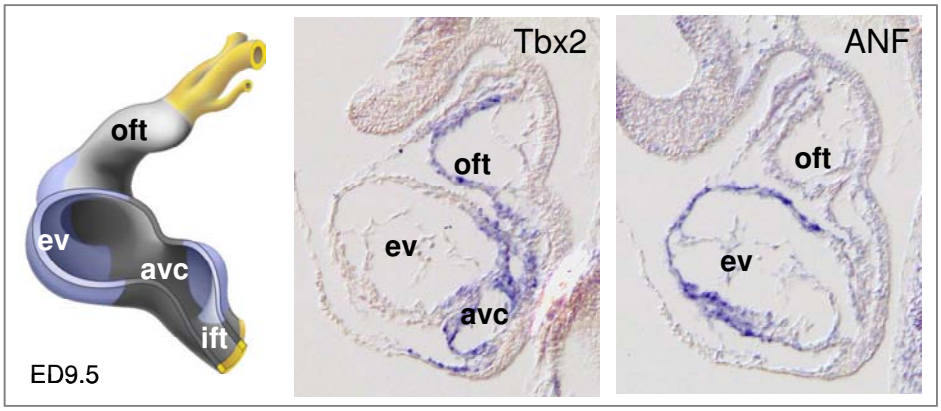

Figure 11. Chamber formation is potentially activated throughout the heart tube, but is kept strictly localized by complementary repression of the chamber-specific gene program. In situ hybridization of adjacent sections of an ED9.5 mouse heart shows chamber-specific expression of the working myocardium-specific marker gene atrial natriuretic factor (anf), and complementary expression of the transcriptional repressor Tbx2 in the primary myocardium of the atrioventricular canal and outflow tract.

resulting in a chamber-like phenotype in the developing inflow tract, atrioventricular canal,inner curvature and outflow tract. Because, as we will explain later, some of these structures give rise to the mature nodes of the conduction system, ectopic expression of chamber-specific genes in these tissues might also lead to arrhythmias. For instance, changes in the essential low electrical coupling between the sinus node and the adjacent atrial myocardium may cause dysfunction of the sinus node. When rapidly conducting gap junctions, such as those containing Connexin40 or Connexin43, become ectopically expressed in the sinus node, the negative resting membrane potential of the atria (-90 mV) will hyperpolarize the more depolarized membrane potential of the small sinus node (-60 mV). The electrical load from the atrial myocardium on the sinus node will slow the rate of diastolic depolarization, and hence spontaneous activity. Should the electrical load become sufficiently large, it may even lead to sinuatrial arrest. Likewise, increased conduction in the atrioventricular node will reduce the conduction time between the atrial and ventricular chambers. Consequently, all four chambers will contract almost simultaneously, which will impair the normal pump function of the heart. An additional disadvantage is that supraventricular tachycardias will be more easily conducted to the ventricles, thereby potentially causing life-threatening ventricular tachycardias. In addition, when the signaling pathways in the primary myocardium are disturbed, it is possible that this may induce formation of rapidly conducting atrioventricular muscular connections across the malformed atrioventricular junctions. Recent experiments from our laboratory, as yet unpublished, show that these accessory tracks can lead to pre-excitation of the ventricles, as seen in humans with Wolff-Parkinson-White syndrome.

In Tbx2-deficient mice, chamber-specific genes are expressed throughout the developing atrioventricular canal (Harrelson et al., 2004). Although an atrioventricular constriction was visible in these mice, it was less than normal, with compromised formation of the endocardial cushions. When Tbx3 was knocked out, mice died before birth, but initially

an obvious macroscopic cardiac phenotype was not reported (Davenport et al., 2003). More recent investigations have shown that, in Tbx3 knock out mice, the gap junction genes Connexin40 and Connexin43 are ectopically expressed in the sinus node (Hoogaars et al., 2007), whereas the bundle branches fail fully to develop (Bakker et al., 2008). Moreover, these mice exhibit ventricular septal defects and double outlet right ventricle. Functional consequences of the genes expressed ectopically in the His bundle and bundle branches, which are normally exclusively expressed in the working myocardium, surprisingly could not be detected (Bakker et al., 2008). The functional consequences for the sinus node, in other words whether these mice suffer from bradycardias or sinuatrial arrests, have yet to be investigated. In humans, mutations of *TBX3* cause the ulnar-mammary syndrome (Bamshad et al., 1997). This syndrome is characterized by defects of the upper limbs on the ulnar side, malformations of the external genital organs, hypoplasia of the mammary glands, and malformations of the teeth (Bamshad et al., 1999). Only very rarely have malformations of the heart been reported, such as ventricular septal defect at birth, and pulmonary stenosis at a later age (Meneghini et al., 2006). Again unexpectedly, thus far no instance has been encountered of abnormal conduction. This relatively mild cardiac phenotype cannot be explained by the redundant expression of Tbx2, because Tbx2 is neither expressed in the sinus node, nor in the atrioventricular bundle. Apparently, half of the normal levels of the TBX3 protein in the embryo are sufficient for appropriate development of the heart, but not the limbs. To the best of our knowledge, mutations of *TBX2* have not yet been reported in man.

Further formation and septation of the atrial chambers

We have explained how ballooning of the appendages from the original caudo-dorsal part of the primary heart tube provides the basis for formation of the right and left atrial appendages. We have also explained that, at this stage, the remainder of the atrial component of the heart tube retains its primary myocardial phenotype (Figure 4). At this stage of development, the systemic venous tributaries drain to the caudal pole of the tube in symmetrical fashion (Figure 12A and B), and as yet there is no formation of either the lungs, or the pulmonary vein. The caudal part of the tube, nonetheless, remains attached to the pharyngeal mesoderm via the dorsal mesocardium. It is through the dorsal mesocardium that new material is added to the venous pole of the developing heart. This newly added mediastinal myocardium functionally is working myocardium because it expresses fast conducting channels composed of Connexin40. However, it is different from the working myocardium of the appendages because it does not express atrial natriuretic factor (Figure 12). In the mouse, the mediastinal myocardium is initially restricted to the area around the persisting dorsal mesocardium (Figure 12 - Soufan et al., 2004). With ongoing development, the area formed by mediastinal myocardium expands considerably, and comes to form the larger part of the body of the developing left atrium, the primary atrial septum, and a significant part of the developing right atrium up to the left venous valve. At the same time, there is a marked realignment of the systemic venous tributaries, such that the left sinus horn diminishes in size, with the left

cranial cardinal vein becoming incorporated, in the mouse, into the left atrioventricular groove, draining to the right atrium as well (Figure 12C and D). This then sets the scene for atrial septation, since the developing pulmonary vein opens to the left atrium through a solitary opening in the dorsal mesocardium, between the so-called pulmonary ridges, adjacent

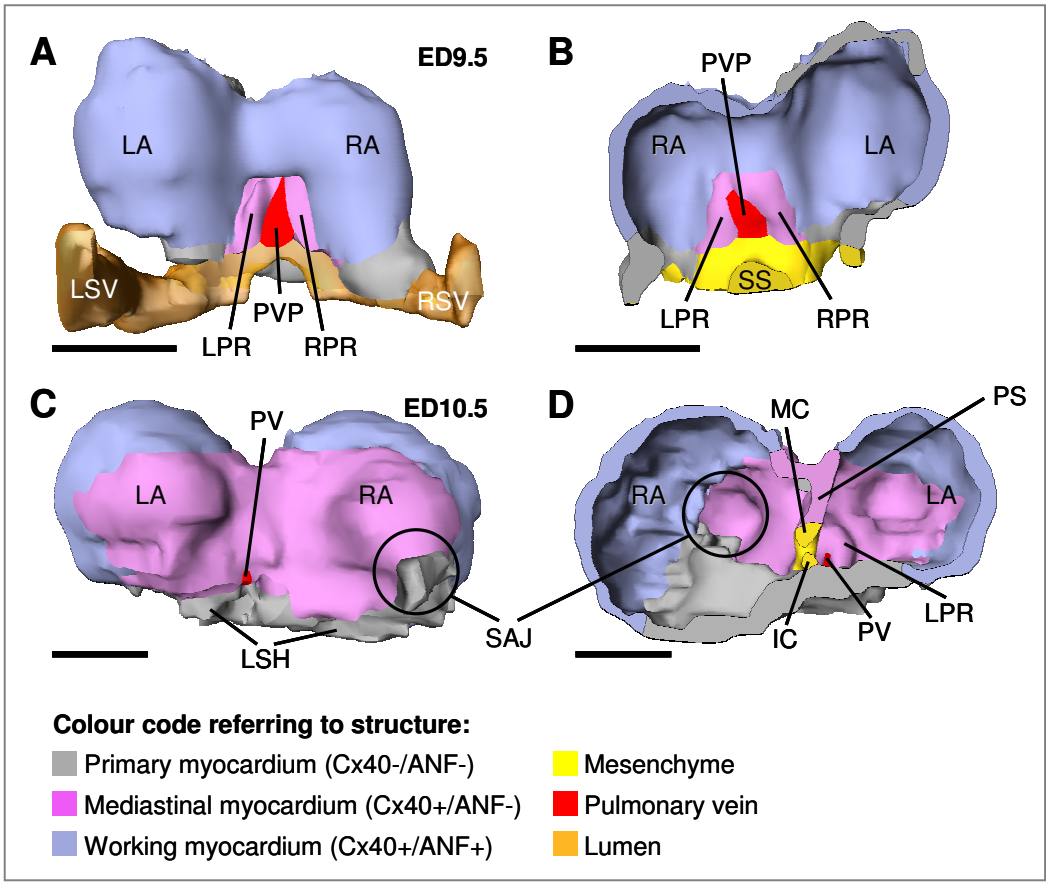

Figure 12. With ongoing development, the area of the atrial dorsal wall that is formed by mediastinal myocardium increases considerably, whereas at the same time the systemic tributaries realign, such that both the right and the left systemic vein drain into the right atrium. Reconstructions of mouse atrial development. Dorsal views (A and C) and ventral views of the dorsal halves (B and D) are shown for ED9.5 (A and B) and ED10.5 (C and D). In the reconstructions, only the myocardium and the intra-cardiac mesenchyme are shown. One should keep in mind that at this stage the heart is surrounded by (extra-cardiac) mesenchyme. (A, B) At stage ED9.5, the ballooning appendages of the atria are mostly composed of working myocardium (blue). The primordium of the lung vein (red), composed of mesenchyme, is enclosed by the left and right pulmonary ridges, which consist of mediastinal myocardium (purple). Still, the left and right systemic veins (orange) drain symmetrically into the left and right atrium, respectively. (C) Via the mesocardium, there has been ongoing recruitment of mediastinal myocardium, which at ED10.5 forms most of the atrial dorsal wall. The lateral appendages still are composed of working myocardium, whereas only the floor of the atrium is still composed of primary myocardium (grey). The wall of the systemic veins have myocardialized, forming the sinus horns. The left sinus horn now is located in the atrioventricular groove and drains, together with the right sinus horn, into the right atrium. (D) The primary atrial septum, composed of newly formed mediastinal myocardium, grows towards the atrioventricular cushions to separate the atria. The pulmonary vein has luminized and drains into the left atrium. LPR, left pulmonal ridge; RPR, right pulmonal ridge; PVP, pulmonary vein primordium; LSV, left systemic vein; RSV, right systemic vein; SS, sinus septum; PV, pulmonary vein; SAJ, sinu-atrial junction; MC, mesenchymal cap; PS, primary septum; IC, inferior atrioventricular cushion; LSH, left sinus horn. See legend to Figure 3 for other abbreviations.

to the developing atrioventricular junction. The primary atrial septum then grows from the newly formed mediastinal myocardial component, approaching the endocardial cushions which themselves are dividing the atrioventricular canal. As the primary atrial septum grows towards the cushions, it carries on its leading edge a mesenchymal cap (Figure 12). It is then fusion of the mesenchymal cap with the fused atrial aspect of the endocardial cushions that closes the primary atrial foramen. Prior to closure of the primary atrial foramen, however, the upper margin of the primary septum breaks down so as to permit the richly oxygenated placental blood returning to the heart through the umbilical and eventually the caudal cardinal vein to continue to reach the left side of the developing heart.

The point of fusion of the mesenchymal cap and the endocardial cushions is then further reinforced by growth of non-endocardium derived mediastinal mesenchyme through the mesocardium into the heart, the so-called vestibular spine or dorsal mesenchymal protrusion (His, 1880; Webb et al., 1998; Mommersteeg et al., 2006; Snarr et al., 2007). We now know that, subsequently, this non-endocardially derived mesenchyme is muscularised to form the basal buttress of the atrial septum (Mommersteeg et al., 2006). The so-called "septum secundum", however, is no more than a fold in the atrial roof. Indeed, in the human heart this superior interatrial fold is not developed until after the solitary pulmonary vein has migrated to the roof of the left atrium, achieving separate opening for the four pulmonary veins in the process (Webb et al., 2001). The "septum secundum" is then simply the deep fold between the connections of the caval veins to the right atrium, and the pulmonary veins to the left atrium. This concept of atrial septal development also shows why sinus venosus and coronary sinus defects are interatrial communications, rather than atrial septal defects, since they are outside the confines of the atrial septum, this being limited to the floor of the oval fossa and the basal buttress formed by muscularisation of the vestibular spine (Anderson et al., 2004).

Primary myocardium signals to adjacent endocardium to form cardiac cushions and later in development gives rise to the mature nodes of the conduction system

Subsequent to ballooning of the atrial appendages and the apical parts of the ventricles, it becomes possible to recognize the atrioventricular canal as the component of the primary tube between the developing atrial and ventricular components. Because of the differences in growth, the inflow tract, atrioventricular canal, and the outflow tract are the persisting components of the primary tube roofed by the primary myocardium of the inner curvature. Responding to signals from this myocardium, the endocardial cells within the canal undergo a process of epithelial-to-mesenchymal transformation, and form the atrioventricular endocardial cushions (Figure 9 - Eisenberg and Markwald, 1995). Later in development, these cushions give rise to some of the leaflets of the mitral and tricuspid valves (de Lange et al., 2004). Furthermore, during development cushion tissue fuses at the atrioventricular border with epicardial tissue of the atrioventricular groove, insulating the atria from the ventricles

electrically (Wessels et al., 1996). In the adult heart the fibrous body only consists of cells from the atrioventricular cushions (de Lange et al., 2004) and forms an integral part of the atrioventricular septum (Kanani et al., 2005). Additional cushions are formed within the outflow tract, which act initially as septal structures (Kanani et al., 2005), but eventually cavitate along their distal margins to form the leaflets of the arterial valves and their supporting sinuses (de Lange et al., 2004). The proximal parts of the cushions, subsequent to their fusion, muscularise to form the subpulmonary infundibulum, which eventually is converted into a free-standing muscular sleeve. The outflow cushions, therefore, play a crucial role in separating the systemic and pulmonary circulations, albeit that no septal structures remain in the definitive heart subsequent to closure of the embryonic interventricular foramen (Anderson et al., 2003).

Concomitant with formation of the chamber myocardium, it is possible to detect a mature electrocardiogram (Figure 13). As we have already discussed, the impulse is generated by the pacemaker cells at the venous pole, which then induces a rapid depolarization of the atrial myocardium. Subsequently, there is a delay in propagation of the impulse through the slowly conducting primary myocardium of the atrioventricular canal, followed by rapid propagation through the ventricles. Later in development, parts of the primary myocardium of the inflow tract and atrioventricular canal become the sinus and the atrioventricular nodes of the definitive conduction system, respectively (Figure 13 - Moorman and Christoffels, 2003). These mature nodes share essential phenotypic characteristics with their embryonic primordiums (Figure 4). The remaining parts of the inflow corridor, the atrioventricular canal, and the outflow tract do not contribute to the histologically discrete conduction system, but instead differentiate into the working myocardium of their appropriate chambers (Rana et al., 2007), albeit that their primary origin can offer explanation for several known cardiac arrhythmias (Moorman et al., 2005).

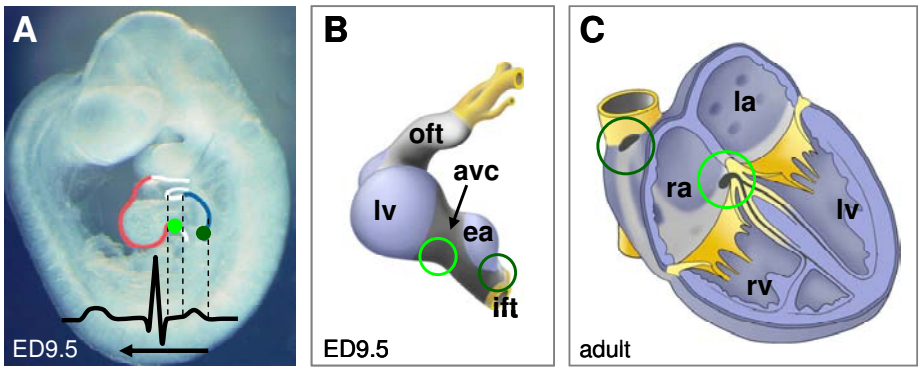

Figure 13. The embryonic myocardium of the inflow tract and atrioventricular canal give rise to the mature sinus node and atrioventricular node, respectively. (A) ED9.5 mouse embryo, with an ECG recording drawn in it. As soon as the chambers form, an "adult-like" ECG can be detected (See text for details). Blue line marks the contour of the atria, red line the ventricles. Arrow gives direction of the action potential. (A,B,C) The inflow tract (dark green dot or circle in A,B) gives rise to the mature sinus node (dark green circle in C), whereas the atrioventricular canal (light green dot or circle in A,B) gives rise to the mature atrioventricular node (light green circle in C). See legend to Figure 3 for abbreviations.

Subsequent to formation of the linear heart tube, cells are continuously added to the heart

Already from 1969 onwards, various labelling studies in chicken suggested that cells were added to both poles of the growing heart from the surrounding mesoderm (Figure 14 - Stalsberg and de Haan, 1969; Virágh and Challice, 1973; De la Cruz et al., 1989; De la Cruz and Sanchez-Gomez, 1998b). Since at that time cardiac development tended to be explained on the basis of the segmental model (Figure 8), in which the primordiums of all future components were postulated to be present in the initial heart tube (Rosenquist, 1970; Garcia-Martinez and Schoenwolf, 1993), these important findings were largely ignored. In 2001, however, studies in chicken (Waldo et al., 2001; Mjaatvedt et al., 2001), and use of transgenic fate mapping techniques in mouse (Kelly et al., 2001), showed conclusively that the cells forming most of the mature right ventricle and outflow tract were added to the heart subsequent to the initial stage of looping. It was then shown by use of other genetically modified mice that cells were also added at the venous pole (Cai et al., 2003; Christoffels et al., 2006). It is now generally accepted that the progenitors within the initial linear tube give rise only to most of the apical part of the mature left ventricle (reviewed in De la Cruz and Markwald, 1998a; Zaffran et al., 2004). In the earliest stage, cells can be added via the mesocardium, which connects the linear tube with the dorsal pericardial wall over its full length. During looping, the mesocardium breaks to form the transverse sinus of the

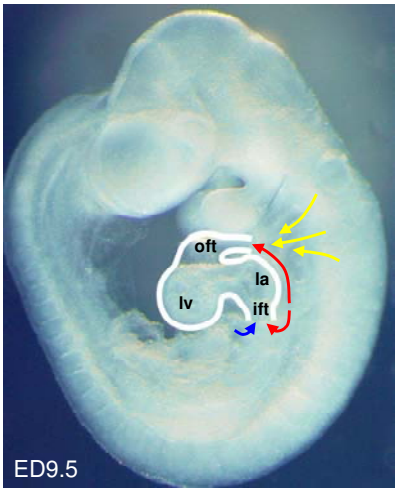

Figure 14. Subsequent to formation of the initial heart tube, extracardiac cells are added to the heart continuously. Left lateral side of ED9.5 mouse embryo with contours of the heart drawn in it. Red arrows depict mesodermal cells from the second heart field which are added to the venous and arterial poles by recruitment. Yellow arrows depict cardiac neural crest cells which are added by migration after formation of the initial heart tube. Blue arrow depicts precursor cells of the sinus venosus. See legend to Figure 3 for abbreviations.

pericardium. Subsequent to this breakdown, the tube is connected to the body wall only at the venous and arterial poles. This enables the heart to beat freely within the pericardial cavity. After the breakdown of the mesocardium, nonetheless, cells can then only be added at the venous or arterial poles of the growing heart. We now know that it is through these poles that further additions are made to the developing heart.

The Second Heart Field

Progenitor cells derived from splanchnic mesoderm bordering the initial heart tube continuously differentiate to myocardium, in a process nowadays often referred to as recruitment (red arrows in Figure 14). This causes the heart tube to elongate at both sides. After the initial differentiation into embryonic myocardium, cells will undergo additional differentiation, thus contributing to different building blocks of the heart. During recruitment, the cells do not move individually or as clusters, but are taken up as sheets, without changing position relative to their neighbours (Stalsberg and de Haan, 1969). The cells are recruited to the initial linear tube from a region in the dorsal wall of the pericardial cavity that has now become known as the second heart field (reviewed in Buckingham et al., 2005). In mouse, the cells from this field are characterized by their expression of the LIM homeodomain transcription factor *Islet1* (Cai et al., 2003). The so-called second heart field is used in this fashion to distinguish the cells of the initial linear tube, which are considered to be derived from a primary heart field. We are comfortable with this nomenclature, although along with others (Abu-Issa et al., 2004), we question the discreteness of the alleged fields (Moorman et al., 2007). This scepticism is, perhaps, reinforced by the recent finding that, in early stages of development, the Islet1 protein can also be detected in the progenitors of the primary heart field among species (Yuan and Schoenwolf, 2000; Prall et al., 2007; Brade et al., 2007). These findings render Islet1 a pan-cardiac marker, and now leave the purported second field without any specific marker, supporting the notion of the existence of a single heart field, from which precursor cells are gradually added to the heart in a temporal sequence. It has been shown, nonetheless, that cells from the cranial part of the purported second field express the fibroblast growth factor gene Fgf10, and it is this population which gives rise to the outflow tract and the right ventricle (Waldo et al., 2001; Mjaatvedt et al., 2001; Kelly et al., 2001). In contrast, most of the atrial myocardium is derived from the more caudal part of the field (Figure 12 and 14 - Cai et al., 2003; Galli et al., 2008). It remains a fact that only the left ventricle is derived from progenitors of the first heart field, which give rise to the initial linear heart tube early in development.

The identification of the second heart field, and its derivatives, has obvious implications for our thinking about congenital cardiac defects. First, it shows that the left and right ventricles have a distinctive transcriptional history. A biopsy of the left ventricle, therefore, does not necessarily tell us anything about the right ventricle! It may also explain why cardiac defects are localized to one side of the heart, albeit that disordered flow subsequent to the completion of septation provides an equally convincing explanation of

lesions such as hypoplastic left heart syndrome or pulmonary atresia with intact ventricular septum. The migration of temporally distinct populations of cells from the heart-forming areas, nonetheless, does show that the primary cause of malformations of the outflow region and right ventricle, varying from functionally univentricular hearts with dominant left ventricles to subtle defects of the outflow tracts, might be located outside the linear heart tube, and be located in the so-called second heart field. DiGeorge syndrome, for example, is a dominant disorder that is linked to a micro-deletion on human chromosome 22q11. It is characterized by a spectrum of abnormalities involving the outflow tracts, such as common arterial trunk or tetralogy of Fallot, and extra-cardiac defects like craniofacial dysmorphologies and hypoplasia of the thymus and parathyroid glands. This spectrum of abnormalities can be attributed to abnormal development of the pharyngeal arches and second heart field (Scambler, 2000). Because the T-box factor *Tbx1* was shown to be both located within this chromosomal deletion, and expressed in the developing pharyngeal arches and second heart field, it was identified as a candidate gene. Indeed, in 2001 it was shown that mice deficient for *Tbx1* phenocopy important aspects of the DiGeorge syndrome, including the malformations involving the outflow tracts (Jerome and Papaioannou, 2001). Also, since the atrial chambers, and the right ventricle, are largely derived from the second heart field, it has been suggested that mutations of genes that are important for correct regulation of the second heart field may lead to congenital malformations at both poles. Indeed, mice lacking the transcription factor *Islet1* display severe malformations of the outflow tract and right ventricle, but also of the atrial chambers (Cai et al., 2003). In humans, however, defects that involve both the inflow and outflow regions of the heart are very rare. This rarity strongly suggests that a defect within the highly proliferative progenitors of the second heart field, sufficiently powerful to disturb both poles of the heart, is lethal.

Cells from the neural crest migrate into the arterial pole to aid in separation of the pulmonary and aortic pathways

Whereas the mesodermal cells are added to the heart by recruitment, cardiac neural crest cells are added to the arterial pole by migration (yellow arrows in Figure 14). After the neural tube and neural crest have been formed from the ectoderm during neurulation, the cells of the neural crest differentiate into ectomesenchyme, breaking up into individual cells that subsequently migrate through the body to give rise to diverse tissues such as neural ganglions, melanocytes, and the adrenal glands. The ectomesenchymal cells of the cardiac neural crest migrate into the outflow tract, populating the outflow cushions formed by endothelial-to-mesenchymal transformation. The cushions, packed by the cells from the neural crest, initially form a septal structure throughout the lumen of the initially solitary outflow tract. They subsequently contribute to the formation of the arterial valvar leaflets and their supporting sinuses, and the most proximal parts muscularise to form the free-standing subpulmonary infundibulum (Anderson et al., 2003). The cells initially separating these structures, however, subsequently disappear, so that eventually there are no septal components between the arterial

valves, or between the subpulmonary infundibulum and the aortic root (Webb et al., 2003). The cardiac neural crest cells also give rise to the connective tissue of the thymus, thyroid gland and parathyroids. Ablation of the cardiac neural crest cells in the chick has been shown to cause malformations such as common arterial trunk, and non-cardiovascular defects like malformations of these glands in the neck (reviewed in Hutson and Kirby, 2003). Indeed, deficiency of the cardiac neural crest mimics the features from DiGeorge syndrome, which has been linked to the *Tbx1* gene. It is nowadays established that, although not the principal perpetrator of the syndrome, disruption of migration of cells from the cardiac neural crest, either directly or indirectly by impairment of the *Tbx1* dose, is an important mediator of the typical phenotype.

Conclusions

The ability genetically to modify mice has rapidly increased our insights into the mechanisms underlying cardiogenesis. These techniques have improved our understanding of several developmental mechanisms essential for shaping the normal developing heart. Awareness of these mechanisms, and of the transcriptional networks which regulate them, provides vital new clues for understanding congenital cardiac malformations. Based on these insights, it has been possible to detect novel candidate genes. Genetic and molecular research exploring these genes has shown them to produce congenitally malformed hearts. This new knowledge, however, should also serve to makes us humble, since the transcriptional networks and cellular interactions regulating cardiac development are shown to be remarkably complex. We have only just started to unravel them.

Acknowledgments

We thank Dr. A.T. Soufan for the preparation of Figure 12. T.H., V.M.C. and A.F.M.M. are supported by the Netherlands Heart Foundation (Grant no.: 1996T203).

References

Abu-Issa R, Waldo K, and Kirby ML. 2004. Heart fields: one, two or more? Dev Biol 272:281-285.

Ai D, Liu W, Ma L, Dong F, Lu MF, Wang D, Verzi MP., Cai C, Gage PJ, Evans S, Black BL, Brown NA, and Martin JF. 2006. Pitx2 regulates cardiac left-right asymmetry by patterning second cardiac lineage-derived myocardium. Dev. Biol. 296:437-449.

Amendt BA, Semina EV, and Alward WL. 2000. Rieger syndrome: a clinical, molecular, and biochemical analysis. Cell Mol. Life Sci. 57:1652-1666.

Anderson RH and Becker AE. 1980. Cardiac anatomy. An integrated text and colour atlas. London: Gower Medical Publ.

Anderson RH, Webb S, Brown NA, Lamers WH, and Moorman AFM. 2003. Development of the heart: 3 - formation of the ventricular outflow tracts, arterial valves, and intrapericardial arterial trunks. Heart 89:1110-1118.

Anderson RH, Webb S, Moorman AFM, and Brown NA. 2004. Morphological correlates of atrial development. John Keith Lecture. Cardiol Young 14:239-254.

Bakker ML, Boukens BJ, Mommersteeg MTM, Brons JF, Wakker V, Moorman AFM and Christoffels VM. 2008. Transcription factor Tbx3 is required for the specification of the atrioventricular conduction system. Circ Res. 102:1340-1349.

Bamshad M, Lin RC, Law DJ, Watkins WC, Krakowiak PA, Moore ME, Franceschini P, Lala R, Holmes LB, Gebuhr TC, Bruneau BG, Schinzel A, Seidman JG, Seidman CE, and Jorde LB. 1997. Mutations in human TBX3 alter limb, apocrine and genital development in ulnar-mammary syndrome. Nat. Genet. 16:311-315.

Bamshad M, Le T, Watkins WS, Dixon ME, Kramer BE, Roeder AD, Carey JC, Root S, Schinzel A, Van Maldergem L, Gardner RJ, Lin RC, Seidman CE, Seidman JG, Wallerstein R, Moran E, Sutphen R, Campbell CE, and Jorde LB. 1999. The spectrum of mutations in TBX3: Genotype/phenotype relationship in ulnar-mammary syndrome. Am. J. Hum. Genet. 64:1550-1562.

Barry A. 1948. The functional significance of the cardiac jelly in the tubular heart of the chick embryo. Anat. Rec. 102:289-298.

Basson CT, Bachinsky DR, Lin RC, Levi T, Elkins JA, Soults J, Grayzel D, Kroumpouzou E, Traill TAL-SJ, Renault B, Kucherlapati R, Seidman JG, and Seidman CE. 1997. Mutations in human TBX5 cause limb and cardiac malformation in Holt-Oram syndrome. Nat. Genet. 15:30-35.

Basson CT, Huang T, Lin RC, Bachinsky DR, Weremowicz S, Vaglio A, Bruzzone R, Quadrelli R, Lerone M, Romeo G, Silengo M, Pereira A, Krieger J, Mesquita SF, Kamisago M, Morton CC, Pierpont MEM, Müller CW, Seidman JG, and Seidman CE. 1999. Different *TBX5* interactions in heart and limb defined by Holt-Oram syndrome mutations. Proc. Natl. Acad. Sci. USA 96:2919-2924.

Brade T, Gessert S, Kuhl M, and Pandur P. 2007. The amphibian second heart field: Xenopus islet-1 is required for cardiovascular development. Dev. Biol. 311:297-310.

Bruneau BG, Logan M, Davis N, Levi T, Tabin CJ, Seidman JG, and Seidman CE. 1999. Chamber-specific cardiac expression of *Tbx5* and heart defects in Holt-Oram syndrome. Dev. Biol. 211:100-108.

Bruneau BG, Nemer G, Schmitt JP, Charron F, Robitaille L, Caron S, Conner DA, Gessler M, Nemer M, Seidman CE, and Seidman JG. 2001. A murine model of Holt-Oram syndrome defines roles of the T-box transcription factor Tbx5 in cardiogenesis and disease. Cell 106:709-721.

Buckingham M, Meilhac S, and Zaffran S. 2005. Building the mammalian heart from two sources of myocardial cells. Nat. Rev. Genet. 6:826-837.

Cai CL, Liang X, Shi Y, Chu PH, Pfaff SL, Chen J, and Evans S. 2003. Isl1 identifies a cardiac progenitor population that proliferates prior to differentiation and contributes a majority of cells to the heart. Dev. Cell 5:877-889.

Capdevila J, Vogan KJ, Tabin CJ, and Izpisua Belmonte JC. 2000. Mechanisms of left-right determination in vertebrates. Cell 101:9-21.

Christoffels VM, Habets PEMH, Franco D, Campione M, de Jong F, Lamers WH, Bao ZZ, Palmer S, Biben C, Harvey RP, and Moorman AFM. 2000. Chamber formation and morphogenesis in the developing mammalian heart. Dev Biol. 223:266-278.

Christoffels VM, Mommersteeg MTM, Trowe MO, Prall OWJ, de Gier-de Vries C, Soufan AT, Bussen M, Schuster-Gossler K, Harvey RP, Moorman AFM, and Kispert A. 2006. Formation of the venous pole of the heart from an *Nkx*2-5-negative precursor population requires Tbx18. Circ Res. 98:1555-1563.

Davenport TG, Jerome-Majewska LA, and Papaioannou VE. 2003. Mammary gland, limb and yolk sac defects in mice lacking Tbx3, the gene mutated in human ulnar mammary syndrome. Dev. 130:2263-2273.

Davis CL. 1927. Development of the human heart from its first appearance to the stage found in embryos of twenty paired somites. Contrib. Embryol. 19:245-284.

De la Cruz MV, Sánchez-Gómez C, and Palomino M. 1989. The primitive cardiac regions in the straight tube heart (stage 9) and their anatomical expression in the mature heart: an experimental study in the chick embryo. J. Anat. 165:121-131.

De la Cruz MV and Markwald RR. 1998a. Living Morphogenesis of the Heart. Boston: Birkhäuser.

De la Cruz MV and Sanchez-Gomez C. 1998b. Straight tube heart. Primitive cardiac cavities vs. primitive cardiac segments. In Living Morphogenesis of the Heart. Chp. 3, De la Cruz and Markwald. Boston: Birkhäuser, pp. 85-98.

de Lange FJ, Moorman AFM, Anderson RH, Manner J, Soufan AT, de Gier-de Vries C, Schneider MD, Webb S, van den Hoff MJB, and Christoffels VM. 2004. Lineage and morphogenetic analysis of the cardiac valves. Circ Res 95:645-654.

Eisenberg LM and Markwald RR. 1995. Molecular regulation of atrioventricular valvuloseptal morphogenesis. Circ. Res. 77:1-6.

Galli D, Dominguez JN, Zaffran S, Munk A, Brown NA, and Buckingham ME. 2008. Atrial myocardium derives from the posterior region of the second heart field, which acquires left-right identity as Pitx2c is expressed. Dev. 135:1157-1167.

Garcia-Martinez V and Schoenwolf GC. 1993. Primitive streak origin of the cardiovascular system in avian embryos. Dev. Biol. 159:706-719.

Goor DA and Lillehei CW. 1975. Congenital malformations of the heart. Embryology, anatomy and operative considerations. New York: Grune and Stratton.

Habets PEMH, Moorman AFM, Clout DEW, van Roon MA, Lingbeek M, Lohuizen M, Campione M, and Christoffels VM. 2002. Cooperative action of Tbx2 and Nkx2.5 inhibits ANF expression in the atrioventricular canal: implications for cardiac chamber formation. Genes Dev. 16:1234-1246.

Harrelson Z, Kelly RG, Goldin SN, Gibson-Brown JJ, Bollag RJ, Silver LM, and Papaioannou VE. 2004. Tbx2 is essential for patterning the atrioventricular canal and for morphogenesis of the outflow tract during heart development. Dev. 131:5041-5052.

Hiroi Y, Kudoh S, Monzen K, Ikeda Y, Yazaki Y, Nagai R, and Komuro I. 2001. Tbx5 associates with Nkx2-5 and synergistically promotes cardiomyocyte differentiation. Nat. Genet. 28:276-280.

His W. 1880. Die area interposita, die Eustachische klappe und die spina vestibuli. Anatomie Menschlicher Embryonen 1880:149-152.

Hochgreb T, Linhares VL, Menezes DC, Sampaio AC, Yan CY, Cardoso WV, Rosenthal N, and Xavier-Neto J. 2003. A caudorostral wave of RALDH2 conveys anteroposterior information to the cardiac field. Dev. 130:5363-5374.

Hoffman JIE. 1995. Incidence of congenital heart disease: II. Prenatal incidence. Pediatr. Cardiol. 16:155-165.

Hoogaars WMH, Tessari A, Moorman AFM, de Boer PAJ, Hagoort J, Soufan AT, Campione M, and Christoffels VM. 2004. The transcriptional repressor Tbx3 delineates the developing central conduction system of the heart. Cardiovasc Res 62:489-499.

Hoogaars WMH, Engel A, Brons JF, Verkerk AO, de Lange FJ, Wong LYE, Bakker ML, Clout DE, Wakker V, Barnett P, Ravesloot JH, Moorman AFM, Verheijck EE, and Christoffels VM. 2007. Tbx3 controls the sinoatrial node gene program and imposes pacemaker function on the atria. Genes Dev. 21:1098-1112.

Hutson MR and Kirby ML. 2003. Neural crest and cardiovascular development: a 20-year perspective. Birth Defects Res Part C. Embryo Today. 69:2-13.

Jerome LA and Papaioannou VE. 2001. DiGeorge syndrome phenotype in mice mutant for the T-box gene, Tbx1. Nat. Genet. 27:286-291.

Kanani M, Moorman AFM, Cook AC, Webb S, Brown NA, Lamers WH, and Anderson RH. 2005. Development of the atrioventricular valves: clinicomorphological correlations. Ann. Thorac. Surg. 79:1797-1804.

Kelly RG, Brown NA, and Buckingham ME. 2001. The arterial pole of the mouse heart forms from Fgf10-expressing cells in pharyngeal mesoderm. Dev. Cell 1:435-440.

Kirby ML. 2001. Getting to the heart of cardiac morphogenesis. Circ. Res. 88:370-372.

Kitamura K, Miura H, Miyagawa-Tomita S, Yanazawa M, Katoh-Fukui Y, Suzuki R, Ohuchi H, Suehiro A, Motegi Y, Nakahara Y, Kondo S, and Yokoyama M. 1999. Mouse Pitx2 deficiency leads to anomalies of the ventral body wall, heart, extra- and periocular mesoderm and right pulmonary isomerism. Dev. 126:5749-5758.

Liu C, Liu W, Lu MF, Brown NA, and Martin JF. 2001. Regulation of left-right asymmetry by thresholds of Pitx2c activity. Dev. 128:2039-2048.

Liu C, Liu W, Palie J, Lu MF, Brown NA, and Martin JF. 2002. Pitx2c patterns anterior myocardium and aortic arch vessels and is required for local cell movement into atrioventricular cushions. Dev. 129:5081-5091.

Meneghini V, Odent S, Platonova N, Egeo A, and Merlo GR. 2006. Novel TBX3 mutation data in families with Ulnar-Mammary syndrome indicate a genotype-phenotype relationship: mutations that do not disrupt the T-domain are associated with less severe limb defects. Eur. J. Med. Genet. 49:151-158.

Mjaatvedt CH, Nakaoka T, Moreno-Rodriguez R, Norris RA, Kern MJ, Eisenberg CA, Turner D, and Markwald RR. 2001. The outflow tract of the heart is recruited from a novel heart-forming field. Dev. Biol. 238:97-109.

Mommersteeg MTM, Soufan AT, de Lange FJ, van den Hoff MJB, Anderson RH, Christoffels VM, and Moorman AFM. 2006. Two distinct pools of mesenchyme contribute to the development of the atrial septum. Circ. Res. 99:351-353.

Mommersteeg MTM, Hoogaars WMH, Prall OWJ, de Gier-de Vries C, Wiese C, Clout DEW, Papaioannou VE, Brown NA, Harvey RP, Moorman AFM, and Christoffels VM. 2007. Molecular pathway for the localized formation of the sinoatrial node. Circ. Res. 100:354-362.

Mone SM, Gillman MW, Miller TL, Herman EH, and Lipshultz SE. 2004. Effects of environmental exposures on the cardiovascular system: prenatal period through adolescence. Ped 113:1058-1069.

Moorman AFM, Schumacher CA, de Boer PAJ, Hagoort J, Bezstarosti K, van den Hoff MJB, Wagenaar GTM, Lamers JMJ, Wuytack F, Christoffels VM, and Fiolet JWT. 2000. Presence of functional sarcoplasmic reticulum in the developing heart and its confinement to chamber myocardium. Dev Biol. 223:279-290.

Moorman AFM and Christoffels VM. 2003. Cardiac chamber formation: development, genes and evolution. Physiol. Rev. 83:1223-1267.

Moorman AFM, Christoffels VM, and Anderson RH. 2005. Anatomic substrates for cardiac conduction. Heart Rhythm 2:875-886.

Moorman AFM, Christoffels VM, Anderson RH, and van den Hoff MJB. 2007. The heart-forming fields: one or multiple? Phil. Trans. R. Soc. B. 362:1257-1265.

Odgers PNB. 1938. The development of the pars membranacea septi in the human heart. J. Anat. 72:247-259.

Patten BM and Kramer TC. 1933. The initiation of contraction in the embryonic chicken heart. Am. J. Anat. 53:349-375.

Postma AV, van de Meerakker JBA, Mathijssen IB, Barnett P, Christoffels VM, Ilgun A, Lam J, Wilde AAM, Lekanne Deprez RH, and Moorman AFM. 2008. A gain-of-function TBX5 mutation is associated with atypical Holt-Oram syndrome and paroxysmal atrial fibrillation. Circ. Res. 102:1433-1442.

Prall OWJ, Menon MK, Solloway MJ, Watanabe Y, Zaffran S, Bajolle F, Biben C, McBride JJ, Robertson BR, Chaulet H, Stennard FA, Wise N, Schaft D, Wolstein O, Furtado MB, Shiratori H, Chien KR, Hamada H, Black BL, Saga Y, Robertson EJ, Buckingham ME, and Harvey RP. 2007. An Nkx2-5/Bmp2/Smad1 negative feedback loop controls heart progenitor specification and proliferation. Cell 128:947-959.

Ramsdell AF. 2005. Left-right asymmetry and congenital cardiac defects: getting to the heart of the matter in vertebrate left-right axis determination. Dev. Biol. 288:1-20.

Rana MS, Horsten NCA, Tesink-Taekema S, Lamers WH, Moorman AFM, and van den Hoff MJB. 2007. Trabeculated right ventricular free wall in the chicken heart forms by ventricularization of the myocardium initially forming the outflow tract. Circ. Res. 100:1000-1007.

Riley P, Anson-Cartwright L, and Cross JC. 1998. The Hand1 bHLH transcription factor is essencial for placentation and cardiac morphogenesis. Nat. Genet. 18:271-275.

Rosenquist GC. 1970. Location and movements of cardiogenic cells in the chick embryo: the heart forming portion of the primitive streak. Dev. Biol. 22:461-475.

Scambler PJ. 2000. The 22q11 deletion syndromes. Hum. Mol. Genet. 9:2421-2426.

Smith A, Ho SY, Anderson RH, Connell MG, Arnold R, Wilkinson JL, and Cook AC. 2006. The diverse cardiac morphology seen in hearts with isomerism of the atrial appendages with reference to the disposition of the specialised conduction system. Cardiol. Young. 16:437-454.

Snarr BS, Wirrig EE, Phelps AL, Trusk TC, and Wessels A. 2007. A spatiotemporal evaluation of the contribution of the dorsal mesenchymal protrusion to cardiac development. Dev. Dyn. 236:1287-1294.

Soufan AT, van den Hoff MJB, Ruijter JM, de Boer PAJ, Hagoort J, Webb S, Anderson RH, and Moorman AFM. 2004. Reconstruction of the patterns of gene expression in the developing mouse heart reveals an architectural arrangement that facilitates the understanding of atrial malformations and arrhythmias. Circ Res. 95:1207-1215.

Soufan AT, van den Berg G, Ruijter JM, de Boer PAJ, van den Hoff MJB, and Moorman AFM. 2006. Regionalized sequence of myocardial cell growth and proliferation characterizes early chamber formation. Circ Res 99:545-552.

Stalsberg H and de Haan RL. 1969. The precardiac areas and formation of the tubular heart in the chick embryo. Dev. Biol. 19:128-159.

Stennard FA and Harvey RP. 2005. T-box transcription factors and their roles in regulatory hierarchies in the developing heart. Dev. 132:4897-4910.

Virágh Sz and Challice CE. 1973. Origin and differentiation of cardiac muscle cells in the mouse. J. Ultrastruct. Res. 42:1-24.

Waldo KL, Kumiski DH, Wallis KT, Stadt HA, Hutson MR, Platt DH, and Kirby ML. 2001. Conotruncal myocardium arises from a secondary heart field. Dev. 128:3179-3188.

Webb S, Brown NA, and Anderson RH. 1998. Formation of the atrioventricular septal structures in the normal mouse. Circ. Res. 82:645-656.

Webb S, Kanani M, Anderson RH, Richardson MK, and Brown NA. 2001. Development of the human pulmonary vein and its incorporation in the morphologically left atrium. Cardiol. Young. 11:632-642.

Webb S, Qayyum SR, Anderson RH, Lamers WH, and Richardson MK. 2003. Septation and separation within the outflow tract of the developing heart. J Anat. 202:327-342.

Wessels A, Markman MWM, Vermeulen JLM, Anderson RH, Moorman AFM, and Lamers WH. 1996. The development of the atrioventricular junction in the human heart. Circ. Res. 78:110-117.

Yuan S and Schoenwolf GC. 2000. Islet-1 marks the early heart rudiments and is asymmetrically expressed during early rotation of the foregut in the chick embryo. Anat. Rec. 260:204-207.

Yutzey KE, Rhee JT, and Bader D. 1994. Expression of the atrial-specific myosin heavy chain AMHC1 and the establishment of anteroposterior polarity in the developing chicken heart. Dev. 120:871-883.

Zaffran S, Kelly RG, Meilhac SM, Buckingham ME, and Brown NA. 2004. Right ventricular myocardium derives from the anterior heart field. Circ. Res. 95:261-268.

Distinct regulation of developmental and heart disease-induced ANF expression by two separate distal sequences

Thomas Horsthuis[1], Arjan C Houweling[1], Petra EMH Habets[1], Frederik J de Lange[1], Hamid el Azzouzi[2], Danielle EW Clout[1], Antoon FM Moorman[1], Vincent M Christoffels[1]

[1]Heart Failure Research Center, Academic Medical Center, University of Amsterdam, the Netherlands. [2]The Hubrecht Institute and Interuniversity Cardiology Institute Netherlands, Royal Netherlands Academy of Sciences, Utrecht, the Netherlands.

Circulation Research 2008. Apr 11;102:849-59.

Abstract

Nppa, encoding atrial natriuretic factor, is expressed in fetal atrial and ventricular myocardium, and is down-regulated in the ventricles after birth. During hypertrophy and heart failure, *Nppa* expression is re-activated in the ventricles, and serves as a highly conserved marker of heart disease. The *Nppa* promoter has become a frequently used model to study mechanisms of cardiac gene regulation. Nevertheless, the regulatory sequences that provide the correct developmental pattern and ventricular re-activation during cardiac disease remain to be defined. We found that proximal *Nppa* fragments ranging from 250 bp to 16 kbp provide robust reporter gene activity in the atria, and correct repression in the atrioventricular canal and the nodes of the conduction system *in vivo*. However, depending on fragment size and site of integration into the genome of mice, the fetal ventricular activity was either absent or present in an incorrect pattern. Furthermore, these fragments did not provide ventricular re-activation in heart disease models. These results indicate that the proximal promoter does not provide a physiologically relevant model for ventricular gene activity. In contrast, two modified bacterial artificial chromosome clones with partially overlapping genomic *Nppa* sequences provided appropriate re-activation of the green fluorescent protein reporter during pressure overload induced hypertrophy and heart failure *in vivo*. However, only one of these bacterial artificial chromosomes provided correct fetal ventricular green fluorescent protein activity. These results show that distinct distal regulatory sequences, and divergent regulatory pathways, control fetal ventricular activity and re-activation of *Nppa* during cardiac disease, respectively.

Introduction

A variety of mechanical, hormonal and genetic stimuli can cause cardiac enlargement and eventually heart failure. In response to these stimuli the ventricular myocytes increase in size and activate a hypertrophy response gene program. This gene program is characterized by induction of cardiac contractile protein genes and re-activation of a 'fetal' gene program, normally only active during cardiac development (reviewed in (Olson and Schneider, 2003;Chien et al., 1991)). Of the known genes that are re-activated, *Nppa*, encoding atrial natriuretic factor (ANF), is probably the best characterized (Chien et al., 1991;Rosenzweig and Seidman, 1991). *Nppa* is expressed specifically in the myocardium of the atria and ventricles of the embryonic and fetal heart, and is the first marker of their formation (Zeller et al., 1987;Christoffels et al., 2000). After birth, *Nppa* expression is down-regulated in the ventricles, where it is re-activated again in situations of cardiac stress.

Proximal promoter fragments (0.5-3.4 kbp) of *Nppa* of human, rat, mouse and *Xenopus* have been shown to drive atrial and fetal ventricular expression both *in vivo* (Field, 1988;Seidman et al., 1991;Knowlton et al., 1995;Habets et al., 2002;Small and Krieg, 2003;von Harsdorf et al., 1997) and in cell cultures (Durocher and Nemer, 1998;Seidman et al., 1988), and to provide a hypertrophy stress response in cardiomyocyte cell cultures and after injection as plasmid DNA in the ventricles of failing dog hearts (Ardati and Nemer, 1993;Shubeita et al., 1990;von Harsdorf et al., 1997). As such, the proximal *Nppa* promoter has become the most widely used model promoter that has importantly contributed to revealing transcriptional networks involved in cardiac gene regulation during cardiac development, health, and disease (reviewed in (Nemer and Nemer, 2001;Temsah and Nemer, 2005;Houweling et al., 2005)). Nonetheless, the *Nppa* promoter fragments have been shown to lack hypertrophy responsiveness *in vivo* (Knowlton et al., 1995). From these findings it has been concluded that the fetal gene program is regulated by sequences within the 0.7 kbp proximal promoter fragment, while the re-activation of the 'fetal' gene program during disease is regulated by sequences residing outside this fragment and therefore by a divergent pathway. However, a recent study indicated that the ventricular activity is absent from an even larger promoter fragment (de Lange et al., 2003), hindering any conclusions regarding the divergence of fetal and hypertrophy pathways. In addition, this lacking function would make the proximal promoter a physiologically less relevant read-out for the activity of cardiac transcriptional pathways. To address these issues, we assessed the regulatory activity of the *Nppa* locus in transgenic mice in detail. We found that the proximal *Nppa* promoter fragments, currently frequently used in studies of cardiac development and disease, lack critical regulatory functions for ventricular activity during development and in disease. Furthermore, the fetal activity of Nppa is regulated independently from its stress-response and re-activation during cardiac disease, both processes requiring distal regulatory sequences. Therefore, ventricular activity before birth and re-activation during disease are regulated by divergent transcriptional pathways.

Materials and methods

Transgenic mice

The transgenic promoter-reporter lines *-0.7rLacZ* and *-3/+4mCre,* and the *αMHC-Gal4* heart failure mouse model have been described previously (Habets et al., 2002;de Lange et al., 2003;Habets et al., 2003). The *-0.7rLacZ* construct was targeted as a single copy to the *Hprt* locus as described (*Hprt-0.7rLacZ)* (Figure 1A-B) (Bronson et al., 1996). To generate the *-0.7mLacZ* construct we replaced the rat *Nppa* promoter sequence by that of the mouse *Nppa* promoter sequence in the *-0.7rLacZ* construct (Figure 1D). Subsequently, to make the *-0.7/+4mLacZ* construct (Figure 1D), we replaced upstream sequences in the *-3/+4mCre* fragment with this *-0.7mLacZ* construct. The *-3mCre* construct was generated by truncating the *-3/+4mCre* construct in the third exon, proximal from the NRSE (Figure 1D). A -380/-138 rat *Nppa* promoter fragment was PCR amplified and fused to the -230/+126 *cTnI-LacZ* construct flanked by insulator sequences previously described (Habets et al., 2002), to generate the *0.25rNppacTnILacZ* construct (Figure 1D).

Two BAC clones of a mouse 129 SvJ BAC library (Incyte, St. Louis, MO) harbouring *Nppa* were end-sequenced to establish the genomic sequences they contain. BAC clone 337 ranges from -27 kbp to +127 kbp, clone 336 from -141 to +58 kbp relative to the transcription start site of *Nppa* (Figure 1C-D). At the translation start site of *Nppa* of both BACs, we replaced sequence cc.cac.gcc.agc.ATG.ggc by *Egfp,* using the BAC modification protocol kindly provided by Shiaoching Gong and Nathaniel Heinz (Gong et al., 2002). Subsequently, the *-11/+5mEgfp* construct was generated from the modified *BAC336-Egfp* construct (Figure 1D).

Supplementary methods are available online and at the end of this chapter.

Results

The activity of the proximal Nppa promoter is context dependent

To assess the spatio-temporal activity profile of the widely used 0.7 kbp *Nppa* promoter fragment, it was targeted as a single copy to the hypoxanthine phosphoribosyltransferase *(Hprt)* locus (Figure 1A, B). This locus is transcriptionally accessible throughout development and adult life, allowing promoter constructs to retain their activity and specificity, while variations in activity resulting from variation in copy number and site of insertion in the chromatin are ruled out (Bronson et al., 1996). Expression of the *lacZ* reporter driven by the promoter was restricted to the heart throughout development (Figure 2). Onset of transgene expression was observed at E8 at the ventral side of the heart tube (not shown), comparable to the onset of *Nppa* expression (Christoffels et al., 2000). From E9.5 onwards both the reporter gene and the endogenous *Nppa* gene were expressed in atrial and ventricular

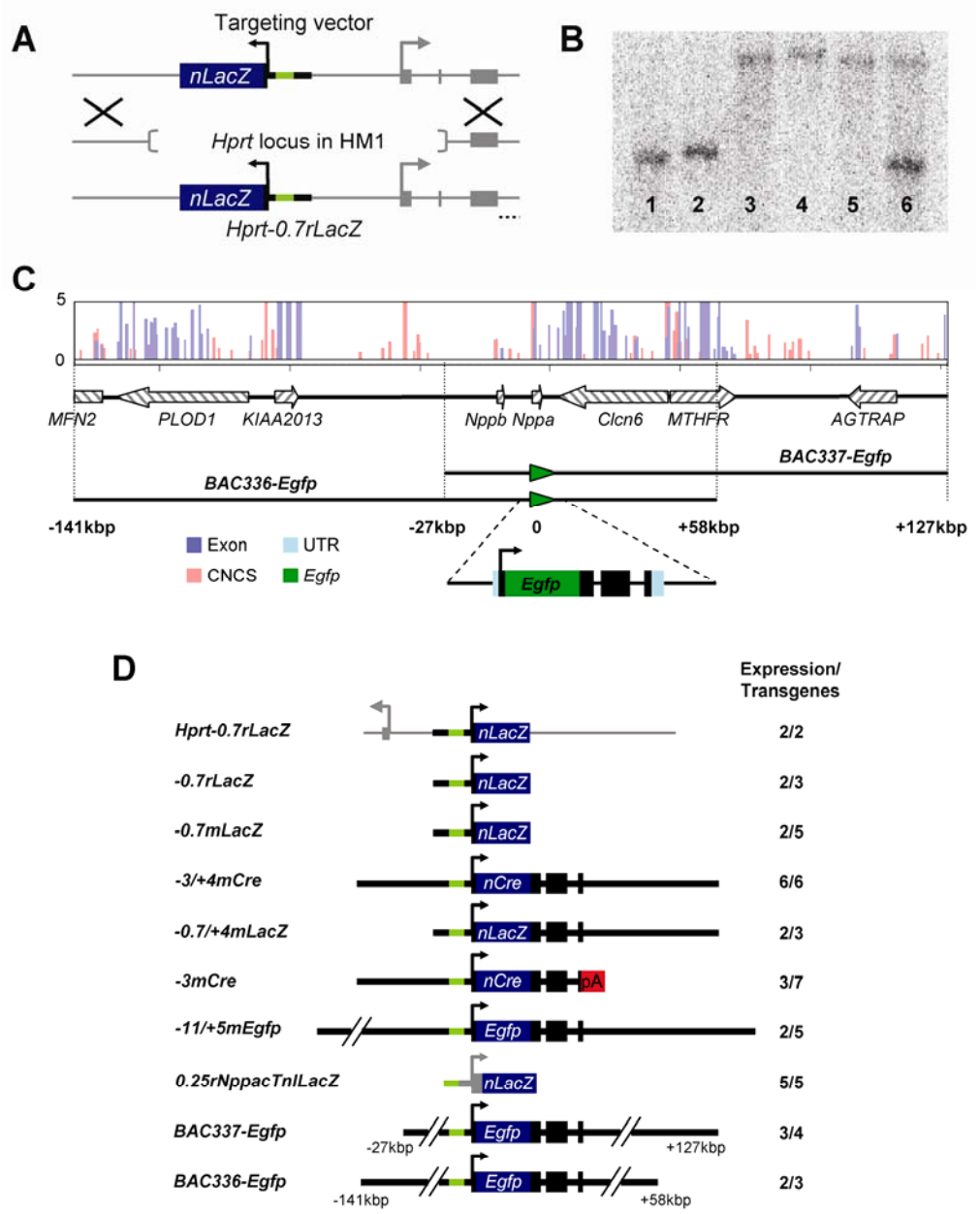

Figure 1. Overview of all *Nppa* promoter constructs used in this study. (A) Targeting vector used to target the 0.7 kbp rat *Nppa* promoter to the *Hprt* locus. (B) Southern blot for verification of single integration at the *Hprt* locus after *Bam*H1 digestion of genomic DNA. 1, wild type; 2, wild type; 3, hemizygous male of line A; 4, homozygous female of line A; 5, hemizygous male of line B; 6, heterozygous female of line B. The position of the *Rsa*I probe used for Southern blotting is indicated (dotted line). (C) Web based RankVISTA alignment of human against mouse *Nppa* genomic region covered by BAC336 and BAC337. BAC336 and BAC337 share 85 kbp of overlapping sequences and both contain unique sequences either up- or downstream, respectively. RankVISTA bars depict evolutionary conserved segments where the heights scale with statistical significance [-log10(P-value)]. (D) Constructs used to generate transgenic mice. The table indicates the number of founders that express the transgene (Expression) over the total number of founders or lines obtained (Transgenes). Grey lines in panel A indicate mouse *Hprt* locus sequences. Thick black lines indicate *Nppa* promoter sequences, green thick lines the 0.25 kb *Nppa* 'atrial' regulatory module, the thick grey line and box in panel D the -230/+126 *cTnI* promoter fragment. Boxes represent exons, dark blue boxes the reporter gene and the red box the human growth hormone polyadenylation signal. CNCS, conserved non-coding sequence; UTR, untranslated region.

chamber myocardium, but not in the atrioventricular canal and outflow tract (Figure 2; 3; 7). *Nppa* expression is absent from the sinoatrial and atrioventricular node (Wharton et al., 1988;Houweling et al., 2002). Analysis of E17.5 embryos revealed that also the *Hprt-0.7rLacZ* construct was not active in these components (Figure 3J-L). However, the transgene was ectopically active in the sinus horns and mediastinal atrial myocardium (Figure 2G-I; 3I). After E9.5 ventricular *Nppa* expression becomes restricted to the trabeculated myocardium, and after birth it largely disappears (Figure 3). In contrast, before and after birth the *Hprt-0.7rLacZ* construct remained active in a transmural pattern in the ventricles (Figure 3; 4A, D). These findings indicate that while the 0.7 kbp promoter drives important aspects of the pattern of *Nppa*, it lacks regulatory sequences for the correct fetal ventricular pattern and postnatal down-regulation, and for correct repression in the mediastinal atrial myocardium and sinus horns.

The pattern of the *Hprt-0.7rLacZ* construct was compared to that of two lines in which the -0.7 kbp promoter-*lacZ* construct was randomly integrated in the genome. Both lines showed similar cardiac expression during development, including ectopic expression in the sinus horns and mediastinal myocardium, albeit that the ventricular activity was relatively weak. In addition, the *-0.7rLacZ* promoter fragment was ectopically active outside the heart (Figure 2). At birth, line A (*-0.7rLacZA*) expressed *lacZ* homogeneously in the atria, whereas some activity was present in the left ventricle (Figure 4B). In the adult heart the atrial expression had become patchy and the ventricular activity had disappeared (Figure 4E). In line B, expression in the atria was patchy at day of birth, while expression in the ventricles was not detectable anymore (Figure 4C). In the adult hearts of this line, only a few atrial cells still expressed the construct (Figure 4F). These observations indicate that the previously observed postnatal ventricular down-regulation of the proximal *Nppa* promoter fragments (Knowlton et al., 1995) may not be specific to the ventricle, and dependent on the site of integration.

Key regulatory functions of Nppa reside within a small 'atrial' module, whereas extension of proximal promoter fragments diminishes ventricular activity

Previous studies indicated that the 0.7 kbp Nppa promoter fragment is organized in three modules, a ventricular and developmental module, an atrial module and a basic cardiac promoter (Argentin et al., 1994;Durocher and Nemer, 1998). We tested the contribution of the ventricular module in vivo, by placing a 0.25 kbp fragment containing only the atrial module upstream of a *cTnI* promoter fragment (*0.25rNppacTnI*) (Figure 1D) that normally is always expressed in the atrioventricular canal and only shows limited expression in the atria (Habets et al., 2002). This resulted in an expression profile comparable to that of the *0.5NppacTnI* fragment containing both the atrial and the ventricular module (Figure 7; Supplementary Figure 1; Habets et al., 2002), with repression of the *cTnI* promoter fragment in the atrioventricular canal, and activity driven in the atria and in the left ventricle. These findings

indicate that the regulatory sequences responsible for the atrial and ventricular activity of the 0.7 kbp proximal *Nppa* promoter reside within the atrial module, and that the ventricular module does not contribute significantly.

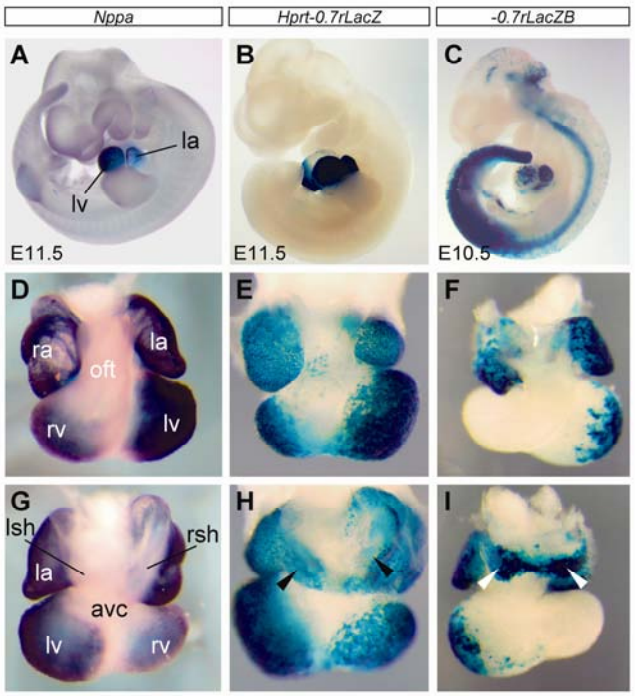

Figure 2. Endogenous *Nppa* expression compared to the targeted *Hprt-0.7rLacZ* and the randomly integrated *-0.7rLacZ* construct. (A, D, G) Whole mount *in situ* hybridisation of *Nppa*. (B-C, E-F, H, I) Whole mount β-galactosidase staining. Both the *Hprt -0.7rLacZ* and the *-0.7rLacZ* constructs showed ectopic expression in the sinus horns (arrow heads in H, I). ra, right atrium; la, left atrium; rv, right ventricle; lv, left ventricle; oft, outflow tract; avc, atrioventricular canal; lsh, left sinus horn; rsh, right sinus horn.

We previously showed that a 7 kbp mouse *Nppa* fragment *(-3/+4mCre*), that includes the 0.7 kbp fragment, is virtually inactive in the ventricles (Figure 7; Supplementary Figure 2A; de Lange et al., 2003). By truncation experiments we tested whether a ventricular repressor either upstream (located between -3 kbp and -0.7 kbp) or downstream (located between -0.7 and +4 kbp) could explain the lack of ventricular activity. Both the up- and downstream truncated construct (Figure 1D) showed almost exclusively atrial expression, similar to *-3/+4mCre* transgenes (Figure 7; Supplementary Figure 2A-C). These findings argue against a repressor located within the 7 kbp fragment that inhibits ventricular expression.

The 7 kbp Nppa fragment is from mouse, whereas the 0.7 kbp promoter fragment that showed activity in the ventricles is from rat. The rat proximal promoter contains marked sequence differences with those of mouse and human (Durocher and Nemer, 1998). To examine whether these differences could account for the lack of ventricular activity in the

larger constructs, we tested the 0.7 kbp of the mouse *Nppa* promoter (*-0.7mLacZ*) (Figure 1D). Similar to the rat 0.7 kbp promoter, this construct was active in both the atria and the ventricles, was correctly inactive in the atrioventricular canal and outflow tract, and was ectopically active in the sinus horns (Figure 7; Supplementary Figure 2D). Thus, the lack of ventricular expression of the larger constructs cannot be explained by a species difference.

In search for lacking sequences responsible for ventricular activity we subsequently generated a larger construct of 16 kbp (*-11/+5mEgfp*) (Figure 1D). However, this construct appeared completely inactive in the ventricles as well (Figure 7; Supplementary Figure 2E). Taken together, our data indicate that enhancers outside a -11 kbp to +5 kbp fragment are required for ventricular activity.

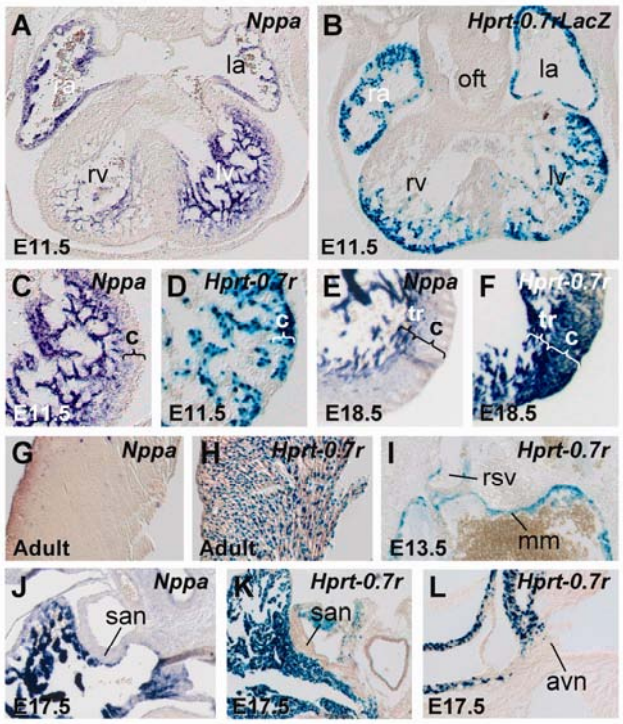

Figure 3. Comparison of expression patterns of endogenous *Nppa* and the *Hprt-0.7rLacZ* transgene. (A, C, E, G, J) Section *in situ* hybridisation of *Nppa*. (B, D, F, H, I, K-L) Section β-galactosidase staining. san, sinoatrial node; avn, atrioventricular node; mm, mediastinal myocardium; rsv, right systemic vein; tr, trabeculated myocardium; c, compact myocardial layer. See legend to Figure 2 for other abbreviations.

Distal regulatory DNA regions for the ventricular pattern and fetal activity

To identify distal regulatory sequences we used two *Nppa* containing BAC clones of 150 to 200 kbp, respectively, with 85 kbp of overlapping sequences (Figure 1C-D). An enhanced green fluorescent protein encoding reporter gene (*Egfp*) was inserted at the translation start site of *Nppa* in both BACs. Transgenic mouse lines were generated carrying the modified

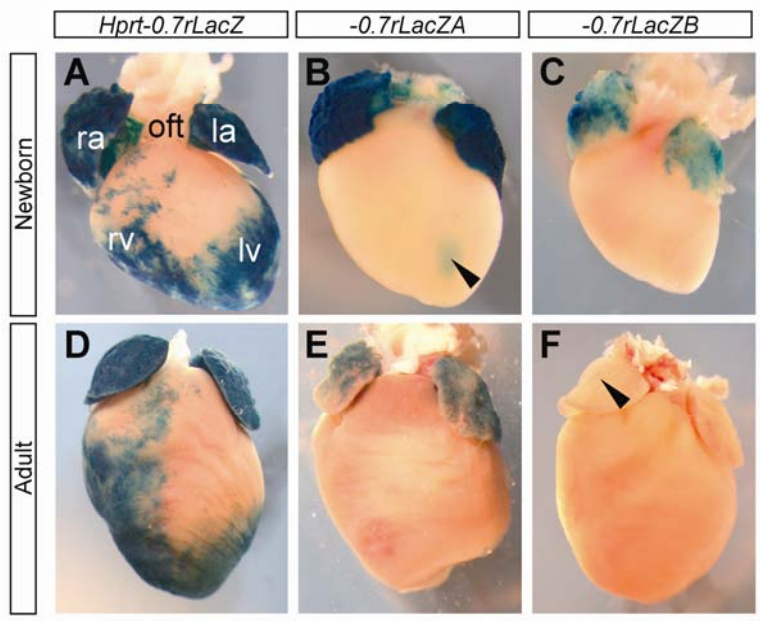

Figure 4. Postnatal expression of the *Hprt-0.7rLacZ* transgene compared to the *-0.7rLacZ* transgenic lines A and B. Whole mount β-galactosidase staining. Ventricular expression in the *Hprt-0.7rLacZ* transgene was not down-regulated after birth and remained active both in atria and ventricles (A, D). The expression in both *-0.7rLacZ* lines was inactivated in the atria as well as in the ventricles (B, E and C, F). Arrowhead in B indicates the small amount of ventricular activity present at day of birth in *-0.7rLacZ* line A. Arrowhead in F indicates the few atrial cells still expressing *-0.7rLacZ* in the adult atrium of line B. For abbreviations, see legend to Figure 2.

BAC clones. EGFP expression in five independent mouse lines carrying *BAC337-Egfp* showed similar spatio-temporal patterns, but different expression levels (Figure 5C-D, G, J). All lines showed ectopic expression in the neural tube (Figure 5C). *In situ* hybridization onsections showed robust expression of *Egfp* in the atria, but also ectopic expression in the sinus horns and in the mediastinal myocardium (Figure 5G), in a pattern similar to that of the *-0.7rLacZ* constructs. In the ventricles, the spatial pattern of *Egfp* expression resembled the endogenous *Nppa* pattern, restricted to the trabecules after E9.5 (Figure 5G, J). However, the observed ventricular fluorescence as well as the signal in *in situ* hybridization was very low when compared to the atria (Figure 5D, G). Three weeks after birth no ventricular fluorescence was detectable anymore (Figure 6D-F).

Two independent mouse lines carrying *BAC336-Egfp* showed a similar pattern and intensity of expression. Expression was restricted to the heart with abundant expression in the atria and ventricles (Figure 5A-B, F, I). The pre- and postnatal patterns of expression of *Nppa* and *BAC336-Egfp* were identical, including absence of expression from the mediastinal myocardium and sinus horns (Figure 5E-F, H-I) and downregulation of ventricular activity after birth (Figure 6A-C), indicating that this BAC clone contains all regulatory sequences involved in fetal spatio-temporal *Nppa* gene regulation.

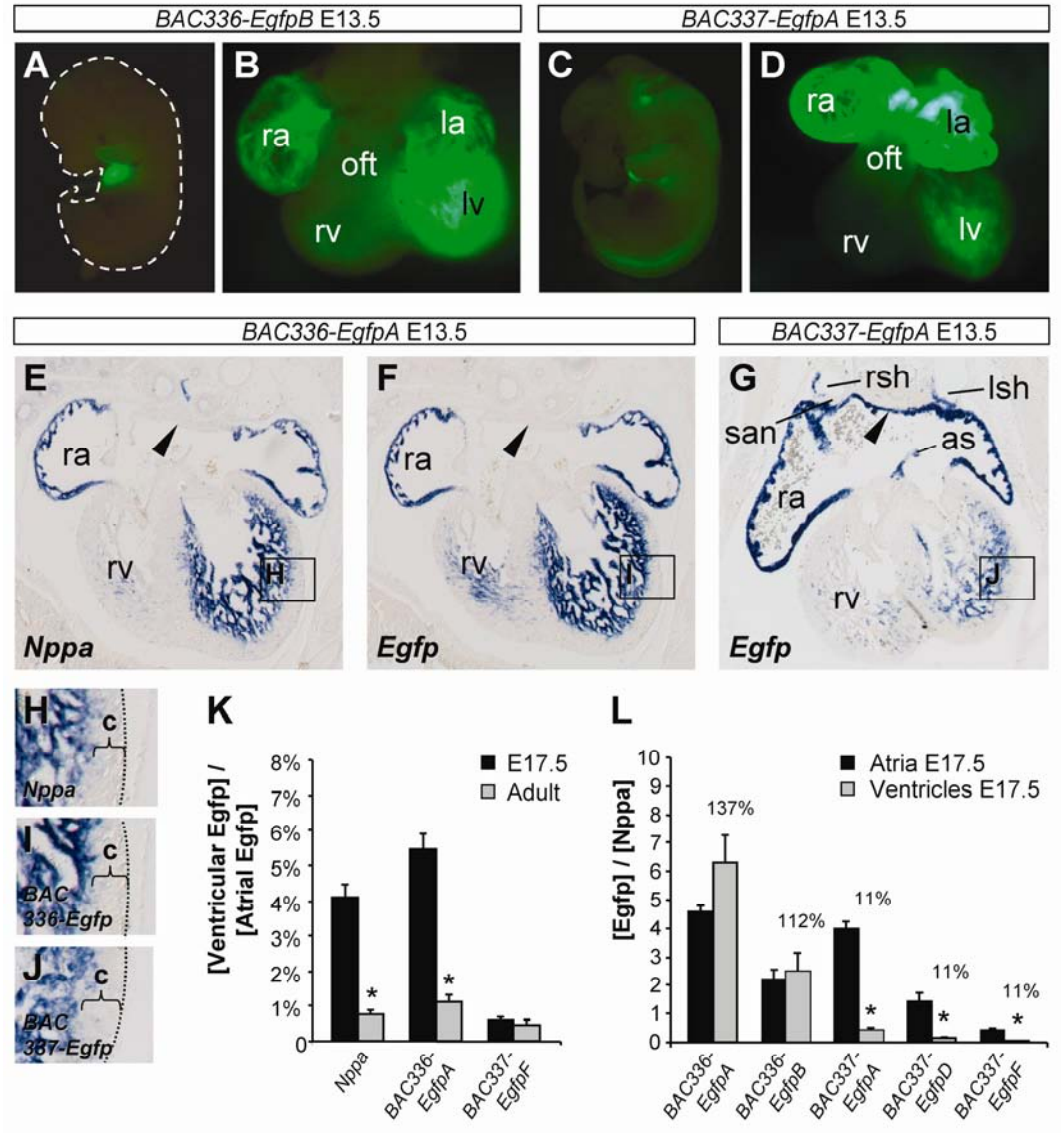

Figure 5. Pre- and postnatal activity and expression patterns of *BAC336-Egfp* and *BAC337-Egfp* transgenes compared to endogenous *Nppa*. Mice carrying *BAC336-Egfp* showed heart-specific expression (A) with high activity both in the atria and the ventricles (B). Transgenic mice carrying *BAC337-Egfp* showed ectopic fluorescence outside the heart (C). Within the heart atrial fluorescence was abundant, but only minor activity was observed in the ventricles (D). *In situ* hybridization revealed that *BAC336-Egfp* mimics both pattern and activity of endogenous *Nppa* expression (E-F and H-I). In contrast, *BAC337-Egfp* in the ventricles recapitulated the pattern of endogenous *Nppa* (E, G and H, J), but was expressed at a very low level relative to atrial expression (G). *BAC337-Egfp* was ectopically active in the right and left sinus horns, the pulmonary vein, the mediastinal myocardium (arrow head) and the developing atrial septum (G). (K-L) qRT-PCR quantification of mRNA levels in E17.5 and adult hearts of *BAC336-Egfp* and *BAC337-Egfp* mice. (K) Ventricular activity of endogenous *Nppa* and *BAC336-Egfp* were approximately 5% of atrial activity before birth, and decreased to 1% of atrial activity after birth. In contrast, fetal ventricular *BAC337-Egfp* expression was less than 1% of atrial expression and after birth remained constant at this level. (L) Ratio of *Egfp* expression relative to endogenous *Nppa* expression in fetal atria and ventricles of two *BAC336-Egfp* and three *BAC337-Egfp* transgenic lines. In both *BAC336-Egfp* lines, the ratio of *Egfp* and *Nppa* expression in the atria and in the ventricles was similar, while in all *BAC337-Egfp* lines ventricular expression was only roughly 10% of atrial expression. *Egfp* and *Nppa* expression in the atria and the ventricles was normalized to *Gapdh* expression. Error bars indicate SEM. as, atrial septum. See legends to Figure 2 and 3 for other abbreviations.

To assess whether the BAC sequences provide correct fetal ventricular activity and perinatal down-regulation, the atrial and ventricular expression levels of *Nppa* and *Egfp* were quantified before and after birth (Figure 5K). At E17.5, ventricular expression of both *Nppa* and *BAC336-Egfp* were around 5% of atrial expression. After birth, both were down-regulated in the ventricles to 1% of atrial expression. In contrast, in E17.5 embryos carrying *BAC337-Egfp*, ventricular *Egfp* expression was less than 1% of atrial *Egfp* expression, and remained at this low level after birth. Subsequently, we calculated the ratios of *Egfp* and *Nppa* mRNA levels in E17.5 atria and ventricles of two *BAC336-* and three *BAC337-Egfp* transgenic lines (Figure 5L). In both *BAC336-Egfp* lines the ratio of the levels of *Egfp* and *Nppa* mRNA in the atria was similar to the ratio in the ventricles, whereas in all *BAC337-Egfp* lines the ratio of *Egfp* and *Nppa* mRNA in the ventricles was around 10% of the ratio found in the atria. These findings indicate that *BAC337-Egfp* lacks a ventricular enhancer that is mainly active before birth, locating this enhancer within the unique sequences of *BAC336-Egfp* (Figure 7).

Distal regulatory sequences control the stress response of Nppa

In the *Hprt* locus ventricular activity is maintained even in the adult heart. To test whether the 0.7 kbp proximal *Nppa* promoter in this transcriptionally favorable context is inducible in the failing ventricle *in vivo*, we subjected these mice to cardiomyopathy, using a transgenic model in which *Gal4* is driven by the *αMHC* promoter (*αMHC-Gal4*) (Habets et al., 2003). All male *Gal4*-positive offspring develop a-specific dilated cardiomyopathy three weeks after birth, which is associated with strong induction of *Nppa*. Although endogenous *Nppa* was strongly induced in double transgenic mice, the *Hprt-0.7rLacZ* construct was not (Figure 6G). Subsequently we tested the 7 kbp fragment, which lacks the capacity for embryonic ventricular expression, but contains an NRSE implicated in induction of *Nppa* promoter fragments in heart failure (Kuwahara et al., 2003). This *-3/+4mCre* construct was not re-activated in the ventricles either (Figure 6G).

In contrast, mice carrying either *BAC336-Egfp* or *BAC337-Egfp* showed strong re-activation of *Egfp* in the failing ventricles (Figure 6A, D, G). In ventricles of *BAC336-Egfp* mice, *Egfp* was up-regulated 12-fold relative to its level in healthy littermates, which is similar to the up-regulation of endogenous *Nppa*. In mice carrying *BAC337-Egfp*, an exceptional 50-fold induction of *Egfp* over basic ventricular expression level was observed, the height of the induction being at least in part due to the low basic expression level of *BAC337-Egfp* in the healthy ventricle. Also transverse aortic constriction of mice carrying these BACs induced the expression of both *Nppa* and *Egfp* (Figure 6B, C, E, F; Supplementary Figure 3), demonstrating that the regulatory sequences in both BACs mediate the response of *Nppa* to pressure overload hypertrophy. These results show that both BAC clones contain the regulatory sequences required for the cardiac stress response of *Nppa* (Figure 7).

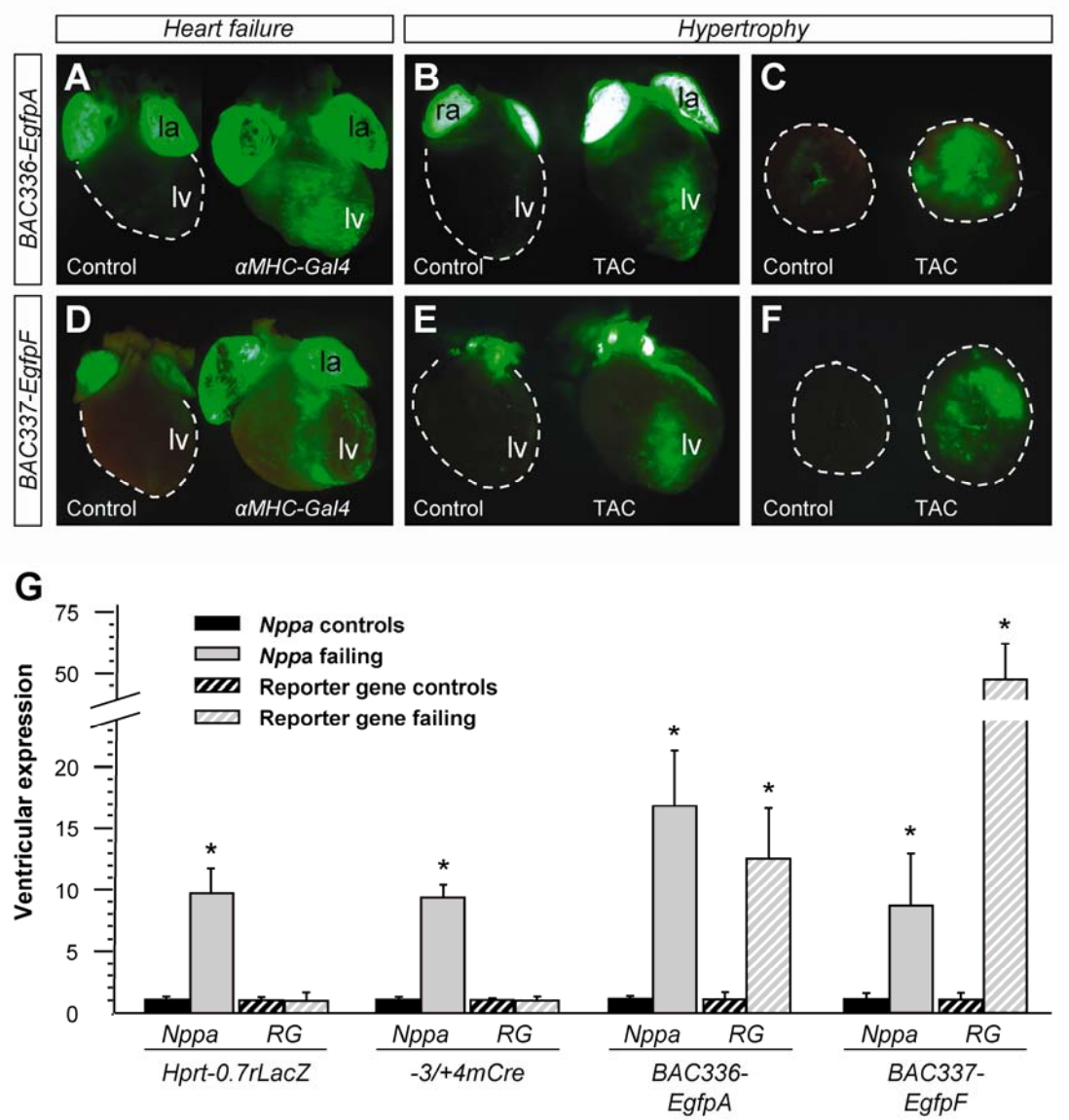

Figure 6. *BAC336-Egfp* and *BAC337-Egfp*, but not the *Hprt-0.7rlacZ* and *-3/+4Cre* constructs, are re-activated in heart failure. (A, D) Heart failure induced by crossing the transgenic mice to the *αMHC-Gal4* heart failure mouse (Habets et al., 2003). (B, E) Hypertrophy induced in adult mice using a pressure overload model (transverse aortic banding (TAC)). From the hearts carrying *BAC337-Egfp* (E) the atria were removed. (C, F) Midventricular transverse sections of hearts shown in B and E. (G) qRT-PCR quantification of ventricular mRNA levels of endogenous *Nppa* and the reporter genes *LacZ*, *Cre* and *Egfp* relative to *Gapdh* mRNA in control (black bars; mean ratio set to 1) and failing hearts (grey bars) in mice carrying the *Hprt-0.7rLacZ, -3/+4mCre, BAC336-Egfp* or *BAC337-Egfp* construct. In all four groups, the level of *Nppa* in failing hearts was significantly higher than in control hearts ($P<0.05$). In contrast, reporter gene expression in neither the *Hprt-0.7rLacZ* (n=4, P=0.3), nor the *-3/+4mCre* failing ventricles (n=3, P=0.9), showed induction. In mice carrying *BAC336-Egfp* (n=4, $P<0.01$) or *BAC337-Egfp* (n=3, $P<0.05$), we detected significant re-activation of *Egfp* in failing ventricles. Error bars indicate SEM. RG, reporter gene. See legend to Figure 2 for other abbreviations.

Discussion

Proximal Nppa promoter fragments lack regulatory functions for ventricular activity

In the developing heart, *Nppa* serves as a marker for differentiating atrial and ventricular working myocardium, whereas its expression is excluded from the sinus horns, atrioventricular canal, outflow tract and nodes of the conduction system (Zeller et al., 1987;Wharton et al., 1988;Christoffels et al., 2000). After birth, *Nppa* is expressed at very high levels in the atria (approximately 1% of total mRNA), whereas its expression in the ventricles is down-regulated (Bloch et al., 1986). Re-activation of *Nppa* expression is part of a highly conserved adaptive change in gene expression in response to hypertrophy and heart failure, serving both diagnostic and potentially therapeutic options. Because of these properties, *Nppa* has become a widely used model gene for studying gene regulation and monitoring phenotypic changes during cardiac disease (reviewed in (Levin et al., 1998;Schmitt et al., 2003;Houweling et al., 2005)). Proximal promoter fragments are frequently used as read-out tools for the activity of a wide range of transcriptional pathways that control patterning of the developing heart and gene regulation in healthy, hypertrophic or failing ventricular myocardium (reviewed in (Nemer and Nemer, 2001;Temsah and Nemer, 2005;Houweling et al., 2005)). It is therefore important to know which regulatory functions the proximal promoter contains. Promoter fragments ranging from -3.4 kbp to -0.5 kbp were reported to efficiently drive expression in the atria, and in several cases also in the ventricles of transgenic mice and *Xenopus* (Field, 1988;Seidman et al., 1991;Knowlton et al., 1995;Habets et al., 2002;Small and Krieg, 2003). Furthermore, analysis of promoter activity in transfected atrial and ventricular myocytes and non-cardiac cells has indicated that the *Nppa* promoter is organized in three modules, a basic cardiac promoter, a developmental- and atrial-specific module, and a ventricular enhancer located just upstream of the atrial module (Durocher et al., 1996;Durocher et al., 1998;Durocher and Nemer, 1998). These studies have led to the current view that the proximal *Nppa* promoter correctly drives atrial and fetal ventricular expression, and postnatal ventricular down-regulation.

Our current data reveal that the proximal promoter fragments lack important regulatory functions required for fetal ventricular activity. All promoter fragments analyzed were active in the atria and correctly inactive in the atrioventricular canal and outflow tract of the developing heart, and in the nodes of the mature heart (Figure 7). The ‘atrial’ module in the context of the *cTnI* promoter was found to be largely sufficient to provide these characteristics (Figure 7; Supplementary Figure 1). These results provide *in vivo* support for previous studies showing that the activity of the promoter is mediated by T-box factors and Nkx2-5 that act on sites within this ‘atrial’ module (Bruneau et al., 2001;Hiroi et al., 2001;Habets et al., 2002). In contrast, the ventricular regulatory characteristics appeared to largely lack from proximal promoter fragments. Firstly, the fetal transmural pattern of expression of the *Nppa* gene was not recapitulated in transgenic mice. Secondly, while

ventricular activity was observed in the favorable genomic context of the *Hprt* locus, in randomly integrated constructs it was weak, and absent in the context of larger *Nppa* fragments (up to -11/+5 kbp). Thirdly, the activity of the 0.7 kbp promoter was not correctly down-regulated in the ventricles after birth. In the context of the *Hprt* locus the *Nppa* promoter fragment remained active, and in the randomly integrated constructs the

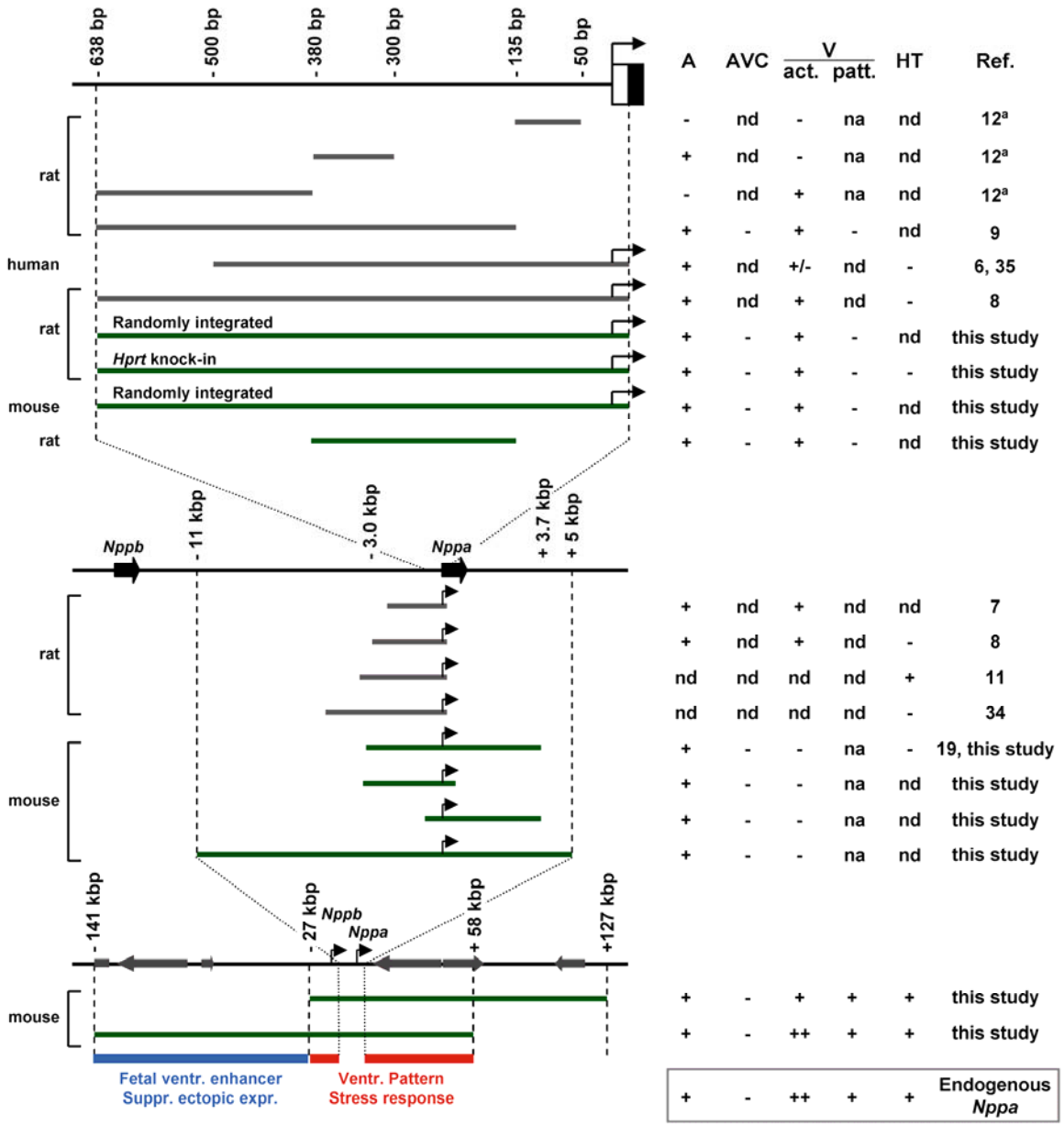

Figure 7. Overview of the activity of regulatory *Nppa* sequences. Black lines depict the *Nppa* locus, gray lines depict DNA fragments described in literature, and dark green lines fragments analyzed in this study. All fragments were studied in transgenic mice, except for the first three ([a]) which were analyzed in cultured cardiomyocytes. act., ventricular activity; patt., ventricular pattern; HT, hypertrophy; Ref, reference; nd, not determined; na, not applicable; -, no expression; +, expression; +/-, expression in some lines; ++, high activity (comparable to endogenous *Nppa*). See legend to Figure 2 for other abbreviations.

inactivation was non-specific, as also the atria lost expression. Finally, analysis of the BAC transgenic mice revealed that fetal ventricular expression requires two distinct distal sequences. The ventricular transmural pattern requires additional regulatory sequences located between -27 kbp to -11 kbp and/or +5 kbp to +58 kbp relative to the *Nppa* gene, whereas fetal ventricular activity is provided by a distinct strong fetal ventricular enhancer that we located more upstream between -141 kbp to -27 kbp (Figure 7). Therefore, the atrial module within the proximal promoter may provide only residual ventricular activity, which is unmasked in a favorable genomic context. Taken together, we conclude that the activity pattern of the *Nppa* proximal promoter region is very useful to study atrial gene activity and repression in the nodes of the conduction system, but does not represent a physiologically relevant read-out for ventricular gene regulation in the developing and adult heart.

Distinct regulatory sequences and divergent pathways drive fetal activity and stress response

The proximal promoter of *Nppa* is responsive to hypertrophic stimuli in some experimental settings (Shubeita et al., 1990;Ardati and Nemer, 1993;von Harsdorf et al., 1997), but does not respond to ventricular hypertrophy in transgenic mice *in vivo* (Knowlton et al., 1995). Our analysis confirms and extends these observations in a different heart disease model. Firstly, we tested a larger fragment that contains an NRSE which has been implicated in the hypertrophy response of *Nppa*. While this NRSE is sufficient to mediate a response to hypertrophic stimuli *in vitro* through NRSF (Kuwahara et al., 2003), our results indicate this is not the case *in vivo*. Secondly, in previous studies the postnatal expression and the inducibility of *Nppa* promoter fragments has been tested in mice carrying randomly integrated promoter constructs, which, according to our findings, may become down-regulated by postnatal silencing that is not specific to the ventricles. We circumvented this potential problem by testing the inducibility of the 0.7 kbp promoter in the context of the *Hprt* locus that stays transcriptionally accessible throughout life. Again, the transgene was found to be non-responsive in the cardiac disease model. Taken together, all data consistently indicate that the proximal promoter region lacks critical sequences that mediate the induction of *Nppa*, rendering the fragment completely non-responsive to cardiac disease *in vivo*.

Based on the assumption that the proximal promoter fragments drive fetal ventricular activity, previous studies indicated that re-activation of the fetal gene program during cardiac disease is regulated by pathways distinct from those that regulate prenatal ventricular activity (Knowlton et al., 1995). As discussed above, our analysis shows that also the fetal ventricular activity functions are lacking from the proximal promoter fragments. Therefore, the previous conclusion regarding the divergent pathways was premature.

The analysis of two BAC transgenic mice revealed that ventricular *Nppa* regulation requires a multi-partite ventricular regulatory module. This module consists of the proximal 0.25 kbp ‘atrial’ module driving residual ventricular expression, and at least two additional distal sequences (Figure 7). Whereas *BAC337-Egfp* provided the correct fetal transmural

ventricular pattern, and was appropriately re-activated during disease, its ventricular activity before birth was similarly low as in the adult heart, indicating that BAC337 lacks a ventricular enhancer inducing activity before birth. In contrast, *BAC336-Egfp* activity mimicked all aspects of ventricular *Nppa* regulation, including fetal transmural pattern, abundant fetal activity, perinatal down-regulation, and re-activation in hypertrophy and in heart failure. These results indicate that shared sequences, residing within both BAC clones, may regulate the typical fetal transmural (trabecular) ventricular pattern and re-activation in cardiac disease (Figure 7). Importantly, this analysis also revealed that the sequences required for activity in the fetal ventricle are located in a different genomic region, more than -27 kbp upstream (Figure 7). Therefore, the re-activation in the failing ventricle and the fetal ventricular activity are regulated by distinct distally located sequences, and, consequently, divergent pathways converging on these sequences. Further mapping will be required to locate the discrete *cis*-elements and factors that mediate these respective activities.

Acknowledgments

We thank Dr. Leon de Windt and Hans van der Linden for their contributions. This work was supported by grants from the Netherlands Heart Foundation (96.002 to V.M.C. and A.F.M.M.); the Netherlands Organization for Scientific Research (Vidi grant 864.05.006 to V.M.C.); European Union FP6 contract “Heart Repair” (LSHM-CT-2005-018630 to V.M.C., A.F.M.M.).

References

Ardati,A. and M.Nemer. 1993. A nuclear pathway for a1-adrenergic receptor signaling in cardiac cells. EMBO J. 12: 5131-5139.

Argentin,S., A.Ardati, S.Tremblay, I.Lihrmann, L.Robitaille, J.Drouin, and M.Nemer. 1994. Developmental stage-specific regulation of atrial natriuretic factor gene transcription in cardiac cells. Mol. Cell Biol. 14: 777-790.

Bloch,K.D., J.G.Seidman, J.D.Naftilan, J.T.Fallon, and C.E.Seidman. 1986. Neonatal atria and ventricles secrete atrial natriuretic factor via tissue-specific secretory pathways. Cell 47: 695-702.

Bronson,S.K., E.G.Plaehn, K.D.Kluckman, J.R.Hagaman, N.Maeda, and O.Smithies. 1996. Single-copy transgenic mice with chosen-site integration. Proc Natl Acad Sci U S A. 93: 9067-9072.

Bruneau,B.G., G.Nemer, J.P.Schmitt, F.Charron, L.Robitaille, S.Caron, D.A.Conner, M.Gessler, M.Nemer, C.E.Seidman, and J.G.Seidman. 2001. A murine model of Holt-Oram syndrome defines roles of the T-box transcription factor Tbx5 in cardiogenesis and disease. Cell 106: 709-721.

Chien,K.R., K.U.Knowlton, H.Zhu, and S.Chien. 1991. Regulation of cardiac gene expression during myocardial growth and hypertrophy: molecular studies of an adaptive physiologic response. FASEB J. 5: 3037-3046.

Christoffels,V.M., P.E.M.H.Habets, D.Franco, M.Campione, F.de Jong, W.H.Lamers, Z.Z.Bao, S.Palmer, C.Biben, R.P.Harvey, and A.F.M.Moorman. 2000. Chamber formation and morphogenesis in the developing mammalian heart. Dev Biol. 223: 266-278.

de Lange,F.J., A.F.M.Moorman, and V.M.Christoffels. 2003. Atrial cardiomyocyte-specific expression of Cre recombinase driven by an Nppa gene fragment. Genesis 37: 1-4.

Durocher,D., C.Y.Chen, A.Ardati, R.J.Schwartz, and M.Nemer. 1996. The atrial natriuretic factor promoter is a downstream target for Nkx-2.5 in the myocardium. Mol. Cell Biol. 16: 4648-4655.

Durocher,D., C.Grepin, and M.Nemer. 1998. Regulation of gene expression in the endocrine heart. Recent Prog Horm Res 53: 7-23.

Durocher,D. and M.Nemer. 1998. Combinatorial interactions regulating cardiac transcription. Developmental Genetics 22: 262.

Field,L.J. 1988. Atrial natriuretic factor-SV40 T antigen transgenes produce tumors and cardiac arrhythmias in mice. Science 239: 1029-1033.

Gong,S., X.W.Yang, C.Li, and N.Heintz. 2002. Highly efficient modification of bacterial artificial chromosomes (BACs) using novel shuttle vectors containing the R6Kgamma origin of replication. Genome Res. 12: 1992-1998.

Habets,P.E.M.H., D.E.W.Clout, R.H.Lekanne Deprez, M.A.van Roon, A.F.Moorman, and V.M.Christoffels. 2003. Cardiac expression of Gal4 causes cardiomyopathy in a dose-dependent manner. J. Muscle. Res. Cell. Motil. 24: 205-209.

Habets,P.E.M.H., A.F.M.Moorman, D.E.W.Clout, M.A.van Roon, M.Lingbeek, M.Lohuizen, M.Campione, and V.M.Christoffels. 2002. Cooperative action of Tbx2 and Nkx2.5 inhibits ANF expression in the atrioventricular canal: implications for cardiac chamber formation. Genes Dev. 16: 1234-1246.

Hiroi,Y., S.Kudoh, K.Monzen, Y.Ikeda, Y.Yazaki, R.Nagai, and I.Komuro. 2001. Tbx5 associates with Nkx2-5 and synergistically promotes cardiomyocyte differentiation. Nat. Genet. 28: 276-280.

Houweling,A.C., S.Somi, M.J.van den Hoff, A.F.M.Moorman, and V.M.Christoffels. 2002. Developmental pattern of ANF gene expression reveals a strict localization of cardiac chamber formation in chicken. Anat Rec 266: 93-102.

Houweling,A.C., M.M.van Borren, A.F.M.Moorman, and V.M.Christoffels. 2005. Expression and regulation of the atrial natriuretic factor encoding gene Nppa during development and disease. Cardiovasc Res 67: 583-593.

Knowlton,K.U., H.A.Rockman, M.Itani, A.Vovan, C.E.Seidman, and K.R.Chien. 1995. Divergent pathways mediate the induction of ANF transgenes in neonatal and hypertrophic ventricular myocardium. J Clin Invest 96: 1311-1318.

Kuwahara,K., Y.Saito, M.Takano, Y.Arai, S.Yasuno, Y.Nakagawa, N.Takahashi, Y.Adachi, G.Takemura, M.Horie, Y.Miyamoto, T.Morisaki, S.Kuratomi, A.Noma, H.Fujiwara, Y.Yoshimasa, H.Kinoshita, R.Kawakami, I.Kishimoto, M.Nakanishi, S.Usami, Y.Saito, M.Harada, and K.Nakao. 2003. NRSF regulates the fetal cardiac gene program and maintains normal cardiac structure and function. EMBO J. 22: 6310-6321.

Levin,E.R., D.G.Gardner, and W.K.Samson. 1998. Natriuretic peptides. N. Engl. J. Med. 339: 321-328.

Nemer,G. and M.Nemer. 2001. Regulation of heart development and function through combinatorial interactions of transcription factors. Ann. Med. 33: 604-610.

Olson,E.N. and M.D.Schneider. 2003. Sizing up the heart: development redux in disease. Genes Dev. 17: 1937-1956.

Rosenzweig,A. and C.E.Seidman. 1991. Atrial natriuretic factor and related peptide hormones. Annu. Rev. Biochem. 60: 229-255.

Schmitt,M., J.R.Cockcroft, and M.P.Frenneaux. 2003. Modulation of the natriuretic peptide system in heart failure: from bench to bedside? Clin. Sci. (Lond) 105: 141-160.

Seidman,C.E., E.V.Schmidt, and J.G.Seidman. 1991. cis-dominance of rat atrial natriuretic factor gene regulatory sequences in transgenic mice. Can. J. Physiol Pharmacol. 69: 1486-1492.

Seidman,C.E., D.W.Wong, J.A.Jarcho, K.D.Bloch, and J.G.Seidman. 1988. Cis-acting sequences that modulate atrial natriuretic factor gene expression. Proc Natl Acad Sci U S A 85: 4104-4108.

Shubeita,H.E., P.M.McDonough, A.N.Harris, K.U.Knowlton, C.C.Glembotski, J.H.Brown, and K.R.Chien. 1990. Endothelin induction of inositol phospholipid hydrolysis, sarcomere assembly, and cardiac gene expression in ventricular myocytes. A paracrine mechanism for myocardial cell hypertrophy. J. Biol. Chem. 265: 20555-20562.

Small,E.M. and P.A.Krieg. 2003. Transgenic analysis of the atrialnatriuretic factor (ANF) promoter: Nkx2-5 and GATA-4 binding sites are required for atrial specific expression of ANF. Dev. Biol 261: 116-131.

Temsah,R. and M.Nemer. 2005. Gata factors and transciptional regulation of cardiac natriuretic peptide genes. Regul Peptides 128: 177-185.

von Harsdorf,R., J.G.Edwards, Y.T.Shen, R.K.Kudej, R.Dietz, L.A.Leinwand, B.Nadal-Ginard, and S.F.Vatner. 1997. Identification of a cis-acting regulatory element conferring inducibility of the atrial natriuretic factor gene in acute pressure overload. J Clin Invest 100: 1294-1304.

Wharton,J., R.H.Anderson, D.Springall, R.F.Power, M.Rose, A.Smith, R.Espejo, A.Khagani, J.Wallwork, M.H.Yacoub, and J.M.Polak. 1988. Localization of atrial natriuretic peptide immunoreactivity in the ventricular myocardium and conduction system of the human fetal and adult heart. Br. Heart J. 60: 267-274.

Zeller,R., K.D.Bloch, B.S.Williams, R.J.Arceci, and C.E.Seidman. 1987. Localized expression of the atrial natriuretic factor gene during cardiac embryogenesis. Gene Dev. 1: 693-698.

Supplementary data

Supplementary materials and methods

Transgenic mice

Hprt-0.7rLacZ

Of the targeted Hprt-0.7rLacZ two independent transgenic lines were established in which we verified a single integration event at the Hprt locus by Southern blot. Both lines showed identical expression patterns.

-3mCre

To generate the -3mCre construct we truncated the -3/+4mCre construct upstream of the NRSE, by cloning the human growth hormone polyadenylation signal into the PvuI site located in the third exon of Nppa.

Bac336-Egfp and BAC337-Egfp

The two-step BAC modification protocol previously described by Shiaoching Gong and Nathaniel Heinz (Gong et al., 2002), consists of two homologous recombination steps. After both the co-integration and the resolution step correct recombination was verified by Southern blot using a hybridization probe against Egfp. The BAC-Egfp constructs were purified using a CsCl gradient following a protocol also kindly provided by Shiaoching Gong and Nathaniel Heinz.

-11/+5mEgfp

To generate the -11/+5mEgfp construct, we started with the modified BAC336-Egfp construct. Using conventional restriction enzymes we cloned a fragment reaching from the first natural Sal1 site at -11 kbp upstream of Nppa, to the first natural Xho1 site at +5 kbp downstream of Nppa.

From all short randomly integrated constructs vector sequences were removed and constructs were injected into pronuclei of zygotes of FVB mice and these were re-implanted into pseudo-pregnant foster mothers by use of standard techniques. Undigested circular BAC constructs were injected into pronuclei to generate transgenic mice.

Heart failure mouse model

Mice carrying the Hprt-0.7rLacZ or -3/+4mCre construct, or one of the modified BAC-Egfp clones, were crossed with the αMHC-Gal4 heart failure mouse previously described (Habets er al., 2003). Gal4 positive and double positive male offspring developed heart failure three

weeks after birth. When dyspnoea was diagnosed, mice were terminated. On postmortal examination all Gal4 positive male mice showed an enlarged heart and a swollen, yellowish liver, signs of heart failure with congestion. Atria and ventricles of double positive hearts and of Cre, LacZ or Egfp single positive hearts of littermates were separated and RNA was isolated using the Nucleospin RNA II kit (Macherey-Nagel, Düren, Germany) following the protocol of the manufacturer. First strand cDNA was synthesized using an optimized reverse transcription protocol (Lekanne Deprez et al., 2002).

Aortic banding

Transverse aortic constriction (TAC) was performed in 3- to 4-month-old mice, carrying the -3/+4mCre construct, or one of the modified BAC-Egfp clones. The aorta was subjected to a defined 25-gauge constriction between the first and second truncus of the aortic arch as described (Rockman et al., 1991). Aged-matched unbanded animals were used as controls. When discomfort (dyspnoe, decreasing mobility) was diagnosed between the 2^{nd} and 3^{rd} week after TAC, mice were terminated and heart tissue was collected. On postmortal examination all mice included in the qRT-PCR experiment had an enlarged heart and/or a stiffened, more solid appearance. RNA isolation and cDNA synthesis was performed as described above.

Animal care was in accordance with national and international guidelines.

Quantitative real time PCR

Quantitative real time PCR was performed using a LightCycler Real-Time PCR system (Roche Diagnostics, Almere, The Netherlands). The relative start concentration [N(0)] was calculated using the following equation: $N(0) = 10[\log(\text{threshold}) - Ct(\text{mean Eff})]$. Values were normalized to Gapdh expression levels.

Non-radioactive in situ hybridisation and β-galactosidase activity detection

Whole mount in situ hybridization, in situ hybridization on sections and whole mount and cryosection β-galactosidase activity staining were performed as described previously (Moorman et al., 2001; Franco et al., 2001).

Supplementary figures

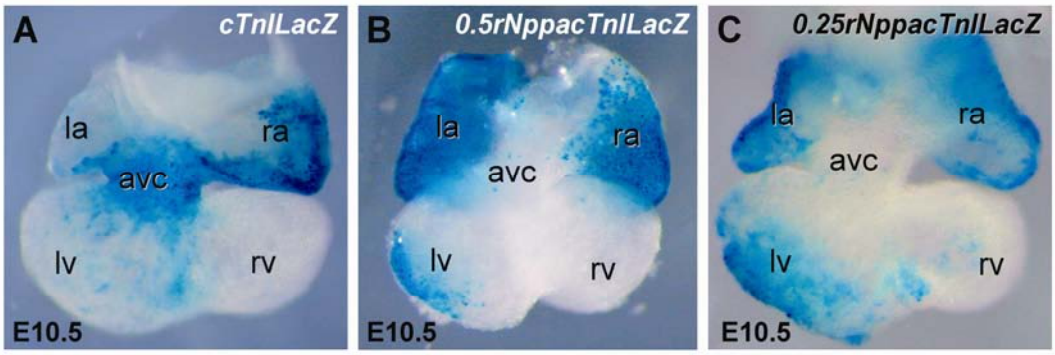

Supplementary Fig. 1. A 0.25 kbp 'atrial' regulatory module correctly represses *Nppa* in the AVC and drives atrial and residual ventricular expression. (A) A 356 bp *cTnI* promoter fragment is always expressed in the atrioventricular canal and only shows limited expression in the atria and ventricles. (B) As previously shown (Habets et al., 2002), a fragment of -638/-138 bp of the rat *Nppa* promoter is able to impose inhibition of expression upon the *cTnI* fragment in the atrioventricular canal, while increase of expression is observed in the atria and to a lesser extent in the ventricles. (C) All elements required to inhibit expression in the atrioventricular canal and to drive the atrial and ventricular expression reside within a 0.25 kbp module of the *Nppa* promoter. ra, right atrium; la, left atrium; rv, right ventricle; lv, left ventricle; avc, atrioventricular canal; oft, outflow tract.

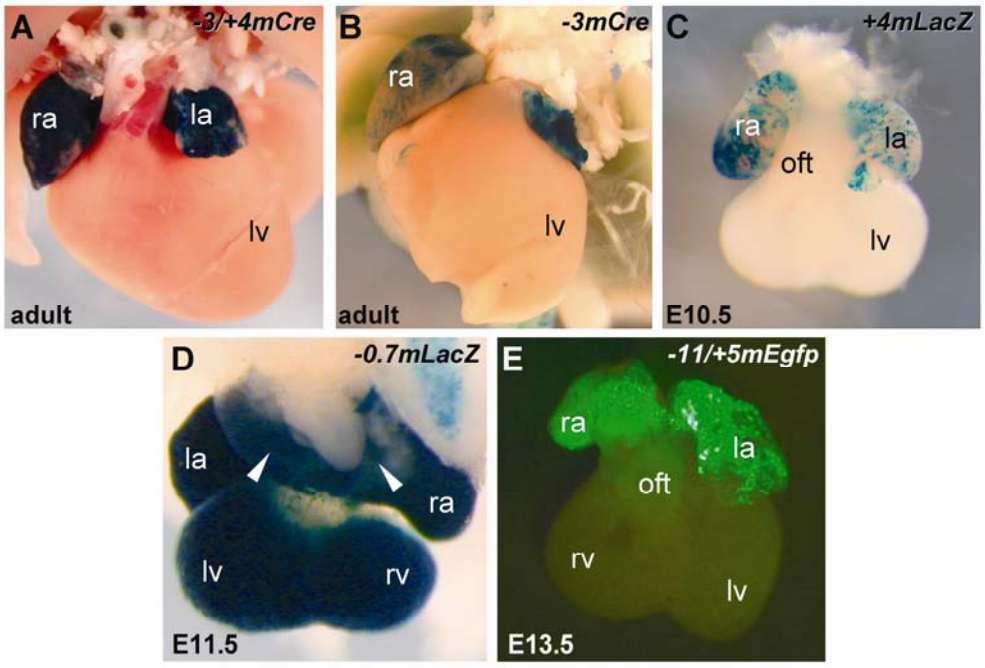

Supplementary Fig. 2. Correct ventricular expression requires distal regulatory sequences that reside outside a -11 to +5 kbp promoter fragment. (A) As previously shown (de Lange et al., 2003), extension of the promoter fragment to 7 kbp (*-3/+4mCre*) diminishes ventricular activity. This lack of activity is not caused by a specific ventricular repressor located either up- or downstream of the 0.7 kb proximal promoter fragment as indicated by the lack of ventricular activity in the *-3mCre* (B) and the *+4mLacZ* transgenes (C). (D) A mouse *-0.7mLacZ* promoter fragment behaves similarly as the rat *-0.7rLacZ* promoter fragment, with activity in both the atria and the ventricles and ectopic expression in the sinus horns. (E) A promoter fragment of 16 kbp (*-11/+5mEgfp*) does not drive any activity in the ventricles either. Arrowheads point at the sinus horns. See legend to supplementary Fig. 1 for other abbreviations.

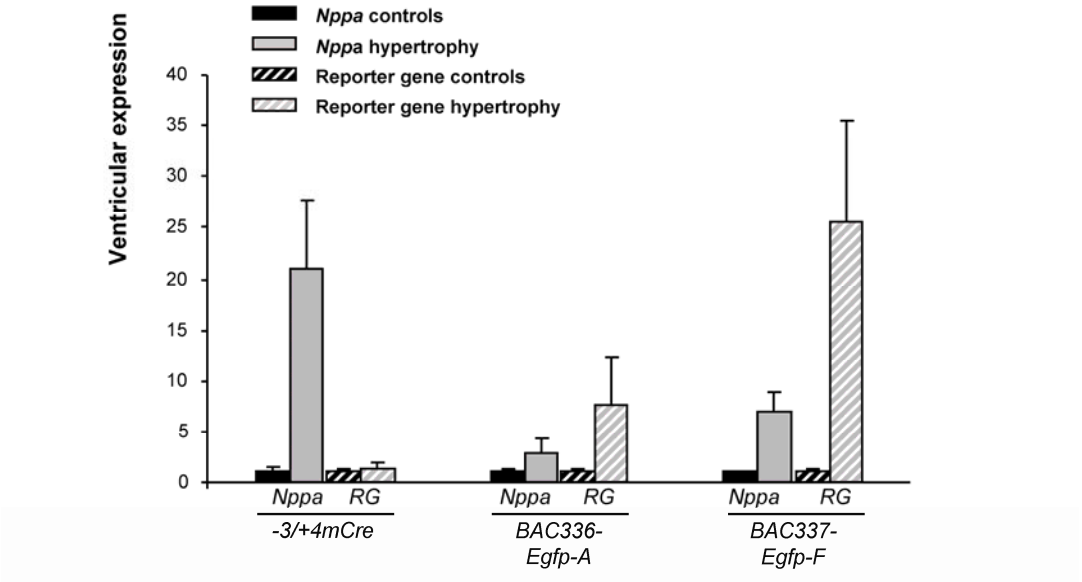

Supplementary Fig. 3. Induction of Nppa, BAC336-Egfp and BAC337-Egfp, but not the -3/+4Cre construct, in mice after induction of hypertrophy by transverse aortic constriction (TAC). In all mice carrying the BAC336-Egfp (n=3) or the BAC337-Egfp (n=3) construct, green fluorescent protein was visibly upregulated upon pressure overload. This finding was confirmed by quantitative RT-PCR. All groups >/=3. Error bars indicate SEM. RG, reporter gene.

References supplementary data

de Lange FJ, Moorman AFM, Christoffels VM. Atrial cardiomyocyte-specific expression of Cre recombinase driven by an Nppa gene fragment. *Genesis* 2003;37:1-4.

Franco D, de Boer PAJ, de Gier-de Vries C, Lamers WH, Moorman AFM. Methods on in situ hybridization, immunohistochemistry and b-galactosidase reporter gene detection. *Eur J Morphol* 2001;39(3):169-91.

Gong S, Yang XW, Li C, Heintz N. Highly efficient modification of bacterial artificial chromosomes (BACs) using novel shuttle vectors containing the R6Kgamma origin of replication. *Genome Res* 2002;12(12):1992-8.

Habets PEMH, Moorman AFM, Clout DEW, van Roon MA, Lingbeek M, Lohuizen M, Campione M, Christoffels VM. Cooperative action of Tbx2 and Nkx2.5 inhibits ANF expression in the atrioventricular canal: implications for cardiac chamber formation. *Genes Dev* 2002;16:1234-46.

Habets PEMH, Clout DEW, Lekanne Deprez RH, van Roon MA, Moorman AF, Christoffels VM. Cardiac expression of Gal4 causes cardiomyopathy in a dosedependent manner. *J Muscle Res Cell Motil* 2003;24:205-9.

Lekanne Deprez RH, Fijnvandraat AC, Ruijter JM, Moorman AFM. Sensitivity and accuracy of quantitative real-time polymerase chain reaction using SYBR green I depends on cDNA synthesis conditions. *Anal Biochem* 2002;307:63-9.

Moorman AFM, Houweling AC, de Boer PAJ, Christoffels VM. Sensitive nonradioactive detection of mRNA in tissue sections: novel application of the whole-mount in situ hybridization protocol. *J Histochem Cytochem* 2001;49:1-8.

Rockman HA, RossRS, Harris AN, Knowlton KU, Steinhelper ME, Field LJ, Ross J, Jr., Chien KR. Segregation of atrial-specific and inducible expression of an atrial natriuretic factor transgene in an in vivo murine model of cardiac hypertrophy. *Proc Natl Acad Sci U S A* 1991;88(18):8277-81.

Interplay between Tbx20, Tbx2/Tbx3 and Bmp/Smad-signaling controls compartmentalization of the developing heart tube into working chambers and the atrioventricular canal

Reena Singh[1#], Thomas Horsthuis[2#], Thomas Grieskamp[1], Willem M.H. Hoogaars[2,3], Henner F. Farin[1], Julia Norden[1], Marianne Petry[1], Henk Buermans[3], Vincent Wakker[2], Antoon F.M. Moorman[2], Peter A.C. 't Hoen[3], Vincent M. Christoffels[2] & Andreas Kispert[1]

#These authors contributed equally to the work

[1]Institut für Molekularbiologie, Medizinische Hochschule Hannover, 30625 Hannover, Germany, [2]Heart Failure Research Center, Academic Medical Center, 1105 AZ Amsterdam, The Netherlands, [3]Department of Human Genetics, Leiden University Medical Center, Leiden.

Submitted for publication in modified form

Abstract

The generation of efficient unidirectional blood flows in the mammalian heart relies on the functional compartmentalization into chambers separated by valves and septa. Here, we report on a genetic network involving the T-box transcription factor genes Tbx20, Tbx2 and Tbx3 and Bmp/Smad-signaling that coordinates the formation of the working chambers and the atrioventricular (AV) canal, from which the AV conduction system and the mesenchymal cushions, primordia of valves and septa, arise during cardiac development. We show that *Tbx2* and its close relative *Tbx3* are redundantly required and individually sufficient to specify AV myocardium, induce formation of the AV cushions and suppress chamber differentiation. *Tbx20* is required for chamber formation independently from *Tbx2*, but suppresses *Tbx2* in the developing chambers, thereby localizing its activity to the AV canal. We identified a Bmp/Smad-dependent enhancer conferring AV canal restricted expression and Tbx20-dependent chamber suppression of *Tbx2 in vivo*. Unexpectedly, Tbx20 does not repress expression of *Tbx2* and other genes by binding to DNA-elements, but attenuates Bmp/Smad-dependent activation by binding Smad1 and 5 and sequestering them from Smad4. Our findings suggest that opposing regulation of Bmp-signaling by Tbx20 and Tbx2 may underlie specification of the chambers and the AV canal, respectively.

Introduction

The complex multi-chambered heart of vertebrates arises from a simple tubular structure through a coordinated program of cellular differentiation and proliferation, and tissue morphogenesis. Elongation of this simple tube is supported by recruitment of precursor cells and differentiation into cardiomyocytes at the two poles. Highly localized processes of further myocardial differentiation and increased proliferation within the growing heart tube mediate the local out-bulging of the atrial and ventricular chambers. Regions separating and bordering the developing chambers retain low proliferation rates and slow impulse conduction and resist differentiation in a working type of myocardium, resulting in the generation of primitive morphological constrictions, the AV canal (AVC) and outflow tract, and a delay in AV conduction (Moorman and Christoffels 2003). The primary AV myocardium, from which the definitive AV node derives, induces the overlying endocardium to undergo an epithelial-mesenchymal transition (EMT) and to invade the cardiac jelly, an extracellular matrix that is deposited by the primary myocardium. These mesenchymal cushions are subsequently remodeled into thin valve leaflets and components of the septa (Person et al. 2005) that ensure structural and functional compartmentalization of the heart.

Formation of the initial heart tube from the cardiac crescent and further elongation of the tube from mesodermal progenitor pools, requires Bmp-signaling, which induces the differentiation into cardiomyocytes (Klaus et al. 2007; Yang et al. 2006). Bmp-signaling regulates expression of an evolutionary conserved network of transcription factor genes that drives the development of chambers and the differentiation of working myocardium therein (Klaus et al. 2007; Prall et al. 2007). Ablation of any member of the network, including Nkx2-5, Gata and Mef2 factors, and the T-box transcription factors Tbx5 and Tbx20 causes major heart defects and early developmental arrest. Mice homozygous mutant for *Nkx2-5* and *Tbx20* establish a heart tube with a primary myocardial phenotype but fail to undergo looping morphogenesis and to initiate chamber formation (Cai et al. 2005; Singh et al. 2005; Stennard et al. 2005; Takeuchi et al. 2005; Prall et al. 2007). *Tbx5* acts independently of *Tbx20* and maintains posterior domains of the heart (Bruneau et al. 2001). Both Tbx20 and Tbx5 synergize on the biochemical level with other members of the conserved network, Nkx2-5 and Gata4, to activate expression of chamber specific genes such as *Nppa* and *Cx40* (for a review see (Hoogaars et al. 2007a)).

Formation of the AVC again relies on Bmp-signaling (Sugi et al. 2004; Ma et al. 2005) and is elaborated and stabilized by other pathways (Rutenberg et al. 2006; Kokubo et al. 2007). Transcriptional repressor Tbx2 acts downstream of Bmp-signaling (Yamada et al. 2000) and regionally inhibits a chamber myocardial gene program in the AV canal by competing with activating T-box proteins such as Tbx5 for binding to conserved T-box binding elements (TBE)s in promoters of chamber specific genes (Habets et al. 2002; Christoffels et al. 2004b; Harrelson et al. 2004; Hoogaars et al. 2004; Chi et al. 2008). Tbx3 is genetically and functionally related to Tbx2, and suppresses chamber differentiation of the

sinus node, the AV bundle and bundle branches (Hoogaars et al. 2007b; Mommersteeg et al. 2007; Bakker et al. 2008). *Tbx2* and *Tbx3* expression overlaps in the AV canal, suggesting that functional redundancy has prevented a full appreciation of their role in the development of this tissue to date (Ribeiro et al. 2007; Bakker et al. 2008; Mesbah et al. 2008).

Although important signaling and transcriptional modules involved in the establishment of the cardiac components have been identified (Olson 2006; Dunwoodie 2007), the genetic hierarchies and the spatial and temporal interplay of these pathways have remained elusive. How for example Bmp-signaling, after inducing cardiogenesis, is redeployed to locally activate *Tbx2* expression and AV canal formation has remained unclear, as has the role of core cardiac transcription factors in orchestrating these morphogenetic processes. The observation that *Tbx2* is ectopically up-regulated in the entire embryonic heart tube of *Tbx20*-deficient embryos, possibly causing the block in chamber differentiation in *Tbx20*-deficient hearts, has suggested that Tbx20 is required to repress *Tbx2* for the progression to a multi-chambered heart (Cai et al. 2005; Singh et al. 2005; Stennard et al. 2005). Here, we present genetic experiments in the mouse that further decipher the molecular pathways that underlie localized formation of the chambers and the AV canal. We show that Tbx20 plays a dual role in compartmentalization of the heart. It stimulates chamber differentiation independently from *Tbx2* and simultaneously suppresses Bmp/Smad-dependent activation of *Tbx2* in the heart tube by a previously unrecognized DNA binding-independent mechanism, thereby restricting its expression to the prospective AVC region. Tbx2, together with Tbx3, subsequently impose the AV canal phenotype on this region of the heart tube. Together, our data provide insight into the hierarchical mechanisms underlying the spatial delimitation of a broadly active signaling pathway and its redeployment to compartmentalize the heart.

Materials and methods

Mice and genotyping

Mice carrying a null allele of Tbx20 ($Tbx20^{tm1Akis}$, synonyms: $Tbx20^{-}$, $Tbx20^{lacZ}$) (Singh et al. 2005), Tbx2 ($Tbx2^{tm1.1(cre)Vmc}$, synonyms: $Tbx2^{-}$, $Tbx2^{Cre}$) and/or Tbx3 ($Tbx3^{tm1.1(cre)Vmc}$, synonyms: $Tbx3^{-}$, $Tbx3^{Cre}$) (Hoogaars et al. 2007b) were maintained on an outbred (NMRI) background. The $Tbx2^{Cre}$ transgenic line, which harbors a Cre gene at the translation start site and from which the Pgk-neo cassette was removed, is a null allele that will be described elsewhere. For the generation of mutant embryos, heterozygous mice were intercrossed. For the generation of double mutant embryos, double heterozygous mice were intercrossed. For timed pregnancies, vaginal plugs were checked in the morning after mating, noon was taken as embryonic day (E) 0.5. Embryos were harvested in PBS, fixed in 4% paraformaldehyde overnight and stored in 100% methanol at –20^{o}C before further use. Wild-type littermates were used as controls. CAG-CAT-TBX3 (CT) and Nppa-Cre4 (Cre4) transgenic mice have

been described (Hoogaars et al. 2007b). Double-transgenic mice conditionally expressing TBX3 in the atria were generated by crossing CT mice with Cre4 mice. Genomic DNA prepared from yolk sacs or tail biopsies was used for genotyping by PCR (Details are available on request).

An expanded Materials and Methods section is available in the online data supplement and included at the end of this chapter.

Results

Tbx20 is required for chamber formation, whereas Tbx2 stimulates cardiac jelly formation

Previous analysis has shown that ectopic expression of *Tbx2* in the simple heart tube leads to arrest of cardiogenesis (Christoffels et al. 2004b). To test the hypothesis that ectopic *Tbx2* expression is responsible for the observed block in chamber differentiation in *Tbx20*-deficient hearts (Cai et al. 2005; Singh et al. 2005; Stennard et al. 2005), we generated embryos with combined deficiencies of *Tbx2* and *Tbx20* by interbreeding double heterozygous animals. Similar to *Tbx20* single mutants, $Tbx20^{lacZ/lacZ};Tbx2^{Cre/Cre}$ embryos were severely growth retarded and died at E10.5 due to hemodynamic failure (data not shown). At E9.5, when cardiac chambers were clearly delineated in wild-type embryos, *Tbx20* single mutant and *Tbx20/Tbx2* double mutant embryos featured a simple heart tube (Fig. 1A-C). On histological stainings of sagittal sections both myocardium and endocardium appeared homogenously thin throughout the $Tbx20^{lacZ/lacZ};Tbx2^{Cre/Cre}$ heart tube that sometimes appeared dilated. This is in contrast to $Tbx20^{lacZ/lacZ}$ hearts, where a thick layer of cardiac jelly filled the space between myocardium and endocardium. Cardiac jelly production was not associated with endocardial EMT and cushion formation in the $Tbx20^{lacZ/lacZ}$ linear heart tube as revealed by histological inspection as well as expression analysis of cushion markers *Sox9* (Akiyama et al. 2004) and *Msx2* (Abdelwahid et al. 2001) (Fig. 1D-F and data not shown). Molecular analysis using markers with differential expression along the linear heart tube (*Tbx5, Myh7*) (Bruneau et al. 1999;Christoffels et al. 2000) confirmed that anterior-posterior patterning occurred normally in $Tbx20^{lacZ/lacZ};Tbx2^{Cre/Cre}$ hearts (Fig. 1G-L). Chamber myocardium, however, was not formed, as shown by absence of expression of *Nppa* (*Anf*) and *Cited1* (Fig. 1M-R). *Bmp2* that is expressed in the primary myocardium of the AV canal in the wild-type (Ma et al. 2005), was found throughout the tubular heart of single and double mutant embryos (Fig. 1S-U). In summary, loss of *Tbx2* does not rescue the *Tbx20*-deficient heart from developmental arrest at the linear heart tube stage, but results in loss of cardiac jelly formation. These data show that *Tbx20* is a critical factor in cardiac chamber development, and that *Tbx2* is sufficient to induce the first step in cushion formation, the production of a thick layer of cardiac jelly in the developing heart.

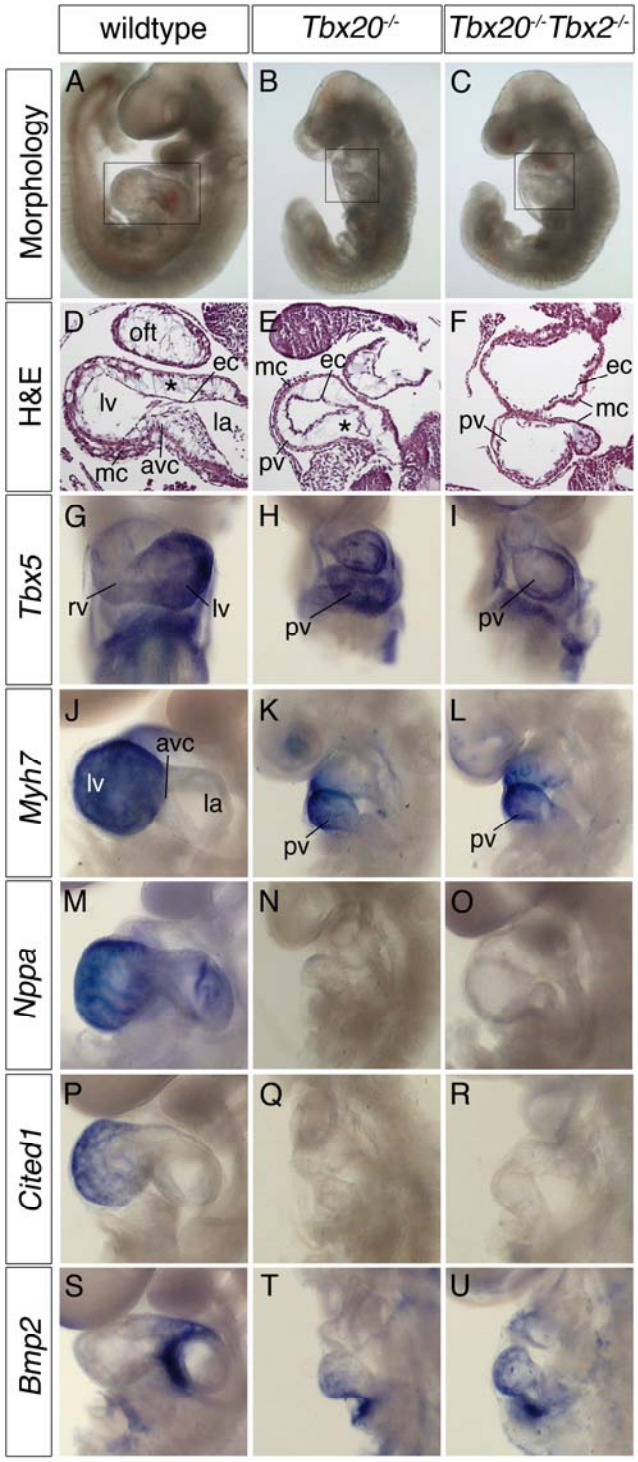

Figure 1. Loss of *Tbx2* does not rescue cardiac arrest of *Tbx20*-deficient mice. Comparative analysis of wild-type, *Tbx20*$^{-/-}$ and *Tbx20*$^{-/-}$*Tbx2*$^{-/-}$ embryos for cardiac morphology, histology and molecular marker expression at E9.5. (*A-C*) Left lateral views of whole E9.5 embryos reveal growth retardation and linear heart tube phenotype in *Tbx20/Tbx2* double mutants similar to *Tbx20*-deficient embryos. Boxes mark the heart regions to be magnified in the following images. (*D-F*) Histological analysis of sagittal sections by hematoxylin and eosin (H&E) staining uncovers loss of cardiac jelly and cushion tissue (asterisk) in the *Tbx20/Tbx2*-deficient linear heart tube that appears as a slightly inflated sac. (*G-U*) *In situ* hybridization analysis of marker gene expression in whole embryos with probes as indicated. avc, atrioventricular canal; ec, endocardium; la, left atrium; lv, left ventricle; mc, myocardium; oft, outflow tract; pv, primitive ventricle; rv, right ventricle.

Tbx2 and Tbx3 are cooperatively required for myocardial patterning and formation of cushion mesenchyme in the AV canal

Previous analyses indicated that *Tbx2* is necessary and sufficient to suppress chamber gene expression in the AV canal (Christoffels et al. 2004b; Harrelson et al. 2004). However, in our *Tbx2* loss-of-function mouse AV canal formation at E9.5 was grossly normal, and *Nppa* and other chamber markers were not ectopically expressed in the AV canal (Fig. 2F,J,N).

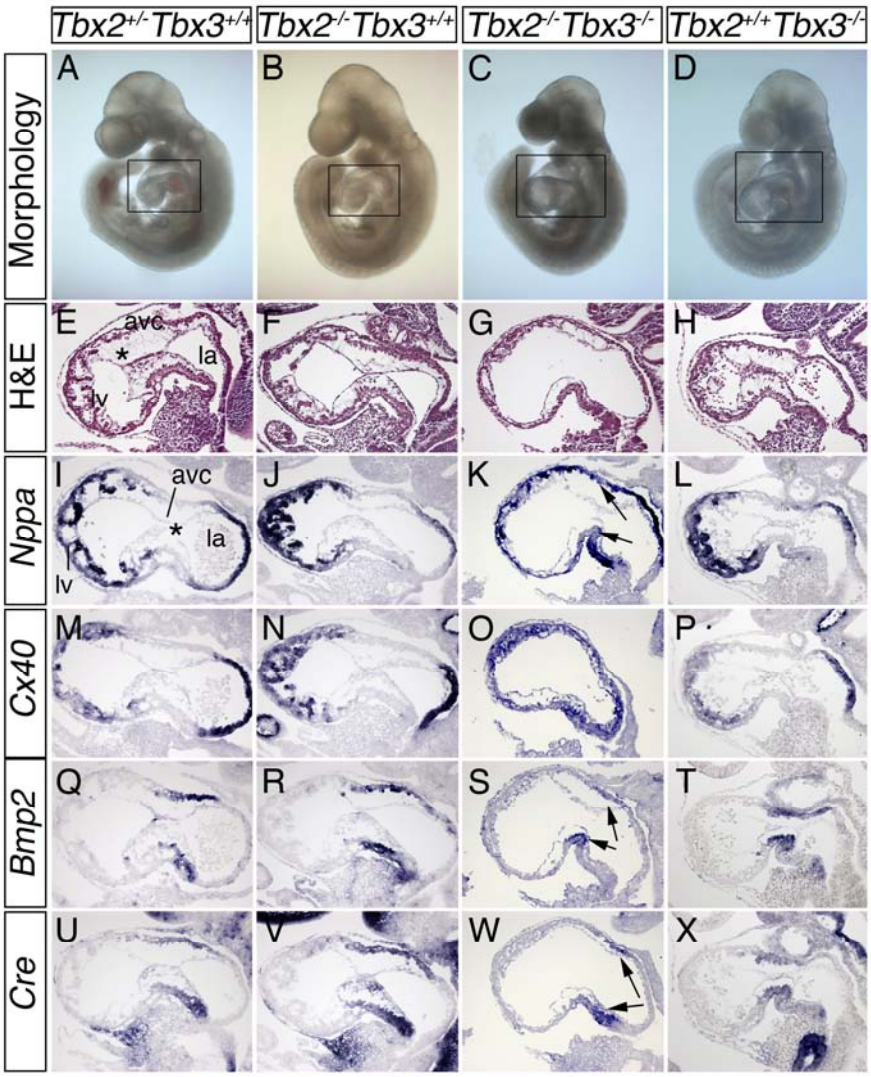

Figure 2. Combined loss of *Tbx2* and *Tbx3* abrogates cushion formation and myocardial patterning in the atrioventricular canal. Comparative analysis of wild-type, *Tbx2*$^{-/-}$, *Tbx2*$^{-/-}$*Tbx3*$^{-/-}$ and *Tbx3*$^{-/-}$ embryos for cardiac morphology, histology and molecular marker expression at E9.5. (*A-D*) Left lateral views of whole E9.5 embryos reveal growth retardation and dilated avc phenotype in *Tbx2/Tbx3* double mutant embryos. Boxes mark the heart regions to be magnified in the following images. (*E-H*) Histological analysis of sagittal sections through the left atrium (la), atrioventricular canal (avc) and left ventricle (lv) by hematoxylin and eosin (H&E) staining uncovers loss of cardiac jelly and cushion tissue (asterisk) in the avc of *Tbx2/Tbx3*-deficient hearts. (*I-X*) In situ hybridization analysis of marker gene expression in sagittal sections through the avc with probes as indicated. Abbreviations are as in Fig.1.

However, co-expression with the close family member *Tbx3* in the AVC myocardium argues that functional redundancy precludes full appreciation of *Tbx2/Tbx3* requirement in this region. We therefore aimed to generate mice double mutant for *Tbx2* and *Tbx3*. Mice double heterozygous for *Tbx2* and *Tbx3* null alleles are afflicted with craniofacial defects that lead to early postnatal lethality (unpubl. observ.). Breeding onto an NMRI wild-type background partially rescued this phenotype so that double heterozygous mice could be interbred. Since pregnancies were badly maintained in these mothers, we obtained only a total of four viable *Tbx2/Tbx3* double homozygous embryos from few litters at E9.5. These embryos appeared slightly retarded in their development, most likely due to arising hemodynamic failure. Morphologically, the constriction between the left ventricle and the atrium in the wild-type was largely absent (Fig. 2C). Histologically, the AV canal appeared as an inflated tube with little investment of cardiac jelly, and, in contrast to the other genotypes, complete absence of cushion tissue (Fig. 2G). Markers of chamber myocardium (*Nppa*, *Gja5* (*Cx40*)) (Christoffels et al. 2004a) were expanded into this region, whereas markers for primary myocardium of the AV canal, *Bmp2* (Ma et al. 2005) and *Cre* from the mutant alleles reflecting endogenous *Tbx2* and *Tbx3* expression, were present but reduced in their expression levels and spatial extent (Fig. 2I-X). A similar phenotype was observed in compound mutants with loss of three functional alleles of *Tbx2* and *Tbx3* (Suppl. Fig. 1), whereas *Tbx2* and *Tbx3* single mutants showed normal cushion formation and proper chamber gene repression in the AV canal (Fig. 2). Hence, *Tbx2* and *Tbx3* are required in a redundant fashion to maintain, expand and differentiate the primary myocardium of the AV canal, and to induce the formation of cushion tissue from the endocardium in this region.

Tbx3 regulates the AV myocardial gene program

The difficulty in obtaining a sufficiently high number of $Tbx2^{Cre/Cre};Tbx3^{Cre/Cre}$ embryos for a more detailed analysis of the molecular consequences of combined loss of *Tbx2* and*Tbx3,* prompted us to use a complimentary gain-of-function approach to further elucidate the role of these factors in AV canal development. We used ectopic expression of *Tbx3* in the atrial myocardium that we have previously shown to be powerful in achieving molecular insight into cardiac *Tbx3* function (Hoogaars et al. 2007b). *Nppa-Cre4* (*Cre4*) mice were crossed with *CT* mice to obtain permanent activation of *Tbx3* in atrial chamber myocardium from E10.5 onwards in double transgenic *Cre4;CT* mice (Hoogaars et al. 2007b). Micro-array analysis comparing the transcriptome of atria of adult *Cre4;CT* and *Cre4* males confirmed earlier findings of strong reduction in expression of the known chamber genes *Nppa*, *Smpx (Chisel)*, *Scn5a* (*Nav1.5*), *Kcnj3* (*Kir3.1*), *Gja1* (*Cx43*) and *Gja5* (*Cx40*) in *Tbx3*-expressing atria of *Cre4;CT* mice (Hoogaars et al. 2007b), and additionally revealed down-regulation of *Ckm, Nppb*, *Bmp10*, *Ednra* and *Aldh1b1* (Suppl. Table 1). qRT-PCR and *in situ* hybridization analysis confirmed normal chamber restricted expression and Tbx3-mediated atrial repression of *Ckm* (Wessels et al. 1990), *Nppb* (Houweling et al. 2005), *Aldh1b1* and *Ednra* (Clouthier et

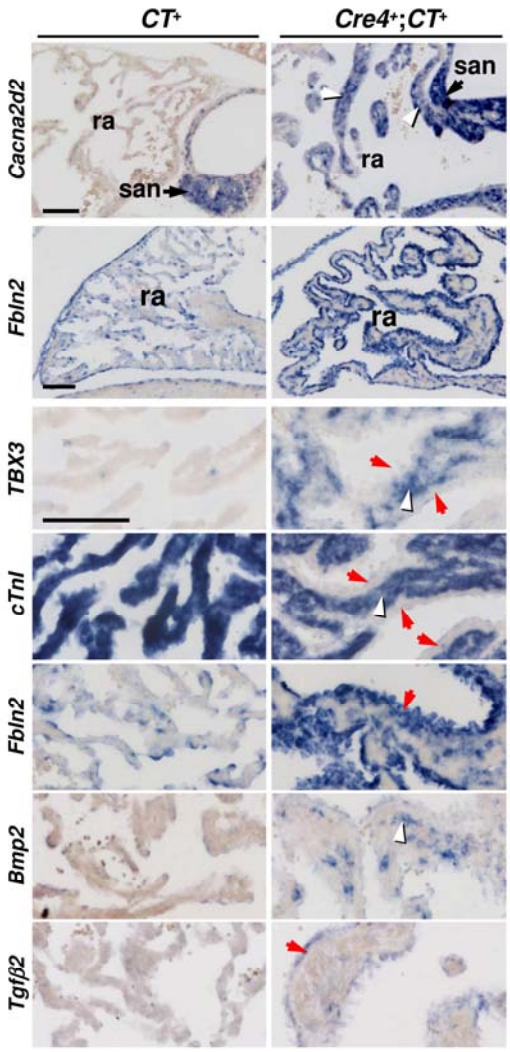

Figure 3. Myocardial Tbx3 expression induces endocardial mesenchyme formation and nodal gene expression. Sections of E17.5 atria of *CT* and *Cre4;CT* mice were probed for expression of indicated genes. Note the reduced complexity and smoothness of the pectinated muscle structure in atria of *Cre4;CT* fetuses. Black arrow head indicates sinus node (san), white arrow head the myocardium in which *Cacna2d2,* transgenic *TBX3* and *Bmp2* expression was seen to be induced in *Cre4;CT* atria. Red arrow heads depict the thick endocardial mesenchymal layer that forms in *Cre4;CT* atria, that is devoid of myocardial gene expression (*cTnI*), but expresses *Fbln2* and *Tgfβ2*. Black bar, 100μm.

al. 1998), and of *Bmp10* (Neuhaus et al. 1999) (Fig. 4, Suppl. Fig. 2). Furthermore, the micro-array data uncovered that atria of *Cre4;CT* mice had reduced expression of genes involved in muscle contractility, such as sarcomere complex genes (e.g. *Myh6*, *Myh7*, *Myh14*, *Myoz2*, *Acta1*, *Tnni2*, *Ttn*, *Dsg2*, *Tmod4*, *Myom1*, *Myom2)*, and genes associated with mitochondria and their energy metabolism, consistent with the less pronounced myofibrillar differentiation and reduced mitochondria number of conduction system compared to working cardiomyocytes (Dehaan 1961).

Previously, we observed that nodal conduction system genes *Hcn1*, *Hcn4*, *Cx30.2*, *Cav3.1* and *Lbh* are induced in *Cre4;CT* mice (Hoogaars et al. 2007b), indicating that Tbx3 stimulates the nodal gene program. Micro-array analysis and subsequent validation by qRT-

PCR and/or *in situ* hybridization revealed induction of additional genes in *Cre4;CT* atria including *Cx45, Itpr1, Slco3A1, Id2, Cacna2d2,* and *Hnt* (Fig. 4). These genes are enriched in the conduction system components, including the AV node, and associated with (*Slco3A1, Cacna2d2, Hnt*) or involved in the formation (*Id2*) or function (*Cx45*, *Itpr1*) of the conduction system (Gorza et al. 1993; Coppen et al. 1999; Kreuzberg et al. 2005; Mery et al. 2005; Moskowitz et al. 2007) (Fig. 3, 4A,B). Together, these data indicate that Tbx3 is able to suppress a large number of chamber genes that are reduced in the AV canal and conduction system, and to induce AV canal-enriched genes implicated in conduction system specification or function.

Tbx3 induces sub-endocardial mesenchyme formation and Bmp-signaling

Histological analysis of *Cre4;CT* atria and controls at E17.5 revealed that the pectinated muscles, trabecule-like structures in the atrial appendages, were abnormally thick, smooth and uncomplicated and that a thick sub-endocardial layer of cells had formed (Fig. 3). This tissue expressed mesenchymal marker genes including *Acta2/αSMA*, *Fbln2, Cspg2/Versican* and *Lumican* (Fig. 3, 4A, Suppl. Table 1) that are associated with AV cushions. In addition, micro-array analysis and *in situ* hybridization revealed strong activation of components of the Tgfß-, Bmp-, Fgf- and Wnt-signaling pathways that have been functionally implicated with AV cushion and valve formation (Armstrong and Bischoff 2004; Person et al. 2005). Notably, we detected induction of *Bmp2* expression in the myocardium, and of *Bmp4* in endocardial layers of *Cre4;CT* mice (Fig. 3, 4A). Since *Bmp2* expression in the AV canal myocardium is both required and sufficient to induce cushion formation (Yamagishi et al. 1999; Sugi et al. 2004; Ma et al. 2005), Bmp2 is likely to be a pivotal downstream mediator of cushion induction by Tbx3. *Tgfß2*, a Bmp2 target in this tissue that is required for cushion formation (Camenisch et al. 2002; Mercado-Pimentel and Runyan 2007) was upregulated in the endocardium (Fig. 3, 4A). In addition, qRT-PCR and *in situ* hybridization analyses confirmed expression of genes in the endocardial mesenchymal layer of *Cre4;CT* mice (*Twist1*, *Msx1*, *Meox1*, *Sox9, Id3* and *Smad6)* (Fig. 4, Suppl. Fig. 2 and 3, Suppl. Table 1), whose expression and functional relevance in EMT and cushion formation in the AV canal have been reported (Galvin et al. 2000; Akiyama et al. 2004; Ma et al. 2005; Lincoln et al. 2006; Chen et al. 2008; Shelton and Yutzey 2008). Furthermore, expression of *Fgfr2*, and of Wnt antagonists *Frzb*, *sFRP2* and *Nkd2* were up-regulated in atria of *Cre4;CT* mice, compatible with the known role for Fgf- and Wnt-signaling in cushion and valve formation (Gitler et al. 2003; Hurlstone et al. 2003; Sugi et al. 2003; Person et al. 2005) (Suppl. Fig. 2, 3). *Pkd2* is normally expressed in the developing valves and was induced in atrial mesenchyme of *Cre4;CT* mice. (Fig. 4A). In human and mouse, mutations of *Pkd2* result in valve abnormalities (Wu et al. 2000; Stypmann et al. 2007). Finally, we identified additional 47 induced genes in the micro-array data whose specific expression in the fetal AV valvular mesenchyme was reported by Genepaint (http://www.genepaint.org/) (Suppl. Table 2).

In summary, these data show that ectopic myocardial expression of *Tbx3* is sufficient to induce the mesenchymal transition of endocardial cells and the formation of AV cushion tissues. Hence, Tbx3 collectively regulates the genetic circuits of signaling pathways and transcriptional activities mediating these processes.

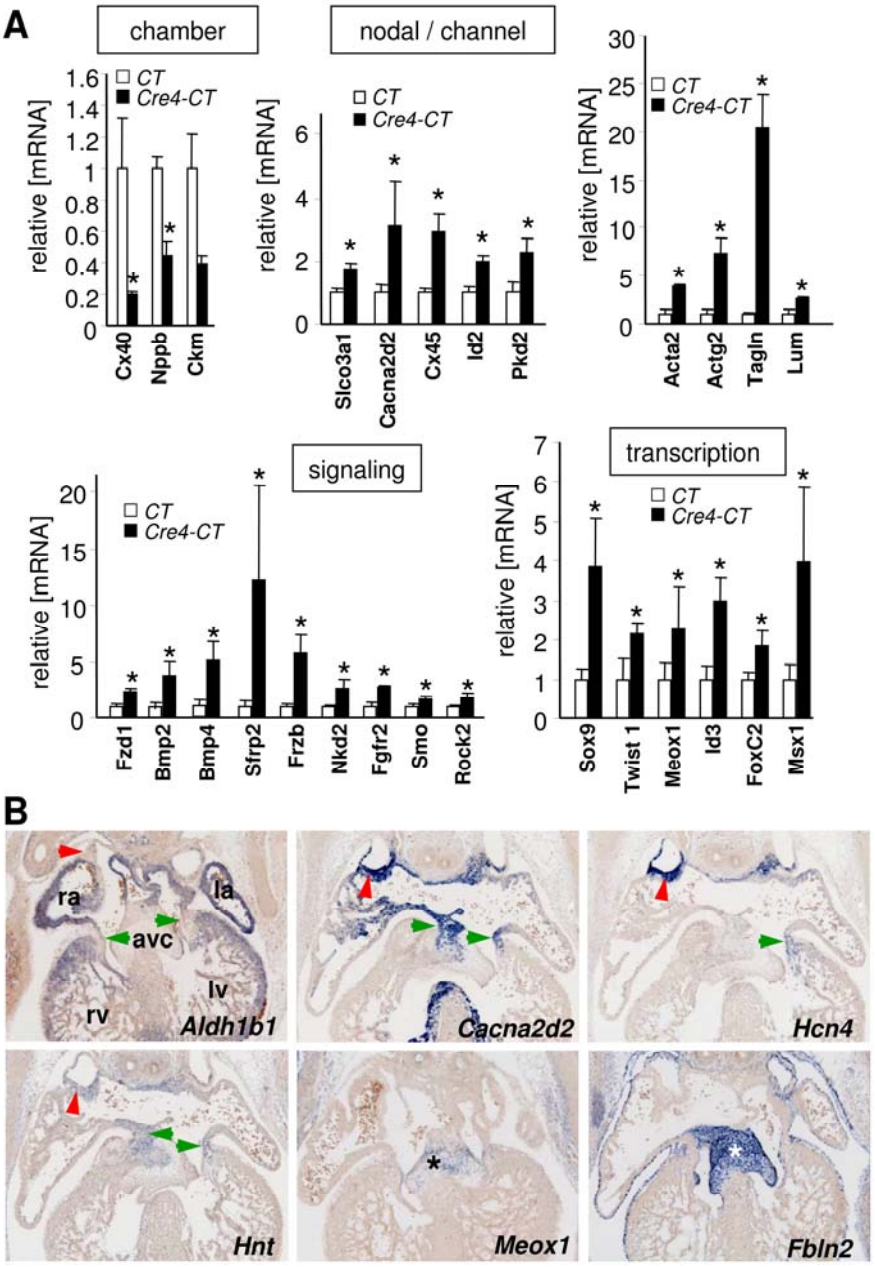

Figure 4. Tbx3 suppresses chamber-specific genes and induces genes involved in cardiac cushion formation and conduction system function. (*A*) qRT-PCR analysis of left atria of *Cre4-CT* double transgenic mice compared to *CT* control mice. Expression levels in *CT* atria were set to 1. Expression of chamber-specific genes was reduced, whereas genes associated with conduction system were induced (nodal/channel). Genes encoding signaling proteins and transcription factors involved in cardiac cushion formation and valve development were induced in atria of *Cre4-CT* mice. Error bars represent SD (n=4 per group). *P<0.05. (*B*) Cross-sections of E12.5 mouse hearts showing expression of genes up-regulated in *Cre4;CT* atria (micro-array) in the developing AV canal and AV cushions and valves.

Regulation of cardiac Tbx2 expression by Bmp/Smad-signaling and Tbx20

To gain insight into the molecular pathways that confine *Tbx2* expression to the developing AVC, we functionally examined the *Tbx2* regulatory region. We first tested a 6 kbp genomic fragment previously shown to mediate AVC expression (Kokubo et al. 2007), and found that Eyfp reporter gene expression driven by this fragment in transgenic animals recapitulated endogenous cardiac expression of *Tbx2* in the AV canal and outflow tract in E9.5 to E11.5 wild-type embryos. Since this fragment also conferred ectopic expression in *Tbx20*-deficient hearts (Fig. 5A-G), all elements required for control of cardiac *Tbx2* expression reside within this genomic DNA fragment that contains several phylogenetically conserved regions (Fig. 5A, Suppl. Fig. 4). Deletion analysis of this fragment showed that the previously identified TBE recognized by Tbx20 (Cai et al. 2005) is neither required for AV canal and outflow tract-specific expression nor Tbx20-mediated repression. We identified a 0.9 kbp genomic fragment located 2.3 kbp upstream of the transcriptional start site, that in combination with a minimal promoter piece of 0.6 kbp (*-1.5mTbx2*) recapitulated cardiac expression of *Tbx2* in wild-type and up-regulation in *Tbx20*-deficient embryos faithfully (Fig. 5H-J, Suppl. Fig. 5). Recent reports have pinpointed the relevance of conserved Foxn and additional TBE sites in the zebrafish *tbx2b* promoter for activation of the gene in the AV canal (Chi et al. 2008). Moreover, ß-catenin has been shown to regulate Tbx3, the T-box factor most closely related to Tbx2, in cancer cells by direct binding to a Lef/Tcf site (Renard et al. 2007). A 1.5 kbp genomic fragment deprived of these conserved sites still drove reporter gene expression to the AV canal and outflow tract, negating a role for T-box factors, Lef/Tcf proteins and Fox transcription factors in regulating cardiac *Tbx2* expression on the DNA level in the mouse (Fig. 5A, Suppl. Fig. 5). However, this *-1.3mTbx2* genomic fragment contained a large number of putative Smad binding sites (SBE), supporting a role of Bmp-signaling in the regulation of cardiac *Tbx2* expression (Suppl. Fig. 4). Taken together, this analysis indicates that a small SBE-containing enhancer in *Tbx2* is sufficient to drive AV canal expression *in vivo*.

We switched to *in vitro* reporter assays in NIH3T3 cells to further investigate the precise role of Tbx20 in conjunction with Bmp/Smad-signaling in cardiac *Tbx2* expression (Fig. 5K,L). We used expression constructs for full-length mouse proteins for Smad5, the constitutively active Bmp receptor Alk3 (Alk3CA) (Wessely et al. 2001) and HA-tagged Tbx20, and a reporter plasmid containing the luciferase reporter gene downstream of the 6 kbp *Tbx2* genomic fragment in these transactivation assays. We observed a strong activation of reporter gene activity upon co-expression of Smad5 and Alk3CA and a reduction to basal activity in the presence of increasing concentrations of Tbx20 (Fig. 5L). Deletion analysis of the *Tbx2* promoter fragment revealed the requirement of a 0.9 kbp *NheI/AflII* fragment for Bmp/Smad-dependent activation of the promoter (Fig. 5K, Suppl. Fig. 6). Since this fragment was found to be sufficient to confer AV canal/outflow tract expression of Eyfp *in vivo*, Bmp/Smad-signaling is likely to activate cardiac *Tbx2* expression *in vivo*. Removal of previously identified TBEs (Cai et al. 2005) did not affect the repression activity of Tbx20 on

the promoter (Fig. 5K, Suppl. Fig. 6). This may suggest the presence of cryptic DNA binding sites for Tbx20. Alternatively, repression by Tbx20 may not be mediated by DNA binding but by protein interaction. To test the latter, we constructed point mutants of Tbx20 that do not exert specific DNA binding any more (Suppl. Fig. 7B,C). Unexpectedly, these mutant Tbx20 proteins still repressed transactivation of the 6 kbp *Tbx2* fragment by Bmp/Smad- signaling

Figure 5. Bmp/Smad-signaling controls cardiac expression of *Tbx2*. *In vivo* and *in vitro* reporter analyses of the control of cardiac *Tbx2* expression. (*A*) Phylogenetic analysis of a 6 kbp genomic region upstream and around the *Tbx2* transcription start site for conserved sequences. The location of conserved T-box binding elements (TBE) and Foxn sites is marked by boxes. Deletion constructs of the 6 kbp *Tbx2* genomic fragment used in vivo to drive Eyfp reporter expression. Presence (+) and absence (-) of Eyfp expression from these deletion constructs in the atrium (A), atrioventricular canal (AVC), ventricle (V) and outflow tract (OFT) in transgenic mouse embryos. Numbers indicate cardiac expression of Eyfp and the number of transgenic embryos analyzed (Card. expr/tg) and extracardiac expression domains detected in the same embryos (Extra card. exp/tg). A 0.9 kbp *NheI*/*AflII* fragment from the *Tbx2* locus contains elements sufficient and required to drive reporter gene activity in the regions of primary myocardium. (*B-J*) Comparative analysis of *Tbx2* mRNA expression (*B-D*), Eyfp activity from the 6.0 kbp *Tbx2* genomic region in transgenic embryos (*E-G*), and Eyfp activity from the 1.5 kbp *Tbx2* genomic region in transgenic embryos (*H-J*) in E9.5 wild-type embryos (*B,E,H*, arrows point to the AVC), E10.5 hearts (*C,F,I*), and E9.5 *Tbx20*-deficient embryos (*D,G,J*, arrows point to mutant linear heart tube). (*K*) In vitro reporter assays to detect transcriptional activation of a luciferase reporter from *Tbx2* genomic fragments. Plasmids encoding constitutively active Bmp receptor Alk3, full length Smad5 protein, full length Tbx20 protein and the luciferase reporter construct were co-transfected in NIH3T3 cells and luciferase activity determined and normalized as fold over the reporter alone. Presence (+) and absence of activation (-) by Bmp/Smad-signaling and repression by Tbx20 is listed for the constructs tested. (*L*), Luciferase reporter assay for the 6 kbp *Tbx2* genomic fragment. Numbers indicate µg of plasmids for the reporter *-6.0mTbx2-luc*, and the expression plasmids for Alk3CA, Smad5, Tbx20 and the non-DNA binding Tbx20 protein (Tbx20 mut) co-transfected into NIH3T3 cells. Reporter activation upon co-transfection of expression constructs for Alk3CA and Smad5 is inhibited by co-expression of Tbx20, independent of its ability to bind to DNA.

both in presence and absence of transfected Smad5 in co-transfection experiments (Fig. 5L). Repression achieved by the DNA-binding deficient mutant of Tbx20 was lower than with the wild-type protein suggesting the co-existence of DNA-binding dependent and independent mechanisms for Tbx20 protein in the regulation of *Tbx2* (Fig. 5L). Together, our analyses of the *Tbx2* promoter argue that temporal and spatial confinement of cardiac *Tbx2* expression is achieved by Tbx20-dependent repression of Bmp/Smad-mediated transcriptional activation.

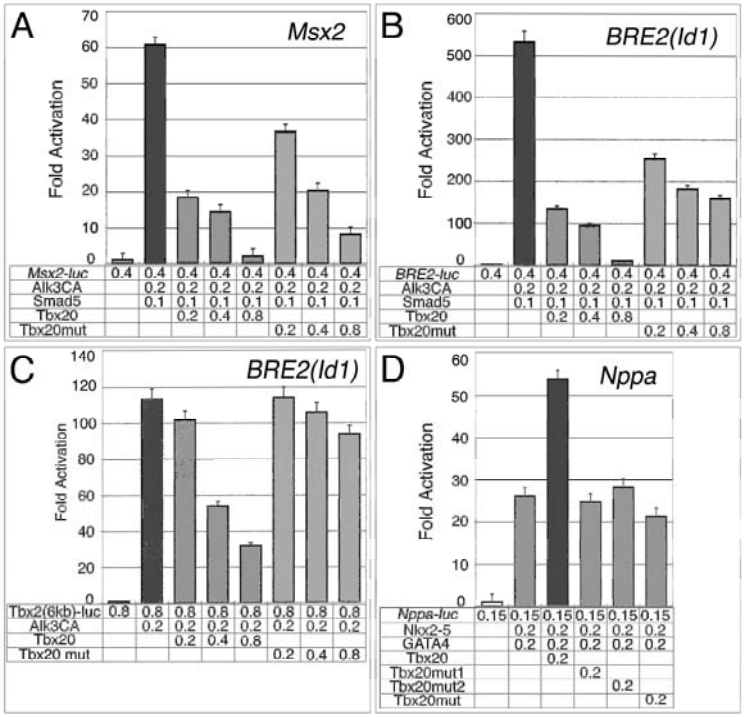

Figure 6. Tbx20 inhibits Bmp/Smad-mediated transcriptional activation. (*A-D*) Luciferase reporter assays on a 0.7 kbp *Msx2* genomic fragment (*A*), a 91 bp array of Smad bindings sites derived from the *Id1* promoter (*B,C*), and the 0.7 kbp *Nppa* promotor fragment (D). Numbers indicate µg of plasmids for the luciferase reporter plasmids, and the expression plasmids for Alk3CA, Smad5, Tbx20 and the non-DNA binding Tbx20 proteins Tbx20mut1 (L126R), Tbx20mut2 (L127R) and Tbx20mut (LL126,127RR) co-transfected into NIH3T3 cells. Wild-type as well as the DNA-binding dead mutant Tbx20 protein inhibit dose-dependently activation by Bmp/Smad whereas the Tbx20 protein activates the Bmp/Smad-independent *Nppa* promoter.

Tbx20 inhibits transcriptional activation of Bmp/Smad-dependent promoters in a DNA-independent manner

We wondered whether the repressive effect of Tbx20 on Bmp/Smad-dependent transcriptional activation might be of a more general nature. We tested minimal fragments of *Msx2* and *Id1* promoters known to be activated by Smad binding in transactivation experiments in NIH3T3 cells (Brugger et al. 2004; Monteiro et al. 2004) (Fig. 6A-C). Both Tbx20 wild-type and Tbx20 DNA-binding mutant proteins repressed Bmp/Smad-mediated activation of *Msx2* and *Id1* promoter in a dose-dependent manner. Repression was independent from the addition of

exogenous Smad5 since it was also observed when cells were only transfected with constructs for Alk3CA. As in the case of the *Tbx2* promoter, repression by the DNA binding-deficient mutant form of Tbx20 did not reach the level of the wild-type protein suggesting participation of direct transcriptional activities of Tbx20 wild-type protein in these assays. Wild-type Tbx20 protein acted as a DNA-dependent transcriptional activator on the Bmp/Smad-independent *Nppa* promoter (Habets et al. 2002) while the Tbx20-mutant protein did not show a transcriptional effect in this context (Fig. 6D). Hence, Tbx20 acts as a transcriptional activator of Bmp/Smad-independent promoters but as an inhibitor of Bmp/Smad-mediated transactivation.

DNA binding-independent inhibition of Bmp/Smad-mediated transactivation by Tbx20

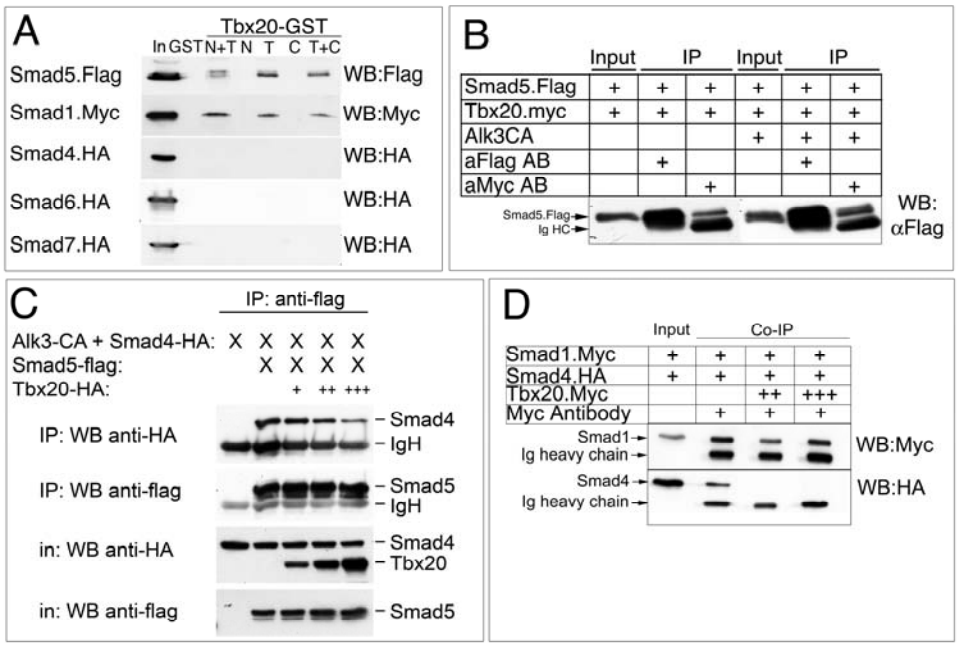

Figure 7. Tbx20 inhibits Bmp/Smad-signaling in a DNA-independent manner by binding to activating Smad1 and Smad5 proteins. (*A*) Pull-down of in vitro synthesized Flag-tagged Smad5, Myc-tagged Smad1 and HA-tagged Smad4, Smad6, and Smad7 proteins by GST fusion proteins bound to GSH-agarose beads and subsequent detection by anti-Flag, anti-Myc and anti-HA immunohistochemistry on Western blot. All GST fusion proteins harboring a T-domain retain Smad5 and Smad1 proteins on the column. (*B*) Co-immunoprecipitation of Myc-tagged Tbx20 and Flag-tagged Smad5 from HeLa cells co-transfected with expression constructs for the two proteins in presence and absence of an expression construct for constitutively active Bmp receptor Alk3 (Alk3CA). Arrow indicates the presence of Smad5 protein after IP with anti-Myc antibody and subsequent detection with anti-Flag antibody. The lower band in the Western blot represents the Ig heavy chain. (*C*) Co-immunoprecipitation of Flag-tagged Smad5, HA-tagged Smad4, and increasing amounts of Tbx20.HA in the presence of AlkCA from HeLa cells. Subsequent immunohistochemistry for different epitopes on Western blot detects competition of Smad4 binding to Smad5 by Tbx20. (*D*) Co-immunoprecipitation of Myc-tagged Smad1 and HA-tagged Smad4 from HeLa cells co-transfected with expression constructs for the two proteins, and subsequent addition of in vitro translated Tbx20 protein to Protein A bound complexes. Anti-HA immunohistochemistry on Western blot detects competition of Smad4 binding to Smad1 by Tbx20.

may rely on physical interaction and/or functional interference with the transcriptional activators Smad5 or Smad1. *In vitro* pull-down assays with GST-Tbx20 fusion proteins showed that Tbx20 directly binds to the activating Smad5 and the closely related Smad1, but not to the regulatory Smad4 and the inhibitory Smads, Smad6 and Smad7 (Fig. 7A, Suppl. Fig. 7A). Binding was mediated by the T-box of Tbx20 as shown by GST pull-down assays with fusion constructs of GST and various Tbx20 protein fragments (Fig. 7A). Tbx20 binding to Smad5 also occurred in a cellular context as shown by co-transfection/co-precipitation experiments in HeLa cells (Fig. 7B). Since Smad4 is a necessary co-factor for nuclear translocation and transcriptional activation by Smad1/Smad5 we investigated whether Tbx20 binding to Smad1/Smad5 competes with Smad1/5-Smad4 complex formation. We transfected expression constructs for Alk3CA, Smad4.HA, Smad5-Flag and increasing amounts of HA-tagged Tbx20 into HeLa cells and precipitated Smad5/Smad4/Tbx20 complexes with anti-Flag antibodies. Detection of HA-epitopes on Western Blots revealed a decrease of co-immunoprecipitated Smad4.HA protein in the presence of increasing amounts of Tbx20 (Fig. 7C).

In an alternative assay, we transfected expression constructs for Myc-tagged Smad1 and HA-tagged Smad4 into HeLa cells and precipitated Smad1/Smad4 complexes by anti-Myc antibodies. Addition of *in vitro* translated Tbx20 protein to resuspended immunocomplexes resulted in a complete release of Smad4 from the complex (Fig. 7D). Thus, Tbx20 effectively competes with Smad4 for binding to Smad1/Smad5 explaining the DNA-independent inhibition of Bmp/Smad-mediated activation of target promoters including *Tbx2*.

Discussion

Mammalian heart development is characterized by an intricate spatial and temporal interplay between morphogenetic programs controlling cellular proliferation and differentiation processes. Bmp-signaling and T-box factor transcriptional activities have been identified to govern some of these programs but the mechanisms that direct and restrict signaling activities and link them to transcriptional circuits to achieve compartmentalization of the heart tube have remained elusive. Our study suggests that the T-box transcription factors Tbx2/Tbx3 and Tbx20 are targets and regulators of Bmp/Smad-signaling, respectively. Tbx20 promotes cardiac chamber formation, and simultaneously suppresses Bmp/Smad-transcriptional activity in the rest of the heart tube in a novel DNA-binding independent manner, thereby restricting Tbx2 activity to the prospective AV canal region. In turn, Tbx2 together with Tbx3, locally stimulate development of the AV canal myocardium and cushions, possibly by up-regulating Bmp-signaling.

Tbx20 restricts Tbx2 to the prospective AV canal by attenuating Bmp/Smad-signaling

Expression analyses, embryological manipulation in the chick and genetic ablation experiments in the mouse have revealed a range of Bmp-dependent processes during amniote heart development (van Wijk et al. 2007). Bmp-signaling is broadly activated in the precardiac mesoderm and the cardiac crescent and is required for differentiation of progenitors of the first and second heart field into cardiomyocytes (Monteiro et al. 2004; Klaus et al. 2007). Ablation of *Bmpr1a* in early mesoderm resulted in a complete failure to establish cardiomyocytes expressing conserved core cardiogenic factors including Tbx5, Tbx20, Nkx2.5 and Gata family members, implicating them as downstream mediators of early Bmp-signaling. After cardiac specification, Bmp-signaling is redeployed for specification of the AV canal. Conditional deletion of *Bmp2* showed that Bmp-signaling is required to establish an AV myocardium, to enhance formation of the cardiac jelly and to induce endocardial EMT (Ma et al. 2005). Bmp2 regulates expression of the transcriptional repressor Tbx2 in the AV canal: *Tbx2* expression is lost in *Bmp2* mutants, and *Tbx2* is induced by Bmp2-loaded beads in chick epiblast cultures (Yamada et al. 2000; Ma et al. 2005). Our analysis of the regulatory region of the *Tbx2* gene identified a genomic fragment that is sufficient to direct AV canal expression *in vivo*. This fragment is rich in Smad-binding sites and responsive to Bmp/Smad-signaling *in vitro*, strongly arguing that *Tbx2* is a direct target gene of this pathway in the heart.

Analysis of the regulatory region of *tbx2b* in the zebrafish heart has identified Foxn4 and Tbx5 as activators of *tbx2b* expression (Chi et al. 2008). Deletion of (conserved) TBE and Foxn4 sites in the *Tbx2* upstream region of the mouse showed that these sites are not relevant for cardiac *Tbx2* expression, suggesting that AV canal restriction of *Tbx2* might have been achieved by different molecular pathways in vertebrate evolution.

Expression of *Tbx2* in the early heart tube prevents chamber formation (Christoffels et al. 2004b), illuminating the necessity to prevent premature activation of *Tbx2* by the first wave of Bmp/Smad-signaling in the cardiac crescent, the heart tube and the prospective chambers. In *Tbx20*-mutant hearts, *Tbx2* is induced in the developing cardiac crescent and throughout the linear heart tube (Singh et al. 2005), demonstrating that temporal and spatial restriction of *Tbx2* to the developing AV canal is not achieved by positive regulatory inputs, but by Tbx20-mediated inhibition of broad activation in regions outside the AV canal. Absence of TBE sites from a minimal *Tbx2* promotor fragment that is sufficient to recapitulate cardiac *Tbx2* expression in wild-type and *Tbx20*-mutant embryos strongly argues against Tbx20 acting as a transcriptional repressor in this context, as indicated by ChIP experiments (Cai et al. 2005).

To our surprise, we discovered that Tbx20 binds to activating Smad1 and 5 and sequesters them from binding to the common Smad4, abolishing the formation of transcriptionally active Smad1/5,Smad4 complexes. Hence, transcriptional modulation of target gene expression by T-box transcription factors may not only rely on the presence of

TBE sites that feature a particular orientation and spacing. Direct binding and sequestration of transcriptional regulators by the conserved T-domain suggests another level of complexity of transcriptional regulation and establishes the T-box as a versatile interface both for DNA and protein interaction.

Tbx20-mediated sequestration of activating Smads may be one of several mechanisms that synergize to shut off Bmp/Smad-signaling after cardiac specification of the lateral plate mesoderm. In *Nkx2.5*-mutant hearts, Bmp/Smad-signaling is dramatically augmented and expanded suggesting that Nkx2.5 represses Bmp/Smad-signaling (Prall et al. 2007). Smad6 that is expressed in the cardiac crescent stably binds to activated type I receptors and competes with regulatory Smad4 for receptor activation (Imamura et al. 1997). Moreover, similar and likely in addition to Tbx20, Smad6 specifically competes with Smad4 for binding to receptor-activated Smad1, yielding an inactive Smad1/Smad6 complex (Hata et al. 1998). Since Tbx20, Nkx2-5 and Smad6 are targets of Bmp-signaling in the cardiac crescent, they may be part of a concerted negative feed-back loop.

Since *Tbx2* is known from other systems like the limb to respond to high levels of Bmp only (Suzuki et al. 2004; Behesti et al. 2006; Yang et al. 2006), all these mechanisms may collectively dampen Bmp/Smad-signaling to a level insufficient to activate *Tbx2*. Intriguingly, we noted that ectopic expression of Tbx2 and Tbx3 resulted in increased expression of *Bmp2, Bmp4* and Smad-target genes (e.g. *Id*). Thus Tbx2/Tbx3 may activate a feed-forward loop of Bmp-signaling that further increases *Tbx2/Tbx3* expression, and thereby development of the AV canal.

Tbx20 and Tbx2/3 regulate chamber versus AV canal development

Previous analyses by a number of research groups revealed the crucial role of *Tbx20* in cardiac chamber formation in vertebrates (Cai et al. 2005; Singh et al. 2005; Stennard et al. 2005; Takeuchi et al. 2005). *Tbx2* expression, normally restricted to the AV canal (Habets et al. 2002) was expanded into the entire heart tube of *Tbx20*-deficient embryos arguing that chambers have been lost at the expense of an AV canal. Since ectopic expression of *Tbx2* in the pre-chamber heart tube resulted in a similar phenotypic outcome (Christoffels et al. 2004b), it was hypothesized that de-repression of *Tbx2* fully explains the cardiac phenotype in *Tbx20*-deficient embryos. Our analysis of *Tbx20/Tbx2* double mutant embryos revealed that loss of *Tbx2* does not rescue the early cardiac arrest, identifying Tbx20 as a positive factor for chamber formation independent from Tbx2. However, given the dominant chamber differentiation-blocking capacity of Tbx2 (Christoffels et al. 2004b), the ectopic expression of *Tbx2* in *Tbx20* mutants is likely to add to its cardiac phenotype. This is further supported by biochemical studies that show that the transcriptional repressor Tbx2 can compete with transcriptional activators of the T-box family including Tbx5 and Tbx20 for binding to conserved DNA-elements such as TBE sites in the *Nppa* promoter (Habets et al. 2002). Thus, Tbx20 has a dual role in cardiac development, acting to stimulate formation of chambers and to confine repressor Tbx2 to the AV canal.

Tbx2 and Tbx3, a pair of evolutionary closely related T-box proteins, share identical biochemical properties (reviewed in (Naiche et al. 2005). Co-expression in the AV canal argues for a role of these genes in regionalization of the simple heart tube and establishment of the AV canal phenotype. In gain-of-function scenarios both Tbx2 and Tbx3 were able to prevent chamber differentiation (Christoffels et al. 2004b; Mommersteeg et al. 2007) and to suppress a broad spectrum of working myocardium associated genes, including sarcomere components and mitochondrial genes. Ectopic expression of Tbx3 in atrial myocardium led to induction of a set of genes associated with the AV canal / conduction system in the atrial working myocardium. Individual loss of function of either *Tbx2* or *Tbx3* did not have a major impact on AV canal development (Harrelson et al. 2004; Ribeiro et al. 2007; Bakker et al. 2008; Mesbah et al. 2008). However, *Tbx2/3* double mutant embryos largely failed to establish a morphological AV canal indicating that the two genes act redundantly in this process, possibly augmented by other factors including *Id* genes that suppress chamber differentiation (Moskowitz et al. 2007). Together, these data indicate that Tbx2 and Tbx3 coordinately regulate the AV gene program by suppressing working myocardial and by activating AV-specific features.

Tbx2/Tbx3 double mutant embryos failed to establish AV swellings (cushions), which are the precursors of the valves, and contribute to the septal structures and to the fibrous insulation. The *Tbx20* mutants formed cardiac jelly in the entire tube, whereas *Tbx2/Tbx20* double mutants did not, suggesting that Tbx2 triggers cardiac jelly formation. These data also suggest that Tbx20 that has been implicated in later aspects of cushion development (Shelton and Yutzey 2007) is not required for the initial steps of cushion formation. Furthermore, we observed a striking mesenchymal layer in the atria of mice ectopically expressing Tbx3 in the atria. Together, these observations strongly suggest that Tbx2 and Tbx3 in the AV canal are required and individually sufficient to initiate cushion formation and EMT. The mechanism of cushion formation has been extensively studied, and important roles for ligands and receptors of the Tgfß-superfamily have been exposed (Bartram et al. 2001; Camenisch et al. 2002; Sugi et al. 2004; Mercado-Pimentel and Runyan 2007). Bmp2 expression in the AV canal myocardium is both required and sufficient to induce cushion formation (Sugi et al. 2004; Ma et al. 2005). *Bmp2* was selectively upregulated in the Tbx3-expressing atrial myocardium, and is likely to be a pivotal downstream mediator of cushion induction by Tbx3. This is further confirmed by enhanced expression in the ectopic mesenchyme of *Tgfß2* and other Bmp2 target genes that are required for cushion formation (Bartram et al. 2001; Camenisch et al. 2002; Sugi et al. 2004; Mercado-Pimentel and Runyan 2007). However, alternative possibilities could be considered, because *Bmp2* is not absent from *Tbx2/Tbx3* double mutant hearts that fail to initiate cushion formation. One possibility is that in addition to its role of directly signaling to the endocardium through receptor Bmpr1a, Bmp2 may act through Tbx2 to activate another intercellular signaling pathway, such as the Notch pathway also implicated in cushion formation (Timmerman et al. 2004).

Together, our loss- and gain-of function analyses suggest that Tbx2/Tbx3 and Tbx20 antagonistically regulate regionalization of the heart. Tbx20 promotes chamber formation

whereas Tbx2/Tbx3 directs the AV canal phenotype in the growing heart tube. Chamber and AV canal formation may be coupled and localized by the antagonistic regulation of Bmp/Smad-signaling pathway by these T-box transcription factors.

Acknowledgements

We thank Corrie de Gier-de Vries for her contributions and advice, M. van Roon of the AMC GGM facility for generating mice, Susan Dymecki for providing *FlpE* deleter mice, Ronald DePinho, Michael Oelgeschläger, Thomas Aigner, Kai Jiao, Olexander Korchynskyi, Peter ten Dijke, Sangita Chauhan, and Nisar Malek for reagents. This work was supported by grants from the Netherlands Heart Foundation (96.002 to V.M.C. and A.F.M.M.); the Netherlands Heart Foundation (2005B076 to V.M.C.); the Netherlands Organization for Scientific Research (Vidi grant 864.05.006 to V.M.C.); the European Community's Sixth Framework Programme contract ('HeartRepair' LSHM-CT-2005-018630 to V.M.C., A.F.M.M. and A.K.), and the German Research Foundation for the Cluster of Excellence REBIRTH (from Regenerative Biology of Reconstructive Therapy) at Hannover Medical School (A.K.).

References

Abdelwahid, E., Rice, D., Pelliniemi, L.J., and Jokinen, E. 2001. Overlapping and differential localization of Bmp-2, Bmp-4, Msx-2 and apoptosis in the endocardial cushion and adjacent tissues of the developing mouse heart. Cell Tissue Res 305: 67-78.

Akiyama, H., Chaboissier, M.C., Behringer, R.R., Rowitch, D.H., Schedl, A., Epstein, J.A., and de Crombrugghe, B. 2004. Essential role of Sox9 in the pathway that controls formation of cardiac valves and septa. Proc Natl Acad Sci U S A 101: 6502-6507.

Armstrong, E.J. and Bischoff, J. 2004. Heart valve development: endothelial cell signaling and differentiation. Circ Res 95: 459-470.

Bakker, M.L., Boukens, B.J., Mommersteeg, M.T., Brons, J.F., Wakker, V., Moorman, A.F., and Christoffels, V.M. 2008. Transcription factor Tbx3 is required for the specification of the atrioventricular conduction system. Circ Res 102: 1340-1349.

Bartram, U., Molin, D.G., Wisse, L.J., Mohamad, A., Sanford, L.P., Doetschman, T., Speer, C.P., Poelmann, R.E., and Gittenberger-de Groot, A.C. 2001. Double-outlet right ventricle and overriding tricuspid valve reflect disturbances of looping, myocardialization, endocardial cushion differentiation, and apoptosis in TGF-beta(2)-knockout mice. Circulation 103: 2745-2752.

Behesti, H., Holt, J.K., and Sowden, J.C. 2006. The level of BMP4 signaling is critical for the regulation of distinct T-box gene expression domains and growth along the dorso-ventral axis of the optic cup. BMC Dev Biol 6: 62.

Brugger, S.M., Merrill, A.E., Torres-Vazquez, J., Wu, N., Ting, M.C., Cho, J.Y., Dobias, S.L., Yi, S.E., Lyons, K., Bell, J.R. et al. 2004. A phylogenetically conserved cis-regulatory module in the Msx2 promoter is sufficient for BMP-dependent transcription in murine and Drosophila embryos. Development 131: 5153-5165.

Bruneau, B.G., Logan, M., Davis, N., Levi, T., Tabin, C.J., Seidman, J.G., and Seidman, C.E. 1999. Chamber-specific cardiac expression of Tbx5 and heart defects in Holt-Oram syndrome. Dev Biol 211: 100-108.

Bruneau, B.G., Nemer, G., Schmitt, J.P., Charron, F., Robitaille, L., Caron, S., Conner, D.A., Gessler, M., Nemer, M., Seidman, C.E. et al. 2001. A murine model of Holt-Oram syndrome defines roles of the T-box transcription factor Tbx5 in cardiogenesis and disease. Cell 106: 709-721.

Cai, C.L., Zhou, W., Yang, L., Bu, L., Qyang, Y., Zhang, X., Li, X., Rosenfeld, M.G., Chen, J., and Evans, S. 2005. T-box genes coordinate regional rates of proliferation and regional specification during cardiogenesis. Development 132: 2475-2487.

Camenisch, T.D., Molin, D.G., Person, A., Runyan, R.B., Gittenberger-de Groot, A.C., McDonald, J.A., and Klewer, S.E. 2002. Temporal and distinct TGFbeta ligand requirements during mouse and avian endocardial cushion morphogenesis. Dev Biol 248: 170-181.

Chen, Y.H., Ishii, M., Sucov, H.M., and Maxson, R.E., Jr. 2008. Msx1 and Msx2 are required for endothelial-mesenchymal transformation of the atrioventricular cushions and patterning of the atrioventricular myocardium. BMC Dev Biol 8: 75.

Chi, N.C., Shaw, R.M., De Val, S., Kang, G., Jan, L.Y., Black, B.L., and Stainier, D.Y. 2008. Foxn4 directly regulates tbx2b expression and atrioventricular canal formation. Genes Dev 22: 734-739.

Christoffels, V.M., Burch, J.B., and Moorman, A.F. 2004a. Architectural plan for the heart: early patterning and delineation of the chambers and the nodes. Trends Cardiovasc Med 14: 301-307.

Christoffels, V.M., Habets, P.E., Franco, D., Campione, M., de Jong, F., Lamers, W.H., Bao, Z.Z., Palmer, S., Biben, C., Harvey, R.P. et al. 2000. Chamber formation and morphogenesis in the developing mammalian heart. Dev Biol 223: 266-278.

Christoffels, V.M., Hoogaars, W.M., Tessari, A., Clout, D.E., Moorman, A.F., and Campione, M. 2004b. T-box transcription factor Tbx2 represses differentiation and formation of the cardiac chambers. Dev Dyn 229: 763-770.

Clouthier, D.E., Hosoda, K., Richardson, J.A., Williams, S.C., Yanagisawa, H., Kuwaki, T., Kumada, M., Hammer, R.E., and Yanagisawa, M. 1998. Cranial and cardiac neural crest defects in endothelin-A receptor-deficient mice. Development 125: 813-824.

Coppen, S.R., Severs, N.J., and Gourdie, R.G. 1999. Connexin45 (alpha 6) expression delineates an extended conduction system in the embryonic and mature rodent heart. Dev Genet 24: 82-90.

Dehaan, R.L. 1961. Differentiation of the atrioventricular conducting system of the heart. Circulation 24: 458-470.

Dunwoodie, S.L. 2007. Combinatorial signaling in the heart orchestrates cardiac induction, lineage specification and chamber formation. Semin Cell Dev Biol 18: 54-66.

Galvin, K.M., Donovan, M.J., Lynch, C.A., Meyer, R.I., Paul, R.J., Lorenz, J.N., Fairchild-Huntress, V., Dixon, K.L., Dunmore, J.H., Gimbrone, M.A., Jr. et al. 2000. A role for smad6 in development and homeostasis of the cardiovascular system. Nat Genet 24: 171-174.

Gitler, A.D., Lu, M.M., Jiang, Y.Q., Epstein, J.A., and Gruber, P.J. 2003. Molecular markers of cardiac endocardial cushion development. Dev Dyn 228: 643-650.

Gorza, L., Schiaffino, S., and Volpe, P. 1993. Inositol 1,4,5-trisphosphate receptor in heart: evidence for its concentration in Purkinje myocytes of the conduction system. J Cell Biol 121: 345-353.

Habets, P.E., Moorman, A.F., Clout, D.E., van Roon, M.A., Lingbeek, M., van Lohuizen, M., Campione, M., and Christoffels, V.M. 2002. Cooperative action of Tbx2 and Nkx2.5 inhibits ANF expression in the atrioventricular canal: implications for cardiac chamber formation. Genes Dev 16: 1234-1246.

Harrelson, Z., Kelly, R.G., Goldin, S.N., Gibson-Brown, J.J., Bollag, R.J., Silver, L.M., and Papaioannou, V.E. 2004. Tbx2 is essential for patterning the atrioventricular canal and for morphogenesis of the outflow tract during heart development. Development 131: 5041-5052.

Hata, A., Lagna, G., Massague, J., and Hemmati-Brivanlou, A. 1998. Smad6 inhibits BMP/Smad1 signaling by specifically competing with the Smad4 tumor suppressor. Genes Dev 12: 186-197.

Hoogaars, W.M., Barnett, P., Moorman, A.F., and Christoffels, V.M. 2007a. T-box factors determine cardiac design. Cell Mol Life Sci 64: 646-660.

Hoogaars, W.M., Engel, A., Brons, J.F., Verkerk, A.O., de Lange, F.J., Wong, L.Y., Bakker, M.L., Clout, D.E., Wakker, V., Barnett, P. et al. 2007b. Tbx3 controls the sinoatrial node gene program and imposes pacemaker function on the atria. Genes Dev 21: 1098-1112.

Hoogaars, W.M., Tessari, A., Moorman, A.F., de Boer, P.A., Hagoort, J., Soufan, A.T., Campione, M., and Christoffels, V.M. 2004. The transcriptional repressor Tbx3 delineates the developing central conduction system of the heart. Cardiovasc Res 62: 489-499.

Houweling, A.C., Somi, S., Massink, M.P., Groenen, M.A., Moorman, A.F., and Christoffels, V.M. 2005. Comparative analysis of the natriuretic peptide precursor gene cluster in vertebrates reveals loss of ANF and retention of CNP-3 in chicken. Dev Dyn 233: 1076-1082.

Hurlstone, A.F., Haramis, A.P., Wienholds, E., Begthel, H., Korving, J., Van Eeden, F., Cuppen, E., Zivkovic, D., Plasterk, R.H., and Clevers, H. 2003. The Wnt/beta-catenin pathway regulates cardiac valve formation. Nature 425: 633-637.

Imamura, T., Takase, M., Nishihara, A., Oeda, E., Hanai, J., Kawabata, M., and Miyazono, K. 1997. Smad6 inhibits signalling by the TGF-beta superfamily. Nature 389: 622-626.

Klaus, A., Saga, Y., Taketo, M.M., Tzahor, E., and Birchmeier, W. 2007. Distinct roles of Wnt/beta-catenin and Bmp signaling during early cardiogenesis. Proc Natl Acad Sci U S A 104: 18531-18536.

Kokubo, H., Tomita-Miyagawa, S., Hamada, Y., and Saga, Y. 2007. Hesr1 and Hesr2 regulate atrioventricular boundary formation in the developing heart through the repression of Tbx2. Development 134: 747-755.

Kreuzberg, M.M., Sohl, G., Kim, J.S., Verselis, V.K., Willecke, K., and Bukauskas, F.F. 2005. Functional properties of mouse connexin30.2 expressed in the conduction system of the heart. Circ Res 96: 1169-1177.

Lincoln, J., Alfieri, C.M., and Yutzey, K.E. 2006. BMP and FGF regulatory pathways control cell lineage diversification of heart valve precursor cells. Dev Biol 292: 292-302.

Ma, L., Lu, M.F., Schwartz, R.J., and Martin, J.F. 2005. Bmp2 is essential for cardiac cushion epithelial-mesenchymal transition and myocardial patterning. Development 132: 5601-5611.

Mercado-Pimentel, M.E. and Runyan, R.B. 2007. Multiple transforming growth factor-beta isoforms and receptors function during epithelial-mesenchymal cell transformation in the embryonic heart. Cells Tissues Organs 185: 146-156.

Mery, A., Aimond, F., Menard, C., Mikoshiba, K., Michalak, M., and Puceat, M. 2005. Initiation of embryonic cardiac pacemaker activity by inositol 1,4,5-trisphosphate-dependent calcium signaling. Mol Biol Cell 16: 2414-2423.

Mesbah, K., Harrelson, Z., Theveniau-Ruissy, M., Papaioannou, V.E., and Kelly, R.G. 2008. Tbx3 is required for outflow tract development. Circ Res 103: 743-750.

Mommersteeg, M.T., Hoogaars, W.M., Prall, O.W., de Gier-de Vries, C., Wiese, C., Clout, D.E., Papaioannou, V.E., Brown, N.A., Harvey, R.P., Moorman, A.F. et al. 2007. Molecular pathway for the localized formation of the sinoatrial node. Circ Res 100: 354-362.

Monteiro, R.M., de Sousa Lopes, S.M., Korchynskyi, O., ten Dijke, P., and Mummery, C.L. 2004. Spatio-temporal activation of Smad1 and Smad5 in vivo: monitoring transcriptional activity of Smad proteins. J Cell Sci 117: 4653-4663.

Moorman, A.F. and Christoffels, V.M. 2003. Cardiac chamber formation: development, genes, and evolution. Physiol Rev 83: 1223-1267.

Moskowitz, I.P., Kim, J.B., Moore, M.L., Wolf, C.M., Peterson, M.A., Shendure, J., Nobrega, M.A., Yokota, Y., Berul, C., Izumo, S. et al. 2007. A molecular pathway including Id2, Tbx5, and Nkx2-5 required for cardiac conduction system development. Cell 129: 1365-1376.

Naiche, L.A., Harrelson, Z., Kelly, R.G., and Papaioannou, V.E. 2005. T-box genes in vertebrate development. Annu Rev Genet 39: 219-239.

Neuhaus, H., Rosen, V., and Thies, R.S. 1999. Heart specific expression of mouse BMP-10 a novel member of the TGF-beta superfamily. Mech Dev 80: 181-184.

Olson, E.N. 2006. Gene regulatory networks in the evolution and development of the heart. Science 313: 1922-1927.

Person, A.D., Klewer, S.E., and Runyan, R.B. 2005. Cell biology of cardiac cushion development. Int Rev Cytol 243: 287-335.

Prall, O.W., Menon, M.K., Solloway, M.J., Watanabe, Y., Zaffran, S., Bajolle, F., Biben, C., McBride, J.J., Robertson, B.R., Chaulet, H. et al. 2007. An Nkx2-5/Bmp2/Smad1 negative feedback loop controls heart progenitor specification and proliferation. Cell 128: 947-959.

Renard, C.A., Labalette, C., Armengol, C., Cougot, D., Wei, Y., Cairo, S., Pineau, P., Neuveut, C., de Reynies, A., Dejean, A. et al. 2007. Tbx3 is a downstream target of the Wnt/beta-catenin pathway and a critical mediator of beta-catenin survival functions in liver cancer. Cancer Res 67: 901-910.

Ribeiro, I., Kawakami, Y., Buscher, D., Raya, A., Rodriguez-Leon, J., Morita, M., Rodriguez Esteban, C., and Izpisua Belmonte, J.C. 2007. Tbx2 and Tbx3 regulate the dynamics of cell proliferation during heart remodeling. PLoS ONE 2: e398.

Rutenberg, J.B., Fischer, A., Jia, H., Gessler, M., Zhong, T.P., and Mercola, M. 2006. Developmental patterning of the cardiac atrioventricular canal by Notch and Hairy-related transcription factors. Development 133: 4381-4390.

Shelton, E.L. and Yutzey, K.E. 2007. Tbx20 regulation of endocardial cushion cell proliferation and extracellular matrix gene expression. Dev Biol 302: 376-388.

Shelton, E.L. and Yutzey, K.E. 2008. Twist1 function in endocardial cushion cell proliferation, migration, and differentiation during heart valve development. Dev Biol 317: 282-295.

Singh, M.K., Christoffels, V.M., Dias, J.M., Trowe, M.O., Petry, M., Schuster-Gossler, K., Burger, A., Ericson, J., and Kispert, A. 2005. Tbx20 is essential for cardiac chamber differentiation and repression of Tbx2. Development 132: 2697-2707.

Stennard, F.A., Costa, M.W., Lai, D., Biben, C., Furtado, M.B., Solloway, M.J., McCulley, D.J., Leimena, C., Preis, J.I., Dunwoodie, S.L. et al. 2005. Murine T-box transcription factor Tbx20 acts as a repressor during heart development, and is essential for adult heart integrity, function and adaptation. Development 132: 2451-2462.

Stypmann, J., Engelen, M.A., Orwat, S., Bilbilis, K., Rothenburger, M., Eckardt, L., Haverkamp, W., Horst, J., Dworniczak, B., and Pennekamp, P. 2007. Cardiovascular characterization of Pkd2(+/LacZ) mice, an animal model for the autosomal dominant polycystic kidney disease type 2 (ADPKD2). Int J Cardiol 120: 158-166.

Sugi, Y., Ito, N., Szebenyi, G., Myers, K., Fallon, J.F., Mikawa, T., and Markwald, R.R. 2003. Fibroblast growth factor (FGF)-4 can induce proliferation of cardiac cushion mesenchymal cells during early valve leaflet formation. Dev Biol 258: 252-263.

Sugi, Y., Yamamura, H., Okagawa, H., and Markwald, R.R. 2004. Bone morphogenetic protein-2 can mediate myocardial regulation of atrioventricular cushion mesenchymal cell formation in mice. Dev Biol 269: 505-518.

Suzuki, T., Takeuchi, J., Koshiba-Takeuchi, K., and Ogura, T. 2004. Tbx Genes Specify Posterior Digit Identity through Shh and BMP Signaling. Dev Cell 6: 43-53.

Takeuchi, J.K., Mileikovskaia, M., Koshiba-Takeuchi, K., Heidt, A.B., Mori, A.D., Arruda, E.P., Gertsenstein, M., Georges, R., Davidson, L., Mo, R. et al. 2005. Tbx20 dose-dependently regulates transcription factor networks required for mouse heart and motoneuron development. Development 132: 2463-2474.

Timmerman, L.A., Grego-Bessa, J., Raya, A., Bertran, E., Perez-Pomares, J.M., Diez, J., Aranda, S., Palomo, S., McCormick, F., Izpisua-Belmonte, J.C. et al. 2004. Notch promotes epithelial-mesenchymal transition during cardiac development and oncogenic transformation. Genes Dev 18: 99-115.

van Wijk, B., Moorman, A.F., and van den Hoff, M.J. 2007. Role of bone morphogenetic proteins in cardiac differentiation. Cardiovasc Res 74: 244-255.

Wessels, A., Vermeulen, J.L., Viragh, S., Kalman, F., Morris, G.E., Man, N.T., Lamers, W.H., and Moorman, A.F. 1990. Spatial distribution of "tissue-specific" antigens in the developing human heart and skeletal muscle. I. An immunohistochemical analysis of creatine kinase isoenzyme expression patterns. Anat Rec 228: 163-176.

Wessely, O., Agius, E., Oelgeschlager, M., Pera, E.M., and De Robertis, E.M. 2001. Neural induction in the absence of mesoderm: beta-catenin-dependent expression of secreted BMP antagonists at the blastula stage in Xenopus. Dev Biol 234: 161-173.

Wu, G., Markowitz, G.S., Li, L., D'Agati, V.D., Factor, S.M., Geng, L., Tibara, S., Tuchman, J., Cai, Y., Park, J.H. et al. 2000. Cardiac defects and renal failure in mice with targeted mutations in Pkd2. Nat Genet 24: 75-78.

Yamada, M., Revelli, J.P., Eichele, G., Barron, M., and Schwartz, R.J. 2000. Expression of chick Tbx-2, Tbx-3, and Tbx-5 genes during early heart development: evidence for BMP2 induction of Tbx2. Dev Biol 228: 95-105.

Yang, L., Cai, C.L., Lin, L., Qyang, Y., Chung, C., Monteiro, R.M., Mummery, C.L., Fishman, G.I., Cogen, A., and Evans, S. 2006. Isl1Cre reveals a common Bmp pathway in heart and limb development. Development 133: 1575-1585.

Supplementary data

Supplementary materials and methods

Histological analysis

Embryos were embedded in paraffin wax and sectioned to 10 µm. For histological analyses sections were stained with Hematoxylin and Eosin.

In situ hybridization analysis

In situ hybridization analyses on whole embryos and on paraffine sections using digoxigenin-labeled antisense riboprobes were performed according to standard protocols (Wilkinson and Nieto 1993; Moorman et al. 2001). Details of probes are available upon request. Stained whole mounts were transferred into 80% glycerol prior to documentation on a Leica M420 microscope with a Fujix digital camera HC-300Z. Sections of in situ hybridizations were photographed using a Leica DM5000 microscope with a Leica DFC300FX digital camera. All images were processed in Adobe Photoshop CS.

Microarray analysis

Left atria of six Cre4-CT mice and six control (Cre4) mice (male, 6 weeks) were dissected and snap frozen in liquid nitrogen. Total RNA was isolated and purified using single prep nucleospin columns according to the manufacturer's instructions (Macherey-Nagel). RNA quality was checked using a bioanalyzer (Agilent Technologies). 250 ng of total RNA was used for biotin-16-UTP cRNA labeling and amplification using the Illumina RNA amplification kit (Ambion Inc., Austin, Txs). Labeled RNA was hybridized to Illumina MouseRef-6 BeadChip following the manufacturer's instructions (Illumina Inc., San Diego, CA). The arrays were scanned using an Illumina Bead array reader confocal scanner. Beadstudio software was used to assess the individual array quality. Unprocessed intensity values were averaged per bead type, exported from beadstudio and subsequently normalized using VSN in R (Huber et al. 2002). Genes were tested for significant differential expression using the empirical Bayes moderated t-statistics test in the R-Limma package (Smyth 2004) at a 5% Benjamini-Hochberg false discovery rate (Reiner et al. 2003). We found that the expression of 737 transcripts was significantly reduced in atria of Cre4-CT mice, whereas 809 transcripts were significantly induced (threshold: P-value<0.05). A comprehensive analysis of this data set will be presented elsewhere.

Quantitative Real-Time PCR analysis

Quantitative real time PCR analysis was performed as described before (Hoogaars et al. 2007). In short, total RNA was isolated from left atrial appendices of 4 week old adult mice using the RNeasy Mini Kit according to the manufacturer's protocol (Qiagen). cDNA was reverse transcribed from 300 ng total RNA using the Superscript II system (Invitrogen) and expression of different genes was assayed with quantitative real time-PCR using the Roche 480 Lightcycler. Relative start concentration ($N_{(0)}$) was calculated using the following equation: $N_{(0)}=10^{(\log(\text{threshold})-Ct\ (\text{mean Eff}))}$. Values were normalized to Gapdh expression levels. Primers sequences can be provided upon request.

Mutagenesis

For construction of a DNA-binding deficient mutant form of Tbx20 conserved amino acid residues in the DNA-binding region were mutated based on reports for the Tbx2 protein (Habets et al. 2002; Lingbeek et al. 2002). Primer sets used for making the DNA binding dead mutant were:
ATCACCAAGTCTGGCGAGAGGATGTTCCCCACCATCC converting arginine 126 to glutamic acid,
ATCACCAAGTCTGGCAGGGAGATGTTCCCCACCATCC converting arginine 127 to glutamic acid and
ATCACCAAGTCTGGCGAGGAGATGTTCCCCACCATCC converting arginines 126 and 127 to glutamic acid residues. pcDNA3.1Tbx20.HA was used as a template for the amplification. Either of the three primers was used for the amplification of the entire plasmid using PfuTurbo DNA polymerase (Stratagene QuickChange XL Site-Directed kit manual). Positive clones were sequenced to confirm the mutation, and protein synthesis was analyzed in transfected Hela cells to check efficiency of expression. Details on all other constructs upon request.

In vitro transcription/in vitro translation

Coding regions of mouse Tbx20, Smad4, Smad6 and Smad7 were amplified by PCR from the respective cDNAs and inserted in pSP64 modified to contain 5'-ß-globin leader and 3'-ß-globin trailer sequences as C-terminal fusion proteins with Myc or HA-epitope tag (Kispert and Herrmann 1993). SP6-coupled in vitro transcription/translation kit (TNT, Promega) was used for synthesis of the proteins in wheat germ lysate.

Expression in cell lines

For cytomegalovirus promoter/enhancer-driven expression of Tbx20, Smad1 and Smad5 proteins in cells, the globin leader/cDNA/globin trailer cassette of pSP64 was shuttled into HindIII and EcoRI sites of pcDNA3 (Invitrogen). Constructs were transfected in HeLa cells using the calcium phosphate method and in NIH3T3 cells employing Fugene reagent (Roche).

In vitro reporter assays

Luciferase reporter assays were used to determine transactivation properties of Tbx20 on various promotor fragments. Promotor fragments cloned in pGL2 or pGL3-luciferase constructs (Promega) were the 6 kbp genomic Tbx2 fragment and deletions thereof (pGL3basic.Tbx2-Luc), a minimal Bmp-responsive Msx2 promotor element (pGL2basic.Msx2-Luc) (Brugger et al. 2004) a short 91 bp Bmp-response element derived from the Id1 promotor (pGL3.BRE2-Luc) (Monteiro et al. 2004) and a 0.7 kbp Nppa genomic fragment (pGL3basic.Nppa(0.7)-Luc) (Habets et al. 2002). Reporter constructs were co-transfected with expression constructs for HA-tagged mouse Tbx20 (pcDNA3.Tbx20.HA), HA-tagged mouse DNA-binding-deficient form of Tbx20 (pcDNA3.Tbx20.HAmut) alone or in the presence of Flag-tagged mouse Smad5 (pcDNA3.Smad5.Flag) and constitutively active Bmp-receptor Alk3 (Alk3CA) (pCS2.BmpR1a.CA)(Wessely et al. 2001). Constructs were transfected into NIH3T3 cells (6×10^5 cells per well of 6-well plates) with the Fugene HD

transfection reagent (Roche). 40 ng of pCMV.ßGal vector were co-transfected to normalize the transfection efficiency by colorimetric determination of X-Gal turnover in the ß-Gal assay. After 48 h of further culture, cell lysates were prepared and the luciferase and ß-galactosidase activities were measured. All transfections were performed in duplicates and experiments were repeated at least three times. After normalization, the mean luciferase activities and standard deviations were plotted as ‘‘fold activation’’ when compared with the empty expression plasmid.

Immunoprecipitation

To determine binding of Tbx20 to Smad5 by co-immunoprecipitation experiments, Hela cells were either transfected with expression constructs for HA-tagged mouse Tbx20 (pcDNA3.Tbx20.HA) alone or in the presence of Flag-tagged mouse Smad5 (pcDNA3.Smad5.Flag) and constitutively active Bmp-receptor Alk3 (Alk3CA) (pCS2.BmpR1a.CA) (Wessely et al. 2001). Transfections were performed using the calcium phosphate method in 10-cm dishes at 50-60% confluency. After 48 h, cells were lysed in 1000 µl of Nonidet P-40 buffer, cellular debri was precipitated by centrifugation for 20 min at 4ºC. The supernatant was split for immunoprecipitation with anti-HA and anti-Flag antibody (2.5 µg). After 1h of incubation, 25 µl of protein G sepharose beads (Amersham Biosciences) were added for 2h at 4 ºC followed by the precipitation and washing of beads. Beads were boiled in SDS-loading buffer and eluted proteins analyzed by Western blot.

To determine competition of Tbx20 and Smad4 for binding to Smad1 in co-immunoprecipitation experiments, Hela cells were transfected with expression constructs for HA-tagged mouse Smad4 (pcDNA3.Smad4.HA) and myc-tagged mouse Smad1 (pcDNA3.Smad1.Myc). Transfections were performed by the calcium phosphate method in 10-cm dishes at 30% confluency. After 48h, cells were lysed in 500 µl of Nonidet P-40 buffer, cellular debri was precipitated by centrifugation for 15 min at 4ºC. The supernatant was split in three aliquots for immunoprecipitation with anti-Myc antibody (2.5 µg). After 2 h of incubation, 30 µl of proteinA agarose beads (Amersham Biosciences) were added for 1 h at 4ºC followed by the precipitation and washing of beads. Beads were resuspended in 300 µl Nonidet P-40 buffer, and 0, 10 and 50 µl of in vitro translated Tbx20 protein was added. After 2 h incubation at 4ºC, beads were precipitated and washed. Proteins were released by boiling in SDS-buffer, and separated by SDS-PAGE. After Western blotting, Myc-tagged proteins (Smad1.Myc, Tbx20.Myc) were detected by anti-Myc, while Smad4.HA was detected by anti HA-immunohistochemistry.

To determine competition of Tbx20 and Smad4 for binding to Smad5 in co-immunoprecipitation experiments, HeLa cells were transfected with expression constructs for Alk3CA, HA-tagged mouse Smad4 (pcDNA3.Smad4.HA), Myc-tagged mouse Smad5 (pcDNA3.Smad5.Myc) using the calcium phosphate method as described. Specific proteins were detected with immunohistochemistry on Western blots as described.

GST pull down

For GST pull-down experiments, GST or GST fusion proteins with five different deletion domains of Tbx20 were expressed in E. coli strain BL21 and bound in the presence of DNAseI to glutathione sepharose 4B beads (Amersham Biosciences) as described (Leger et al. 1995). An aliquot of the washed and equilibrated beads, now carrying GST or GST fusion protein, was incubated with one-tenth of an extract of HeLa cells transfected with pcDNA3.1 expression constructs for Smad5.Flag or Smad1.Myc protein (from 10cm plates), or with an

aliquot of in vitro translated protein of Smad4.HA, Smad6.HA and Smad7.HA in interaction buffer (20 mM HEPES, pH 7.9, 100 mM NaCl, 10 mM KCl, 5mM $MgCl_2$, 0.5 mM EDTA, 5% glycerol, 0.05% Triton X-100, and 1 mM DTT). After extensive washing, the proteins were eluted and analyzed by SDS-PAGE and Western blot.

Electrophoretic mobility shift assay

EMSA was done as previously described (Farin et al. 2007). The probe for Tbx20 binding was generated by annealing the two oligonucleotides BS.dirF, 5'-GATCCGGAGGTGTGAAGGTGTGAAAGGA-3'; and BS.dirR, 5'-GATCTCCTTTCACACCTTCACACCTCCG-3'. Protein for the binding assay was prepared using TNT SP6 High-Yield protein expression system (Promega) (Farin et al. 2007).

In vivo reporter assays

The -6mTbx2-Eyfp construct for generating transgenic Tbx2 promoter-reporter lines (Fig. 5A) was generated by inserting a 6 kbp Tbx2-promoter fragment (from -5.557 bp to +310 bp relative to the human TBX2 transcription start site) into expression vector pCS2, upstream of Eyfp (Venus) (Nagai et al. 2002), removing the CMV promoter. The -3.6mTbx2-Eyfp and -2.7mTbx2-Eyfp constructs were generated by truncation of the -6mTbx2-Eyfp construct using the restriction sites NheI and AflII, respectively (Fig. 5A). To generate the -1.5mTbx2-Eyfp and -1.3mTbx2-Eyfp constructs, the -3.6mTbx2-Eyfp construct was restricted with AflII and BglII, after which a fragment was cloned in between with an artificial AflII site at -314 bp and -63 bp, respectively. Within the -1.5mTbx2-Eyfp construct, a conserved LEF1/Tgf binding site CTTTGTT (Arce et al. 2006) at -2620 bp was mutated into CcgcGcgGT to generate the -1.5(LEFmut)mTbx2-Eyfp construct. Vector sequences were removed and constructs were injected into pronuclei of zygotes of FVB mice.

Supplementary figures

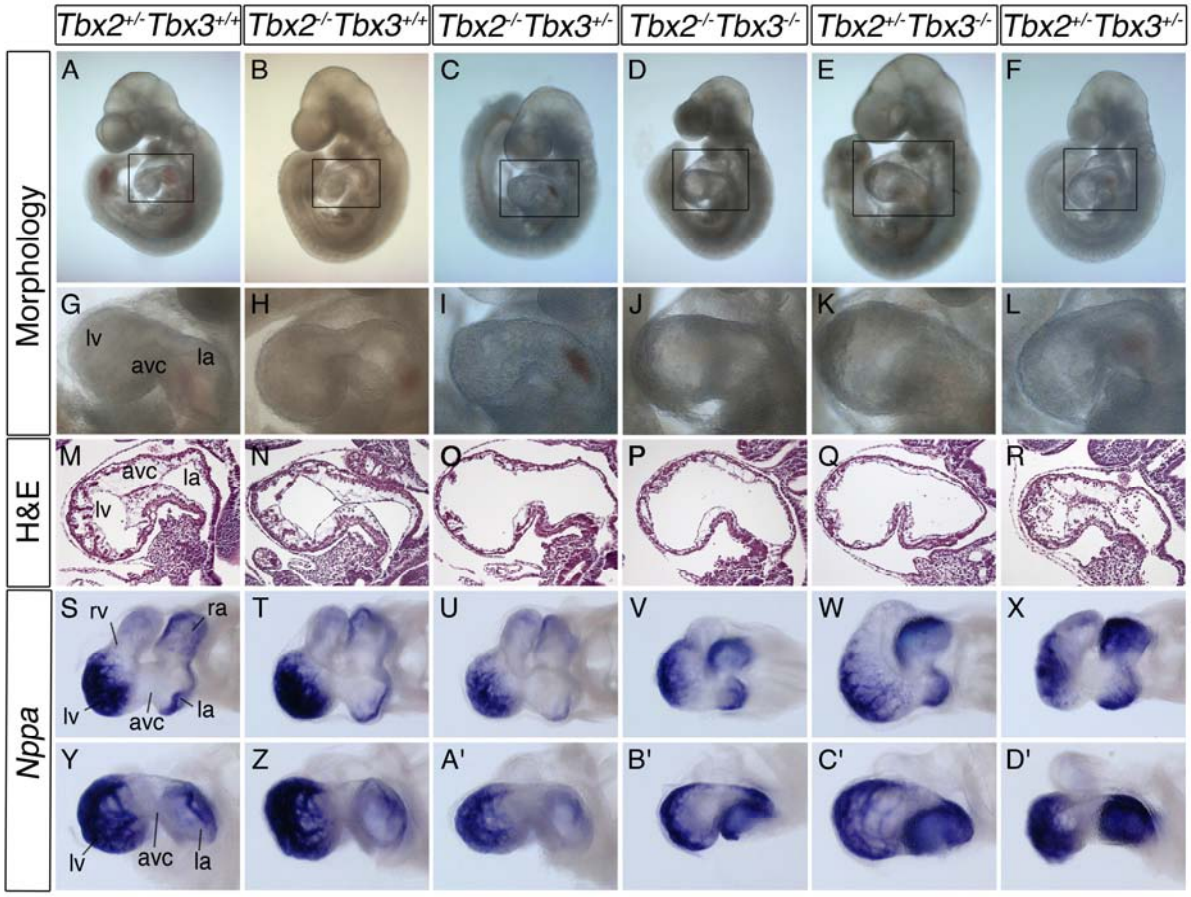

Supplementary Figure 1. Analysis of AVC formation in an allelic series of Tbx2 and Tbx3 embryos by cardiac morphology, histology and expression of the chamber marker Nppa at E9.5; genotypes are as indicated. (A-F) Left lateral views of whole embryos. Boxes mark the heart regions to be magnified in the following figures (G-L). (M-R) Histological analysis of sagittal sections through the left atrium (la), atrioventricular canal (avc) and left ventricle (lv) by hematoxylin and eosin staining (H&E). (S-D') in situ hybridization analysis of Nppa expression in whole hearts in dorsal views (S-X) and in left lateral views (Y-D'). Embryos with a loss of three functional alleles of Tbx2 and Tbx3 exhibit expansion of chamber myocardium in the AVC, and lack of AVC cushion formation, while single mutants appear phenotypically normal in this respect.

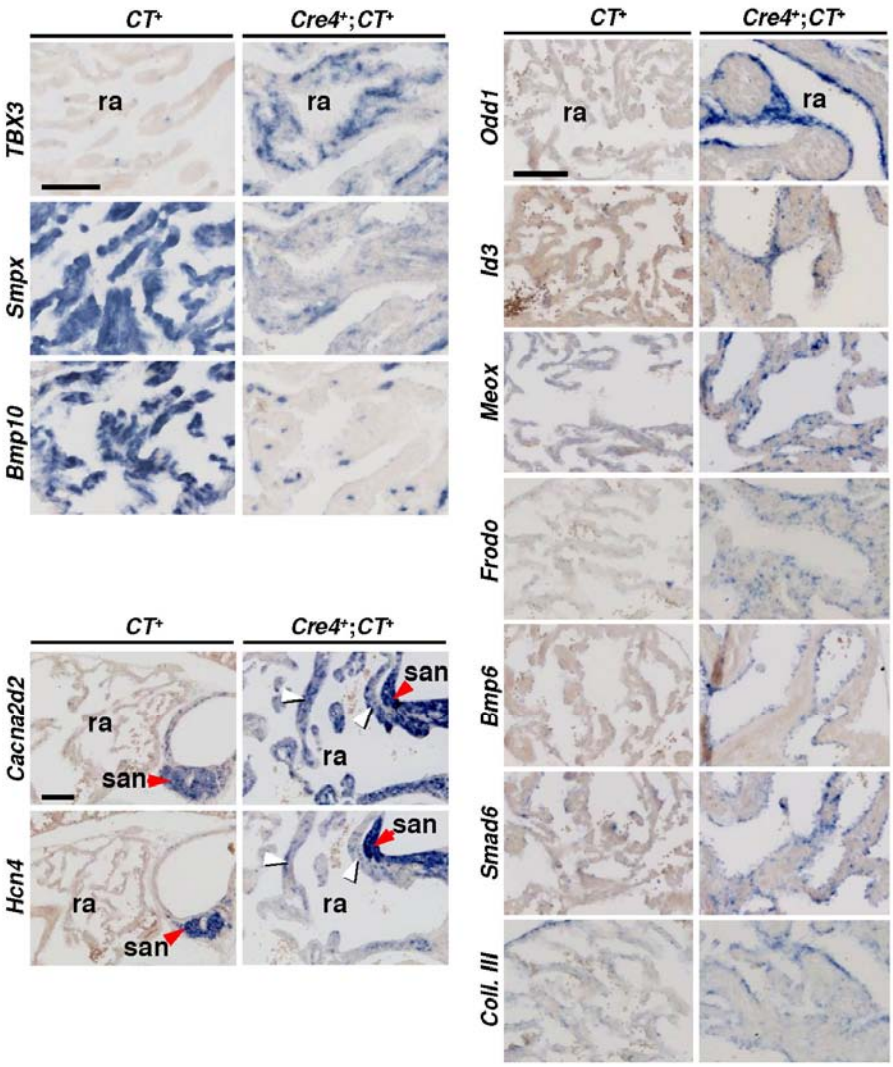

Supplementary Figure 2. Tbx3 induces expression of genes involved in cardiac cushion formation and valve development. Serial sections of E17.5 hearts of CT and Cre4;CT mice, showing induced myocardial expression of transgenic TBX3, reduced myocardial expression of Smpx and Bmp10, induced myocardial expression of Cacna2d2 and Hcn4, and induced mesenchymal expression of Odd1, Id3, Meox1 (also myocardial), Frodo (also myocardial), Bmp6, Smad6 and Collagen III. ra, right atrium; san, sinoatrial node. Black bar, 100 μm.

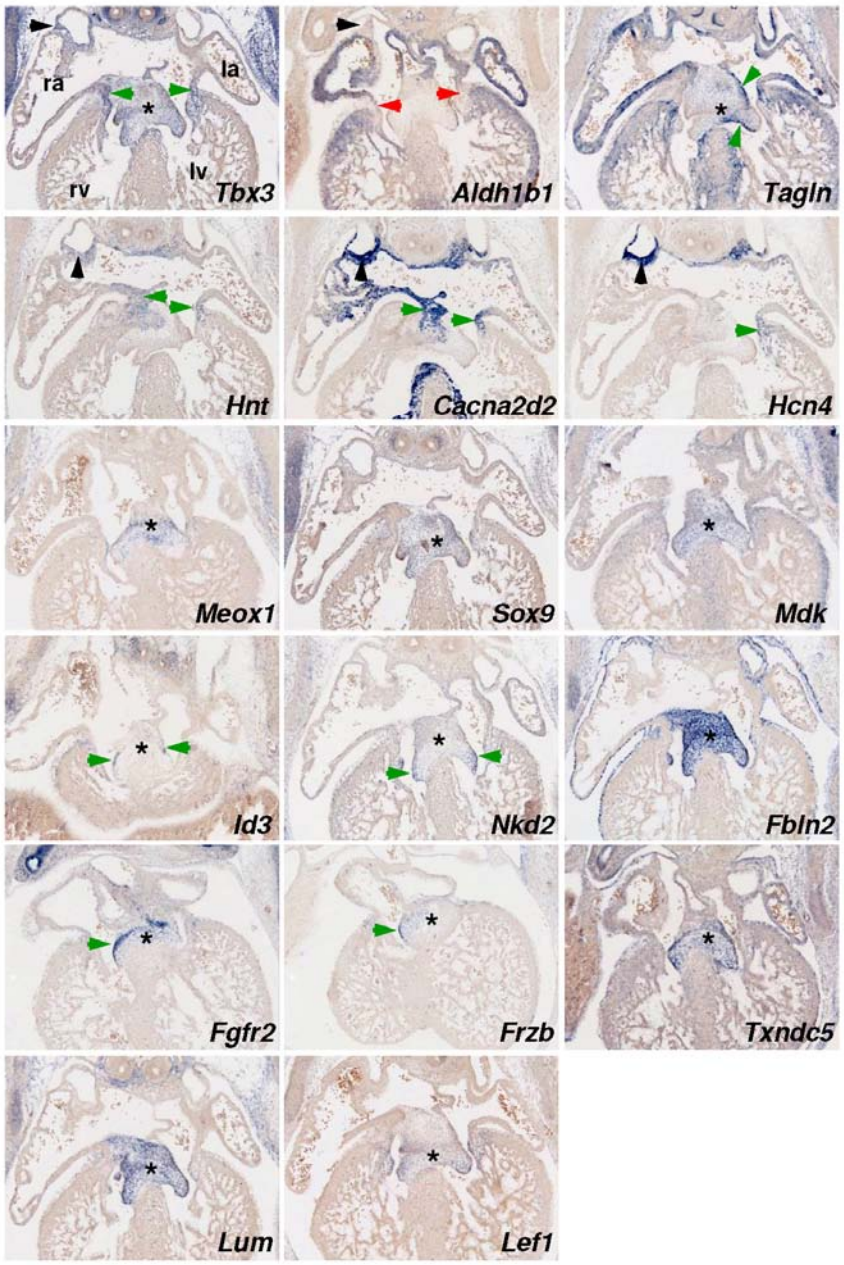

Supplementary Figure 3. Cross-sections of E12.5 mouse hearts showing expression of genes up-regulated in Cre4;CT atria (micro-array) in the developing AVC and AV cushions and valves. In situ hybridization shows expression of Tbx3 in AVC myocardium (green arrow heads) and endocardial cushions (asterisk). Aldh1b1 expression is absent from the AVC, whereas Hnt, Cacna2d2 and Hcn4 are expressed in the AVC and sinus node. We observed broad expression of Sox9, Mdk, Fbln2, Txndc5, Lum and Lef1 in the AV cushions (black asterisk) and the valve leaflets, whereas expression of Meox1, Id3, Nkd2, Fgfr2 and Frzb was more restricted.

Supplementary Figure 4. Sequence analysis of the 6 kbp promoter region of Tbx2 identifies conserved elements.

Reference sequence NCBI July 2007: >ref|NT_096135.5|Mm11_95772_37:51144025-51167297 Mus musculus chromosome 11 genomic contig, strain C57BL/6J.

Positions of restriction sites and putative binding sites refer to the middle of a site.

-6mTbx2 promoter
The first nucleotide (G) and last (A) are depicted in green. Total length is 5867bp, from -5557 to +310 relative to the transcription start site.

5'-GGGATGGTAGAGAAGCTCTGCATAGCATGACCCCTGCACCCACCCTTCTGCTACACAAAG
ATGGGACCTTTCTCAGCCCCGCAGGGGACCTACGGACCCTGGCCCAGCCCTTTACAGTGGGCAAAAAAAC
AGATGTGGCCTCCTCCAGTCAGGGAAAGCAGTGGGTGTAGCGCTGGACGTGCTGGCTGAGCTTGCAGGAC
AATCTGGTTATTCATCTGCTTGCAGTCAGGGCAAGTCTAAGTAAATGGGGGAAGGGTGAGGATCAGAGAG
CTTAGATAAGCCGGCCCCATAGCGGCTGCGGGTTGCAGTTCAGGTTATCTGAAAGGCCCTGGGCCTGGCC
TCCAGCTAATTGGGAAGGTTAGGGACCCAGCCACAGCCTGTAATCAGCTGAAGGTGAGAGCTAGACCGGG
GACCTTACTGCCACTAACCCTAGAGGGGCCAGCTTCTTATCCTCTACAGATAACATCCGAAACAACCTCA
ACCTCTCCCCCCCCCCCCTTAACCCCTAGACCGCATGATACCATCACTCAGAAAGCCATCAGAACATGAA
TCTAATTGTGACTGGGCCAGGTGACCTTGAGGAAGGCAAGTGACCTCCTACTTCTCACAGCACTACCTAC
TTACGGGGCTCCCTTTCAATCTGGGAGGAAGAGGCTGCTGGGAACTGGCCACTCATAAGGTATGGCACTG
TCTGGGAGTGAATCAGTAAAAAGCCCAATGGTCCAAGAGCAAAAATCACACAAAACACAGACACAAGGGC
CGACTCTGCCAGGAGCATGCAGAAGACAGCCACTGGGCTGTAACTGAGGATAATTTCCTAGTGATCGGTT
CTAAATGTTAAAGATCGGAGACTAACCCCCACTCATTCCACCCTCCTTTTATTGATGACAAGCCTGAGCC
CCCAAGAAGGGCAGGGACTTTGCCAAGGTCATGGAGTCACAGCTAGTCAGCTGACCCCTGTCTGCACCTT
GCTACCCTGTGAGCTGTGTCTTGTTCCTGTTCAGCCACCTGAAGCCCAGCTGATCTCTCTCTCTCTCTCT
CTCTCTCTCTCTCTCTCTCTCTCTCTCTCTCCCTCCCTCCCTCTCTCTCTCTCTCTCTCTCTCTCTCT
CTCTCTCTCTCTCTCTCTCTCTCTCTCTCGTGCCCCCAGGACATTCCCACACTTCACACACACACACACA
CACACACACACACACACACACACACACACCTGCACACCTCCCCGCACACCTGCTGTCTGTAAAGCCAGAACC
AGTGGAGTTTCTGGGATGCCAGTGTGGCTTTGCTCTCTGAGCAGGACAGCAATACCACCTTTCTAAGGAG
TGGATGTGGGATTCCATTCTGGCTTTTCCACCTGGAGCCATGTGACCTTAGGCAAATTAGCCTCTAGGTA
GGCTTCTGATTCTCATCTGTAAGGAGAGGGACTGTGAAGAGCAGCAGAGACTGGCATGGCAGACGAAAAG
GGACCGCTGTGGGTCAGAAAGGTGCTTAGAGGCTACTGCCCCGTAGCTCTTTGGTAGGGGTGGGACTGCG
GGGACACCCACAGATTGTGACCGCGCTGTACCCCAGGTACTCTTGAGAACCAGCCTGCAGTGCCCACAGA
CCAGCCCCGCCCCACTGTTGTCGGTAGGCCTATATTGGGGACCCTTCTCAAGTCGGTTCGCTCTTGTGAG
ATCCCAAACACGCACCACGTCCAGGCTCAAGTTCAAGACTGGCACCTCACTTTTGCCACCCAGTGTGTAC
CAAGAGCGACAGCTGCACCTCCTGGGACCAAGGCTCAGGGTAGCAAGTATTTAGCAGTTTTTTAGGAGTT
ATACGATTCCTAAAGCTCCCCCAAATCGACTATAACCTATCTTCCTAACCGCGTGATCTCTCACTATGCA
AAGAAATGCCCGCCCACCGGAGCAAGTGTGTCCCTGACAGAGACAGTTTGGTTGGGCCTCGCCTTTGCAT
TAACCTGGAAGGCAGTGGCCATACAGGAGGTAACTGTTCCAATACTTCCCATAACCTGATGAGGAAGTGG
TCCCGCGGCTGGTCCTGGCACCAGACTAGGGGCACAGCGTCACCAGAAAGAAGGTCGGGCAGCCCACTCT
TCCCGCGCCGCCTGCCGCACCCCAGCCTGTTGGCCAGACCCTGCGCTGGGTAATTGGGACGAAGAGAGCC
GGCCGGCGAGCGGCTCCAGGGAGACTGCAAGCCTGTCAGCCACAATTTGTTTAAGTGGACGGGACAGGCT
GGGCCGCCGGGGGCTGGGGTCACCGAGGCCGCGGCCCCCAGCCTGGCCAGACCCAGGACCGCGGGGGAGC
CCAGCCCTACTGCTTAACCGGGCTAGCTGGCGCCAAGGCTCTGGAAGGCGCGGGTCCGGTGGAGAAGCCA
TGGATGGGAACAACGAATGCACCTAGTGTCTTCTACCGACCACTTTTCCTAAGCATAGGGCCACACATGT
CACCCCAGCTTTTCCCGGGCACATTTATAAGTCAAGGCGCGCTTAGTACCCAGTTATTGGTGCTCACGTG
CCCTCACTCAACTCTGCCACAGGACTACACATTCCCCAGCCTTCCCGCATCCATTCTATGAGGGCTCAGG
CAAATCTTCACGCATGCAGACACATCCGCAGGGACCTATGCTATTTAGAGATCAACTCTTGAGAGAGGACTT
AGCCTTATCTCTTGACCATTCTCGATGTAACTCGGCCAAAAGACGGACCCGGCAGCCCTGCCAGGCTTGG
GAGGGCAGTCCCCTCCGGCCCAGGCTACTGGTGCTGGATTTGATTGTTGCGGGAAGCTAAGACTACAGAC
CACGTGAAAGGGGCCTGGGACCACGAAGCCAGCGCCTGCCCGACGCCCCCGCCCAGAACTGCCTGGGAGA
GGGAGGGGCGGCTGAGCGCGCGTCCCCCACCCGTCTGCGGGTCCCGGCCGATGCGAAGTGACAGGGGCCG
LEF1 / TBE
GAGCTTTGTTGTGGAGCCTCGGCCGCCTGGCGCCAGGCGCCCTCGTCCGTGCCCTCCCCCTCCAGCCCCG
GGCGGCCCGCGAGGCGCCCCCCGGGGCCTCTTAAAGAGACACGCACACTCTGCCCAGGGGACTCCCCCAG
GGGCGCCTGTTCCTGGGAAGGGGAGATGAGTGGGGGTAGACCCAGGCGGGGGTAGGGCGAAGCAGGAGTT
GCGAGCCGCAAGGCGCCGCTCGAGAGGCTGCTTAGGCCGCCCCAGCACCAGTTTTCGATGCTACAAGGAT
ATTCTAAGAAAATTTTGTTGGGGATGGGTCGATAAAGAATCTTAAGAGCGGCTAAAGCAGGTCATCCAGG
TGACTACGTGATGGGGGTGGGGGTGGGGGGGTGGCTGGAGCTGTTGGTGGAAACCCAACCTGCCCTGAAA
ACGTCTCTGACCAGTCGCAGGTCCTTAGCTCTATAGGTGGGATTCAGATCCCCTAATGTAGCCACTGGGC

GACAGCTGTCCGATTTCGTGGACCAATAACT**CAGAC**CTTCATGTTTTAACTCTCAGGCCTAAACGGGTAG
ACCAGCTACTGTATGCTACCCAGGAAAATGACCAAAATACATACTTCGATACATACACATTTTTACAAGG
TACTAAAGTGCCTGTCCCCATACACACAACTTAGCAAATGTCCTGCCAACTCGGAAAGCTGAACTGACTA
CTTCTTGTTCACCTCACTAACTGTCCAAGTGTGTT**CAGAC**ACATCTCTCCTGGAGGAGCCACATCCTGTC
TGAATTGGAAGCAGTGCAAAGCTGCAATGGATCTCTCACCGGCTGCGAACACCGCGAAGCTAGAGCTGAA
GGTTCACTGTGGGCAGAGAAAAGAGTGAGAAAAGCGACCTAGGAGTAAGGTCCTGAAGAAAAACCCAGTG
GGGCAGGCGCGCACAGGGTTATGAAGAATTACAAGCGCCTGGTGTTGGCTCAGATGTATAGGAAAAAAGG
TCGTGGAGGCCAAACGACTCCTGCTGGTCTCAACCCCGTACTGCCGGGGGCAACTAGCTTTTAAACGCCT
TTCTGGGCGGTCAGCTACCAAGTGCCTGAAGACCTGGTGTATGCAGCGGAGGGGCAAGCTGCCTGGGCCA
CTTACGTGGTAGGTGCCTACCACGGGGACATAGGGCTGGAGCGGCAGAATTCGCTTATACTGGTTGGGAG
GGTGGGAGTATCCACTGTGGCTAGTTCACACCCTGCTTCCCCTCCCCAACAAGCACAAGGGTGTGAGCCT
CAACCCTAAACAGGCAAGTGTATGATCGTTTTACTCTGGGCACACCTGATTATGGTTTTACACACACACA
CACACAGAGAGAGAGAGAGAGAGAGAGAGAAAGAGAGAGAGAGAGAGAGAGAGAGAGAGAGAGAGAGA
GAGAGAGAGAGAGAGAGAGAGAGGAAGATGCATTGGGGCTGTTGCCAGAGAGATAACGAAGACTGATCGT
CGAAGGGGGTGTTCACACTTGCTGGCAAACACCTCGATTCCCATCCGCATTACTCAGCTTTCCTGAACTA
GGGAGCCTTGAGCTTCCAAGGGACGGAAACAATCTCTAGAGAAGTGACTGAGAAGAAAAGATGCCAGAGT
TTAGGAAGAGATAGATGGGCTTGCATCTCCAGTACCGGATGCGGCGAAAATTCCTTCTGGCGCGTGTGGA
GAATCTGAGTTCTAGGATCAACTAGCGCGGCACCGCCTTGGGCTCTGTAGAAGGTGCGCTCACCTACCTG
GTCCCAAGGATCCATTTTCCTACTCGCCAGAAGGTTTTGGCTTAGTGACCTGACA**CAGAC**CTTCTTTAGG
CTAAATGCCCGGCCCTTCTGGAACCCCAGGTTCCTGAGTCTACGAGGGGAGGAGCAGGTGGGGGTGGGGA
CCCTTCGTTTCCCCAGCGCAAGGCGGCGTCCCGTTCCCGCCCGTGCCGGCCCCATCAGGGTTCTGCCATG
GCTCCCCACTCACCGGCTCCGGACACCTGATTCGGCTCCGGGACCTCGGCCGCCCGAGCCTCCTGATTTG
CCCGCCCACCGGCCTCGCTTTCCAGTGCCCGCAGCCTCCCTCTGAAGTGCATGGACCCGGGGCGGTGACC
GGGAGTGGGGTGGGAGGCCAGGCTGGGTCGCAGGCAAGAGCGGCCGGGCCTCCCGGCGCGGGAGGGAAAG
GGCGCCCCCTCTCCTCTCCGGAACGTGTCAATGCTTTGCACTTGGGGCCGGCATGCGGCTAGGGGGTCCT
TCCCCAAGGCCCCGGGACCCGGGCGCCCCTGCCTCAGGCCCTTACGGCGGGTCAGATCGGTCCTCTGCG
 −314
CTTTCCAGCCCTCGCCCAGGCAGCGGCGGGCGCGGGCGGCGAGGTGGGGGCCAGGCCAGGGGGAGGGGTC
TCGGGGCCCGCTGGCCCGTCATTGGTTAATATTTTATTCTGTTGACATGTTTTCTTACTGCTGAGGCTTC
CGACACCTTCTCCCTGGCCTCCCCTCCCGTCCAGAGCTTGGCCTGAGCTGTCAAAACCCCGCCCCCGGAG
−63
ACCCACAATTGGTCCAAAAAGCGTAAAATCAGCAATCAAGGGGGGCCTGGCTCGTTAGCGCAGGGGATCC
+1
GAACAGGGCAGGACATGTGAGATAGTCACAGTTTTC**CAG**AGATCAGGACAAGATCTAACCAGTCGCGCGT
GGTCCCCGGCGCCGGAGCCGGCCAGCCCAGCCCAGCCCAGCCCAGCCCAGCCCCGCGCAGCGCCCCCTCC
GCCCCCGCGTCCAGAGCCCTGCGCCCCTTGAGGTGCGCGGGACGGGGAGCCGGGAGAAGCCGCTGCCGCG
CCCGCCGCCCCGGGCCGTCCGTCCTCCGCGCGCGCCGCCGCCCGGGCCGGGGGTCCGAGGCGCGCGCCCCC
+310
GGCCCCGGCCCCGGCTCCCAGGAGCCTGGGCCGGATGTCCCGATGAGAGAGCCGGCGCTGGCAGCCAgcg
ccATG−3′

Transcription start site +1 = **CAG**AGATCA, conserved across species. Translation start site at +316 (ATG), conserved across species. The 5′ untranslated region has been underlined. Transcription and translation start site of mouse have been inaccurately assigned in the NCBI database.

0.9 kb NheI-AflII enhancer
This fragment of 929 bp reaches from the unique restriction site NheI at -3233 to the unique restriction site AflII at -2305 bp. Its sequence has been marked in light grey.

-1.5 kb construct: promoter starts at -314
It contains the 0.9 kb NheI-AflII enhancer, which has been cloned upstream of a -0.6 kb promoter fragment from -314 to +310. The 5′ nucleotide of the proximal promoter has been marked black.

-1.3 kb construct: promoter starts at -63
It contains the 0.9 kb NheI-AflII enhancer, which has been cloned upstream of a -0.4 kb proximal promoter fragment from -63 to +310. The 5′ nucleotide of the proximal promoter has been marked light grey.

Putative binding sites previous literature on Tbx2 promoter:
1) Cai CL 2005. Development 132:2475-87:
TBE at -426: GTGTCAATGCTTTGCAC

2) Chi NC 2008. Genes Dev 22:734-739:
Tbx5 BE at -173: AAGGTGTCGGAA (anti-sense)
Foxn binding site at -84: TTTACGCTTT (anti-sense)

Novel localized putative LEF1 and T-box binding sites present study
1) LEF1 binding site at -2620: 5'-GCTTTGTT-3' (reviewed in Arce L 2006. Oncogene 25:7492-7504), found to be conserved between human and mouse using Transfac matrices. To inactivate the binding site in the context of the -1.5(LEFmut)mTbx2-Eyfp construct it has been mutated into: GCcgcGcg (Giese K 1992. Cell 69:185-195).

2) Non-consensus putative Tbx5 site (for consensus sites see Sinha S 2000. Gene 258:15-29; Farin HF 2007. J Biol Chem 282:25748-59), localized using rVISTA and Transfac matrices, at -2615: 5'-TGTTGTGGA-3'. It partially overlaps with the LEF1 binding site. Within the -1.5(LEFmut)mTbx2-Eyfp construct the site has been inactivated by mutation to: 5'-cGcgGTGGA-3'.

Novel localized putative SMAD binding sites present study

Consensus Smad Binding Elements (SBEs)
5'-***GTCTG***-3' or 5'-***CAGAC***-3' was the original consensus binding sequence; 5'-T***GTCTG***-3' or 5'-***CAGAC***A-3 was indicated by Jonk LJC 1998. J Biol Chem 273:21145-52. However, also 5'-GTCT-3'or 5'-AGAC-3' has been published to be sufficient (Shi Y 1998. Cell 94:585-594; Zawel L 1998. Mol Cell 1:611-617; reviewed in Massagué J 2000. EMBO J 19:1745-1754). All sites have been indicated in the regulatory sequence.

GC-rich palindromes shown to be important for SMAD activation
5'-GGCGCC-3' (Korchynskyi O and ten Dijke P 2002. J Biol Chem 277:4883-4891)

Non-consensus SMAD-binding sequences
5'-*GTGGAGCCTCGGCCGCCTGGCGCCAGGCG*-3': Sequence at -2608, found to contain several SMAD binding elements which are conserved between mouse-human-chicken, using rVISTA and Transfac matrices. The sequence has been underlined.

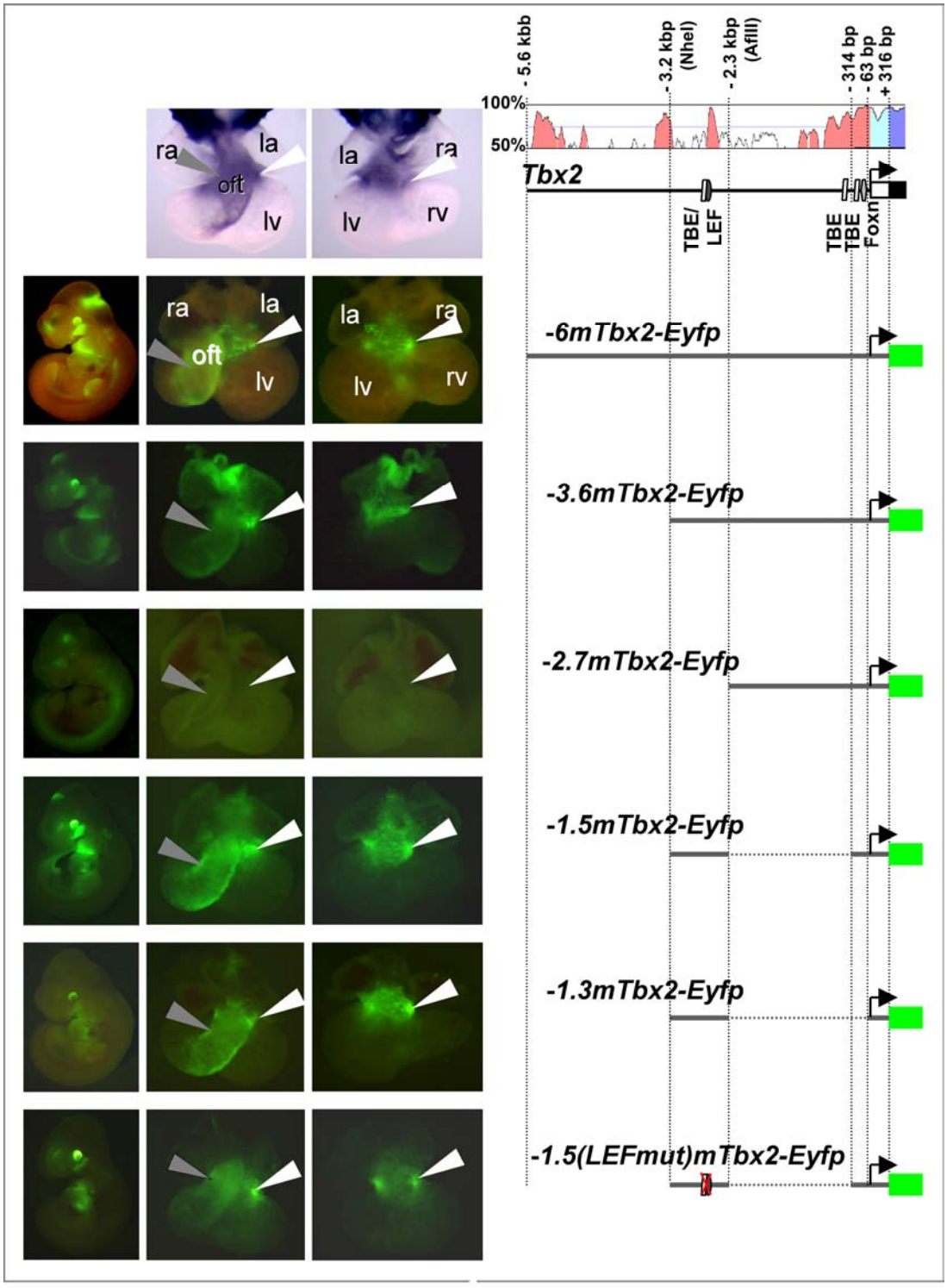

Supplementary Figure 5. Identification of cardiac regulatory elements by deletion analysis of the Tbx2 promoter in transgenic embryos. RankVISTA alignment of human against mouse Tbx2 regulatory sequences show conserved regions. Conserved T-box binding elements (TBE), LEF and Foxn sites are marked by boxes. Top panels show pictures of the Tbx2 expression pattern in E10.5 hearts visualized by whole mount in situ hybridization. Below these are fluorescence pictures of hearts of representative embryos with constructs depicted in the right panel. White arrowheads depict the atrioventricular canal (AVC), grey arrowheads the outflow tract (OFT). Grey lines indicate Tbx2 regulatory sequences, boxes represent exons, green boxes reporter gene Egfp. la, left atrium; lv, left ventricle; ra, right atrium; rv, right ventricle.

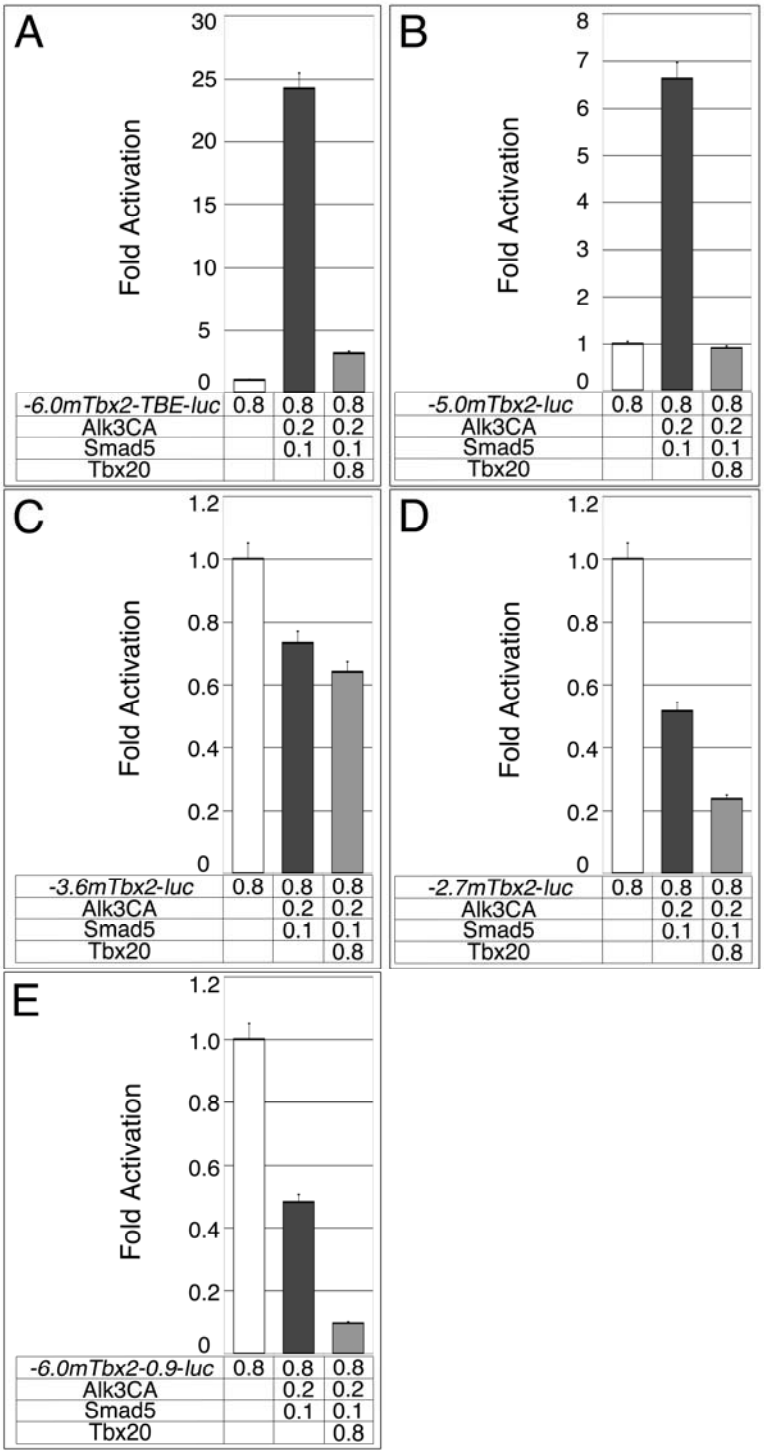

Supplementary Figure 6. Identification of regions of the Tbx2 promoter conferring transcriptional activation by Bmp/Smad-signaling and repression by Tbx20 in transactivation experiments in vitro by deletion analysis. Plasmids encoding constitutively active Bmp receptor Alk3 (Alk3CA), full length Smad5 protein, full length Tbx20 protein and the luciferase reporter constructs were co-transfected in NIH3T3 cells and luciferase activity determined and normalized as fold activation over the reporter alone. Numbers indicate µg of plasmids for the reporter -6.0Tbx2-TBE-luc (A), -5.0mTbx2-luc (B), -3.6mTbx2-luc (C), -2.7mTbx2-luc (D) and -6.0mTbx2-0.9-luc (E), and the expression plasmids for Alk3CA, Smad5 and Tbx20 co-transfected into NIH3T3 cells.

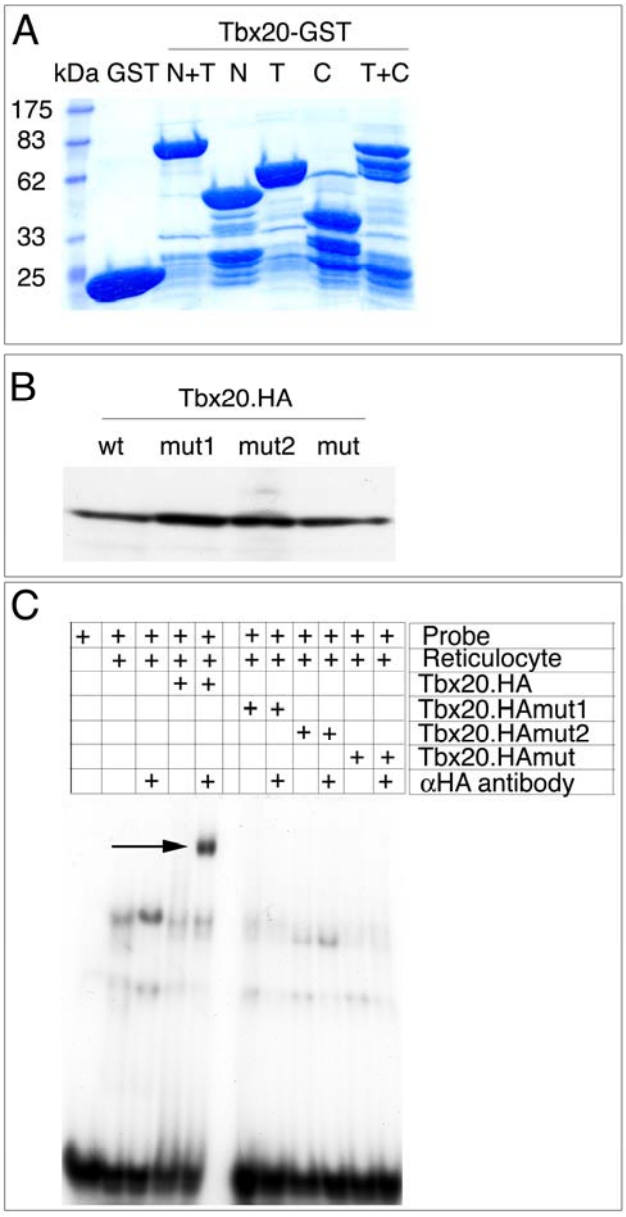

Supplementary Figure 7. Biochemical analyses of Tbx20 proteins. (A) Coomassie staining of Tbx20-GST fusion proteins shows that all proteins are expressed in and purified equally well from bacteria. N refers to the N-terminal protein domain, T to the T-box region and C to the C-terminal protein domain. (B) Western blot analysis of the HA-tag of different Tbx20 proteins in transfected HeLa cells shows that the wild-type (wt), and the non-DNA binding Tbx20mut1 (L126R), Tbx20mut2 (L127R) and Tbx20mut (LL126,127RR) forms are expressed equally well. (C) Electrophoretic mobility shift assay of wild-type and mutant Tbx20 proteins confirms that amino acid changes L126R and L127R abolish binding of the Tbx20 protein to the DNA probe. Note the absence of the supershift band (arrow) in the mutant situations (Tbx20.HAmut1, mut2, mut).

References supplementary data

Arce, L., Yokoyama, N.N., and Waterman, M.L. 2006. Diversity of LEF/TCF action in development and disease. *Oncogene* 25: 7492-7504.

Brugger, S.M., Merrill, A.E., Torres-Vazquez, J., Wu, N., Ting, M.C., Cho, J.Y., Dobias, S.L., Yi, S.E., Lyons, K., Bell, J.R., Arora, K., Warrior, R., and Maxson, R. 2004. A phylogenetically conserved cis-regulatory module in the Msx2 promoter is sufficient for BMP-dependent transcription in murine and Drosophila embryos. *Development* 131: 5153-5165.

Farin, H.F., Bussen, M., Schmidt, M.K., Singh, M.K., Schuster-Gossler, K., and Kispert, A. 2007. Transcriptional repression by the T-box proteins Tbx18 and Tbx15 depends on Groucho corepressors. *J. Biol. Chem.* 282: 25748-25759.

Habets, P.E., Moorman, A.F., Clout, D.E., van Roon, M.A., Lingbeek, M., van Lohuizen, M., Campione, M., and Christoffels, V.M. 2002. Cooperative action of Tbx2 and Nkx2.5 inhibits ANF expression in the atrioventricular canal: implications for cardiac chamber formation. *Genes Dev.* 16: 1234-1246.

Hoogaars, W.M., Engel, A., Brons, J.F., Verkerk, A.O., de Lange, F.J., Wong, L.Y., Bakker, M.L., Clout, D.E., Wakker, V., Barnett, P., Ravesloot, J.H., Moorman, A.F., Verheijck, E.E., and Christoffels, V.M. 2007. Tbx3 controls the sinoatrial node gene program and imposes pacemaker function on the atria. *Genes Dev.* 21: 1098-1112.

Huber, W., von Heydebreck, A., Sultmann, H., Poustka, A., and Vingron, M. 2002. Variance stabilization applied to microarray data calibration and to the quantification of differential expression. *Bioinformatics* 18 Suppl 1: S96-104.

Kispert, A. and Herrmann, B.G. 1993. The Brachyury gene encodes a novel DNA binding protein. *Embo J.* 12: 3211-3220.

Leger, H., Sock, E., Renner, K., Grummt, F., and Wegner, M. 1995. Functional interaction between the POU domain protein Tst-1/Oct-6 and the high-mobility-group protein HMG-I/Y. *Mol. Cell. Biol.* 15: 3738-3747.

Lingbeek, M.E., Jacobs, J.J., and van Lohuizen, M. 2002. The T-box repressors TBX2 and TBX3 specifically regulate the tumor suppressor gene p14ARF via a variant T-site in the initiator. *J. Biol. Chem.* 277: 26120-26127.

Monteiro, R.M., de Sousa Lopes, S.M., Korchynskyi, O., ten Dijke, P., and Mummery, C.L. 2004. Spatio-temporal activation of Smad1 and Smad5 in vivo: monitoring transcriptional activity of Smad proteins. *J. Cell. Sci.* 117: 4653-4663.

Moorman, A.F., Houweling, A.C., de Boer, P.A., and Christoffels, V.M. 2001. Sensitive nonradioactive detection of mRNA in tissue sections: novel application of the whole-mount in situ hybridization protocol. *J. Histochem. Cytochem.* 49: 1-8.

Nagai, T., Ibata, K., Park, E.S., Kubota, M., Mikoshiba, K., and Miyawaki, A. 2002. A variant of yellow fluorescent protein with fast and efficient maturation for cell-biological applications. *Nat. Biotechnol.* 20: 87-90.

Reiner, A., Yekutieli, D., and Benjamini, Y. 2003. Identifying differentially expressed genes using false discovery rate controlling procedures. *Bioinformatics* 19: 368-375.

Smyth, G.K. 2004. Linear models and empirical bayes methods for assessing differential expression in microarray experiments. *Stat. Appl. Genet. Mol. Biol.* 3: Article3.

Wessely, O., Agius, E., Oelgeschlager, M., Pera, E.M., and De Robertis, E.M. 2001. Neural induction in the absence of mesoderm: beta-catenin-dependent expression of secreted BMP antagonists at the blastula stage in Xenopus. *Dev. Biol.* 234: 161-173.

Wilkinson, D.G. and Nieto, M.A. 1993. Detection of messenger RNA by in situ hybridization to tissue sections and whole mounts. *Methods Enzymol*. 225: 361-373.

Gene expression profiling of the forming atrioventricular node using a novel Tbx3-based node-specific transgenic reporter

Thomas Horsthuis[1], Henk PJ Buermans[2#], Janynke F Brons[1#], Arie O Verkerk[1], Martijn L Bakker[1], Vincent Wakker[1], Danielle EW Clout[1], Antoon FM Moorman[1], Peter AC 't Hoen[2], Vincent M Christoffels[1]

#These authors contributed equally to the work

[1]Heart Failure Research Center, Academic Medical Center, University of Amsterdam, the Netherlands. [2]Center for Human and Clinical Genetics, Leiden University Medical Center, Leiden, the Netherlands.

Submitted for publication

Abstract

The atrioventricular (AV) node is a recurrent source of potentially life-threatening arrhythmias. Nevertheless, limited data are available on its developmental control or molecular phenotype. We used a novel AV node-specific reporter mouse to gain insight into the gene programs determining the formation and phenotype of the AV node. In this reporter, green fluorescent protein (GFP) expression was driven by 160 kbp of *Tbx3* and flanking sequences. GFP was selectively active in the AV canal of embryos, and AV node of adults, whereas all other *Tbx3*$^{+}$ conduction system components, including the AV bundle, were devoid of GFP. These findings demonstrate that distinct regulatory sequences and pathways control expression in the components of the conduction system. Fluorescent AV nodal *(Tbx3BAC-Egfp)* and complementary working myocardial (*NppaBAC336-Egfp*) cell populations of E10.5 embryos and E17.5 fetuses were purified using fluorescence-activated cell sorting, and their expression profiles were assessed by microarray analysis. We constructed a comprehensive list of sodium, calcium, and potassium channels specific for nodal or working myocardium. Furthermore, the data revealed that the AV node and the working myocardium phenotypes diverge during development, but that the functional gene classes characterizing both subtypes are maintained. One of the repertoires identified in the AV node-specific gene profiles consists of multiple neurotrophic factors and semaphorins, not yet appreciated to play a role in nodal development, revealing shared characteristics between nodal and nervous system development. These data present the first genome-wide transcription profiles of the AV node during development, providing valuable information concerning its molecular identity.

Introduction

The electrical impulse is initiated in the sinus node, propagated rapidly through the muscular tissues of the atria, delayed in the AV node, and then rapidly propagated through the ventricular conduction system, activating the ventricles from apex to base. The slow conduction through the AV node ensures sequential, synchronized contractions of the atria and ventricles (reviewed in(Meijler and Janse, 1988;Anderson et al., 1981)). This guarantees the ventricles to benefit from the atrial contraction, adding 15% to cardiac output, and prevents one to one conduction of potentially life-threatening supraventricular arrhythmias. Furthermore, the AV node is the major subsidiary pacemaker in case of failure of the sinus node (reviewed in(Meijler and Janse, 1988;Mangoni and Nargeot, 2008)). However, the AV node is also a recurrent source of tachy- and brady- arrhythmias, notably AV node reentrant tachycardia and AV block, requiring lifelong medication, ablation, or electronic pacemaker implantation. Knowledge regarding development (Virágh and Challice, 1977b;Moorman and Christoffels, 2003;Gourdie et al., 2003;Myers and Fishman, 2003;Stroud et al., 2007), anatomy (Anderson et al., 1981), and molecular background of the physiological function (Marionneau et al., 2005;Li et al., 2008;Boyett et al., 1996;Schram et al., 2002;Nerbonne and Kass, 2005) of the AV node has increased gradually. Nevertheless, insights into the transcriptional pathways regulating its development, and the gene expression profiles underlying its phenotype and function are limited.

The T-box transcription factor Tbx3 belongs to an evolutionary conserved family of factors, plays key roles in development and cancer, and is mutated in the ulnar mammary syndrome of congenital defects (Naiche et al., 2005). *Tbx3* is specifically expressed in the components of the cardiac conduction system, i.e. the sinus node, AV node, AV bundle and bundle branches, throughout development and in the adult (Hoogaars et al., 2004), where it plays important roles in their formation (Hoogaars et al., 2007;Bakker et al., 2008). We analyzed the function of regulatory sequences of *Tbx3* to gain insight into transcriptional regulation during conduction system formation. We identified a large regulatory fragment driving *GFP* reporter gene expression specifically in the AV node. Subsequently, this transgenic mouse model was used to study the transcription profiles of the developing AV node through microarray analysis, providing new insights into the molecular pathways underlying differentiation and function of the AV canal and maturing AV node.

Materials and methods

Transgenic mice

The transgenic working myocardium-specific promoter-reporter line *NppaBAC336-Egfp* has been described previously (Horsthuis et al., 2008). Bacterial artificial chromosome (BAC)

clone 366H17, containing genomic sequences from -83 kbp to +77 kbp relative to the transcription start site of *Tbx3*, was obtained from a C57BL/6J mouse BAC/PAC library (CHORI, Oakland, CA). To generate the *Tbx3BAC-Egfp* construct, the sequence ATG.agc.ctc.t was replaced by *GFP* using the BAC modification method kindly provided by Gong and Heintz (Gong et al., 2002). An expanded Materials and Methods section is available in the online data supplement and at the end of this chapter.

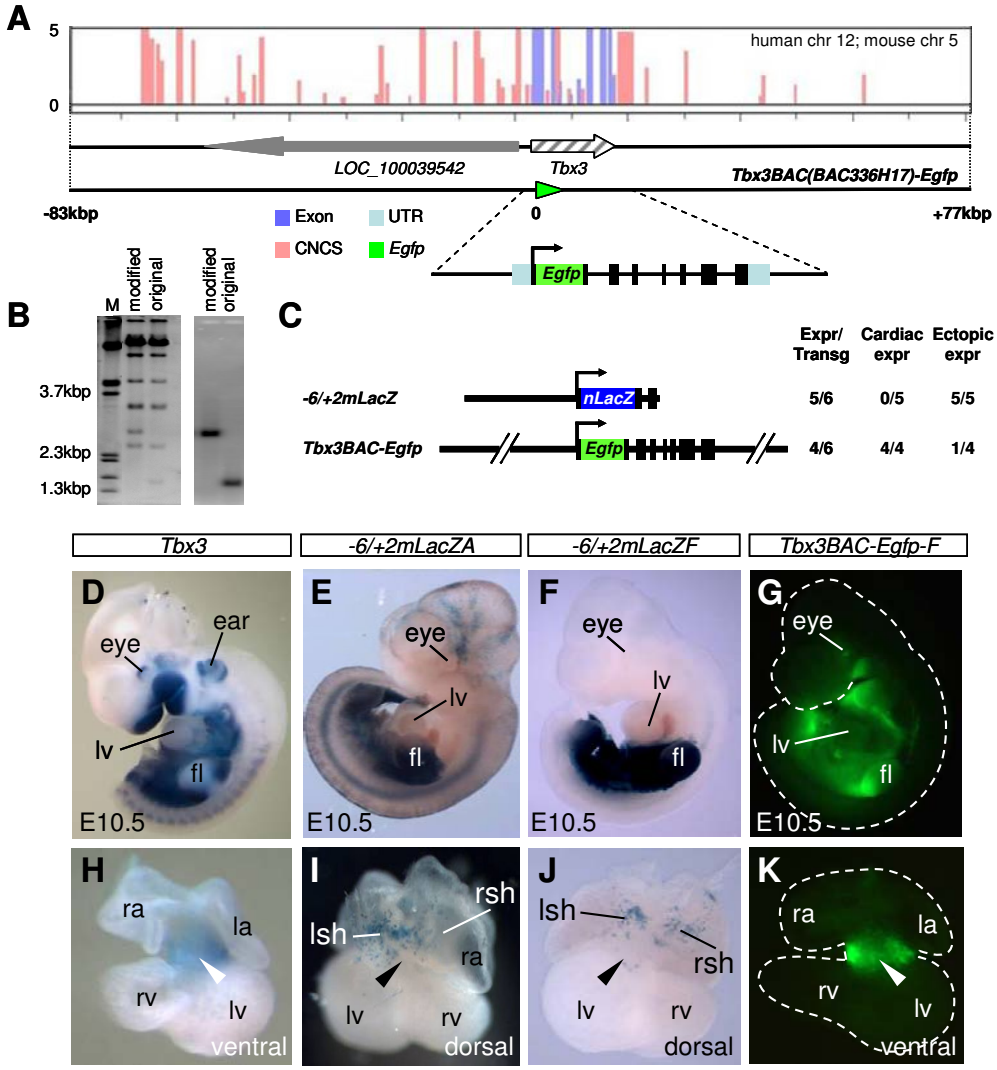

Figure 1. Overview of *Tbx3* regulatory sequences containing reporter constructs used in this study. (A) RankVISTA alignment of human against mouse *Tbx3* genomic region covered by Tbx3BAC336H17. Bars depict evolutionary conserved segments where the heights scale with statistical significance [-log10(P-value)]. (B) After SstII restriction of the original Tbx3BAC and the modified *Tbx3BAC-Egfp* construct, an ethidium bromide stained gel (left) and Southern blot (right) depict the modified fragment. (C) Constructs used to generate transgenic mice. Fraction of founders (transg) expressing GFP (expr) and fraction of expressing transgenes expressing GFP in the heart (cardiac) and ectopically (ectopic), have been indicated. (D, H) Whole mount *in situ* hybridization of *Tbx3*. (E-F and I-J) Whole mount ß-galactosidase staining of two independent founders carrying the *-6/+2mLacZ* construct. (G,K) Fluorescence pictures of mice carrying *Tbx3BAC-Egfp* construct. Black lines in A and C indicate *Tbx3* regulatory sequences, boxes represent exons, dark blue or green boxes the reporter genes. CNCS, conserved non-coding sequence; M, λ-BsteII marker; UTR, untranslated region; lv, left ventricle; fl, forelimb; ra, right atrium; la, left atrium; rv, right ventricle; lsh, left sinus horn; rsh, right sinus horn.

Results

Tbx3 activity is driven by distal regulatory sequences

To assess the spatiotemporal activity of the proximal regulatory sequences of *Tbx3*, transgenic mice were generated in which a fragment ranging from 6 kbp upstream to 2 kbp downstream of the *Tbx3* translation start site drives *LacZ* reporter gene expression (Figure 1C). 5 of 6 independently obtained lines expressed *LacZ* in a pattern unlike that of *Tbx3*. In 4 of these lines *LacZ* was expressed mainly ectopically in the caudal part of the embryo and the forelimbs, whereas no expression was detected in the *Tbx3*$^{+}$ tissues such as the mammary glands or heart (Figure 1D-F,H-J). These observations indicate that the regulatory sequences driving correct spatiotemporal *Tbx3* expression are located outside the 8 kbp regulatory DNA region.

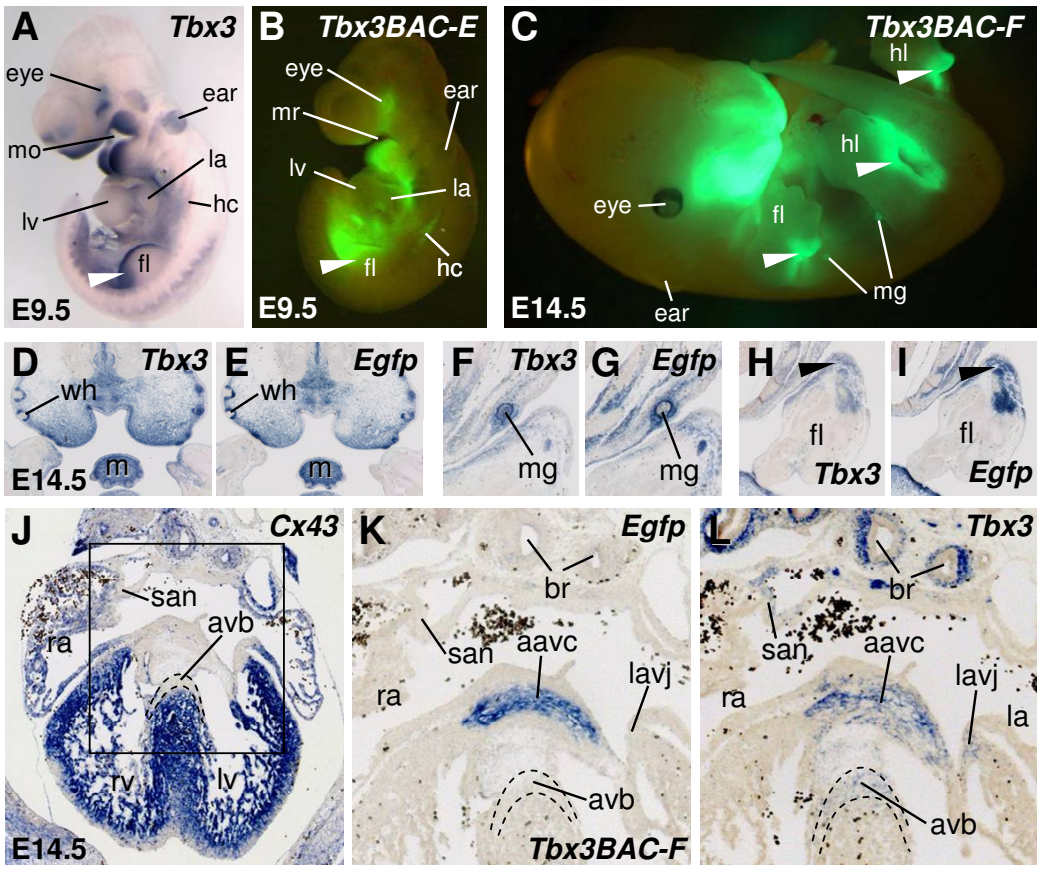

Figure 2. Comparison of expression patterns of endogenous *Tbx3* and the *Tbx3BAC-Egfp* transgene. (A) Whole mount and (D-L) section *in situ* hybridization, and (B-C) fluorescence pictures. Arrowheads point at ulnar site limbs. hc, hypoglossal cord; hl, hindlimb; mg, mammary gland; mr, mandibular and maxillary region; wh, whisker; m, mandibula; san, sinoatrial (sinus) node; avb atrioventricular bundle; br, bronchi; aavc, anterior atrioventricular canal; lavj, left atrioventricular junction. See legend to Figure 1 for other abbreviations.

We next used a BAC clone containing *Tbx3* flanked by 83 kbp upstream sequences and 77 kbp downstream sequences (Figure 1A-C). An enhanced green fluorescent protein (GFP) encoding reporter gene was inserted at the translation start site of *Tbx3*, thereby functionally inactivating *Tbx3*. 4 independent mouse lines carrying *Tbx3BAC-Egfp* showed comparable spatiotemporal GFP patterns (Figure 1G,K and 2B,C) highly similar to the pattern of *Tbx3* (1D,H and 2A). *In situ* hybridizations on serial sections confirmed that in the eye, snout, mammary glands and limbs *Tbx3BAC-Egfp* mimicked *Tbx3* expression (Figure 1G and 2A-I, Supplementary Table 1). However, the construct appeared inactive in the ear (Figure 1G and 2B,C) and the lung mesenchyme (Figure 2K,L), showing that not all DNA sequences regulating *Tbx3* expression were present in the 160 kbp BAC.

Tbx3BAC drives AV node-specific expression

Tbx3 is expressed in the sinus node, AV node, AV bundle and bundle branches (Hoogaars et al., 2004), but *Tbx3BAC-Egfp* was not active in the $Tbx3^{+}/Cx43^{-}$ sinus node, AV bundle and bundle branches (Figure 2J-L). In contrast, *Tbx3BAC-Egfp* was active in the AV canal from E9 onwards. Until E14.5 *Tbx3BAC-Egfp* was active in the dorsal, ventral and right side of the AV canal, colocalizing with the developing AV node (Virágh and Challice, 1977b), right atrioventricular ring bundle (Moorman et al., 1998), retro-aortic root branch (Moorman et al., 1998), and the anterior node-like structure (Blom et al., 1999) or retroaortic node (Anderson et al., 2008), respectively (Figure 2K,L and 3A-D). No activity was detected in the $Tbx3^{+}$ left AV canal. Also the $Tbx3^{+}$ AV mesenchymal cushions were devoid of GFP (Figure 4A). At E17.5, the area of activity in the AV junction (Figure 3E) further diminished, resulting in *Tbx3BAC-Egfp* activity progressively restricted to the AV node. In the adult, we detected *GFP* expression strictly limited to the $Tbx3^{+}/Hcn4^{+}$ tissue of the AV node and the anterior node, complementary to the $Cx40^{+}$ AV bundle (Figure 3G-O).

To further verify AV nodal specificity of *Tbx3BAC-Egfp*, we performed patch-clamp experiments on single GFP^{+} and GFP^{-} cardiac cells of E17.5 embryos. All action potential parameters, except overshoot, differed significantly between both groups (Figure 3P,Q and Supplementary Table 2). Importantly, all GFP^{+} cells (n=4) showed diastolic depolarization resulting in spontaneous activity, and exhibit the hyperpolarization-activated current (I_f), whereas all GFP^{-} cells (n=5) had a stable resting membrane potential, were quiescent and lacked I_f (Figure 3P,Q and Supplementary Table 2). In conclusion, GFP^{+} cells had electrical properties typical for nodal cells and GFP^{-} cells for working myocardial cells. The combined data of the marker expression analysis and patch-clamp experiments indicate that the 160 kbp *Tbx3BAC-Egfp* construct contains regulatory sequences driving specific AV nodal expression, but lacks additional enhancers driving expression in the sinus node, AV bundle and bundle branches.

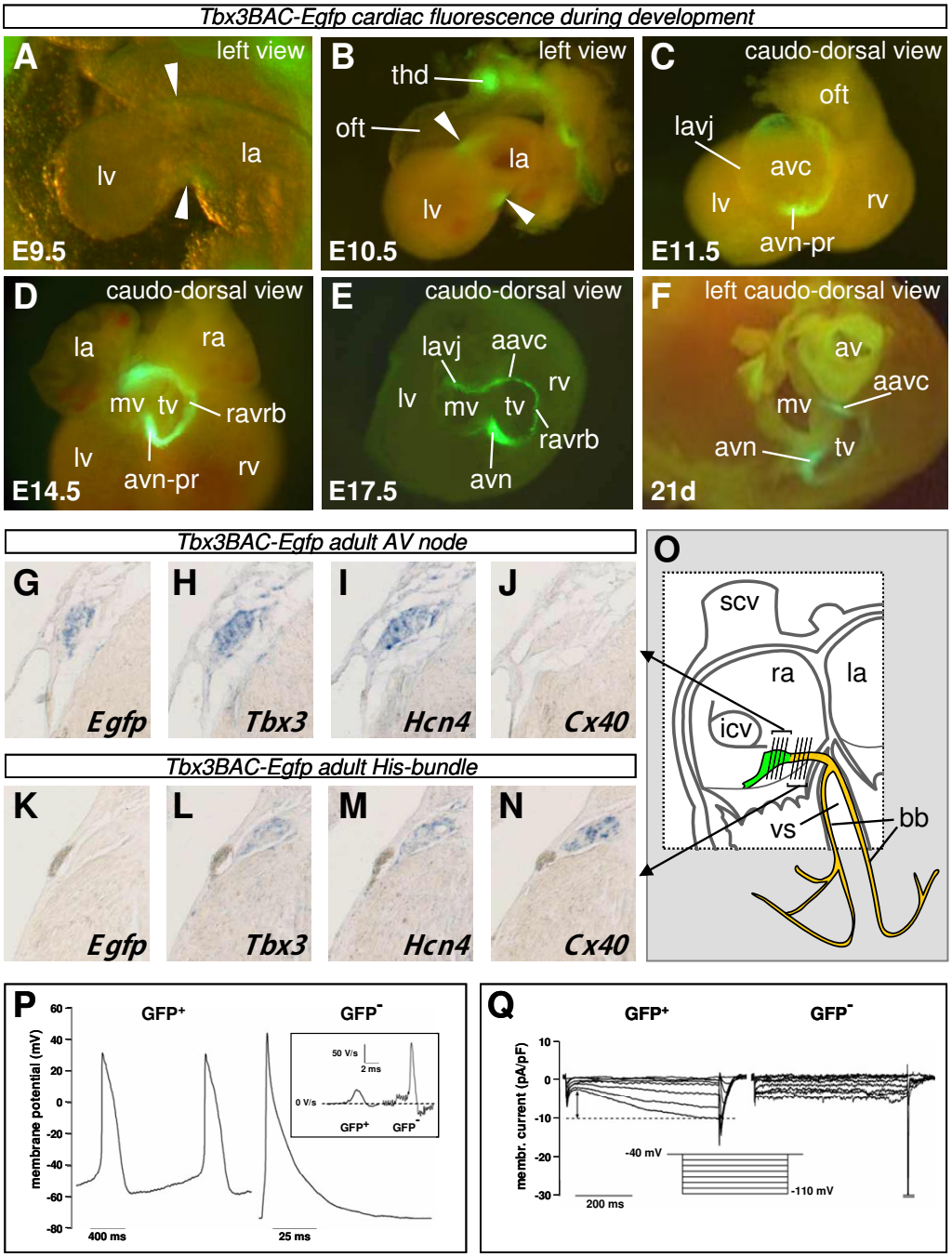

Figure 3. *Tbx3BAC-Egfp* expression in the AV canal is progressively restricted to the developing AV node. (A-F) Atrioventricular fluorescence of mice carrying *Tbx3BAC-Egfp* shown from E9.5 till 3 weeks after birth. (G-O) *In situ* hybridization on serial sections confirmed that *GFP* was expressed only in the $Tbx3^{+}/Hcn4^{+}/Cx40^{-}$ AV node, and not in the $Tbx3^{+}/Hcn4^{+}/Cx40^{+}$ AV bundle. (P) Typical examples of action potentials (APs) from an E17.5 GFP^{+} and an GFP^{-} cell obtained by patch-clamp experiments. APs recorded from all GFP^{+} cells were spontaneous (n=4); APs from GFP^{-} cells were elicited by current injection through the pipette (n=5). Note the differences in time scale. Inset shows the maximal dV/dt, a measure for sodium current availability (Q) Membrane currents activated by 500 ms hyperpolarizing voltage-clamp steps from -40 mV (inset). Note the presence of the hyperpolarizing current (I_f) in the GFP^{+} cells (arrow). This current was never detected in non-fluorescent cells. avn(-pr), atrioventricular node(-primordium); oft, outflow tract; thd, thyroid gland; ravrb, right atrioventricular ring bundle; mv, mitral valve; tv, tricuspid valve; av, aortic valve; scv, superior caval vein; ivc, inferior caval vein; vs, ventricular septum; bb, bundle branches. See legends to Figure 1 and 2 for other abbreviations.

Gene expression profiles of the developing AV node and working myocardium

The property of *Tbx3BAC-Egfp* to drive GFP expression specifically in the AV node myocardium allowed assessing the genome wide expression profiles of these cells during development. *Nppa,* the gene encoding atrial natriuretic factor, is specifically expressed in developing working myocardium complementary to the *Tbx3*$^{+}$ conduction system (Moorman and Christoffels, 2003). The expression of GFP in the *NppaBAC336-Egfp* transgene recapitulates the *Nppa* expression pattern precisely (Horsthuis et al., 2008). Embryonic E10.5 *Tbx3BAC-Egfp* cells (E10.5 AV canal) were compared with age-matched pooled atrial and ventricular cardiomyocytes expressing *NppaBAC336-Egfp* (E10.5 WM (working myocardium)). Fetal E17.5 *Tbx3BAC-Egfp* (E17.5 AV nodal) cells were compared with E17.5 *NppaBAC336-Egfp* atrial working myocardium (E17.5 WM) (Figure 4A and 5A). For every sample, transgenic hearts were dissected, the GFP-positive tissues pooled, dissociated to obtain single cells, and purified using FACS (Figure 4B). Fluorescent cells comprised, on average, 1-4% of live-gated AV nodal, and 3-8% of live-gated WM cell populations, whereas

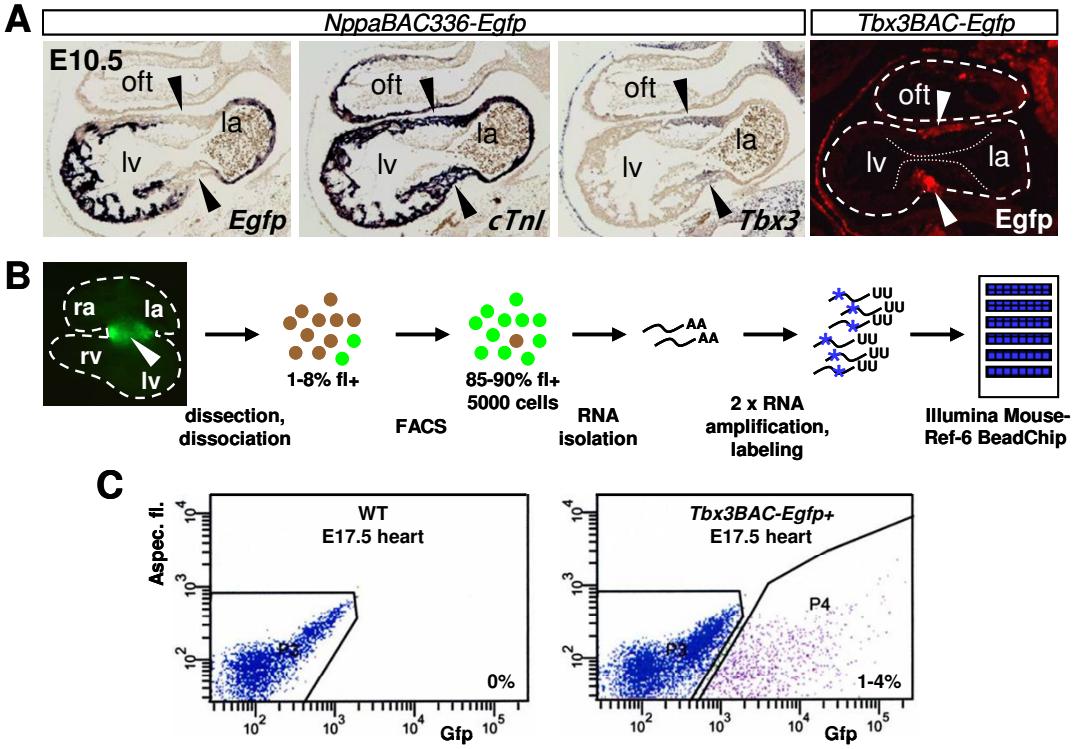

Figure 4. Purification of working myocardium- and AV node myocardium-specific myocyte populations for transcriptome analyses. (A) *In situ* hybridization and immunofluorescent labeling on sections of mice carrying the *NppaBAC336-Egfp* or *Tbx3BAC-Egfp* construct, respectively. (B) Successive steps of fluorescent cell preparation from dissection of the Egfp^{+} hearts till hybridization of amplified and labeled aRNA to the microarray. (C) FACS profiles of hearts of an E17.5 *Tbx3BAC-Egfp*$^{+}$ transgene (right) and a wild type littermate (left). The percentage of Egfp^{+} cells in the live gate is shown. Arrowheads in A point at atrioventricular canal. See legends to Figure 1 and 3 for abbreviations.

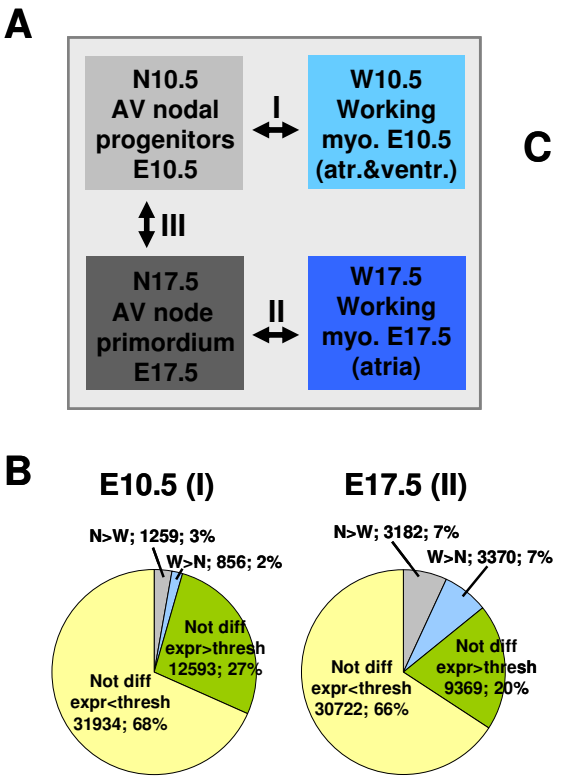

C

Gene	Accession #	E10.5	Fold higher	E17.5	Fold higher
AV canal / node > working myocardium					
Cacna1g (Cav3.1)	NM_009783	N>W	5.6	N>W	48.0
Id2	NM_010496	N=W		N>W	3.5
Kcna6 (Kv1.6)	NM_013568	N>W	9.1	N>W	73.0
Msx2	NM_013601	N>W	9.4	-	
Tbx2	NM_009324	N>W	5.6	N>W	5.9
Tbx3	AK031708	N>W	13.5	N>W	149.9
Tbx20	NM_020496	N=W		N>W	6.8
Working myocardium > AV canal / node					
Cited1	NM_007709	W>N	19.9	W>N	86.5
Gja1 (Cx43)	NM_010288	W>N	2.5	W>N	12.2
Gja5(Cx40)	NM_008121	W>N	157.0	W>N	566.0
Nppa	NM_008725	W>N	32.5	W>N	1587.6
Nppb	NM_008726	W>N	28.5	W>N	13629.6
Scn5a	NM_021544	W>N	47.5	W>N	81.5
Smpx (Chisel)	NM_025357	W>N	10.3	-	

Figure 5. Microarray experiments comparing E10.5 and E17.5 AV nodal myocardium with stage-matched working myocardium cell populations. (A) Scheme of microarray experiments. In present study experiment I and II were performed, after which data regarding III were deduced (For details about III, see Figure 6C). (B) Pie charts summarizing microarray experiment I (E10.5) and II (E17.5), showing number of transcripts enriched in AV nodal tissue relative to age-matched WM (N>W), transcripts enriched in WM relative to age-matched AV nodal myocardium (W>N), transcripts expressed above threshold (expr>thresh) in nodal myocardium and/or WM which are not differentially expressed between both groups, and transcripts not detected above threshold (expr<thresh). (C) Genes previously established to be differentially expressed between AV nodal and age-matched chamber/working myocardium at E10.5 and E17.5 were picked up in the array experiment.

post-sort analysis revealed 85-90% purity of GFP^+ cell populations after flow cytometry (Figure 4B,C). Because the number of E10.5 AV canal GFP^+ cells per embryo were low (typically 0.6 – 0.9 thousand per embryo), 5000 cells per sample were gated and used for RNA isolation. RNA was subjected to 2 rounds of linear amplification and biotin labeling. Within each group (Figure 5A) 6 labeled antisense RNA samples were hybridized to separate Illumina Mouse-Ref-6 BeadChips (Figure 4B). Present and absent calls were calculated, transcripts were counted as differentially expressed at a p-value, adjusted for multiple testing, of <0.01. Microarray data have been submitted to the Gene Expression Omnibus database [http://www.ncbi.nlm.nih.gov/projects/geo] under series GSE13614.

Genes known to be specific to the AV myocardium, including *Tbx3* itself, were highly enriched in both E10.5 and E17.5 AV myocardial groups (Fig. 5C). Also the array data regarding *Tbx20* were consistent with its initial broad and later AV canal-enriched pattern. Genes known to be specific to working myocardium were strongly enriched in working myocardium at both stages (Figure 5C). These data validate the microarray analysis,

and indicate it efficiently identified genes differentially expressed between the developing AV node and age-matched working myocardium. Mutations in *Nkx2-5*, *Tbx5* and *Gata4* result in AV conduction defects or structural AV canal defects in human and mouse (Bruneau, 2008). However, they were not enriched in the AV canal.

Diverging phenotypes of the developing AV node and working myocardium

Of 46643 transcripts present on the array, 14708 transcripts (32%) gave a signal above threshold and were considered to be expressed. Of these, 1259 (3%) were over- and 856 (2%) were underrepresented in the E10.5 AV canal compared to E10.5 WM (Figure 5A, B). In the E17.5 AV node and E17.5 WM, 15921 transcripts were expressed, similar to E10.5. However, the number of differentially expressed enrich genes strongly increased. 3182 (7%) transcripts were upregulated, and 3370 (7%) were under-represented in the E17.5 AV node relative to E17.5 WM, revealing an evident divergence of gene profiles of the differentiating AV node and complementary working myocardium. To assess this deviation in gene profiles we used the GLOBAL test (Goeman et al., 2004). Using standardized test-conditions, we identified 124 differentially expressed Gene Ontology (GO)-categories at E10.5, and 432 terms at E17.5. The test-conditions are shown in the online data supplement. The extensive lists of differentially expressed GO terms will not be discussed here, but are shown in the online data sets IIA and IIB. These data confirmed divergence of gene expression profiles and phenotypes between maturing AV nodal and working myocardium.

Node-specific gene expression increases during development

To evaluate AV nodal gene expression during development independently of developmental changes in working myocardial gene expression, the expression profile data of the E10.5 WM cell population was used as common reference for the three other data sets. We calculated genes differentially expressed between E10.5 WM and E17.5 AV nodal and E10.5 WM and E17.5 WM, respectively, and combined these data with the values found comparing both E10.5 groups. Whereas 2115 transcripts were expressed differentially between E10.5 WM and AV canal myocardium, the difference between E10.5 WM and E17.5 AV nodal myocardium had increased to 11388, implying an increase in differential expression of 9273 transcripts in the maturing AV nodal cells (Figure 6A). Of these, 4611 transcripts appeared differentially expressed between E10.5 WM and E17.5 WM as well, indicating these were not node-specific, but characteristic for myocardial maturation in general (Figure 6B). To gain insight into nodal differentiation, we assessed transcripts differentially expressed between E10.5 WM and E10.5 and/or E17.5 nodal tissue (Figure 6C), excluding those transcripts associated with myocardial maturation. In the E10.5 AV canal, 1092 transcripts were differentially expressed, in the E17.5 AV node 5856. Of the transcripts differentially expressed at E10.5, 249 (23%) transcripts were differentially expressed only early in

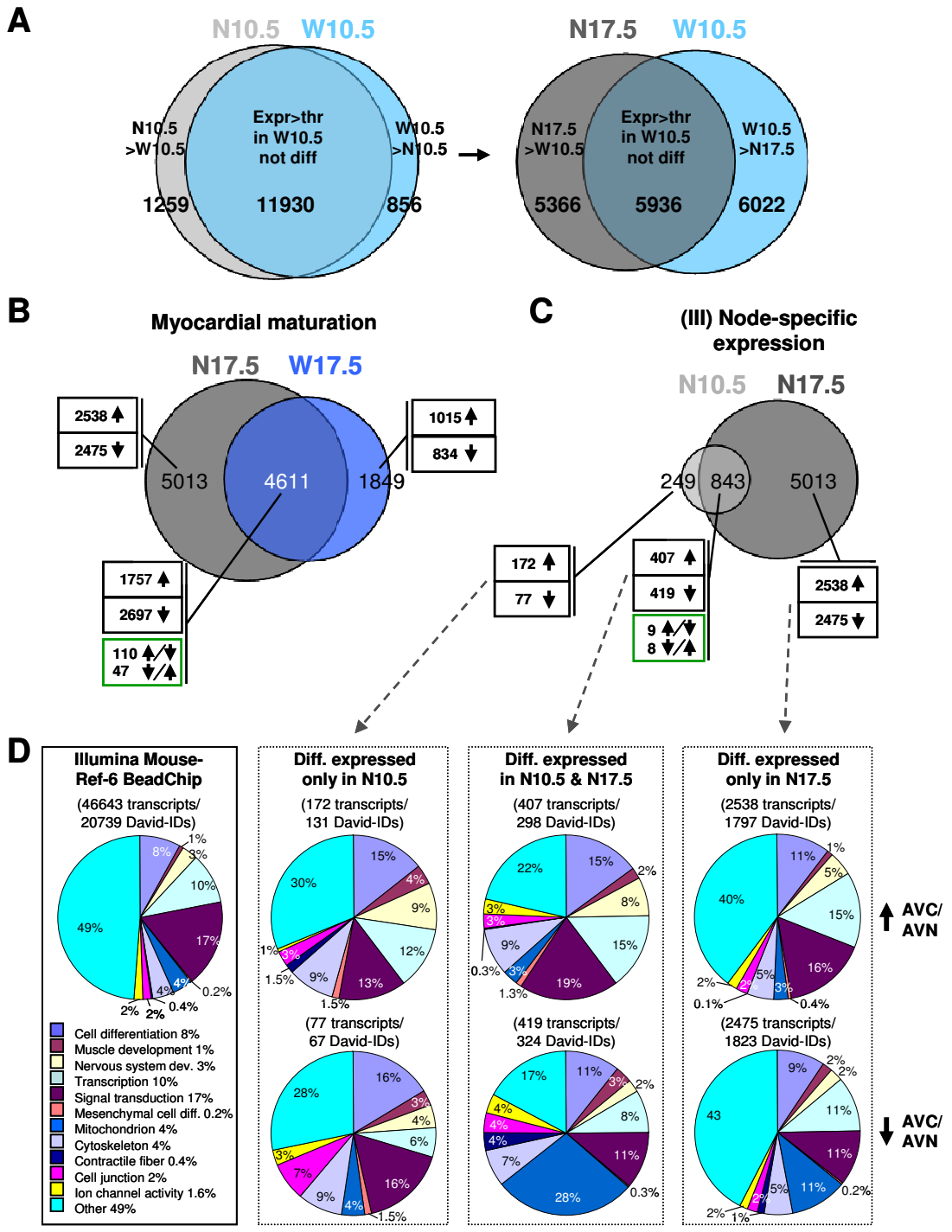

Figure 6. Evaluation of node-specific gene expression during development. (A) Venn diagrams showing transcripts (differentially) expressed in E10.5 AV canal (N10.5) and E17.5 AV node (N17.5) myocardium compared to common reference E10.5 WM (W10.5). Expression levels in E17.5 working myocardium (W17.5) were not taken into account. (B) Transcripts which, relative to W10.5, were differentially expressed in N17.5 and/or W17.5, but not N10.5. Overlap indicates genes involved in cardiac maturation. (C) Transcripts differentially expressed in N10.5 and/or N17.5 (relative to W10.5), but not W17.5. Overlap reveals genes involved in node-specific expression throughout development (See Figure 5A, III). Boxes specify the number of transcripts over- or under-represented relative to W10.5. (D) Functional classification, using GO terms, of transcripts present on the microarray, and of differentially expressed transcripts of node-specific groups mentioned in Figure 6C. By converting the transcript-list into DAVID gene IDs which are unique per gene entry, potential redundancy was removed.

development, whereas 77% (843) were still differentially expressed at E17.5. Together, these data indicate that the AV node differentiates considerably during development, but that the late fetal AV node largely maintains the AV canal program acquired at E10.5.

To gain insight into the 3 groups of differentially expressed genes in the developing AV node, we used the Database for Annotation, Visualization and Integrated Discovery (http://david.abcc.ncifcrf.gov) bioinformatics tool to functionally categorize the transcripts, using GO annotations (Figure 6D). Found percentages were compared to the relative presence of specific GO terms on the Illumina Mouse-Ref-6 BeadChip (Figure 6D). Among transcripts enriched in both the AV canal and AV node, GO categories associated with *cell differentiation*, *transcription* and *nervous system development* were overrepresented. Among *nervous system development,* neurotrophic factors Nrn1, Ntng1, Ntnt2l, Gdnf, Slit2 and Rtn4, the receptors for these neurotrophic factors Unc5b, Unc5c, Ret, and Robo2, and several semaphorins, including *Sema3f*, *Sema3b*, *Sema4c*, *Sema4g* and *Sema6a*, were found to be enriched in the AV canal and / or node. Contamination of nervous tissue at E10.5 can be excluded as the innervation of the heart has not yet taken place at this stage. Therefore, the latter finding should be attributed to shared molecular properties between developing nodal myocardium and nervous tissue. In addition, structure-related GO term *cytoskeleton* was up in both the AV canal and AV node. Among transcripts expressed at a lower level in nodal tissue at both stages, GO terms associated with contraction, energy and electrophysiology were overrepresented (*muscle development, mitochondrion, cytoskeleton, contractile fiber, cell junction, ion channel activity*). These processes and structures are typically more developed in the working myocardium (de Haan, 1961), further elaborating the notion that while AV canal cells substantially differentiate to form AV nodal cells, their primitive, non-working properties are maintained.

Transcripts differentially expressed exclusively in the E10.5 AV canal define its embryo-specific characteristics and might reveal important information regarding the initiation of conduction-system development. Among these, GO categories *cell differentiation, muscle development* and *cytoskeleton* were overrepresented both in the group of AV enriched and in the group of AV reduced transcripts (Fig. 6D). These representations highlight both the further differentiation of cardiac muscle during development, and the divergence in muscular phenotypes between both myocardial subpopulations.

The AV canal / node population could be contaminated with co-purified mesenchymal cells of the AV cushions / fibrous insulation that are in close association with these nodal cells. Resorting of purified GFP^+ cells revealed approximately 85-90% pure cell populations. Indeed, in both E10.5 and E17.5 AV nodal groups, mesenchymal transcripts like *Postn* (Kruzynska-Frejtag et al., 2004) that are highly expressed specifically in the cushion mesenchyme were found to be significantly enriched, whereas the signals for these transcripts was low or absent in both WM groups. It is difficult to estimate contamination because of most transcripts the precise spatial distribution has not been established.

Genome-wide profile of ion channel families expressed in AV nodal tissue

The AV myocardium has highly specific electrophysiological properties. To gain insight into the associated gene profiles, we examined the ion channel expression profiles of the E10.5 and E17.5 AV nodal myocardium relative to age-matched working myocardium (Table 1; Supplementary Table 3). In addition to previously established differences (Schram et al., 2002;Marionneau et al., 2005), we noted several novel channel transcripts to be enriched in the AV node or working myocardium. Of voltage-gated Na^+ (Nav) channels and accessory genes, α-subunit Scn7A (Nav2(.3)) and β-subunit Scn2B (Navβ2) were higher expressed in the E10.5 AV canal and E17.5 node, whereas sodium channel modifier gene 1 (*Scnm1*) was enriched only in the E17.5 AV node. In working myocardium, the prominent cardiac α-subunit Scn5A (Nav1.5) was higher expressed at both developmental stages (Nerbonne and Kass, 2005), as well as fibroblast growth factor Fgf12, a growth factor recently shown to interact with Scn5A and modulate its properties (Liu et al., 2003). Additionally, Scn10A (Nav1.8), another neuronal type Nav α-subunit, was overrepresented in the working myocardium.

Of pore-forming voltage-gated calcium (Cav) channel α-subunits, Cacna1g (Cav3.1) was higher expressed in AV nodal cells at both stages, Cacna1c (Cav1.2), Cacna2d1 (Cavα2δ1) and Cacna2d2 (Cavα2δ2) were picked up at comparable levels in nodal and working myocardial tissue, and Cacna1h (Cav3.2) was expressed at comparable levels throughout E10.5 myocardium, but at E17.5 was enriched in atrial myocardium. Of accessory β-subunits, Cacnab1 (Cavβ1) was overrepresented in the E17.5 AV node, Cacnab2 (Cavβ2) was up in working myocardium at both stages. Other Cav related proteins were not detected above threshold. Of genes involved in Ca^{2+} homeostasis, Calmodulin3 (Calm3) was expressed at high levels throughout the myocardium, yet Calmodulin1 was not detected. Interestingly, of the Calcium/Calmodulin-dependent protein kinase family, several genes were enriched in the node, others in working myocardium. In addition to transient receptor potential (Trp) cation channels Trpc2, Trpc6, Trpm8, known to function in calcium homeostasis, several novel members of this family were enriched in AV nodal (Trpc1, Trpm5, Trpv4) or working myocardial tissue (Trpm2). Inositol 1,4,5-triphosphate receptor 3 (Itpr3), previously associated with pacemaker activity in differentiating cardiomyocytes,(Kapur and Banach, 2007) and *Trpv4* were enriched only in the AV canal. Ankyrin-1,-2 and -3, ATPases, calsequestrin-2 (Casq2), histidine rich calcium binding protein (Hrc), phospholamban (Pln) and ryanodine receptor-2 (Ryr2) were all (much) higher expressed in working myocardium.

Among the voltage-gated potassium (Kv) channel family, α-subunits Kcna6 (Kv1.6), Kcnc4 (Kv3.4) and Kcnh1 (Meag) were enriched moderately in E10.5 AV canal and highly in E17.5 AV node. Auxiliary Kv channel subunits Kcne4 (MiRP), Kcne5 (Mink), Kcnip3 (KChiP3) and Pias3 (KChap) were enriched in the E17.5 AV node. The genes encoding α-subunits Kv1.4, Kv3.2, Kv4.2, Kv4.3, Kv6.2, erg6, Kcnq1 (KvLQT1) and channel modifier

Gene	Alias/ Protein	Accession #	E10.5	Fold higher	E17.5	Fold higher
Sodium channel and auxiliary subunits, modifier genes						
Scn2b	Navβ2	NM_001014761	N>W	2.6	N>W	16.1
Scn7a	Nav2(.3)	NM_009135	N>W	3.8	N>W	2.8
Scnm1		NM_027013	N=W		N>W	2.4
Fgf12		NM_183064	W>N	9.2	W>N	403
Scn5a	Nav1.5	NM_021544	W>N	47.5	W>N	81.5
Scn10a	Nav1.8	NM_009134	W>N	6.9	W>N	92.8
Calcium channel and auxiliary subunits, Ca homeostasis						
Cacna1g	Cav3.1	NM_009783	N>W	5.6	N>W	48.9
Cacnb1	Cavβ1	NM_031173	N=W		N>W	3.1
Camk2n1		NM_025451	N>W	10.3	N>W	8.1
Camk4		NM_009793	N=W		N>W	4.1
Camkk1		NM_018883	-		N>W	3.4
Camkk2		AK044660	N>W	2.7	N>W	3.4
Cask		NM_009806	N=W		N>W	2.6
Gria3		NM_016886	N=W		N>W	18.2
Itpr3	RIP-3	NM_080553	N>W	5.3	N=W	
Pkd2		NM_008861	N>W	2.6	N>W	9.0
Trpc1		AK005144	N=W		N>W	4.1
Trpc2		AK030267	N=W		N>W	2.4
Trpm5		NM_020277	-		N>W	5.7
Trpv4		NM_022017	N>W	63.4	-	
Ank1	Ank-R	NM_031158.1	N=W		W>N	88.2
Ank2	Ank-B	NM_001034168	N=W		W>N	5.2
Ank3	Ank-G	NM_009670.4	N=W		W>N	6.0
Atp2a2	SERCA2	NM_009722	N=W		W>N	8.9
Camk1d		NM_177343	-		W>N	28.5
Camk1g		NM_144817	N=W		W>N	5.0
Camk2a		NM_177407	W>N	8.5	W>N	12.9
Camk2b		NM_007595	N=W		W>N	3.9
Camk2d		NM_001025438	W>N	4.1	W>N	3.5
Camk2g		NM_178597	N=W		W>N	2.6
Cacna1h	Cav3.2	NM_021415	N=W		W>N	8.0
Cacnb2	Cavβ2	NM_023116	W>N	4.0	W>N	8.3
Casq2		NM_009814	W>N	5.8	W>N	45.2
Hrc		NM_010473	N=W		W>N	83.1
Pln	PLB	NM_023129	W>N	5.5	W>N	29.7
Ryr2	RYR2	NM_023868	W>N	4.7	W>N	55.7
Trpm2		AK036731	-		W>N	10.0
Potassium channel and auxiliary subunits, modifier genes						
Kcna6	Kv1.6	NM_013568	N>W	9.1	N>W	73.0
Kcnc4	Kv3.4	NM_145922	N>W	16.3	N>W	42.5
Kcne4	MiRP3	NM_021342	-		N>W	7.0
Kcne5	Mink	NM_021487	N=W		N>W	9.4
Kcnh1	Meag	NM_001038607	N>W	15.8	N>W	54.1
Kcnip3	KChIP3	NM_019789	N=W		N>W	4.6
Kcnj15	Kir4.2	NM_019664	-		N>W	33.1
Kcnk2	TREK-1	NM_010607	N=W		N>W	34.8
Kcnk6	Twik2	NM_001033525	N>W	10.9	N=W	
Kcnma1		NM_010610	-		N>W	4.4
Kcnn4		NM_008433	-		N>W	9.1
Kcns1	Kv9.1	NM_008435	-		N>W	3.9
Pias3	KChap	NM_146135	N=W		N>W	2.3
Dpp6	Dppx	NM_010075	-		W>N	29.0
Kcmf1	Pmcf	NM_019715	N=W		W>N	1.8
Kcna4	Kv1.4	NM_021275	-		W>N	4.5
Kcnc2	Kv3.2	NM_001025581	-		W>N	3.7
Kcnd2	Kv4.2	NM_019697	W>N	22.9	W>N	16.1
Kcnd3	Kv4.3	AK033962	-		W>N	1.9
Kcng2	Kv6.2	XM_140499	W>N	2.4	W>N	2.8
Kcnh7	erg6	AK052366	W>N	4.9	W>N	83.9
Kcnj3	Kir3.1	NM_008426	-		W>N	22.0
Kcnj5	Kir3.4	NM_010605	N=W		W>N	28.5
Kcnj8	Kir6.1	NM_008428	N=W		W>N	4.5
Kcnj11	Kir6.2	NM_010602	-		W>N	6.0
Kcnj12	Kir2.2	NM_010603	-		W>N	28.8
Kcnk3	TASK-1	NM_010608	W>N	5.3	W>N	12.4
Kcnmb1		NM_031169	W>N	6.9	W>N	10.2
Kcnq1	KvLQT1	NM_008434	W>N	4.1	W>N	47.9
Gap junctional subunits:						
Gjc2	Cx47	NM_080454	-		N>W	5.6
Gja1	Cx43	NM_010288	W>N	2.5	W>N	12.2
Gja5	Cx40	NM_008121	W>N	158	W>N	567
Gjd3	Cx30.2	NM_178596	-		W>N	2.3

Table 1. Ion channel gene families, auxiliary subunits, modifier genes and gap junctional subunits that were found to be differentially expressed in E10.5 AV canal and/or E17.5 AV node compared to stage-matched WM. Genes were counted as differentially expressed if the adjusted p-value was <0.01. N>W, enriched in AV canal/node; W>N, enriched in WM; N=W, signal above threshold in nodal and/or working myocardium, but no differential expression; -, no signal detected above threshold. See Supplementary Table 3 for an extensive overview categorized in functional subclasses.

genes *Dpp6* and *Kcmf1* (Pmcf) predominated in working myocardium, of which several already at E10.5. Of the inwardly rectifying K+ (Kir) channel family, α-subunits Kir3.1, Kir2.4, Kir6.1, Kir6.2 and Kir2.2 were higher expressed in the working myocardium. Of 3 differentially expressed members of a novel type of K^+ pore-forming subunits (K2P), Kcnk2 (TREK-1) and Kcnk6 (Twik2) predominated in nodal (Kcnk2 only at E10.5) and Kcnk3 (TASK-1) in working myocardial tissue. Also, 3 calcium-activated channels were differentially expressed, of which Kcnma1 and Kcnn4 were enriched in the AV node. Other channel, accessory subunit and gap junctional transcripts are shown in Supplementary Table 3.

Discussion

Assessing the unique gene profile of the developing AV node myocardium

The adult AV node is a morphologically complex structure with heterogeneous molecular and functional characteristics containing not only cardiomyocytes, but also mesenchymal cells, fibroblasts, smooth muscles, innervating neurons and extracellular matrix. Here, we identified novel *Tbx3* sequences that in the heart are exclusively active in the AV canal- and node myocardium, allowing their selective fluorescent labeling. The specificity of GFP expression was confirmed by detailed expression analysis and patch-clamp analyses of fluorescent cells. Using FACS we obtained purified AV myocardial cell populations largely free of other cell types, and their expression profiles were compared to those of age-matched working myocardial cells obtained from *NppaBAC336-Egfp* mice (Horsthuis et al., 2008). Some contamination of other cells-types, such as AV mesenchymal cells, was observed in the purified AV myocardial populations, but these appeared minor. All transcripts that we are aware of to be enriched in either AV- or (developing) working myocardium were found to be enriched in the corresponding cell populations (Figure 5 and Table 1). Furthermore, genes associated with mitochondria and contractile fibers were underrepresented in both the AV canal and AV node, whereas *Nervous system development* (especially a subclass of neurotrophic genes and semaphorins) was prominently overrepresented in both the AV canal and AV node. These data not only confirm previous findings (de Haan, 1961;Virágh and Challice, 1977a;Virágh and Challice, 1977b;Moorman et al., 1998;Walls, 1947), but provide a much more elaborate picture of the transcriptional landscape of the developing AV node and working myocardium. Taken together, we have generated a potentially valuable transgenic tool to study AV node development and function *in vivo*.

To gain insight into the molecular underpinning of the physiologically complex AV node, we analyzed the expression profile data sets for expression of 'electrophysiological' transcripts (ion channel, accessory subunit, etc). Previous expression studies of the adult AV node have provided valuable data on the expression distribution of those genes (Marionneau et al., 2005). However, those were performed on dissected adult tissues contaminated with adjacent working myocardium and the non-myocardial cell populations, potentially affecting the observed expression profiles. Furthermore, they examined expression of 82 pre-defined genes (Marionneau et al., 2005). The microarray approach presented here largely confirmed these findings, and in addition identified a considerable number of novel cardiac transcripts enriched in either AV nodal or working myocardium that may be important for understanding AV node function (Table 1 and Supplementary Table 3).

The origin and modular development of the AV node

Histological studies and marker analyses revealed that the conduction system (sinus node, AV node, AV bundle and bundle branches) is formed from a contiguous network of myocardial cells distinctive from the surrounding atrial and ventricular (working)

myocardium (Virágh and Challice, 1977a;Virágh and Challice, 1977b;Moorman and Christoffels, 2003;Gourdie et al., 2003). This network can be discriminated already early in development by poorly developed sarcomeres and sarcoplasmatic reticulum, high automaticity, low proliferation rate, sparse mitochondria, selective expression of markers (e.g. Gln2, HNK-1, *Tbx3*, *minK-lacZ*, *CCS-lacZ*) and absence of high-conductance gap junctions (e.g. Cx43) (de Haan, 1961;Virágh and Challice, 1977a;Virágh and Challice, 1977b;de Jong et al., 1992;Moorman et al., 1998). These properties, which are controlled by Tbx3 (Hoogaars et al., 2007;Bakker et al., 2008) and other factors, are largely maintained in the adult components. The existence of this contiguous precursor network with shared properties suggests a common regulatory mechanism for conduction system gene expression and formation. On the other hand, arguments in favor of a modular composition have been put forward as well. During mid-fetal stages, the initially 'nodal' AV bundle acquires rapid conduction and Cx40 expression (Chuck et al., 1997;Bakker et al., 2008). In Nkx2-5/Tbx5 and Tbx5/Id2 double heterozygous mutants and Tbx3 mutants, which develop severe AV bundle defects, the AV node may be less affected (Moskowitz et al., 2007;Bakker et al., 2008), suggestive for differential sensitivity of these components to loss of transcription factor function. In the present study, we found that 160 kbp of *Tbx3* and flanking sequences drive expression highly selectively in the AV canal of embryos, and AV node of adults, but not in the *Tbx3*$^{+}$ AV bundle or sinus node. These data unambiguously demonstrate that separable regulatory sequences and regulatory pathways (regulatory modules) control gene expression and formation of the AV node, AV bundle and other conduction system components.

The AV node may be derived from the embryonic AV canal or AV ring, or may form *de novo* from other sources (Virágh and Challice, 1977a;Virágh and Challice, 1977b;Arguëllo et al., 1988). From E9 onwards, the expression of GFP was observed selectively in the myocardium of the AV canal, and gradually became confined to the AV node and anterior node-like structure (Blom et al., 1999). Further, the expression profile of the embryonic AV canal showed a large overlap with the profile of the late fetal AV node, whereas both profiles were found to be consistently distinctive from both E10.5 and E17.5 working myocardium. These findings indicate early segregation of AV canal cells and adjacent developing working myocardial cells from E10.5 or earlier, arguing the AV node arises from myocardium in the dorsal wall of the AV canal as proposed by Viragh and Challice (Virágh and Challice, 1977a;Virágh and Challice, 1977b).

Specialization of the AV nodal myocardium during development

The embryonic AV canal and the derived AV node maintain many properties (see above) found already in the embryonic heart tube, whereas the surrounding myocardium acquires working myocardial properties (Moorman and Christoffels, 2003). These observations have led to the idea that suppression of (working myocardial) differentiation in the AV canal domain is an important contributing mechanism to AV node formation, an idea that gained

strong support by the functional identification of suppressors Tbx2 and Tbx3 in the AV canal and conduction system (Moorman and Christoffels, 2003). However, the AV myocardium itself is likely to also specialize during development (Milan et al., 2006), an aspect that has not been thoroughly examined thus far. When comparing the AV gene expression profiles at an early (E10.5) and late (E17.5) time point of development with the common reference, 249 transcripts were found to be differentially expressed only at E10.5. These are interesting candidates potentially involved in the initiation and early differentiation of the AV node. 77% of transcripts (843 transcripts) differentially expressed at E10.5 still are differentially expressed in the fetal AV node, indicative for maintenance of properties during AV node development. On the other hand, around 5 thousand transcripts not differentially expressed at E10.5 were differentially expressed in the E17.5 AV node, indicating that the AV node undergoes substantial specialization during development.

Acknowledgments

We thank Berend Hooibrink for excellent technical support, Corrie de Gier-de Vries and Wim TJ Aanhaanen for their contributions, Daniel J Garry and Amanda M Masino for providing protocols, and Marian van Roon of the AMC GGM facility for generating transgenic mice. This work was supported by grants from the Netherlands Heart Foundation (96.002 to V.M.C. and A.F.M.M.); European Community's Sixth Framework Programme contract ('HeartRepair') LSHM-CT-2005-018630 to AMC (V.M.C., A.F.M.M.) and LUMC (P.A.C.H.).

References

Anderson,R.H., A.E.Becker, J.Tranum-Jensen, and M.J.Janse. 1981. Anatomico-electrophysiological correlations in the conduction system--a review. Br. Heart J. 45: 67-82.

Anderson,R.H., J.Yanni, M.R.Boyett, N.J.Chandler, and H.Dobrzynski. 2008. The anatomy of the cardiac conduction system. Clin. Anat.

Arguëllo,C., J.Alanis, and B.Valenzuela. 1988. The early development of the atrioventricular node and bundle of His in the embryonic chick heart. An electrophysiological and morphological study. Dev. 102: 623-637.

Bakker,M.L., B.J.Boukens, M.T.M.Mommersteeg, J.F.Brons, V.Wakker, A.F.M.Moorman, and V.M.Christoffels. 2008. Transcription factor Tbx3 is required for the specification of the atrioventricular conduction system. Circ Res. 102: 1340-1349.

Blom,N.A., A.C.Gittenberger-de Groot, M.C.deRuiter, R.E.Poelmann, M.M.T.Mentink, and J.Ottenkamp. 1999. Development of the cardiac conduction tissue in human embryos using HNK- 1 antigen expression: possible relevance for understanding of abnormal atrial automaticity. Circulation. 99: 800-806.

Boyett,M.R., S.M.Harrison, N.C.Janvier, S.O.McMorn, J.M.Owen, and Z.Shui. 1996. A list of vertebrate cardiac ionic currents nomenclature, properties, function and cloned equivalents. Cardiovasc. Res. 32: 455-481.

Bruneau,B.G. 2008. The developmental genetics of congenital heart disease. Nature 451: 943-948.

Chuck,E.T., D.M.Freeman, M.Watanabe, and D.S.Rosenbaum. 1997. Changing activation sequence in the embryonic chick heart: implications for the development of the His-Purkinje system. Circ. Res. 81: 470-476.

de Haan,R.L. 1961. Differentiation of the atrioventricular conducting system of the heart. Circulation 24: 458-470.

de Jong,F., T.Opthof, A.A.M.Wilde, M.J.Janse, R.Charles, W.H.Lamers, and A.F.M.Moorman. 1992. Persisting zones of slow impulse conduction in developing chicken hearts. Circ. Res. 71: 240-250.

Goeman,J.J., S.A.van de Geer, de Kort F., and H.C.van Houwelingen. 2004. A global test for groups of genes: testing association with a clinical outcome. Bioinformatics. 20: 93-99.

Gong,S., X.W.Yang, C.Li, and N.Heintz. 2002. Highly efficient modification of bacterial artificial chromosomes (BACs) using novel shuttle vectors containing the R6Kgamma origin of replication. Genome Res. 12: 1992-1998.

Gourdie,R.G., B.S.Harris, J.Bond, C.Justus, K.W.Hewett, T.X.O'Brien, R.P.Thompson, and D.Sedmera. 2003. Development of the cardiac pacemaking and conduction system. Birth Defects Res. Part C. Embryo. Today 69: 46-57.

Hoogaars,W.M.H., A.Engel, J.F.Brons, A.O.Verkerk, F.J.de Lange, L.Y.E.Wong, M.L.Bakker, D.E.Clout, V.Wakker, P.Barnett, J.H.Ravesloot, A.F.M.Moorman, E.E.Verheijck, and V.M.Christoffels. 2007. Tbx3 controls the sinoatrial node gene program and imposes pacemaker function on the atria. Genes Dev. 21: 1098-1112.

Hoogaars,W.M.H., A.Tessari, A.F.M.Moorman, P.A.J.de Boer, J.Hagoort, A.T.Soufan, M.Campione, and V.M.Christoffels. 2004. The transcriptional repressor Tbx3 delineates the developing central conduction system of the heart. Cardiovasc Res 62: 489-499.

Horsthuis,T., A.C.Houweling, P.E.M.H.Habets, F.J.de Lange, H.el Azzouzi, D.E.W.Clout, A.F.M.Moorman, and V.M.Christoffels. 2008. Distinct regulation of developmental and heart disease induced atrial natriuretic factor expression by two separate distal sequence. Circ Res. 102: 849-859.

Kapur,N. and K.Banach. 2007. Inositol-1,4,5-trisphosphate-mediated spontaneous activity in mouse embryonic stem cell-derived cardiomyocytes. J. Physiol 581: 1113-1127.

Kruzynska-Frejtag,A., J.Wang, M.Maeda, R.Rogers, E.Krug, S.Hoffman, R.R.Markwald, and S.J.Conway. 2004. Periostin is expressed within the developing teeth at the sites of epithelial-mesenchymal interaction. Dev. Dyn. 229: 857-868.

Li,J., I.D.Greener, S.Inada, V.P.Nikolski, M.Yamamoto, J.C.Hancox, H.Zhang, R.Billeter, I.R.Efimov, H.Dobrzynski, and M.R.Boyett. 2008. Computer three-dimensional reconstruction of the atrioventricular node. Circ. Res. 102: 975-985.

Liu,C.J., S.D.Dib-Hajj, M.Renganathan, T.R.Cummins, and S.G.Waxman. 2003. Modulation of the cardiac sodium channel Nav1.5 by fibroblast growth factor homologous factor 1B. J. Biol. Chem. 278: 1029-1036.

Mangoni,M.E. and J.Nargeot. 2008. Genesis and regulation of the heart automaticity. Physiol Rev. 88: 919-982.

Marionneau,C., B.Couette, J.Liu, H.Li, M.E.Mangoni, J.Nargeot, M.Lei, D.Escande, and S.Demolombe. 2005. Specific pattern of ionic channel gene expression associated with pacemaker activity in the mouse heart. J. Physiol 562: 223-234.

Meijler,F.L. and M.J.Janse. 1988. Morphology and electrophysiology of the mammalian atrioventricular node. Physiol. Rev. 68: 608-647.

Milan,D.J., A.C.Giokas, F.C.Serluca, R.T.Peterson, and C.A.MacRae. 2006. Notch1b and neuregulin are required for specification of central cardiac conduction tissue. Dev. 133: 1125-1132.

Moorman,A.F.M. and V.M.Christoffels. 2003. Cardiac chamber formation: development, genes and evolution. Physiol. Rev. 83: 1223-1267.

Moorman,A.F.M., F.de Jong, M.M.F.J.Denyn, and W.H.Lamers. 1998. Development of the cardiac conduction system. Circ Res 82: 629-644.

Moskowitz,I.P., J.B.Kim, M.L.Moore, C.M.Wolf, M.A.Peterson, J.Shendure, M.A.Nobrega, Y.Yokota, C.Berul, S.Izumo, J.G.Seidman, and C.E.Seidman. 2007. A molecular pathway including id2, tbx5, and nkx2-5 required for cardiac conduction system development. Cell 129: 1365-1376.

Myers,D.C. and G.I.Fishman. 2003. Molecular and functional maturation of the murine cardiac conduction system. TCM 13: 289-295.

Naiche,L.A., Z.Harrelson, R.G.Kelly, and V.E.Papaioannou. 2005. T-Box Genes in Vertebrate Development. Annu. Rev. Genet. 39: 219-239.

Nerbonne,J.M. and R.S.Kass. 2005. Molecular physiology of cardiac repolarization. Physiol Rev. 85: 1205-1253.

Schram,G., M.Pourrier, P.Melnyk, and S.Nattel. 2002. Differential distribution of cardiac ion channel expression as a basis for regional specialization in electrical function. Circ. Res. 90: 939-950.

Stroud,D.M., V.Gaussin, J.B.Burch, C.Yu, Y.Mishina, M.D.Schneider, G.I.Fishman, and G.E.Morley. 2007. Abnormal conduction and morphology in the atrioventricular node of mice with atrioventricular canal-targeted deletion of Alk3/Bmpr1a receptor. Circulation 116: in press.

Virágh,Sz. and C.E.Challice. 1977a. The development of the conduction system in the mouse embryo heart. I. The first embryonic A-V conduction pathway. Dev Biol 56: 382-396.

Virágh,Sz. and C.E.Challice. 1977b. The development of the conduction system in the mouse embryo heart. II. Histogenesis of the atrioventricular node and bundle. Dev Biol 56: 397-411.

Walls,E.W. 1947. The development of the specialized conducting tissue of the human heart. J. Anat. 81(Pt 1): 93-110.6.

Supplementary data

Expanded materials and methods

Transgenic mice

-6/+2mLacZ construct

To generate the *-6/+2mLacZ* construct, an nlsLacZ-pA cassette was placed at the translation start site of *Tbx3* in an 8 kbp fragment from the endogenous Sca1 restriction site at 6 kbp upstream to the endogenous PshA1 site at 2 kbp downstream of the translation start site. Vector sequences were removed before introduction into the mouse genome.

Tbx3BAC-Egfp construct

The two-step BAC modification protocol previously described by Shiaoching Gong and Nathaniel Heinz (Gong et al., 2002), consists of two homologous recombination steps. After both the co-integration and the resolution step correct recombination was verified by Southern blot using a hybridization probe against *Egfp*. The *BAC-Egfp* constructs were purified using a CsCl gradient following a protocol also kindly provided by Shiaoching Gong and Nathaniel Heinz. Constructs were linearized before introduction into the mouse genome. To generate transgenic mouse lines, constructs were injected into pronuclei of zygotes of FVB mice and these were re-implanted into pseudo-pregnant foster mothers by use of standard techniques. Animal care was in accordance with national and international guidelines.

Non-radioactive in situ hybridisation, β-galactosidase activity detection and immunohistochemistry

Embryos were fixed in 4% formaldehyde, embedded in paraplast and sectioned at 10 μm for immunohistochemistry and *in situ* hybridization on sections. Whole mount *in situ* hybridization, *in situ* hybridization on sections and whole mount β-galactosidase activity staining were performed as described previously (Moorman et al., 2001;Franco et al., 2001). For immunohistochemistry GFP rabbit polyclonal primary antibody (1:250; Santa Cruz) was used. The secondary antibody used was Alexa 568 goat-anti-rabbit (1:250; Invitrogen).

Electrophysiology

Cell isolation. Hearts isolated from E17.5 heterozygous *BACTbx3-Egfp*$^{+}$ embryos were immersed in a standard solution containing (mmol/l) 140 NaCl, 5.4 KCl, 1.8 $CaCl_2$, 1.0 $MgCl_2$, 5.5 glucose, 5 HEPES; pH7.4 (NaOH). After removal of the atria, fluorescent cells of the atrioventricular (AV) region were visualized with a stereomicroscope equipped for GFP detection. The fluorescent AV regions of 10 embryo's were dissected and pooled. Cells were

dissociated in an enzyme mix (Gibco 14170-070 with pancreatine, 60 mg/ml and trypsine 1.25 mg/ml) in a multiple rotate-harvest procedure, using a rotator and water bath at 37°C. To get rid of cardiac fibroblasts cells were incubated for 2 hours, next myocytes were plated on collagen coated cover slips and cultured for 24 hours.

Data acquisition. Action potentials (APs) and hyperpolarizing-activated current (I_f) were recorded at 36±0.2°C from single *BACTbx3-Egfp*$^+$ and *BACTbx3-Egfp*$^-$ cells with the amphotericin-B perforated patch-clamp technique using an Axopatch 200B patch-clamp amplifier (Molecular Devices Corporation, Sunnyvale, CA, USA). Superfusion solution contained (mmol/l): 140 NaCl, 5.4 KCl, 1.8 $CaCl_2$, 1 $MgCl_2$, 5.5 glucose, 5 HEPES; pH 7.4 (NaOH). Pipettes (3-4 MΩ, borosilicate glass) were filled with solution containing (mmol/l): 125 K-gluc, 20 KCl, 5 NaCl, 0.22 amphotericin-B, 10 HEPES; pH 7.2 (KOH). APs were low-pass filtered with a 10-kHz cut-off frequency, and digitized at 25-kHz; I_f recordings were both filtered and digitized at 5-KHz. Membrane capacitance (C_m) was estimated by dividing the decay time constant of the capacitive transient in response to 5-mV hyperpolarizing voltage-clamp steps from -40 mV by the series resistance (R_s). Potentials were corrected for liquid junction potential, and C_m and R_s were compensated for >80%. For voltage control, data acquisition, and analysis, custom-made software was used.

Stimulation protocols. (Supplementary Table 2) In cells without pacemaker activity, APs were elicited at 2-Hz by 3-ms, 1.5× threshold current pulses through the patch pipette. We analyzed cycle length, maximal diastolic potential (MDP), diastolic depolarization rate (DDR, measured over the 100-ms time interval starting at MDP + 1 mV), maximal upstroke velocity (dV/dt_{max}), maximal AP amplitude (APA), and AP duration at 20, 50, and 90% repolarization (APD_{20}, APD_{50} and APD_{90}). Parameters from 10 consecutive APs were averaged. I_f was measured by 500-ms hyperpolarizing voltage clamp steps from a holding potential of –40 mV. I_f was normalized to C_m.

Statistics. Results are expressed as mean±SEM. Data are considered different if $p<0.05$. The Mann-Whitney U test, unpaired *t*-test, or Fisher's exact test was used if appropriate.

Fluorescent-activated cell sorting and RNA handling

Hearts from stage-matched embryos were removed, pooled, and single-cell FACS samples were prepared using a protocol described by Masino and Garry (Masino et al., 2004). Cells were sorted on a FacsAria flow cytometer (BD Biosciences) using FacsDIVA software. Samples from wild-type age-matched hearts were used for gating. Samples were gated to exclude debris and cell clumps. Per sample 5000 live-gated cells were collected directly in RA1 Nucleospin RNA cell lysis buffer and RNA was isolated following the protocol of the manufacturer (Machery-Nagel). RNA integrity was checked on a Agilent Bioanalyzer 2100, using RNA 6000 pico chips. Samples were subjected to 2 rounds of linear amplification, using the MessageAmp II aRNA Amplification Kit (Ambion) for the first round, and the

Illumina TotalPrep RNA Amplificaton Kit (Ambion) for the second round and biotin-16-UTP labelling.

Microarray analysis

Labeled RNA was hybridized to Illumina MouseRef-6 BeadChip following the manufacturer's instructions (Illumina Inc.). Beadstudio software was used to assess the individual array quality. Intensity values were averaged per bead type and subsequently normalized using VSN in R (Huber et al., 2002). Present/absent call calculation was based on more than 300 negative controls per array. Analysis of differentially expressed genes was done with LIMMA package in R (Smyth et al., 2004). P-values were adjusted for multiple testing using the method proposed by Benjamin and Hochberg. Transcripts were counted as differentially expressed if the adjusted p-value was <0.01.

Bioinformatics

Settings GLOBAL test determining global (differential) expression patterns of functional groups of genes

A Gene Ontology (GO) functional category is considered to be significantly associated with the difference in genotypes tested when all of the following selection criteria are met.
Per GO catagory:

1) at least 10, maximum 75 genes
2) at least 5 genes with an influence >5
3) at least 25% of genes for N>W with influence >5, or at least 25% of genes for W>N with influence >5, or both
4) BY-FDR <= 0.1

Geneplots of differentially expressed GO categories:

The bar height for each of the genes in the geneplots indicates the standardized influence of each gene represented in the specific GO term. The scales in the individual bars represent the number of standard deviations that the gene influence exceeds the null hypothesis that the gene is not associated with the difference in phenotype between N and W for the specific time point. Genes with red bars have higher expression levels in W, genes with green bars have higher expression levels in N. The blue dashed line indicates the critical influence value of 5 that was used in the selection of the GO terms. For practical reasons, geneplots have not been included here. For geneplots of differentially expressed GO categories please contact the corresponding author (e-mail: v.m.christoffels@amc.uva.nl).

Supplementary Table 1. Overview of expression patterns of the endogenous Tbx3 gene and the 160 kbp BACTbx3-Egfp construct, E9.5-E17.5. +, expression; -, no expression; +/-, incomplete expression.

		Tbx3	Egfp
heart	sinus node	+	-
	AV canal	+	+/-
	AV cushions	+	-
	AV node	+	+
	AV (His) bundle	+	-
	second heartfield	+/-	-
	OFT cushions/valves	+	-
	cardiac neural crest	+	+
	cardiac plexus	+	+/-
head	mandibula mesenchyme	+	+
	maxilla mesenchyme	+	+
	whisker	+	+
	teeth	+	+
	tongue	+	+
	optic vesicle (dorsal region)	+	+
	otic vesicle	+	-
	Rathke	+	-
	infundibulum	+	+
	thyroid	+	+
	hypoglossal cord	+	+
body	laryngeal groove mesenchyme	+	+
	laryngeal groove epithelium	-	+
	trachea mesenchyme	+	-
	lung mesenchyme	+	-
	muscles thorax	+	+
	cartilage ribs	+	+
	body wall	+	+
	mammary gland epithelial bud	+	+/-
	mammary gland mesothelium	+	+
	dorsal root ganglia	+	+
	limbs (ulnar side)	+	+
	diaphragm	+	+
	septum transversum	+	+
	trigeminal ganglion	+	+
	urogenital sinus	+	+
	urogenital ridge	+	-
	metanephric duct	+	+
	metanephric blastema	+	-
	genital tubercle	+	+
	liver	+	+/-

Supplementary Table 2. Action potential properties of single BACTbx3-Egfp-positive and BACTbx3-Egfp-negative cells

	GFP^+ cells	GFP^- cells
	n=4	n=5
cycle length (ms)	472±138	–
MDP (mV)	-58.9±5.1	-74.2±2.7*
DDR_{100} (mV/s)	55±27	–
dV/dt_{max} (V/s)	27±14	111±30*
APA (mV)	97±7	123±5*
overshoot (mV)	38±10	48±5
APD_{20} (ms)	27.8±7.1	4.4±1.0*
APD_{50} (ms)	61.2±8.4	14.8±5.1*
APD_{90} (ms)	98.6±13.0	44.8±7.4*

Data are mean±SEM; n, number of cells; MDP, maximal diastolic potential; DDR_{100}, diastolic depolarization rate over the 100-ms time interval starting at MDP; dV/dt_{max}, maximal upstroke velocity; APA, action potential amplitude; APD_{20}, APD_{50}, and APD_{90}, action potential duration at 20, 50, and 90% repolarization. *p<0.05.

Supplementary Table 3. Expression profiles of all electricity-associated transcripts on the microarray, categorized in functional subclasses.

Gene	Alias/ Protein	Accession #	E10.5	Fold higher	E17.5	Fold higher
Sodium channel and auxiliary subunits, modifier genes						
Scn1a	Nav1.1	NM_018733	-		-	
Scn2a1	Nav1.2	XM_980330	-		-	
Scn3a	Nav1.3	NM_018732	-		-	
Scn4a	Nav1.4	NM_133199	-		-	
Scn5a	Nav1.5	NM_021544	W>N	47.5	W>N	81.5
Scn7a	Nav2(.3)	NM_009135	N>W	3.8	N>W	2.8
Scn8a	Nav1.6	NM_001077499	-		-	
Scn10a	Nav1.8	NM_009134	W>N	6.9	W>N	92.8
Scn11a	Nav1.9	NM_011887	-		-	
Scn1b	Navβ1	NM_011322	-		-	
Scn2b	Navβ2	NM_001014761	N>W	2.6	N>W	16.1
Scn3b	Navβ3	NM_153522	-		-	
Scn4b	Navβ4	NM_001013390	-		N=W	
Fgf12		NM_183064	W>N	9.2	W>N	403
Scnm1		NM_027013	N=W		N>W	2.4
Calcium channel and auxiliary subunits, Ca homeostasis						
Ank1	Ank-R	NM_031158.1	N=W		W>N	88.20
Ank2	Ank-B	NM_001034168	N=W		W>N	5.2
Ank3	Ank-G	NM_009670.4	N=W		W>N	6.0
Atp2a1	SERCA1	NM_007504	N=W		-	
Atp2a2	SERCA2	NM_009722	N=W		W>N	8.9
Cacna1a	Cav2.1	NM_007578	-		-	
Cacna1b	Cav2.2	NM_007579	-		-	
Cacna1c	Cav1.2	NM_009781	N=W		N=W	
Cacna1d	Cav1.3	NM_028981	-		-	
Cacna1e	Cav2.3	NM_009782	-		-	
Cacna1f	Cav1.4	NM_019582	-		-	
Cacna1g	Cav3.1	NM_009783	N>W	5.6	N>W	48.9
Cacna1h	Cav3.2	NM_021415	N=W		W>N	8.0
Cacna1i	Cav3.3	NM_001044308	-		-	
Cacna2d1	Cavα2δ1	NM_009784	N=W		N=W	
Cacna2d2	Cavα2δ2	NM_020263	N=W		N=W	
Cacna2d3	Cavα2δ3	NM_009785	-		-	
Cacna2d4	Cavα2δ4	NM_001033382	-		-	
Cacnb1	Cavβ1	NM_031173	N=W		N>W	3.1
Cacnb2	Cavβ2	NM_023116	W>N	4.0	W>N	8.3
Cacnb4	Cavβ4	NM_001037099	-		-	
Cacng1	Cavγ1	NM_007582	-		-	
Cacng2	Cavγ2	NM_007583	-		-	
Cacng3	Cavγ3	NM_019430	-		-	
Cacng4	Cavγ4	NM_019431	-		-	
Cacng5	Cavγ5	NM_080644	-		-	
Cacng6	Cavγ6	NM_133183	-		-	
Cacng7	Cavγ7	NM_133189	-		-	
Calm1		NM_009790	-		-	
Calm3		NM_007590	N=W		N=W	
Camk1d		NM_177343	-		W>N	28.5
Camk1g		NM_144817	N=W		W>N	5.0
Camk2a		NM_177407	W>N	8.5	W>N	12.9
Camk2b		NM_007595	N=W		W>N	3.9
Camk2d		NM_001025438	W>N	4.1	W>N	3.5
Camk2g		NM_178597	N=W		W>N	2.6
Camk2n1		NM_025451	N>W	10.3	N>W	8.1
Camk4		NM_009793	N=W		N>W	4.1
Camkk1		NM_018883	-		N>W	3.4

Gene	Alias/ Protein	Accession #	E10.5	Fold higher	E17.5	Fold higher
Camkk2		AK044660	N>W	2.7	N>W	3.4
Cask		NM_009806	N=W		N>W	2.6
Casq2		NM_009814	W>N	5.8	W>N	45.2
Gria3		NM_016886	N=W		N>W	18.2
Hrc		NM_010473	N=W		W>N	83.1
Itpr1		NM_010585	N=W		N=W	
Itpr2	RIP3-2	NM_010586	-		-	
Itpr3	RIP-3	NM_080553	N>W	5.3	N=W	
Pkd2		NM_008861	N>W	2.6	N>W	9.0
Pln	PLB	NM_023129	W>N	5.5	W>N	29.7
Ryr2	RYR2	NM_023868	W>N	4.7	W>N	55.7
Trpc1	Trp1	AK005144	N=W		N>W	4.1
Trpc2		AK030267	N=W		N>W	2.4
Trpm2		AK036731	-		W>N	10.0
Trpm5		NM_020277	-		N>W	5.7
Trpv4		NM_022017	N>W	63.4	-	
Potassium channel and auxiliary subunits, modifier genes						
Dpp6	Dppx	NM_010075	-		W>N	29.0
Freq	NCS1	NM_019681	*		*	
Kcmf1	Pmcf	NM_019715	N=W		W>N	1.8
Kcna1	Kv1.1	NM_010595	-		-	
Kcna2	Kv1.2	NM_008417	-		-	
Kcna3	Kv1.3	NM_008418	-		-	
Kcna4	Kv1.4	NM_021275	-		W>N	4.5
Kcna5	Kv1.5	NM_145983	N=W		-	
Kcna6	Kv1.6	NM_013568	N>W	9.1	N>W	73.0
Kcna7	Kv1.7	NM_010596	-		-	
Kcna10	Kv1.10	NM_001081140	-		-	
Kcnab1	Kvβ1	NM_010597	-		-	
Kcnab2	Kvβ2	NM_010598	N=W		N=W	
Kcnab3	Kvβ3	NM_010599	-		N=W	
Kcnb1	Kv2.1	NM_008420	-		-	
Kcnc1	Kv3.1	NM_008421	-		-	
Kcnc2	Kv3.2	NM_001025581	-		W>N	3.7
Kcnc3	Kv3.1	NM_008422	-		-	
Kcnc4	Kv3.4	NM_145922	N>W	16.3	N>W	42.5
Kcnd1	Kv4.1	NM_008423	-		-	
Kcnd2	Kv4.2	NM_019697	W>N	22.9	W>N	16.1
Kcnd3	Kv4.3	AK033962	-		W>N	1.9
Kcne1	MinK	NM_008424	N=W		N=W	
Kcne2	MIRP1	NM_134110	-		-	
Kcne3	MIRP2	NM_020574	-		-	
Kcne4	MiRP3	NM_021342	-		N>W	7.0
Kcne5	Mink	NM_021487	N=W		N>W	9.4
Kcnf1	Kv5.1	NM_201531	-		-	
Kcng2	Kv6.2	XM_140499	W>N	2.4	W>N	2.8
Kcng3	Kv6.3	NM_153512	-		-	
Kcng4	Kv6.4	NM_025734	-		-	
Kcnh1	Meag	NM_001038607	N>W	15.8	N>W	54.1
Kcnh2	erg1	AF034762	-		-	
Kcnh3	erg2	NM_010601	-		-	
Kcnh5	erg4	NM_172805	-		-	
Kcnh6	erg5	NM_001037712	-		-	
Kcnh7	erg6	AK052366	W>N	4.9	W>N	83.9
Kcnh8	erg7	NM_001031811	-		-	
Kcnip1	KChIP1	NM_027398	-		-	
Kcnip2	KChIP2	NM_145703	-		-	
Kcnip3	KChIP3	NM_019789	N=W		N>W	4.6
Kcnip4	KChIP4	NM_030265	-		-	
Kcnj1	Kir1.1	NM_019659	-		-	

Gene	Alias/ Protein	Accession #	E10.5	Fold higher	E17.5	Fold higher
Kcnj2	Kir2.1	NM_008425	-		-	
Kcnj3	Kir3.1	NM_008426	-		W>N	22.0
Kcnj5	Kir3.4	NM_010605	N=W		W>N	28.5
Kcnj6	Kir3.2	NM_010606	-		-	
Kcnj8	Kir6.1	NM_008428	N=W		W>N	4.5
Kcnj11	Kir6.2	NM_010602	-		W>N	6.0
Kcnj12	Kir2.2	NM_010603	-		W>N	28.8
Kcnj15	Kir4.2	NM_019664	-		N>W	33.1
Kcnk1	TWIK1	NM_008430	-		-	
Kcnk2	TREK-1	NM_010607	N=W		N>W	34.8
Kcnk3	TASK-1	NM_010608	W>N	5.3	W>N	12.4
Kcnk4	TRAAK	NM_008431	-		-	
Kcnk5	TASK2	NM_021542	-		N=W	
Kcnk6	Twik2	NM_001033525	N>W	10.9	N=W	
Kcnk13		NM_146037	-		N=W	
Kcnk15	TASK5	NM_001030292	-		-	
Kcnk16	TALK-1	XM_907162.1	-		-	
Kcnk18		NM_207261.3	-		-	
Kcnma1		NM_010610	-		N>W	4.4
Kcnmb1		NM_031169	W>N	6.9	W>N	10.2
Kcnn1	SK1	NM_032397	N=W		N=W	
Kcnn2	SK2	NM_080465	-		-	
Kcnn3	SK3	NM_080466	-		-	
Kcnn4		NM_008433	-		N>W	9.1
Kcnq1	KvLQT1	NM_008434	W>N	4.1	W>N	47.9
Kcnq2	Kcnq2	NM_001006680	-		-	
Kcnq3	Kcnq3	NM_152923	-		-	
Kcnq5	Kv7.5	AK039046	-		-	
Kcns1	Kv9.1	NM_008435	-		N>W	3.9
Kcns2	Kv9.2	NM_181317	-		-	
Kcns3	Kv9.3	NM_173417	-		-	
Kcnu1		NM_008432	-		-	
Kcnv1	Kv8.1	NM_026200	-		-	
Kcnv2	Kv8.2	NM_183179	-		-	
Pias3	KChap	NM_146135	N=W		N>W	2.3
Gap junctional subunits:						
Gja1	Cx43	NM_010288	W>N	2.5	W>N	12.2
Gja4	Cx37	NM_008120	N=W		N=W	
Gja5	Cx40	NM_008121	W>N	158	W>N	567
Gjc1	cx45	NM_008122	N=W		N=W	
Gjc2	Cx47	NM_080454	-		N>W	5.6
Gjd3	Cx30.2	NM_178596	-		W>N	2.3
Miscellaneous genes associated with ion channels or calcium homeostasis						
Abcc8	SUR1	NM_011510	N=W		W>N	982
Abcc9	SUR2	NM_021041	W>N	17.1	W>N	6.6
Accn2	ASIC1	NM_009597	N>W	5.9	N>W	14.6
Accn3	ASIC3	NM_183000	-		W>N	2.8
Atp1a1		NM_144900	N=W		W>N	3.3
Atp1b1		NM_009721	N=W		W>N	2.3
Cftr		NM_021050	-		-	
Clcn1		NM_013491	-		N=W	
Clcn2	ClC2	NM_009900	N=W		N>W	2.9
Clcn3	ClC3	NM_007711	N=W		W>N	2.6
Clcn6		AK045787	W>N	3.2	W>N	4.9
Clcn7		NM_011930	N=W		N=W	
Clic1		NM_033444	N=W		N=W	
Clic3		NM_027085	-		W>N	162
Clic4		NM_013885	N=W		W>N	2.2
Clic5		NM_172621	-		W>N	7.2

Gene	Alias/ Protein	Accession #	E10.5	Fold higher	E17.5	Fold higher
Clic6		NM_172469	N=W		W>N	9.0
Clns1a		NM_023671	N=W		N=W	
Hcn1	HCN1	NM_010408	-		-	
Hcn2		NM_008226	-		-	
Hcn3		NM_008227	-		N>W	5.5
Hcn4	HCN4	NM_001081192	-		-	
P2rx1		NM_008771	-		W>N	4.4
P2rx4		NM_011026	N=W		N>W	2.5
P2rx5		NM_033321	-		N=W	
P2rx7		NM_001038887	-		N>W	3.0
P2rxl1		NM_011028	-		-	
Slc4a3		NM_009208	N=W		W>N	8.3
Slc8a1		NM_011406	*		*	
Slc26a7		NM_145947	-		N>W	11.8
Slco3a1		NM_001038643	N=W		N=W	
Trpc4ap		NM_019828	N=W		N=W	
Trpc6		AK086446	N=W		N=W	
Trpc7		NM_012035	-		-	
Trpm4	Mls2s	NM_175130	N=W		N=W	
Trpm7		AK009470	N=W		N=W	
Trpv2		NM_011706	N=W		W>N	6.4

E10.5 and E17.5 AV canal/node (N) compared with age-matched working myocardium (W). N>W, higher expression in N than in W ($p<0.01$); W>N, higher expression in W than in N ($p<0.01$); N=W, not differentially expressed between N and W ($p>0.01$), expression level above threshold in N and/or W; -, not differentially expressed between N and W ($p>0.01$), expression level not above threshold in N and W; *, Expressed above threshold, some probes of gene higher signal in N, some in W

References supplementary data

Franco D, de Boer PAJ, de Gier-de Vries C, Lamers WH, Moorman AFM. Methods on in situ hybridization, immunohistochemistry and b-galactosidase reporter gene detection. Eur J Morphol 2001;39:169-91.

Gong S, Yang XW, Li C, Heintz N. Highly efficient modification of bacterial artificial chromosomes (BACs) using novel shuttle vectors containing the R6Kgamma origin of replication. Genome Res 2002 December;12:1992-8.

Huber W, von Heydebreck A., Sultmann H, Poustka A, Vingron M. Variance stabilization applied to microarray data calibration and to the quantification of differential expression. Bioinformatics 2002;18 Suppl 1:S96-104.

Masino AM, Gallardo TD, Wilcox CA, Olson EN, Williams RS, Garry DJ. Transcriptional regulation of cardiac progenitor cell populations. Circ Res 2004;95:389-97.

Moorman AFM, Houweling AC, de Boer PAJ, Christoffels VM. Sensitive nonradioactive detection of mRNA in tissue sections: novel application of the whole-mount in situ hybridization protocol. J Histochem Cytochem 2001;49:1-8.

Smyth GK. Linear models and empirical Bayes methods for assessing differential expression in microarray experiments. Stat Appl Genet Mol Biol 2004;3:article 3.

Summary

Within 3 weeks of conception in humans (comparable with mouse embryonic day E8.5), it is already possible to identify the beating heart. At this early stage, the heart is a tube-like structure, which contracts in a peristaltoid fashion, pumping the blood from the venous to the arterial pole. Its wall consists of an inner endocardial layer and an outer myocardial layer, the latter containing muscle cells sharing important 'embryonic' characteristics, among which high automaticity, low contractility and low conduction velocity. Subsequent to its formation the tube starts to loop to the right, and at specific places on the outer curvature of the looping heart a chamber-specific gene program is turned on, marking the initiation of the development of the atrial and ventricular chambers. The myocardium of the newly evolving atria and ventricles share typical 'working myocardial' characteristics, i.e. high contractility, high conduction velocity and low automaticity, making these chambers ideally equipped to pump the blood ahead in the now rapidly growing embryo. The rest of the looping heart tube, that is the inflow tract, atrioventricular canal (the embryonic structure connecting the developing atria and ventricles), inner curvature and outflow tract, does not differentiate into chamber myocardium, but maintains its embryonic phenotype for a longer period. From these structures the nodal parts of the conduction system, still characterized by the previously mentioned embryonic characteristics, will develop. The inflow tract gives rise to the sinus node, whereas the atrioventricular node develops from the back wall of the atrioventricular canal. During subsequent steps of embryonic development, by an interplay of additional steps of differentiation, cell growth, proliferation and recruitment of cells to the cardiac lineage, the 4-chambered heart is formed, containing numerous phenotypically different cells. In the mature heart, the atria and ventricles are fully septated, the pulmonal and the systemic circulation functioning in parallel. The heart contains valves ensuring efficient unidirectional blood flow, and the highly specialized cardiac conduction system ensures sequential, synchronized contractions of the atria and ventricles. On a molecular level many decisions have to be made before embryonic cardiac cells develop in a correct pattern from their primitive to their mature terminally differentiated state. This thesis focuses on the deciphering of some of the molecular regulatory networks, which orchestrate the decision of an embryonic myocardial cell to become a myocardial cell of the atrioventricular node or chamber.

Many of the decisions taken in (cardiac) morphogenesis are enforced by a complex interplay of transcription factors and signaling molecules. Transcription factors are proteins that are able to bind to specific sequences of DNA. When they bind, together with other transcription factors, signaling molecules and co-factors, they turn on, or turn off, the transcription of downstream target genes. These target genes, in turn, induce the changes in cellular differentiation. Whereas transcription factors are expressed intracellularly and direct their action upon the cell in which they are expressed, signaling molecules are excreted

extracellularly. These proteins act upstream of a 'signal transduction pathway'. Upon excretion, signaling molecules bind to the extracellular part of highly specific trans-membrane receptors present only on target cells. Following binding, the signal is transduced intracellularly, as the intracellular part of the activated receptor turns on an intracellular signaling cascade. Eventually, this intracellular signaling cascade results in proteins shuttling from the cytoplasm into the nucleus of the target cell, where – just like transcription factors – they often bind to specific regulatory sequences of DNA, thereby activating or repressing the transcription of downstream target genes. In heart development, the T-box family of transcription factors plays a pivotal role as will be discussed in this thesis. Several signal transduction pathways play a role in the morphogenesis of the heart. Of these, several members of the subfamily of bone morphogenetic proteins (Bmp)s, which belongs to the transforming growth factor β superfamily, are known to closely interact with T-box transcription factors. The Bmp subfamily consists of more than 20 members, of which, in this thesis, Bmp2 – and the intracellular molecules Smad1, 5, 8 and 4, which shuttle into the nucleus upon Bmp activation - will be discussed in detail. *Nppa*, the gene encoding atrial natriuretic factor (ANF), of which our study of its regulatory DNA sequences is described in Chapter 2, is a typical example of a target gene.

Chapter 1 reviews recent insights into some key morphogenetic processes underlying early cardiac development and the implications of this new knowledge for our thinking about the genesis of congenital heart defects. First, we discuss current understanding of patterning along the cranio-caudal, dorso-ventral, and left-right axes of the initially straight heart tube, explaining, among other malformations, why in the heart only the atria can be truly isomeric. Then, recent insights into the formation of the atrial and ventricular chambers, and their underlying transcriptional networks, are discussed. In many cardiac textbooks still the incorrect segmental model of cardiac formation is described, in which it was inaccurately assumed that already in the early heart tube all progenitors of the building blocks of the mature heart are present as a linear array of transverse precursor segments. Here, we review the up-to-date ballooning model of chamber formation, the first model which clearly explains how an initially solitary tube, with laminar flow through a single lumen, can transform into a 4-chambered heart in which the pulmonary and systemic circulations work in parallel. Finally, we discuss novel information on the origin of the cells that are added to the heart after formation of the initial tube, and their fate during further development.

In **Chapter 2** we explore the regulatory DNA sequences driving expression of *Nppa*, the gene encoding atrial natriuretic factor (ANF), during development and disease. Before birth *Nppa* is expressed specifically in the evolving atrial and ventricular chambers, marking their development. After birth the gene is silenced in the ventricles, where, in case of cardiac hypertrophy or heart failure, it is reactivated again as part of a larger 'fetal' gene program. To get insight into the regulatory sequences of *Nppa*, we generated several transgenic mice, all of them carrying a different transgenic construct integrated into their genome, in which a unique sequence of regulatory DNA, cloned from the endogenous *Nppa* locus, drives a reporter gene

(green fluorescent protein (*GFP), LacZ* or *Cre*). Then we induced heart failure in the reporter mice by crossbreeding them with another transgenic mouse model, in which the yeast transcription factor Gal4 is expressed throughout the myocardium, causing aspecific cardiomyopathy in males three weeks after birth. In some of the reporter mice, cardiac hypertrophy was induced by aortic banding, a procedure in which the ascending aorta is ligated, causing a pressure-overload hypertrophy model. Comparison of the expression patterns of the reporter genes in the diverse transgenic mice, both in embryos and in diseased hearts, with the expression pattern of endogenous *Nppa*, then provided insight into the potency of the diverse regulatory DNA sequences. From previous studies in transgenic mice, in which only short regulatory sequences were tested, it had been concluded that a proximal sequence of 0.7 kbp (kilo basepairs) contains all regulatory modules necessary to drive correct expression before birth. In those studies, the sequences driving *Nppa* expression during disease had never been located. By combining data from reporter mice carrying short regulatory fragments randomly integrated into the genome, with data from mice harboring a short fragment that was knocked in as a single copy into the genome, and data from reporter mice carrying very large regulatory fragments (up to 200 kbp in bacterial artificial chromosomes (BACs)), we came to very different conclusions. We show that, to drive correct ventricular activity during development, the proximal *Nppa* regulatory fragment lacks regulatory sequences. We then demonstrate that for correct ventricular expression before birth, at least two separate distally located activating sequences (enhancers) are required, one providing the correct pattern and one providing the correct fetal activity. Regulatory sequences driving *Nppa* expression during disease (stress response) might overlap or cooperate with those regulating the fetal expression pattern, but appear to function independently of the enhancer regulating ventricular activity before birth. Therefore, we conclude that ventricular *Nppa* activity before birth and reactivation during disease are regulated by separate regulatory sequences, and as a consequence by divergent transcriptional pathways. These findings implicate that all previous data on gene regulation obtained from transgenic mouse models using the short *Nppa* regulatory sequences, either during chamber development or cardiac hypertrophy and heart failure, should be re-evaluated. Additionally, they implicate that data on gene regulation obtained from fetal mouse models cannot automatically be applied on hypertrophy models, and vice versa.

In **Chapter 3** we aim to deepen our knowledge on the molecular pathways underlying the localized formation of the chambers versus the atrioventricular canal. From previous studies, the T-box transcription factors Tbx2, Tbx3 and Tbx20, together with Bmp/Smad-signaling, already had been established to play pivotal roles in the development of the chambers (Tbx20) and the atrioventricular canal (Tbx2, Tbx3 and Bmp/Smad). However, their genetic hierarchies and spatial and temporal interplay had remained unclear. By investigating mice homozygous mutant for *Tbx2,* for *Tbx3*, or double mutant for both genes, we found that Tbx2 and its close relative Tbx3 are redundantly required and individually sufficient to specify atrioventricular myocardium, induce formation of the atrioventricular cushions and suppress chamber differentiation in the atrioventricular canal. Furthermore, by

studying reporter mice harboring diverse Tbx2-reporter constructs and transfection experiments in which the constructs were temporally introduced into cell cultures *in vitro*, we identified a Bmp/Smad-dependent enhancer conferring atrioventricular canal-restricted expression and Tbx20-dependent chamber suppression of Tbx2 *in vivo*. Then we show that the T-box transcription factor Tbx20 plays a dual role in the compartmentalization of the heart. Contrary to what had been hypothesized previously, Tbx20 appears to stimulate chamber differentiation independently of Tbx2, and at the same time suppresses the activation of Tbx2 in the developing chambers, thereby localizing Tbx2 activity to the atrioventricular canal. Unexpectedly, Tbx20 does not repress Tbx2 expression directly by binding to its regulatory DNA sequences, but indirectly by binding to activated Smad1 and Smad5, sequestering these proteins from Smad4. Since Tbx2 is activated in the atrioventricular canal by Bmp2 in a Smad-dependent manner and Smad4 is a necessary co-factor for nuclear translocation and transcriptional activation by Smad1/Smad5, by this indirect mechanism Tbx20 effectively inhibits the Bmp/Smad-mediated activation of the target promoter of *Tbx2*. In conclusion, our findings suggest that opposing regulation of Bmp signaling by Tbx20 and Tbx2 may underlie specification of the chambers and the atrioventricular canal, respectively.

In **Chapter 4** we describe the generation of a novel reporter mouse, in which green fluorescent protein (GFP) is driven by 160 kbp of regulatory DNA sequences of the T-box transcription factor Tbx3. Whereas endogenous Tbx3 is expressed in the different components of the cardiac conduction system, i.e. the sinus node, the atrioventricular node, the atrioventricular bundle and the bundle branches, the reporter gene was expressed specifically in the developing atrioventricular node but not in the other components of the cardiac conduction system. This finding demonstrates that the components of the conduction system are driven by distinct regulatory sequences, and therefore separate transcriptional pathways. The reporter mice were then used to purify atrioventricular nodal cells at two development stages (embryonic E10.5 and fetal E17.5). Subsequently, the gene expression profiles of these purified nodal cells were compared with age-matched working myocardial cells (purified using transgenic mice described in Chapter 2) using microarray analysis, a technique allowing examination of the activity of more than 20,000 genes at the same time. We constructed a comprehensive list of genes associated with electrical impulse propagation, which were picked up specifically in the nodal or working myocardium. Many of these were ion channels, not previously associated with nodal or working myocardium and several not even with cardiac expression. Furthermore, the data revealed that the atrioventricular node and the working myocardium phenotypes diverge during development, but that the functional gene classes characterizing both subtypes are maintained. One of the repertoires identified in the atrioventricular node-specific gene profiles consists of multiple factors previously only associated with neural development, revealing shared characteristics between nodal and nervous system development. These data present the first genome-wide transcription profiles of the atrioventricular node during development, providing valuable information concerning its molecular identity.

Nederlandse samenvatting

Drie weken na de bevruchting is het al mogelijk een kloppend hart waar te nemen in het zich ontwikkelende menselijke embryo. Zo vroeg in de ontwikkeling is het hart een buisvormige structuur, die het bloed van de veneuze instroom naar de arteriële uitstroom pompt door middel van peristaltische contracties. De wand van de hartbuis bestaat uit een binnenste endocardiale laag en een buitenste myocardiale spierlaag. De cellen van de spierlaag worden cardiomyocyten genoemd en hebben een aantal belangrijke 'embryonale' eigenschappen gemeenschappelijk, waaronder hoge automaticiteit (de eigenschap van een cel om zelf een elektrische prikkel te kunnen genereren), lage contractiliteit (de mogelijkheid tot samentrekken), en een lage impuls-voortgeleidingssnelheid. Nadat de rechte hartbuis is gevormd begint deze uit te bochten naar voren en naar rechts. Rond dezelfde tijd wordt op specifieke plaatsen van de nu ontstane buitenste bocht van de hartbuis een specifiek genprogramma aangeschakeld, waardoor de eigenschappen van de cellen ter plaatse veranderen (differentiëren). Dit proces markeert het begin van de ontwikkeling van de boezems (atria) en de kamers (ventrikels). De spiercellen van de zich ontwikkelende atria en ventrikels hebben andere, typische 'werk' eigenschappen gemeenschappelijk, zoals hoge contractiliteit en hoge voortgeleidingssnelheid, maar lage automaticiteit. Met deze eigenschappen zijn de kamers perfect toegerust om het bloed met kracht voort te pompen in het nu snel groeiende embryo. De rest van het uitbochtende hart, namelijk het instroom gebied (inflow tract), het atrioventriculaire kanaal (de embryonale structuur die de atria met de ventrikels verbindt), de binnenste curvatuur (dat gedeelte van de hartbuis dat zich aan de binnenbocht bevindt) en het uitstroom gebied (outflow tract), differentieert niet tot kamer-spiercel, maar behoudt zijn embryonale eigenschappen gedurende een langere periode (zie ook figuur 3 in hoofdstuk 2, waarin bovenstaand proces aan de hand van een tekening wordt uitgelegd). Uit deze laatstgenoemde structuren ontwikkelen zich onder andere de knopen van het geleidingssysteem van het hart, welke ook in het volwassen stadium gekarakteriseerd worden door de eerder genoemde 'embryonale' spiercel-eigenschappen. De sinusknoop, die ontstaat in het instroom gebied, is een gespecialiseerde spiercel-structuur bij de instroom van de bovenste lichaamsader in het rechter atrium. Deze structuur heeft de hoogste automaticiteit van alle hartspiercellen en genereert de elektrische prikkel die het hart aanzet samen te trekken. Vanuit de sinusknoop wordt de elektrische impuls voortgeleid door de atriale wand, welke als reactie samentrekt, waarna de impuls terecht komt in de atrioventriculaire knoop. De atrioventriculaire knoop ontstaat uit het atrioventriculaire kanaal. In het volwassen stadium is de atrioventriculaire knoop de enige myocardiale structuur die de atria, via de atrioventriculaire bundel, met de ventrikels verbindt. Verder zijn de atria en ventrikels elektrisch gescheiden door bindweefsel. De atrioventriculaire knoop heeft twee belangrijke eigenschappen. Ten eerste vertraagt de atrioventriculaire knoop de impuls voordat hij deze

doorgeeft aan de ventrikels, waardoor deze net iets later samentrekken dan de atria. Hierdoor profiteren de ventrikels optimaal van de extra instroom van bloed door de atria-contractie, en pompen dus een zo groot mogelijk volume per slag. Ten tweede heeft ook de atrioventriculaire knoop een hoge automaticiteit, zodat, wanneer de sinusknoop uitvalt, de atrioventriculaire knoop een prikkel kan genereren die de kamers aanzet samen te trekken. Gedurende hieropvolgende stappen van ontwikkeling wordt, door een samenspel van differentiatie, celgroei, celdeling, en toevoeging van cellen aan het hart, het vierkamerige volwassen hart gevormd. Dit bevat veel fenotypisch verschillende cellen. In het volwassen hart zijn het linker en rechter atrium, evenals de linker en rechter ventrikel, volledig van elkaar gescheiden door tussenschotten, waardoor de long- en de lichaams-bloedsomloop gescheiden functioneren. Het hart bevat kleppen die een efficiënte bloedstroom in één richting verzekeren, en het gespecialiseerde geleidingssysteem van het hart verzekert opeenvolgende, synchrone contractie van de atria en de ventrikels. Op moleculair niveau moeten veel beslissingen worden genomen voordat de embryonale hartcellen zich in een correct patroon ontwikkelen van hun primitieve tot hun terminaal gedifferentieerde staat. Dit proefschrift richt zich op het ontrafelen van sommige van de moleculaire regel-netwerken, die ten grondslag liggen aan de beslissing van een embryonale spiercel om zich te ontwikkelen tot een spiercel van de atrioventriculaire knoop, dan wel tot een spiercel van de (atriale of ventriculaire) kamers.

Binnen één organisme bevat elke cel hetzelfde erfelijk materiaal (genoom of DNA). De reden dat elke cel toch andere eigenschappen heeft (een ander fenotype heeft), is dat in elke cel verschillende genen aan en uit staan. Als een gen aan staat, wordt deze afgelezen in RNA, een proces dat transcriptie wordt genoemd. Vervolgens wordt dit RNA omgezet in eiwit. Dit proces heet translatie. Alle eiwitten die aanwezig zijn in een specifieke cel bepalen samen het fenotype van deze cel, met andere woorden bepalen welke eigenschappen deze cel heeft. Binnen elke cel wordt zowel de transcriptie als de translatie nauwkeurig gereguleerd. Veel van de beslissingen die worden genomen gedurende de ontwikkeling worden op transcriptieniveau opgelegd door een complex samenspel van transcriptiefactoren en signaalmoleculen. Transcriptiefactoren zijn eiwitten die kunnen binden aan een specifieke DNA regel-sequentie. Elk gen heeft zijn eigen regulatoire sequenties, welke bestaan uit een specifieke volgorde van de bouwstenen van het DNA (basenparen). Als transcriptiefactoren binden, in samenspel met andere transcriptiefactoren, signaalmoleculen en co-factoren, schakelen ze de transcriptie van doelwit-genen aan of uit. De hieruit resulterende verhoogde of verlaagde aanwezigheid van doelwit-eiwitten in de cel induceert uiteindelijk de veranderingen in cellulaire differentiatie. Terwijl transcriptiefactoren intracellulair (binnen de cel) tot expressie komen en dus de differentiatie van de cel beïnvloeden waarin ze actief zijn, worden signaalmoleculen extracellulair (buiten de cel) uitgescheiden. Deze signaaleiwitten fungeren als meest ‘stroomopwaarts’ gelegen spelers van een ‘signaal-transductie pad’. Na uitscheiding binden de signaaleiwitten aan het extracellulaire gedeelte van specifieke trans-membraanreceptoren die alleen aanwezig zijn op doelwit-cellen. Na binding wordt het signaal naar het binnenste van de cel (het cytoplasma) doorgegeven, doordat het intracellulaire

gedeelte van de geactiveerde receptor een intracellulaire signaalcascade activeert. Uiteindelijk leidt deze cascade ertoe dat specifieke eiwitten vanuit het cytoplasma de celkern in migreren, waar ze – net als transcriptiefactoren – meestal aan specifieke DNA regel-sequenties binden, en zo de transcriptie van doelwit-genen activeren of onderdrukken.

Zoals wordt besproken in dit proefschrift, speelt de T-box familie van transcriptiefactoren een centrale rol tijdens de ontwikkeling van het hart. Ook spelen meerdere signaal-transductie paden een belangrijke rol. Verschillende leden van de signaal-transductie subfamilie van 'bone morphogenetic proteins' (Bmp)s werken nauw samen met T-box transcriptiefactoren. De Bmp subfamilie kent meer dan 20 leden, van welke in dit proefschrift vooral Bmp2 en de intracellulaire moleculen Smad1, 5, 8 en 4, die uiteindelijk de celkern in migreren na extracellulaire Bmp activatie, in detail worden besproken. Nppa, het gen dat codeert voor 'atriale natriuretische factor' (ANF), waarvan we in onze studie in hoofdstuk 2 de regulatoire DNA sequenties beschrijven, is een typisch voorbeeld van een doelwit-gen.

In **Hoofdstuk 1** bespreken we recent verkregen inzichten in enige vormbepalende processen die een centrale rol spelen tijdens de vroege hartontwikkeling. Daarnaast gaan we in op de implicaties van deze nieuwe inzichten voor ons denken over het ontstaan van aangeboren hartafwijkingen. We beginnen met een bespreking van ons huidige begrip van patroonvorming van de in eerste instantie rechte hartbuis langs de verschillende assen van het lichaam (cranio-caudaal (kop-staart), dorso-ventraal (rug-buik), links-rechts). Patroonvorming maakt dat de cellen in de hartbuis 'weten' waar ze zich bevinden, en zich als zodanig gedragen en zich verder ontwikkelen. We leggen uit wat hierbij mis kan gaan en geven inzicht in verschillende relatief veel voorkomende aangeboren afwijkingen, waaronder isomerie van de atria. Vervolgens gaan we in op de huidige kennis over de ontstaanswijze van de atriale en ventriculaire kamers, en de moleculaire regel-netwerken die hieraan ten grondslag liggen. In vrijwel alle tekstboeken over hartontwikkeling wordt nog altijd het segmentmodel beschreven. In dit model wordt er ten onrechte van uit gegaan dat in de initiële hartbuis alle voorlopercellen van de bouwstenen van het volwassen hart aanwezig zijn. Deze voorlopercellen zouden bovendien lineair gerangschikt zijn als opeenvolgende over de gehele diameter verlopende voorlopersegmenten. Hier bespreken we het 'ballooning model van kamer ontwikkeling'. Dit is het eerste model dat inzichtelijk maakt hoe een initieel enkelvoudige buis, met een bloedstroom door een enkele holte, zich kan ontwikkelen tot een vierkamerig hart waarin de long- en de lichaams-circulatie gescheiden functioneren. Als laatste bespreken we recente inzichten in de afkomst van die cellen die worden toegevoegd nadat de embryonale hartbuis is gevormd, en over de uiteindelijke plaats en functie van deze cellen in het volwassen hart.

In **Hoofdstuk 2** beschrijven we ons onderzoek naar de regulatoire DNA sequenties die de expressie van het gen Nppa reguleren in het zich ontwikkelende en in het zieke hart. Voor de geboorte komt Nppa specifiek tot expressie in de zich vormende atriale en ventriculaire kamers. Na de geboorte wordt het gen uitgezet in de ventrikels, waar het weer wordt aangezet bij het optreden van hypertrofie (verdikking van de hartspier) en bij hartfalen. Algemeen

wordt aangenomen dat deze re-activering plaats vindt als onderdeel van de re-activering van een groter embryonaal genprogramma. Om inzicht te krijgen in de lokatie van de regulatoire sequenties van Nppa, en zo op termijn in de eiwitten die hieraan binden en dit gen reguleren, hebben we verschillende transgene muizen gegenereerd. Alle muizen hebben een ander transgeen (lichaamsvreemd) DNA construct geïntegreerd in hun erfelijk materiaal (in hun genoom), waarin steeds een ander stuk regel-DNA is gekloneerd vanuit de natuurlijke Nppa locus, dat een 'reportergen' aanstuurt. Een reportergen is een gen (bijvoorbeeld groen fluorescerend proteïne (GFP), LacZ of Cre) waarvan het expressiepatroon makkelijk gedetecteerd kan worden in het transgene dier. Vervolgens hebben we hartfalen geïnduceerd in de reportermuizen door ze te kruisen met een andere transgene muis die een uit gist afkomstige transcriptiefactor (Gal4) tot expressie brengt in alle hartspiercellen. Hierdoor ontstaat drie weken na de geboorte aspecifieke cardiomyopathie (ziekte van de hartspier) in alle mannetjes van deze lijn. In enkele van de reportermuizen hebben we bovendien hypertrofie geïnduceerd door 'aortic banding'. Dit is een operatie waarbij om de aorta, net nadat deze ontspringt uit het linker ventrikel, een bandje wordt gelegd die de aorta vernauwt. Hierdoor ontstaat een druk-overbelasting, waardoor een type hypertrofie wordt geïnduceerd die ook bij bijvoorbeeld langdurige hypertensie (hoge bloeddruk) wordt gezien. Vergelijking van de expressiepatronen van de reportergenen in de diverse transgene muizen, zowel tijdens het embryonale stadium als in het zieke hart, met het expressiepatroon van endogeen (lichaamseigen) Nppa, gaf vervolgens inzicht in de potentie van de diverse regulatoire DNA sequenties. In voorafgaande studies werden alleen korte regulatoire sequenties getest. Uit deze studies werd geconcludeerd dat een dicht bij het gen liggend (proximaal) DNA fragment van 0.7 kilobasenparen alle regulatoire modules bevat die nodig zijn voor een correcte expressie voor de geboorte. De sequenties die Nppa expressie in het zieke hart aansturen werden in eerdere studies nooit gelokaliseerd. In onze studie onderzoeken we reportermuizen die korte regulatoire fragmenten op een willekeurige plek in het genoom hebben geïntegreerd, met een muis die een enkele kopie van een kort fragment heeft geïntegreerd op een welomschreven plek in het genoom (knockin muis), met muizen met een groot regulatoir fragment (tot 200 kilobasenparen in 'bacterial artificial chromosomes' (BACs)), en komen zo tot heel andere conclusies. We laten zien dat de proximale fragmenten regulatoire elementen missen voor correcte ventriculaire activiteit tijdens de ontwikkeling. Vervolgens laten we zien dat voor correcte ventriculaire expressie voor de geboorte minimaal twee extra, op grote afstand (distaal) van het eigenlijke gen gelokaliseerde, activerende regulatoire sequenties nodig zijn. Eén van deze verzorgt het correcte patroon, de andere sequentie verzorgt de correcte embryonale activiteit. Ook de regulatoire sequenties die Nppa expressie in tijden van cardiale ziekte (stress respons) reguleren blijken distaal gelegen. Mogelijk overlappen deze, of werken samen, met de sequenties die het embryonale expressiepatroon reguleren. Echter, ze blijken onafhankelijk te functioneren van de activerende sequenties die de ventriculaire activiteit voor de geboorte reguleren. Om die reden concluderen we dat de ventriculaire Nppa activiteit voor de geboorte gereguleerd wordt door andere regulatoire sequenties en dus door andere transcriptie-paden dan de re-activatie van Nppa in tijden van cardiale stress. Deze nieuwe

informatie impliceert dat alle voorgaande data over genregulatie, verkregen uit onderzoek aan transgene muismodellen met enkel korte regulatoire Nppa fragmenten, opnieuw moeten worden geïnterpreteerd. Ook impliceert dit inzicht dat data over genregulatie die zijn verkregen uit embryonale muismodellen niet automatisch mogen worden geëxtrapoleerd naar situaties waarbij cardiale stress in het spel is, en vice versa.

Hoofdstuk 3 bevat een studie, die al bestaande kennis verdiept over de moleculaire netwerken die de gelokaliseerde formatie van de atriale en ventriculaire kamers, versus het tussenliggende atrioventriculaire kanaal, reguleren. Voorgaande studies hadden al aangetoond dat de T-box transcriptiefactoren Tbx2, Tbx3 en Tbx20, in nauwe samenwerking met het Bmp/Smad signaal transductie pad, een centrale rol spelen in de ontwikkeling van de kamers (Tbx20) en het atrioventriculaire kanaal (Tbx2, Tbx3 en Bmp/Smad). Echter, hun onderlinge hiërarchie en precieze samenspel in tijd en plaats waren nog onduidelijk. Knock-out muizen zijn muizen waarin de werking van één specifiek gen, van een totaal van meer dan 20.000 genen, is kapot gemaakt. Door een knock-out muis te onderzoeken, kan vervolgens de functie van het specifieke gen worden afgeleid. In de hier beschreven studie hebben we muizen onderzocht waarin of alleen Tbx2, of alleen Tbx3, of zowel Tbx2 als Tbx3 was uitgeschakeld. Hieruit komt naar voren dat de transcriptiefactoren Tbx2 en het genetisch zeer verwante Tbx3 onafhankelijk van elkaar voldoende zijn om zowel de ontwikkeling van de spiercellen van het atrioventriculaire kanaal te reguleren, als de formatie van de atrioventriculaire kussens (voorlopers van kleppen en tussenschotten) te initiëren, en bovendien de kamerontwikkeling in het atrioventriculaire kanaal te onderdrukken. Kortom, beide genen zijn in het atrioventriculaire kanaal ‘redundant’ actief, wat wil zeggen dat ze essentiële functies van elkaar kunnen overnemen, mocht het andere gen niet werkzaam zijn. Vervolgens hebben we verschillende Tbx2-reportermuizen bestudeerd en de data hiervan gecombineerd met data uit experimenten waarbij we het gedrag van diezelfde reporterconstructen in vitro (buiten het lichaam) testen door de constructen tijdelijk te introduceren in cellen. Het voordeel van deze laatste proefopzet is dat een laboratoriumsituatie wordt gecreëerd, waarbij heel specifiek de gevoeligheid van elk construct voor allerlei bij te voegen factoren kan worden getest. Aldoende hebben we een Bmp/Smad-afhankelijk regulatoir DNA-fragment geïdentificeerd, dat zowel de atrioventriculaire kanaal-specifieke expressie van Tbx2, als de Tbx20-afhankelijke repressie van Tbx2 in de kamers reguleert. Vervolgens laten we zien dat Tbx20 een dubbele rol speelt in de compartimentalisatie van het hart. Ten eerste blijkt, in tegenstelling tot wat tot nu toe werd verondersteld, dat Tbx20 kamerontwikkeling stimuleert onafhankelijk van Tbx2. Tegelijkertijd onderdrukt Tbx20 de activatie van Tbx2 in de zich onwikkelende kamers, waardoor Tbx2 expressie tot het atrioventriculaire kanaal wordt beperkt. Daarbij onderdrukt Tbx20 Tbx2 niet rechtstreeks door te binden aan de regulatoire DNA sequenties van Tbx2, maar indirect door te binden aan geactiveerd Smad1 en Smad5, waardoor deze eiwitten gescheiden blijven van Smad4. In het atrioventriculaire kanaal wordt Tbx2 geactiveerd door Bmp2 op een Smad-afhankelijke manier. Als resultaat van de Bmp2-binding moet, als onderdeel van de geactiveerde intracellulaire signaalcascade, Smad4 als co-factor eerst binden aan Smad1 of Smad5 voordat dit gehele Smad-complex vanuit het

cytoplasma de celkern in kan migreren om de transcriptie van Tbx2 te activeren. Daardoor onderdrukt Tbx20 op een indirecte manier (namelijk, door te voorkómen dat er geactiveerde Smad-complexen ontstaan die de celkern in migreren om hier Tbx2 te activeren) de Bmp/Smad-gemedieerde activatie van het doelwit-gen Tbx2 zeer effectief. Samenvattend suggereren onze data dat tegengestelde regulatie van Bmp-signalering door Tbx20 en Tbx2 aan de basis ligt van de specificatie van respectievelijk de kamers en het atrioventriculaire kanaal.

In **Hoofdstuk 4** beschrijven we het genereren van een nieuwe reportermuis, welke in zijn genoom een construct draagt waarin een groen fluorescerend eiwit (GFP) wordt aangestuurd door 160 kilobasenparen van de regulatoire sequenties van de T-box transcriptiefactor Tbx3. Terwijl endogeen Tbx3 tot expressie komt in de verschillende componenten van het cardiale geleidingssysteem, namelijk in de sinusknoop, de atrioventriculaire knoop, de atrioventriculaire (His) bundel en de bundeltakken, laten we zien dat GFP heel specifiek tot expressie komt alleen in de zich ontwikkelende atrioventriculaire knoop en niet in de andere componenten van het geleidingssysteem. Deze vinding toont aan dat de verschillende componenten van het geleidingssysteem worden gereguleerd door verschillende regulatoire DNA sequenties, en dus door verschillende transcriptionele paden. Vervolgens hebben we deze reportermuizen, die gekenmerkt worden door een fel groen fluorescerende atrioventriculaire knoop, gebruikt om sterk gezuiverde atrioventriculaire knoopcel-populaties te verkrijgen op twee verschillende stadia van ontwikkeling (embryonaal E10.5 en foetaal E17.5). Vervolgens hebben we het genexpressieprofiel (de specifieke hoeveelheid RNA van alle individuele genen) bepaald van deze atrioventriculaire knoopcellen, en dit profiel vervolgens vergeleken met het genexpressieprofiel van kamer-spiercellen van dezelfde leeftijd (die we hebben gezuiverd door gebruik te maken van de transgene muizen beschreven in hoofdstuk 2). Hiertoe hebben we gebruik gemaakt van microarrays, een moderne techniek die het mogelijk maakt de expressie van meer dan 20.000 genen simultaan te bepalen. Uit de hieruit gegenereerde data hebben we een volledige lijst geconstrueerd van genen die geassocieerd zijn met elektrische impulsvoortgeleiding, en die specifiek in de atrioventriculaire knoopspiercellen, dan wel in de kamerspiercellen tot expressie kwamen. Vele van deze zijn ionkanalen die niet eerder werden geassocieerd met knoop- of werk-spiercellen, terwijl verschillende zelfs niet eerder werden geassocieerd met het hart. Bovendien komt uit deze data naar voren dat hoewel de fenotypen van de kamerspiercellen en van de atrioventriculaire knoopspiercellen gedurende de ontwikkeling divergeren, binnen elk subtype de aanwezigheid van de karakteristieke functionele genklassen grotendeels behouden blijft. Eén van de functionele genrepertoires die we hebben geïdentificeerd in de atrioventriculaire knoopcellen, bestaat uit genen die voorheen alleen werden geassocieerd met de ontwikkeling van zenuwen. Dit suggereert dat knoopspiercel-ontwikkeling en zenuw-ontwikkeling vele kenmerken delen. De informatie die uit deze microarray naar voren komt representeert het eerste genexpressieprofiel van de zich ontwikkelende atrioventriculaire knoop op genoombreed niveau en geeft ons waardevolle informatie over zijn moleculaire identiteit.

Dankwoord

‘Jongens waren we - maar aardige jongens.’ Eén van de mooiste zinnen uit de Nederlandse literatuur, waar ik vaak en lang met vrienden over gesproken heb tijdens mijn studenten- en co-schaptijd. Een boek schrijven wilden we. Daarbij ging het om de eerste en de laatste zin. Als die één keer op papier zouden staan – en er waren ideeën te over – zou het invullen van die 300 bladzijden er tussenin een koud kunstje zijn, waarna grootse oplagen en beroemdheid in het verschiet zouden liggen. Nou, het boek is er bij deze gekomen. Het blijkt er echter geen van Literatuur, maar van Wetenschap. En de invulling tussen de eerste en laatste regel had meer voeten in de aarde dan toentertijd verwacht. Ook het romantisch idee van geïnspireerd schrijver (of wetenschapper) eenzaam achter zijn typemachine op zolder bleek onjuist. Dit proefschrift is tot stand gekomen door noeste arbeid en bovenal door fantastisch teamwork binnen de afdeling Anatomie & Embryologie (AEL), de overige afdelingen binnen het HartFaalCentrum, en enige onderzoeksgroepen daarbuiten. Vanaf deze plaats dank ik iedereen die op enige wijze aan dit proefschrift heeft bijgedragen, waarbij ik natuurlijk enkele mensen in het bijzonder wil noemen.

Ik dank Prof. dr. A.F.M. Moorman en dr. V.M. Christoffels, respectievelijk mijn promotor- en co-promotor. Beste Antoon en Vincent, jullie beiden hebben me vijf jaar geleden het vertrouwen gegeven om als medisch dokter de pipet ter hand te nemen, en me met vallen en opstaan gesmeed tot enthousiast moleculair onderzoeker. Antoon, uit je opmerking, gemaakt in mijn eerste week als fundamenteel onderzoeker ‘Promoveren is een dikke huid kweken’, blijkt je mensenkennis en relativeringsvermogen. Als wetenschappelijk mentor stond jij als stabiliserende factor op de achtergrond en enthousiasmeerde waar dat nodig was, en hield een oogje in het zeil dat het proefschrift ook daadwerkelijk werd afgerond. Vincent, hoewel ons verschil in karakters enige gewenning beiderzijds noodzakelijk maakte, werkten je gedrevenheid en perfectionisme aanstekelijk. Je wist elke proef en elke tekst weer vlot te trekken, en altijd een nieuwe hypothese te formuleren. Van jullie beiden waardeer ik bovenal de bevlogenheid de ontstaanswijze van het 4-kamerige hart te ontrafelen. Een enthousiasme dat aanstekelijk is gebleken, en dat ik meeneem naar de kliniek.

Mijn leermeesters op de werkvloer: Daan en Vincent W, jullie leerden me knutselen met DNA (kloneren – nog steeds mijn favoriete tak van moleculaire sport) en van één streng vele identieke kopieën maken (PCR-en – blijkt een stuk saaier). Janynke, samen kloneerden wij de eerste bacterial artificial chromosomes op de afdeling en overwonnen alle kinderziektes van dat ogenschijnlijk zo eenvoudige protocol. Corrie, dank voor je introductie in de wondere wereld van paraplast, coupes en in situ hybridisaties. Alex P, Kees-Jan en Phil, vraagbaken tijdens mijn bioinformatische zoektochten op het www naar nieuwe bindingssites en geconserveerde sequenties – helaas bleek de natuur steeds weerbarstiger dan onze modellen.

Arjan, ik heb genoten van het enthousiaste sparren over ANF-expressie – en er tot op heden spijt van dat ik je goede raad betreffende BACs in de wind heb geslagen. Geweldig dat het zo'n mooi artikel is geworden. Dan natuurlijk die hele oude garde jonge onderzoekers – Chris, Suzanne, Boudewijn, Frederik, Saskia, André, Tamara, Willem – die kort na mijn aankomst nooit te beroerd waren de basics van het vak (het verschil tussen dTTPs en dNTPs, de kunst van het lyseren der staartjes) toe te lichten. Kennis die ik later met veel plezier heb overgedragen aan de jonge enthousiaste garde na mij, vaak net als ik hartstikke groen in het vak.

Zonder de faciliterende backbone van het AEL hadden wij jonge onderzoekers nooit zo vrij kunnen spelen. Structuur en sfeer werden en worden gebracht door Roelof-Jan, Ruth, Paul, André, Petra, Maurice, Jaco, Jan, Sabine, Piet (altijd in voor een belangrijk gesprek over de beste tandwielen voor de juiste helling, en organisator van de groene HartFaal tocht), Anita, Pamela. Het AEL is inmiddels met de afdeling Fysiologie en Experimentele Cardiologie georganiseerd in het HartFaalCentrum, waardoor eenieder nog beter van elkaars kennis kan profiteren – een samenwerking die steeds meer vruchten afwerpt. Zo dank ik Arie Verkerk voor de electrofysiologische metingen, cruciaal voor hoofdstuk 4.

I am greatly indepted to my thesis committee. Dear dr. C.R. Bezzina, dr. P.A.C. 't Hoen, Prof. dr. A. Kispert, Prof. dr. Y.M. Pinto and Prof. dr. A.C. van Rossum, I am honored to have been able to submit my work to your expert opinion.

De externe samenwerkingsverbanden en hulptroepen met wie we onze expertise hebben gebundeld om de verschillende artikelen van dit proefschrift tot volle wasdom te laten komen dank ik hartelijk. Tijdens de altijd inspirerende en scherpe brainstormsessies met de groep Humane Genetica van het Leids Universitair medisch centrum combineerden we onze moleculaire kennis van het embryonale hart met jullie kunde en kennis van genomics. Sessies die hebben geleid tot hoofdstuk 4 en een bijdrage leverden aan hoofdstuk 3. Henk en Peter-Bram, bedankt! Andreas, I enjoyed the discussions with you and Vincent about the genesis of the atrioventricular canal versus the chambers. Your enthusiasm in science and thorough experimental approach were an example for me. Hamid el Azouzzi, jij ombond binnen twee dagen meer dan 20 aortas en maakte zo de re-submissie van hoofdstuk 2 mogelijk. Berend Hooibrink hielp mij op fantastische wijze met het FACS-en van mijn schaarse fluorescente cellen. Student Hans van der Linden deed vele prachtige ANF *in situ* hybridisaties.

In het bijzonder dank ik mijn mede AIO's, die nooit te beroerd waren met hun grappen alles te relativeren, ook als ik daar nu eens absoluut niet op te wachten stond. Jullie hebben mijn jaren in het lab tot onvergetelijke gemaakt. Ik mis de koffie tussen de stoffige boeken en keurig ingepakte en gerangschikte schedels bij Laurens, beschermheer van de collectie Vrolik; de (on)geleide wetenschappelijke projectielen van Wim; de observeringen in de patiëntenrecreatie met Alex S; de alternatieve bandjes van Willem op de vrijdagmiddag; de

Lunterense plattelandsverhalen van Bram; het geroddel en gemopper van – en discussies over de (on)leesbaarheid van Grunberg met – Gert; de broodnodige blikjes cola met Kees-Jan; en alle andere AIO's met wie ik in één tent heb geslapen, heb gekanood, congressen heb bezocht, in de Smoky Mountains heb gehiked, of gewoon heb geborreld.

Ik dank mijn nieuwe collega's van de afdeling Cardiologie in het VU medisch centrum voor de hartelijke ontvangst, het getoonde geduld bij mijn her-intrede in de kliniek en bij mijn verhalen over het ver-pdf-en van mijn manuscript, en natuurlijk voor de goede borrels in Amsterdam en op lokatie in de Oostenrijkse sneeuw.

Dan dank ik eenieder buiten het vakgebied, die telkens weer dezelfde vraag stelde: 'En, hoe is het met de muizen, zijn ze nog steeds groen?' Kortom, mijn vriendenschare die met nimmer aflatende (dan wel goed geveinsde) interesse naar mijn escapades in het lab luisterde, en zo mijn enthousiasme deelde: De onnavolgbare en mij zeer dierbare Elandsstraat-posse – 'Een feest is pas een feest als jij en de politie zijn geweest'; mijn geliefde geneeskunde-vriend(inn)en – voor (helaas te infrequente) etentjes, fietstochten Luik-Bastenaken-Luik en sterven op de Redoute; de steeds hechter wordende groep bergliefhebbers – voor een avondje wegdromen in de Doffer, dan wel in ijle lucht in de Alpen of Nepal; en alle andere vrienden die mij het gevoel gaven te leven in de breedte, wanneer het keurslijf van de promotie knelde.

Marloes, lieve zus, András, grootmoedige vriend. Jullie vanzelfsprekende vriendschap maakt jullie tot gedroomde paranimfen. Betere metgezellen in mijn leven, en tijdens mijn promotie, zou ik mij niet kunnen wensen.

Lieve Janneke, onze ontmoeting nu bijna twee jaar geleden in de Hortus Botanicus relativeert elke maat voor 'impactfactor'. De ongewisse wetenschappelijke reis die wij beiden in 2003 alleen begonnen aan onze eigen uiterste α-, respectievelijk β- zijde van het evolutionaire spectrum, is sindsdien verstrengeld geraakt. Het laatste half jaar hebben we deze schouder aan schouder afgelegd, monter werkend aan onze eigen bureaus die nu in één kamer staan. De lange reis zit er nu bijna op, en ik zal de wetenschappelijke avonden en weekenden nog gaan missen. Maar vooral zie ik uit naar onze toekomstige reizen.

Vanzelfsprekend eindig ik dit dankwoord met een woord aan mijn ouders. Lieve papa en mama, jullie positieve levenshouding, arbeidsethos, toewijding en niet aflatende belangstelling hebben mij gevormd en het zelfvertrouwen gegeven dit proefschrift in goede banen te leiden. Ik ben er trots op dit proefschrift hierbij aan twee zulke bijzondere mensen op te dragen.

Thomas